ISSN 1948-0210 (online)

World Journal of *Stem Cells*

World J Stem Cells 2024 March 26; 16(3): 228-323

Published by Baishideng Publishing Group Inc

World Journal of Stem Cells

Contents

Monthly Volume 16 Number 3 March 26, 2024

EDITORIAL

228 O-linked β-N-acetylglucosaminylation may be a key regulatory factor in promoting osteogenic differentiation of bone marrow mesenchymal stromal cells

Zhou XC, Ni GX

232 Understanding host-graft crosstalk for predicting the outcome of stem cell transplantation

Labusca L, Zugun-Eloae F

237 High glucose microenvironment and human mesenchymal stem cell behavior

Mateen MA, Alaagib N, Haider KH

MINIREVIEWS

245 How mesenchymal stem cells transform into adipocytes: Overview of the current understanding of adipogenic differentiation

Liu SS, Fang X, Wen X, Liu JS, Alip M, Sun T, Wang YY, Chen HW

ORIGINAL ARTICLE

Retrospective Study

257 Long-term outcome of stem cell transplantation with and without anti-tumor necrotic factor therapy in perianal fistula with Crohn's disease

Park MY, Yoon YS, Park JH, Lee JL, Yu CS

Basic Study

267 Low-intensity pulsed ultrasound reduces alveolar bone resorption during orthodontic treatment *via* Lamin A/C-Yes-associated protein axis in stem cells

Wu T, Zheng F, Tang HY, Li HZ, Cui XY, Ding S, Liu D, Li CY, Jiang JH, Yang RL

287 Self-assembly of differentiated dental pulp stem cells facilitates spheroid human dental organoid formation and prevascularization

Liu F, Xiao J, Chen LH, Pan YY, Tian JZ, Zhang ZR, Bai XC

305 Evaluation of genetic response of mesenchymal stem cells to nanosecond pulsed electric fields by whole transcriptome sequencing

Lin JJ, Ning T, Jia SC, Li KJ, Huang YC, Liu Q, Lin JH, Zhang XT

World Journal of Stem Cells

Monthly Volume 16 Number 3 March 26, 2024

Contents

ABOUT COVER

Editorial Board Member of *World Journal of Stem Cells*, Yu-Hong Li, PhD, Associate Professor, Department of Cell Biology, Army Medical University, Chongqing 400038, China. liyuhongtmmu@hotmail.com

AIMS AND SCOPE

The primary aim of *World Journal of Stem Cells* (*WJSC*, *World J Stem Cells*) is to provide scholars and readers from various fields of stem cells with a platform to publish high-quality basic and clinical research articles and communicate their research findings online. *WJSC* publishes articles reporting research results obtained in the field of stem cell biology and regenerative medicine, related to the wide range of stem cells including embryonic stem cells, germline stem cells, tissue-specific stem cells, adult stem cells, mesenchymal stromal cells, induced pluripotent stem cells, embryonal carcinoma stem cells, hemangioblasts, lymphoid progenitor cells, *etc*.

INDEXING/ABSTRACTING

The *WJSC* is now abstracted and indexed in Science Citation Index Expanded (SCIE, also known as SciSearch®), Journal Citation Reports/Science Edition, PubMed, PubMed Central, Scopus, Biological Abstracts, BIOSIS Previews, Reference Citation Analysis, China Science and Technology Journal Database, and Superstar Journals Database. The 2023 Edition of Journal Citation Reports® cites the 2022 impact factor (IF) for *WJSC* as 4.1; IF without journal self cites: 3.9; 5-year IF: 4.5; Journal Citation Indicator: 0.53; Ranking: 15 among 29 journals in cell and tissue engineering; Quartile category: Q3; Ranking: 99 among 191 journals in cell biology; and Quartile category: Q3. The *WJSC*'s CiteScore for 2022 is 8.0 and Scopus CiteScore rank 2022: Histology is 9/57; Genetics is 68/325; Genetics (clinical) is 19/90; Molecular Biology is 119/380; Cell Biology is 95/274.

RESPONSIBLE EDITORS FOR THIS ISSUE

Production Editor: *Xiang-Di Zhang*; **Production Department Director:** *Xu Guo*; **Cover Editor:** *Jia-Ru Fan*.

NAME OF JOURNAL
World Journal of Stem Cells

ISSN
ISSN 1948-0210 (online)

LAUNCH DATE
December 31, 2009

FREQUENCY
Monthly

EDITORS-IN-CHIEF
Shengwen Calvin Li, Carlo Ventura

EDITORIAL BOARD MEMBERS
https://www.wjgnet.com/1948-0210/editorialboard.htm

PUBLICATION DATE
March 26, 2024

INSTRUCTIONS TO AUTHORS
https://www.wjgnet.com/bpg/gerinfo/204

GUIDELINES FOR ETHICS DOCUMENTS
https://www.wjgnet.com/bpg/GerInfo/287

GUIDELINES FOR NON-NATIVE SPEAKERS OF ENGLISH
https://www.wjgnet.com/bpg/gerinfo/240

PUBLICATION ETHICS
https://www.wjgnet.com/bpg/GerInfo/288

PUBLICATION MISCONDUCT
https://www.wjgnet.com/bpg/gerinfo/208

ARTICLE PROCESSING CHARGE
https://www.wjgnet.com/bpg/gerinfo/242

STEPS FOR SUBMITTING MANUSCRIPTS
https://www.wjgnet.com/bpg/GerInfo/239

ONLINE SUBMISSION
https://www.f6publishing.com

World Journal of Stem Cells

Submit a Manuscript: https://www.f6publishing.com

World J Stem Cells 2024 March 26; 16(3): 228-231

DOI: 10.4252/wjsc.v16.i3.228

ISSN 1948-0210 (online)

EDITORIAL

O-linked β-N-acetylglucosaminylation may be a key regulatory factor in promoting osteogenic differentiation of bone marrow mesenchymal stromal cells

Xu-Chang Zhou, Guo-Xin Ni

Specialty type: Cell and tissue engineering

Provenance and peer review: Invited article; Externally peer reviewed.

Peer-review model: Single blind

Peer-review report's scientific quality classification

Grade A (Excellent): 0
Grade B (Very good): 0
Grade C (Good): C
Grade D (Fair): 0
Grade E (Poor): 0

P-Reviewer: Naik D, India

Received: December 7, 2023
Peer-review started: December 7, 2023
First decision: January 29, 2024
Revised: February 2, 2024
Accepted: February 29, 2024
Article in press: February 29, 2024
Published online: March 26, 2024

Xu-Chang Zhou, School of Sport Medicine and Rehabilitation, Beijing Sport University, Beijing 100084, China

Guo-Xin Ni, Department of Rehabilitation Medicine, The First Affiliated Hospital of Xiamen University, Xiamen 361003, Fujian Province, China

Corresponding author: Guo-Xin Ni, Doctor, MD, PhD, Chief Doctor, Chief Physician, Professor, Department of Rehabilitation Medicine, The First Affiliated Hospital of Xiamen University, No. 55 Zhenhai Road, Siming District, Xiamen 361003, Fujian Province, China. nigx@xmu.edu.cn

Abstract

Cumulative evidence suggests that O-linked β-N-acetylglucosaminylation (O-GlcNAcylation) plays an important regulatory role in pathophysiological processes. Although the regulatory mechanisms of O-GlcNAcylation in tumors have been gradually elucidated, the potential mechanisms of O-GlcNAcylation in bone metabolism, particularly, in the osteogenic differentiation of bone marrow mesenchymal stromal cells (BMSCs) remains unexplored. In this study, the literature related to O-GlcNAcylation and BMSC osteogenic differentiation was reviewed, assuming that it could trigger more scholars to focus on research related to O-GlcNAcylation and bone metabolism and provide insights into the development of novel therapeutic targets for bone metabolism disorders such as osteoporosis.

Key Words: O-GlcNAcylation; Osteogenic differentiation; Bone marrow mesenchymal stromal cells; Osteoporosis

Core Tip: O-linked β-N-acetylglucosaminylation (O-GlcNAcylation), an important post-translational modification of proteins, widely involved in the regulation of biological processes such as signal transduction and proteasomal degradation, plays an essential role in the initiation and progression of various diseases such as bone metabolism. In this study, we emphasized that maintaining appropriate levels of O-GlcNAcylation is beneficial for the osteogenic differentiation of bone marrow mesenchymal stem cells (BMSCs). Insufficient or excessive levels of O-GlcNAcylation are detrimental to BMSC osteogenic differentiation.

Citation: Zhou XC, Ni GX. O-linked β-N-acetylglucosaminylation may be a key regulatory factor in promoting osteogenic differentiation of bone marrow mesenchymal stromal cells. *World J Stem Cells* 2024; 16(3): 228-231
URL: https://www.wjgnet.com/1948-0210/full/v16/i3/228.htm
DOI: https://dx.doi.org/10.4252/wjsc.v16.i3.228

INTRODUCTION

Bone marrow mesenchymal stromal cells (BMSCs), important precursors of osteoblastic lineage cells, are pluripotent stem cells with self-renewal, immunomodulatory, and multidifferentiation potentials[1]. As the major source of osteoblasts, BMSCs are important contributors to the bone tissue repair process. The abnormal osteogenic differentiation of BMSCs is an important cause of bone metabolism-related diseases, including osteoporosis[2,3]. O-linked β-N-acetylglucosaminylation (O-GlcNAcylation) is an important post-translational modification in which involves the attachment of a single O-linked N-acetylglucosamine (O-GlcNAc) moiety to Ser or Thr residues of cytoplasmic, nuclear, and mitochondrial proteins. O-GlcNAcylation can regulate fundamental cellular processes ranging from gene transcription and translation to protein localization, interaction, and degradation[4]. The donor for O-GlcNAcylation is a nucleoside sugar, such as uridine diphosphate GlcNAc (UDP-GlcNAc). UDP-GlcNAc, a key metabolite produced by the hexosamine biosynthetic pathway, is synthesized by consumption of uridine triphosphate, glucose, glutamine, and acetyl-CoA[5]. As a ubiquitous post-translational modification of proteins, O-GlcNAcylation is regulated by two conserved enzymes: O-GlcNAc transferase (OGT), which can add O-GlcNAc to proteins, and O-GlcNAc enzyme (OGA), which can remove O-GlcNAc from proteins. O-GlcNAcylation maintains optimal homeostatic balance through mutual regulation of OGT and OGA[4]. However, uncoupled OGT and OGA homeostasis have been shown to be associated with the pathogenesis of multiple human diseases, including bone metabolic diseases. Emerging evidence shows that O-GlcNAc modification is closely related to the osteogenic differentiation of BMSCs[6].

BMSCs have the potential to differentiate into osteoblasts, adipocytes, and chondrocytes[7,8]. A recent study showed that OGT knockout in mouse BMSCs inhibited bone formation while promoting bone marrow adipogenesis[9] , indicating that O-GlcNACylation may be a key regulatory factor affecting the differentiation fate of BMSCs. Runt-related transcription factor 2 (RUNX2) is a member of the polyomavirus enhancer-binding protein 2/core-binding factor superfamily[10,11]. The balance between osteogenesis and adipogenic differentiation in BMSC is coordinated regulated by transcription factors Runx2 and CCAAT/enhancer-binding protein beta (C/EBPβ) through O-GlcNAc post-translational modifications. The increased O-glycosylation of Runx2 is not only critical for osteogenic differentiation, but also promotes B lymphocytes by activating interleukin-7. Knockdown of OGT can activate the transcriptional activity of C/EBPβ to promote the adipogenic differentiation of BMSCs[12,13], and upregulate the expression of myelopoietic stem cell factor encoded by the Kitl gene, thereby increasing myopoiesis[14-17]. In addition, Kim *et al*[6] observed that elevated protein O-GlcNAc modification enhances the binding of Runx2 to Ose2 by promoting the transcriptional activity of Runx2 and inducing an increase in the expression of the osteoblast-specific marker osteocalcin (OCN)[18-21]. Another study reported that the osteogenic differentiation marker bone morphogenetic protein 2/7 reduced OGA activity[18]. During osteogenic differentiation process of BMSC, the overall level of O-GlcNACylation increases. Pharmacological inhibition of OGA promotes the expression of osteogenic differentiation makers, including alkaline phosphatase (ALP), OCN, and bone sialoprotein[6,18,22,23].

Hyperglycemia is reported to be closely related to bone formation inhibition and is a major factor in diabetic osteoporosis[24-27]. Previous studies have shown that high blood sugar levels increase the O-GlcNAcylation of proteins. Abnormal regulation of O-GlcNAcylation is closely associated with the pathogenesis of diabetes mellitus[28]. Therefore, hyperglycemia-induced excessive and abnormal O-GlcNAcylation may lead to reduced osteogenic differentiation and diabetic osteoporosis. Gu *et al*[29] demonstrated that excessive O-GlcNAcylation induced by high glucose, glucosamine, or GlcNAc treatment or OGT overexpression can reduce the expression levels of osteoblast markers, such as ALP, type I collagen, OCN, Runx2, and osterix, thereby inhibiting osteogenic differentiation. These results are consistent with the phenotypic reduction in bone formation observed in patients with type 2 diabetes. However, other studies have shown that the upregulation of O-GlcNAcylation through supplementation with OGA inhibitors promotes osteogenic differentiation and increases Runx2 transcriptional activity and matrix mineralization[6,18]. One explanation for aforementioned difference is that the effects of metabolic treatment (high concentration glucose treatment) and drug treatment (OGA inhibitors) may be different. Pharmacological inhibition of OGA increases the O-GlcNAcylation level by breaking the dynamic on/off cycle, whereas metabolic treatment or OGT overexpression increases the O-GlcNAcylation level by shifting the balance toward modification[30].

CONCLUSION

The osteogenic differentiation of BMSCs requires a moderate increase of O-GlcNAcylation, and an excessive increase in overall O-GlcNAcylation may inhibit the osteogenic differentiation of BMSCS. Therefore, the overall O-GlcNAcylation level should be maintained within an optimal range to protect normal cellular functions. The precise regulation of O-GlcNAcylation may be an effective strategy for promoting the osteogenic differentiation of BMSCs, correcting abnormal bone metabolism, and preventing bone-related diseases. Further elucidation of the potential regulatory mechanism between O-GlcNAcylation and the osteogenic differentiation of BMSCs will help to better understand the pathogenesis of bone metabolic diseases and provide novel ideas for the treatment and prevention of bone metabolic diseases.

FOOTNOTES

Author contributions: Zhou XC and Ni GX designed and coordinated the study; Zhou XC wrote the manuscript; and all authors approved the final version of the article.

Conflict-of-interest statement: All the authors report no relevant conflicts of interest for this article.

Country/Territory of origin: China

ORCID number: Xu-Chang Zhou 0000-0003-1390-7659; Guo-Xin Ni 0000-0001-9181-8155.

S-Editor: Wang JJ
L-Editor: A
P-Editor: Yuan YY

REFERENCES

1 **Zhang X**, Cao D, Xu L, Xu Y, Gao Z, Pan Y, Jiang M, Wei Y, Wang L, Liao Y, Wang Q, Yang L, Xu X, Gao Y, Gao S, Wang J, Yue R. Harnessing matrix stiffness to engineer a bone marrow niche for hematopoietic stem cell rejuvenation. *Cell Stem Cell* 2023; **30**: 378-395.e8 [PMID: 37028404 DOI: 10.1016/j.stem.2023.03.005]

2 **Jensen PR**, Andersen TL, Chavassieux P, Roux JP, Delaisse JM. Bisphosphonates impair the onset of bone formation at remodeling sites. *Bone* 2021; **145**: 115850 [PMID: 33465485 DOI: 10.1016/j.bone.2021.115850]

3 **Zhang Y**, Ma L, Lu E, Huang W. Atorvastatin Upregulates microRNA-186 and Inhibits the TLR4-Mediated MAPKs/NF-κB Pathway to Relieve Steroid-Induced Avascular Necrosis of the Femoral Head. *Front Pharmacol* 2021; **12**: 583975 [PMID: 33995003 DOI: 10.3389/fphar.2021.583975]

4 **Yang Y**, Yan Y, Yin J, Tang N, Wang K, Huang L, Hu J, Feng Z, Gao Q, Huang A. O-GlcNAcylation of YTHDF2 promotes HBV-related hepatocellular carcinoma progression in an N(6)-methyladenosine-dependent manner. *Signal Transduct Target Ther* 2023; **8**: 63 [PMID: 36765030 DOI: 10.1038/s41392-023-01316-8]

5 **Paneque A**, Fortus H, Zheng J, Werlen G, Jacinto E. The Hexosamine Biosynthesis Pathway: Regulation and Function. *Genes (Basel)* 2023; **14** [PMID: 37107691 DOI: 10.3390/genes14040933]

6 **Kim SH**, Kim YH, Song M, An SH, Byun HY, Heo K, Lim S, Oh YS, Ryu SH, Suh PG. O-GlcNAc modification modulates the expression of osteocalcin *via* OSE2 and Runx2. *Biochem Biophys Res Commun* 2007; **362**: 325-329 [PMID: 17707335 DOI: 10.1016/j.bbrc.2007.07.149]

7 **Huang M**, Xu S, Liu L, Zhang M, Guo J, Yuan Y, Xu J, Chen X, Zou J. m6A Methylation Regulates Osteoblastic Differentiation and Bone Remodeling. *Front Cell Dev Biol* 2021; **9**: 783322 [PMID: 34993198 DOI: 10.3389/fcell.2021.783322]

8 **Uzieliene I**, Bernotiene E, Rakauskiene G, Denkovskij J, Bagdonas E, Mackiewicz Z, Porvaneckas N, Kvederas G, Mobasheri A. The Antihypertensive Drug Nifedipine Modulates the Metabolism of Chondrocytes and Human Bone Marrow-Derived Mesenchymal Stem Cells. *Front Endocrinol (Lausanne)* 2019; **10**: 756 [PMID: 31781032 DOI: 10.3389/fendo.2019.00756]

9 **Zhang Z**, Huang Z, Awad M, Elsalanty M, Cray J, Ball LE, Maynard JC, Burlingame AL, Zeng H, Mansky KC, Ruan HB. O-GlcNAc glycosylation orchestrates fate decision and niche function of bone marrow stromal progenitors. *Elife* 2023; **12** [PMID: 36861967 DOI: 10.7554/eLife.85464]

10 **Kim WJ**, Shin HL, Kim BS, Kim HJ, Ryoo HM. RUNX2-modifying enzymes: therapeutic targets for bone diseases. *Exp Mol Med* 2020; **52**: 1178-1184 [PMID: 32788656 DOI: 10.1038/s12276-020-0471-4]

11 **Chen Y**, Zhao X, Wu H. Transcriptional Programming in Arteriosclerotic Disease: A Multifaceted Function of the Runx2 (Runt-Related Transcription Factor 2). *Arterioscler Thromb Vasc Biol* 2021; **41**: 20-34 [PMID: 33115268 DOI: 10.1161/ATVBAHA.120.313791]

12 **Qian K**, Wang S, Fu M, Zhou J, Singh JP, Li MD, Yang Y, Zhang K, Wu J, Nie Y, Ruan HB, Yang X. Transcriptional regulation of O-GlcNAc homeostasis is disrupted in pancreatic cancer. *J Biol Chem* 2018; **293**: 13989-14000 [PMID: 30037904 DOI: 10.1074/jbc.RA118.004709]

13 **Li X**, Molina H, Huang H, Zhang YY, Liu M, Qian SW, Slawson C, Dias WB, Pandey A, Hart GW, Lane MD, Tang QQ. O-linked N-acetylglucosamine modification on CCAAT enhancer-binding protein beta: role during adipocyte differentiation. *J Biol Chem* 2009; **284**:

19248-19254 [PMID: 19478079 DOI: 10.1074/jbc.M109.005678]

14 **Zhang Z**, Huang Z, Ong B, Sahu C, Zeng H, Ruan HB. Bone marrow adipose tissue-derived stem cell factor mediates metabolic regulation of hematopoiesis. *Haematologica* 2019; **104**: 1731-1743 [PMID: 30792196 DOI: 10.3324/haematol.2018.205856]

15 **Fistonich C**, Zehentmeier S, Bednarski JJ, Miao R, Schjerven H, Sleckman BP, Pereira JP. Cell circuits between B cell progenitors and IL-7(+) mesenchymal progenitor cells control B cell development. *J Exp Med* 2018; **215**: 2586-2599 [PMID: 30158115 DOI: 10.1084/jem.20180778]

16 **Asada N**, Kunisaki Y, Pierce H, Wang Z, Fernandez NF, Birbrair A, Ma'ayan A, Frenette PS. Differential cytokine contributions of perivascular haematopoietic stem cell niches. *Nat Cell Biol* 2017; **19**: 214-223 [PMID: 28218906 DOI: 10.1038/ncb3475]

17 **Cordeiro Gomes A**, Hara T, Lim VY, Herndler-Brandstetter D, Nevius E, Sugiyama T, Tani-Ichi S, Schlenner S, Richie E, Rodewald HR, Flavell RA, Nagasawa T, Ikuta K, Pereira JP. Hematopoietic Stem Cell Niches Produce Lineage-Instructive Signals to Control Multipotent Progenitor Differentiation. *Immunity* 2016; **45**: 1219-1231 [PMID: 27913094 DOI: 10.1016/j.immuni.2016.11.004]

18 **Nagel AK**, Ball LE. O-GlcNAc modification of the runt-related transcription factor 2 (Runx2) links osteogenesis and nutrient metabolism in bone marrow mesenchymal stem cells. *Mol Cell Proteomics* 2014; **13**: 3381-3395 [PMID: 25187572 DOI: 10.1074/mcp.M114.040691]

19 **Sun C**, Lan W, Li B, Zuo R, Xing H, Liu M, Li J, Yao Y, Wu J, Tang Y, Liu H, Zhou Y. Glucose regulates tissue-specific chondro-osteogenic differentiation of human cartilage endplate stem cells *via* O-GlcNAcylation of Sox9 and Runx2. *Stem Cell Res Ther* 2019; **10**: 357 [PMID: 31779679 DOI: 10.1186/s13287-019-1440-5]

20 **Komori T**. Mechanism of transcriptional regulation by Runx2 in osteoblasts. *Clin Calcium* 2006; **16**: 801-807 [PMID: 16679622]

21 **Shui C**, Spelsberg TC, Riggs BL, Khosla S. Changes in Runx2/Cbfa1 expression and activity during osteoblastic differentiation of human bone marrow stromal cells. *J Bone Miner Res* 2003; **18**: 213-221 [PMID: 12568398 DOI: 10.1359/jbmr.2003.18.2.213]

22 **Koyama T**, Kamemura K. Global increase in O-linked N-acetylglucosamine modification promotes osteoblast differentiation. *Exp Cell Res* 2015; **338**: 194-202 [PMID: 26302267 DOI: 10.1016/j.yexcr.2015.08.009]

23 **Weng Y**, Wang Z, Fukuhara Y, Tanai A, Ikegame M, Yamada D, Takarada T, Izawa T, Hayano S, Yoshida K, Kamioka H, Okamura H. O-GlcNAcylation drives calcium signaling toward osteoblast differentiation: A bioinformatics-oriented study. *Biofactors* 2021; **47**: 992-1015 [PMID: 34418170 DOI: 10.1002/biof.1774]

24 **Botolin S**, McCabe LR. Chronic hyperglycemia modulates osteoblast gene expression through osmotic and non-osmotic pathways. *J Cell Biochem* 2006; **99**: 411-424 [PMID: 16619259 DOI: 10.1002/jcb.20842]

25 **Schwartz AV**. Diabetes Mellitus: Does it Affect Bone? *Calcif Tissue Int* 2003; **73**: 515-519 [PMID: 14517715 DOI: 10.1007/s00223-003-0023-7]

26 **Strotmeyer ES**, Cauley JA, Orchard TJ, Steenkiste AR, Dorman JS. Middle-aged premenopausal women with type 1 diabetes have lower bone mineral density and calcaneal quantitative ultrasound than nondiabetic women. *Diabetes Care* 2006; **29**: 306-311 [PMID: 16443878 DOI: 10.2337/diacare.29.02.06.dc05-1353]

27 **Botolin S**, McCabe LR. Bone loss and increased bone adiposity in spontaneous and pharmacologically induced diabetic mice. *Endocrinology* 2007; **148**: 198-205 [PMID: 17053023 DOI: 10.1210/en.2006-1006]

28 **Bolanle IO**, Palmer TM. Targeting Protein O-GlcNAcylation, a Link between Type 2 Diabetes Mellitus and Inflammatory Disease. *Cells* 2022; **11** [PMID: 35203353 DOI: 10.3390/cells11040705]

29 **Gu H**, Song M, Boonanantanasarn K, Baek K, Woo KM, Ryoo HM, Baek JH. Conditions Inducing Excessive O-GlcNAcylation Inhibit BMP2-Induced Osteogenic Differentiation of C2C12 Cells. *Int J Mol Sci* 2018; **19** [PMID: 29315243 DOI: 10.3390/ijms19010202]

30 **Vaidyanathan K**, Wells L. Multiple tissue-specific roles for the O-GlcNAc post-translational modification in the induction of and complications arising from type II diabetes. *J Biol Chem* 2014; **289**: 34466-34471 [PMID: 25336652 DOI: 10.1074/jbc.R114.591560]

World Journal of Stem Cells

Submit a Manuscript: https://www.f6publishing.com

World J Stem Cells 2024 March 26; 16(3): 232-236

DOI: 10.4252/wjsc.v16.i3.232

ISSN 1948-0210 (online)

EDITORIAL

Understanding host-graft crosstalk for predicting the outcome of stem cell transplantation

Luminita Labusca, Florin Zugun-Eloae

Specialty type: Cell and tissue engineering

Provenance and peer review: Invited article; Externally peer reviewed.

Peer-review model: Single blind

Peer-review report's scientific quality classification

Grade A (Excellent): 0
Grade B (Very good): B
Grade C (Good): C
Grade D (Fair): 0
Grade E (Poor): 0

P-Reviewer: Li K, China; Wang Z, China

Received: December 22, 2023
Peer-review started: December 22, 2023
First decision: January 11, 2024
Revised: January 14, 2024
Accepted: February 18, 2024
Article in press: February 18, 2024
Published online: March 26, 2024

Luminita Labusca, Magnetic Materials and Sensors, National Institute of Research and Development for Technical Physics, Iasi 700050, Romania

Luminita Labusca, Orthopedics and Trauma, Emergency County Hospital Saint Spiridon, Iasi 700000, Romania

Florin Zugun-Eloae, Transcend, Regional Oncology Institute, Iasi 7000000, Romania

Corresponding author: Luminita Labusca, MD, PhD, Senior Scientist, Magnetic Materials and Sensors, National Institute of Research and Development for Technical Physics, Boulevard Dimitrie Mangeron 47, Iasi 700050, Romania. drlluminita@yahoo.com

Abstract

Mesenchymal stromal cells (MSCs) hold great promise for tissue regeneration in debilitating disorders. Despite reported improvements, the short-term outcomes of MSC transplantation, which is possibly linked to poor cell survival, demand extensive investigation. Disease-associated stress microenvironments further complicate outcomes. This debate underscores the need for a deeper understanding of the phenotypes of transplanted MSCs and their environment-induced fluctuations. Additionally, questions arise about how to predict, track, and comprehend cell fate post-transplantation. *In vivo* cellular imaging has emerged as a critical requirement for both short- and long-term safety and efficacy studies. However, translating preclinical imaging methods to clinical settings remains challenging. The fate and function of transplanted cells within the host environment present intricate challenges, including MSC engraftment, variability, and inconsistencies between preclinical and clinical data. The study explored the impact of high glucose concentrations on MSC survival in diabetic environments, emphasizing mitochondrial factors. Preserving these factors may enhance MSC survival, suggesting potential strategies involving genetic modification, biomaterials, and nanoparticles. Understanding stressors in diabetic patients is crucial for predicting the effects of MSC-based therapies. These multifaceted challenges call for a holistic approach involving the incorporation of large-scale data, computational disease modeling, and possibly artificial intelligence to enable deterministic insights.

Key Words: Mesenchymal stem cells; Phenotype; Transplantation; Host; Microenvironment; Cellular imaging; Diabetes mellitus

Core Tip: Deterministic methods for modeling stem cell–host interactions are needed to ensure the safety and efficacy of stem cell-based therapies. This requires an in-depth understanding of the mechanism of action of the transplanted cells for each and every host condition(s) and asks for the establishment of adequate methods to predict, follow-up and determine the safety profile of the respective therapies.

Citation: Labusca L, Zugun-Eloae F. Understanding host-graft crosstalk for predicting the outcome of stem cell transplantation. *World J Stem Cells* 2024; 16(3): 232-236
URL: https://www.wjgnet.com/1948-0210/full/v16/i3/232.htm
DOI: https://dx.doi.org/10.4252/wjsc.v16.i3.232

INTRODUCTION

Mesenchymal stromal cells (MSCs) continue to be the most explored type of stem cell because of their regenerative impact on restoring organ and tissue structure and function. Such cell-based therapies are tested within various regenerative approaches in the hope of enabling the treatment of disabling diseases[1]. However, the consistent improvement in disease-associated biomarkers reported after MSC transplantation proved to be short-lived. This transitory effect could be related to a poor cell survival rate, which requires extensive investigation[2]. The disease environment is characterized by the presence of numerous stressors that include but are not limited to hypoxia, inflammation, and metabolic imbalances that can impact the duration and efficiency of MSC transplantation. To further complicate this matter, disease association and side effects of concurrent therapies result in an extremely complex and intricate situation for a specific individual or group of individuals potential recipients of MSC therapies. It has been proposed that in the context of cell therapies, host microenvironmental modulators can be used as therapeutics. This requires a deep understanding of the mechanism of action of the transplanted cells for specific host condition(s) and asks for the establishment of adequate, probably multi-biomarker panels to predict, follow-up and determine the safety profile of the respective therapies[3].

This largely open debate invites several considerations with respect to MSCs (and probably other stem cell types). therapies at large. What is known about the phenotype of transplanted MSCs, and what do they represent from an informational and physiological perspective?

The question of whether cultured expanded MSCs faithfully reflect any stage of natural *in vivo* MSCs or whether cells are present akin to developmental stages is prominent. It is essential to note the intricate embryological development of mesenchymal tissues that have double embryological origins within trunk and head mesenchymal lineages (neural crest-derived), with these origins intricately intertwined, particularly in tissues such as the myocardium or head and neck, including sensory organs[4]. In the natural context of a developing organism, cellular differentiation appears deterministic, allowing predictions about the fate of similar cells in subsequent generations even in unrelated species. However, embryological studies reveal that cells from one presumptive tissue, when implanted into another tissue, can assume a different fate[5]. The local regulation of their destiny by the new environment underscores the selective rather than directive development of implanted cells, a characteristic inherent to MSCs. The development of human mesenchymal tissues involves a sequence of precisely coordinated series of time-dependent events distinct from the tissue repair mechanisms observed in adults 15-80 years later[6]. A classic example of such a mismatch is the long-tested and highly argued approach in which MSCs from various sources are used for regeneration or tissue engineering of articular cartilage. Chondrogenic primed adult tissue-derived MSCs notoriously undergo hypertrophic ossification since endochondral bone repair appears to be the "default" function after organism maturation. Manipulation of the Wnt/β-catenin pathway or pulsed exposure to parathyroid hormone related protein, which are reportedly used to suppress or delay hypertrophic differentiation[7], involves the use of several attached strings. Challenges in describing the timing and duration of such pharmacological intervention are not negligible, while adding steps in cell manipulation complicates both prospective cell therapy manufacturing and regulatory approval altogether. Although insights from early development may offer insight into utilizing cultured MSCs for repairing and regenerating adult tissues, the precise underlying mechanisms remain unknown.

Another question refers to the ability to predict, track and monitor cell fate after transplantation. From a regulatory perspective, the ability to fully comprehend cell fate after delivery is vital for understanding safety and efficiency. Translation from animal models to clinical studies often requires an upgraded set of tests in an attempt to describe parameters such as biodistribution, cell survival or engraftment after transplantation[8]. Preclinical studies rely on data gathered through invasive sample collection for safety studies. Such assessments commonly utilize polymerase chain reaction or immunohistochemistry as standards for good laboratory practice to detect cell-specific markers *in vivo*. This approach involves the termination of *in vivo* experiments to enable sample collection. Time-series results and long-term follow-up require a substantial number of animals and are obviously impractical for clinical studies. Consequently, there is a critical demand for *in vivo* cellular imaging that facilitates both short- and long-term pharmacological studies, as well as monitoring of therapeutic response. Cellular imaging has become necessary in the context of short- and long-term

safety and efficacy of cell therapies. However, translation of imaging methods from preclinical studies is challenging. Clinically available imaging methods, such as computer tomography, single-photon emission spectroscopy computer tomography, and magnetic resonance imaging, need to be used to balance sensitivity, specificity, resolution and the need for cell labeling. Radiolabeling, positron-emitting isotopes and nanomagnetic tracers are intensely tested alone or in combination to enable imaging at the cellular level. Cell trackers themselves can modify both transplanted cells and the host environment, introducing another set of variables that need to be taken into account when predicting the behavior of the two intertwining systems. Notably, to date, no relevant modality for noninvasively imaging the viability of transplanted cells has made its way to clinical settings despite several smart solutions being proposed experimentally.

However, the most difficult question may be whether the fate and function of the transplanted cell population are predicted within the context of the host environment. In addition to the much-investigated issue of cell engraftment and direct involvement in tissue regeneration *vs* the so-called "trophic" role that MSCs are supposed to play in the quality of small molecules releasing "medicinal cells"[9], other crucial points require careful consideration. Specifically, molecular-level descriptions of therapeutic cell mechanisms of action, donor- and tissue-type-dependent MSC variability, consistent differences between preclinical data and existing results from available clinical trials are the only major challenges to be addressed. In addition, predicting the content of MSC-released cytokines "black box" and their environment-induced licensing after transplantation are still unresolved problems[3].

A significant challenge for stem cell therapy is cell survival and maintenance of the phenotype after transplantation. The harsh microenvironment of the host commonly includes ischemia, inflammation, oxidative stress, and mechanical stress, which contribute to important cell loss and to the release of proinflammatory cytokines, potentially increasing local damage[10].

The multifaceted aspects of these challenges point toward the necessity of approaching them by means of a holistic view where large amounts of data, computational disease modeling and perhaps the use of artificial intelligence could offer valuable insights. Several possible developments in this context consist of data-driven optimization of cell delivery. Thus, a large amount of data analysis can inform the optimization of cell delivery methods to increase the survival of transplanted stem cells in hostile microenvironments[11]. With respect to the existing knowledge regarding the use of biomaterial-based nanocarrier systems, tailored methods for cell delivery to fit a specific clinical situation (such as intraarticular or intracardiac), cell preconditioning or cell engineering can be used to inform decision-making regarding pharmacological aspects of cell transplantation for a given clinical need.

MSCs can display a bidirectional immune modulatory effect, as shown by numerous *in vivo* studies and clinical trials. MSCs are actually used to modulate the hyperactive immune response in coronavirus disease 2019 or graft-*versus*-host disease patients[12]. MSCs act through secretomes and exosomes *via* paracrine effects, promoting the production of regulatory T cells and preventing the infiltration of proinflammatory cytokines such as tumor necrosis factor-α and interleukin-6[13].

Cell engineering strategies can be used to mitigate the immune response in the context of cell therapy. Genome editing strategies and immune checkpoint inhibitors, such as programmed cell death ligand 1, CD47, and human leukocyte antigen-G, are being explored to mitigate immune rejection caused by various cellular components of the immune system, either in the presence or absence of human leukocyte antigen, particularly in human induced pluripotent stem cells and progenitor-based therapies[14].

Despite the progress made in developing strategies to mitigate immune responses in patients receiving stem cell therapies, these approaches still have limitations. One of the main challenges is that none of the current treatment modalities are successful at abolishing the immune response in a manner that does not influence transplanted cell viability or therapeutic efficacy[15]. The human immune system is extremely accurate at identifying non-self cells, which poses a significant risk of antigraft immune responses resulting from allogeneic MSC sources. Another limitation is that the refinement of stem cell culture protocols, including cell engineering strategies to increase the "therapeutic phenotype", may increase the immunogenicity of the transplanted cells.

AI and large-scale data analysis could be used to identify methods for cell preconditioning as well as genetic engineering techniques that increase the survival and viability of transplanted stem cells, offering new possibilities for improving engraftment and functionality. A holistic view, informed by large amounts of data and computational modeling, can aid in understanding the complex interplay of factors affecting the survival and functionality of transplanted stem cells, leading to more effective therapeutic strategies.

Using artificial intelligence in stem cell research introduces a new set of challenges mostly related to ethical considerations, policy implications, and intellectual property, demanding a risk-based approach to balance the potential benefits and risks. Abu-El-Rub *et al*[16] discussed one important aspect of MSC transplantation within the survival-challenging environment of diabetes mellitus (DM) patients. MSC transplantation has been proposed as a potential treatment for type I and II DM mainly due to its immunosuppressive properties and anti-inflammatory effects. The authors present evidence that high glucose concentrations adversely affect MSC survival by disrupting mitochondrial regulatory factors, leading to apoptosis. These findings advance the idea that understanding and preserving factors such as the mitochondrial membrane potential, the NAD+/NADH pool, and the mechanistic target of rapamycin protein may enhance MSC survival in diabetic microenvironments. Future strategies could involve genetic modification, biomaterials, and nanoparticles aimed at overcoming poor MSC survival under high-glucose conditions. Additionally, studying the impact of other stressors in DM patients is crucial in the attempt to predict the effect of potential MSC-based therapies. The role of frequent fluctuations in glucose levels in DM patients, systemic inflammation and the possible uremic milieu still need to be considered.

CONCLUSION

The incoming field of MSC-based cellular therapies faces multifaceted challenges, including poor cell survival rates, complex host microenvironments, and immune responses. Addressing these challenges requires a holistic approach informed by large amounts of data, computational modeling, and possibly the use of artificial intelligence. Future strategies could involve genetic modification, biomaterials, and nanoparticles aimed at overcoming poor MSC survival in specific microenvironments, such as those found in diabetic patients. Awaiting the true potential of cell-based therapies to unfold, the need for comprehensive and multidisciplinary approaches to overcome these obstacles and to advance the field toward more effective and safer clinical applications appears to be more imperative.

FOOTNOTES

Author contributions: Labusca L and Zugun-Eloae F contributed to this paper, and the writing and editing of the manuscript; Labusca L designed the overall concept and outline of the manuscript; Zugun-Eloae F contributed to the discussion and design of the manuscript.

Supported by the Romanian Ministry of Research, Innovation and Digitization, CNCS/CCCDI-UEFISCDI, project number ERANET-EURONANOMED-3-OASIs, within PNCDI III (contract number 273/2022).

Conflict-of-interest statement: All the authors report no relevant conflicts of interest for this article.

Country/Territory of origin: Romania

ORCID number: Luminita Labusca 0000-0001-9635-6893.

S-Editor: Wang JJ
L-Editor: A
P-Editor: Zhang XD

REFERENCES

1 **Ebrahimi A**, Ahmadi H, Pourfraidon Ghasrodashti Z, Tanide N, Shahriarirad R, Erfani A, Ranjbar K, Ashkani-Esfahani S. Therapeutic effects of stem cells in different body systems, a novel method that is yet to gain trust: A comprehensive review. *Bosn J Basic Med Sci* 2021; **21**: 672-701 [PMID: 34255619 DOI: 10.17305/bjbms.2021.5508]
2 **Brianna**, Ling APK, Wong YP. Applying stem cell therapy in intractable diseases: a narrative review of decades of progress and challenges. *Stem Cell Investig* 2022; **9**: 4 [PMID: 36238449 DOI: 10.21037/sci-2022-021]
3 **Krampera M**, Le Blanc K. Mesenchymal stromal cells: Putative microenvironmental modulators become cell therapy. *Cell Stem Cell* 2021; **28**: 1708-1725 [PMID: 34624232 DOI: 10.1016/j.stem.2021.09.006]
4 **Cumpata AJ**, Labusca L, Radulescu LM. Stem Cell-Based Therapies for Auditory Hair Cell Regeneration in the Treatment of Hearing Loss. *Tissue Eng Part B Rev* 2023 [PMID: 37440318 DOI: 10.1089/ten.TEB.2023.0084]
5 **Sheng G**. The developmental basis of mesenchymal stem/stromal cells (MSCs). *BMC Dev Biol* 2015; **15**: 44 [DOI: 10.1186/s12861-015-0094-5]
6 **Pittenger MF**, Discher DE, Péault BM, Phinney DG, Hare JM, Caplan AI. Mesenchymal stem cell perspective: cell biology to clinical progress. *NPJ Regen Med* 2019; **4**: 22 [PMID: 31815001 DOI: 10.1038/s41536-019-0083-6]
7 **Fischer J**, Aulmann A, Dexheimer V, Grossner T, Richter W. Intermittent PTHrP(1-34) exposure augments chondrogenesis and reduces hypertrophy of mesenchymal stromal cells. *Stem Cells Dev* 2014; **23**: 2513-2523 [PMID: 24836507 DOI: 10.1089/scd.2014.0101]
8 **Helfer BM**, Ponomarev V, Patrick PS, Blower PJ, Feitel A, Fruhwirth GO, Jackman S, Pereira Mouriès L, Park MVDZ, Srinivas M, Stuckey DJ, Thu MS, van den Hoorn T, Herberts CA, Shingleton WD. Options for imaging cellular therapeutics in vivo: a multi-stakeholder perspective. *Cytotherapy* 2021; **23**: 757-773 [PMID: 33832818 DOI: 10.1016/j.jcyt.2021.02.005]
9 **Caplan AI**. Mesenchymal Stem Cells: Time to Change the Name! *Stem Cells Transl Med* 2017; **6**: 1445-1451 [PMID: 28452204 DOI: 10.1002/sctm.17-0051]
10 **Li X**, Huang M, Zhao R, Zhao C, Liu Y, Zou H, Chen L, Guan Y, Zhang YA. Intravenously Delivered Allogeneic Mesenchymal Stem Cells Bidirectionally Regulate Inflammation and Induce Neurotrophic Effects in Distal Middle Cerebral Artery Occlusion Rats Within the First 7 Days After Stroke. *Cell Physiol Biochem* 2018; **46**: 1951-1970 [PMID: 29719282 DOI: 10.1159/000489384]
11 **Abubakar M**, Masood MF, Javed I, Adil H, Faraz MA, Bhat RR, Fatima M, Abdelkhalek AM, Buccilli B, Raza S, Hajjaj M. Unlocking the Mysteries, Bridging the Gap, and Unveiling the Multifaceted Potential of Stem Cell Therapy for Cardiac Tissue Regeneration: A Narrative Review of Current Literature, Ethical Challenges, and Future Perspectives. *Cureus* 2023; **15**: e41533 [PMID: 37551212 DOI: 10.7759/cureus.41533]
12 **Morata-Tarifa C**, Macías-Sánchez MDM, Gutiérrez-Pizarraya A, Sanchez-Pernaute R. Mesenchymal stromal cells for the prophylaxis and treatment of graft-versus-host disease-a meta-analysis. *Stem Cell Res Ther* 2020; **11**: 64 [PMID: 32070420 DOI: 10.1186/s13287-020-01592-z]

13 **Manoharan R**, Kore RA, Mehta JL. Mesenchymal stem cell treatment for hyperactive immune response in patients with COVID-19. *Immunotherapy* 2022; **14**: 1055-1065 [PMID: 35855633 DOI: 10.2217/imt-2021-0245]

14 **Meissner TB**, Schulze HS, Dale SM. Immune Editing: Overcoming Immune Barriers in Stem Cell Transplantation. *Curr Stem Cell Rep* 2022; **8**: 206-218 [PMID: 36406259 DOI: 10.1007/s40778-022-00221-0]

15 **Petrus-Reurer S**, Romano M, Howlett S, Jones JL, Lombardi G, Saeb-Parsy K. Immunological considerations and challenges for regenerative cellular therapies. *Commun Biol* 2021; **4**: 798 [PMID: 34172826 DOI: 10.1038/s42003-021-02237-4]

16 **Abu-El-Rub E**, Almahasneh F, Khasawneh RR, Alzu'bi A, Ghorab D, Almazari R, Magableh H, Sanajleh A, Shlool H, Mazari M, Bader NS, Al-Momani J. Human mesenchymal stem cells exhibit altered mitochondrial dynamics and poor survival in high glucose microenvironment. *World J Stem Cells* 2023; **15**: 1093-1103 [PMID: 38179215 DOI: 10.4252/wjsc.v15.i12.1093]

World Journal of Stem Cells

Submit a Manuscript: https://www.f6publishing.com

World J Stem Cells 2024 March 26; 16(3): 237-244

DOI: 10.4252/wjsc.v16.i3.237

ISSN 1948-0210 (online)

EDITORIAL

High glucose microenvironment and human mesenchymal stem cell behavior

Muhammad Abdul Mateen, Nouralsalhin Alaagib, Khawaja Husnain Haider

Specialty type: Cell and tissue engineering

Provenance and peer review: Invited article; Externally peer reviewed.

Peer-review model: Single blind

Peer-review report's scientific quality classification

Grade A (Excellent): 0
Grade B (Very good): B
Grade C (Good): C
Grade D (Fair): 0
Grade E (Poor): 0

P-Reviewer: Wang L, China; Zhou X, China

Received: December 25, 2023
Peer-review started: December 25, 2023
First decision: January 11, 2024
Revised: January 11, 2024
Accepted: January 29, 2024
Article in press: January 29, 2024
Published online: March 26, 2024

Muhammad Abdul Mateen, Nouralsalhin Alaagib, Basic Sciences, Sulaiman AlRajhi University, AlQaseem 52736, Saudi Arabia

Khawaja Husnain Haider, Cellular and Molecular Pharmacology, Sulaiman AlRajhi Medical School, Al Bukairiyah 51941, Saudi Arabia

Corresponding author: Khawaja Husnain Haider, BPharm, BSc, PhD, Chairman, Full Professor, Professor, Cellular and Molecular Pharmacology, Sulaiman AlRajhi Medical School, PO Box 777, Al Bukairiyah 51941, Saudi Arabia. kh.haider@sr.edu.sa

Abstract

High glucose (HG) culture conditions *in vitro* and persistent exposure to hyperglycemia in diabetes patients are detrimental to stem cells, analogous to any other cell type in our body. It interferes with diverse signaling pathways, *i.e.* mammalian target of rapamycin (mTOR)-phosphoinositide 3-kinase (PI3K)-Akt signaling, to impact physiological cellular functions, leading to low cell survival and higher cell apoptosis rates. While elucidating the underlying mechanism responsible for the apoptosis of adipose tissue-derived mesenchymal stem cells (MSCs), a recent study has shown that HG culture conditions dysregulate mTOR-PI3K-Akt signaling in addition to mitochondrial malfunctioning due to defective mitochondrial membrane potential (MtMP) that lowers ATP production. This organelle-level dysfunction energy-starves the cells and increases oxidative stress and ultrastructural abnormalities. Disruption of the mitochondrial electron transport chain produces an altered mitochondrial NAD+/NADH redox state as evidenced by a low NAD+/NADH ratio that primarily contributes to the reduced cell survival in HG. Some previous studies have also reported altered mitochondrial membrane polarity (causing hyperpolarization) and reduced mitochondrial cell mass, leading to perturbed mitochondrial homeostasis. The hostile microenvironment created by HG exposure creates structural and functional changes in the mitochondria, altering their bioenergetics and reducing their capacity to produce ATP. These are significant data, as MSCs are extensively studied for tissue regeneration and restoring their normal functioning in cell-based therapy. Therefore, MSCs from hyperglycemic donors should be cautiously used in clinical settings for cell-based therapy due to concerns of their poor sur-vival rates and increased rates of post engraftment proliferation. As hypergly-cemia alters the bioenergetics of donor MSCs, rectifying the loss of MtMP may be an excellent target for future research to restore the normal functioning of MSCs in hyperglycemic patients.

Key Words: Adipose tissue; Apoptosis; Bioenergetics; Cell survival; Cell therapy; Hyperglycemia; Mitochondria; Mesenchymal stem cells; Stem cells

Core Tip: High glucose (HG) conditions, seen *in vitro* as well as in diabetic patients, adversely affect stem cells by disrupting mammalian target of rapamycin-phosphoinositide 3-kinase-Akt signaling, resulting in reduced cell survival and increased apoptosis. A recent study of adipose tissue-derived mesenchymal stem cells (MSCs) found dysregulation of this signaling pathway and defective mitochondrial membrane potential (MtMP) under HG conditions. This leads to decreased ATP production, heightened oxidative stress, and structural abnormalities, causing diminished cell survival. Altered mitochondrial NAD+/NADH redox state and disrupted mitochondrial homeostasis worsen the hostile microenvironment induced by HG exposure. These findings are a note of caution for using MSCs from hyperglycemic donors in cell-based therapy owing to their poor survival and proliferation rates. Future research targeting MtMP restoration may enhance the therapeutic efficacy of MSCs in hyperglycemic patients.

Citation: Mateen MA, Alaagib N, Haider KH. High glucose microenvironment and human mesenchymal stem cell behavior. *World J Stem Cells* 2024; 16(3): 237-244
URL: https://www.wjgnet.com/1948-0210/full/v16/i3/237.htm
DOI: https://dx.doi.org/10.4252/wjsc.v16.i3.237

INTRODUCTION

Chronic exposure to a high glucose (HG) microenvironment *in vitro* and *in vivo* is detrimental to cells and has physiological and pathological consequences (Figure 1). At the cellular level, the damaging effects of HG exposure for a prolonged period can cause glucose cytotoxicity that invariably affects every body cell, encompassing red blood cells to stem cells[1-3].

Insulin resistance, pancreatic beta cell damage, and decreased insulin production lead to hyperglycemia that drastically affects the whole body at the organ and cellular levels. An uncontrolled hyperglycemic state leads to chronic systemic inflammation that brings about morphological and functional changes in the body cells, including stem cells[4]. This persistent uncontrolled hyperglycemia also produces changes in the bone marrow (BM) microenvironment that cause functional impairment of stem cells[5]. Nguyen *et al*[6] reported a reduced proliferation rate and increased expression of stress-associated genes, activating transcription factor 4, and C/EBP homologous protein in mesenchymal stem cells (MSCs). On the same note, Kim *et al*[7] reported defective osteogenic differentiation but an increased adipogenic differentiation rate in BM-derived MSCs. MSCs from streptozotocin (STZ)-induced diabetic rats have a slow proliferation rate and poor myogenic potential[8]. These studies show that hyperglycemia causes changes in progenitor cell biology and affects their normal behavior and functions during tissue repair[9]. Hence, attempts have been made in some cases to predifferentiate MSCs into insulin-producing cells before transplantation in hyperglycemic experimental animal models [10].

Antihyperglycemic therapy to regain glucose homeostasis can also interfere with the quality and efficacy of MSC treatment. Hsiao *et al*[11] reported that metformin caused apoptosis of MSCs *via* the AMP-activated protein kinase (AMPK)-mammalian target of rapamycin (mTOR) pathway. Interestingly, the authors observed that hyperglycemia protected cells from metformin-induced apoptosis. In another study involving a rat model of diabetic cardiomyopathy, Ammar *et al*[12] observed impaired angiogenesis and higher myocardial fibrosis in response to concomitant treatment with metformin and MSCs compared to MSCs treated animals. These data were attributed to impaired MSC functionality in the presence of metformin treatment.

HG CULTURE- AND HYPERGLYCEMIA-INDUCED SIGNALING

Hyperglycemic conditions *in vivo* are simulated *in vitro* by culturing the cells in HG conditions to study the effects of hyperglycemia. HG culture conditions have been shown to cause rapid cellular dysfunction by promoting transcriptional changes[13]. Some of the essential mechanisms involved therein include the formation of advanced glycation products (AGEs), PKC activation, mTOR/Akt dysregulation, *etc*, that lead to elevated reactive oxygen species (ROS) stress, increased pro-inflammatory cytokines production, growth factors, abnormally high gas transmitters, altered cell bioenergetics, *etc*.

For example, Aguiari *et al*[14] reported that muscle-derived stem cells and adipose tissue-derived stem cells under HG culture conditions preferentially adopted adipogenic phenotype in response to ROS accumulation and activation of PKC-β in the cells. They supported their findings by treating the cells with oxidizing agents and silencing PKC-β in the cells to inhibit their adipogenic differentiation. In a subsequent study, culture of human aortic endothelial cells in HG was re-

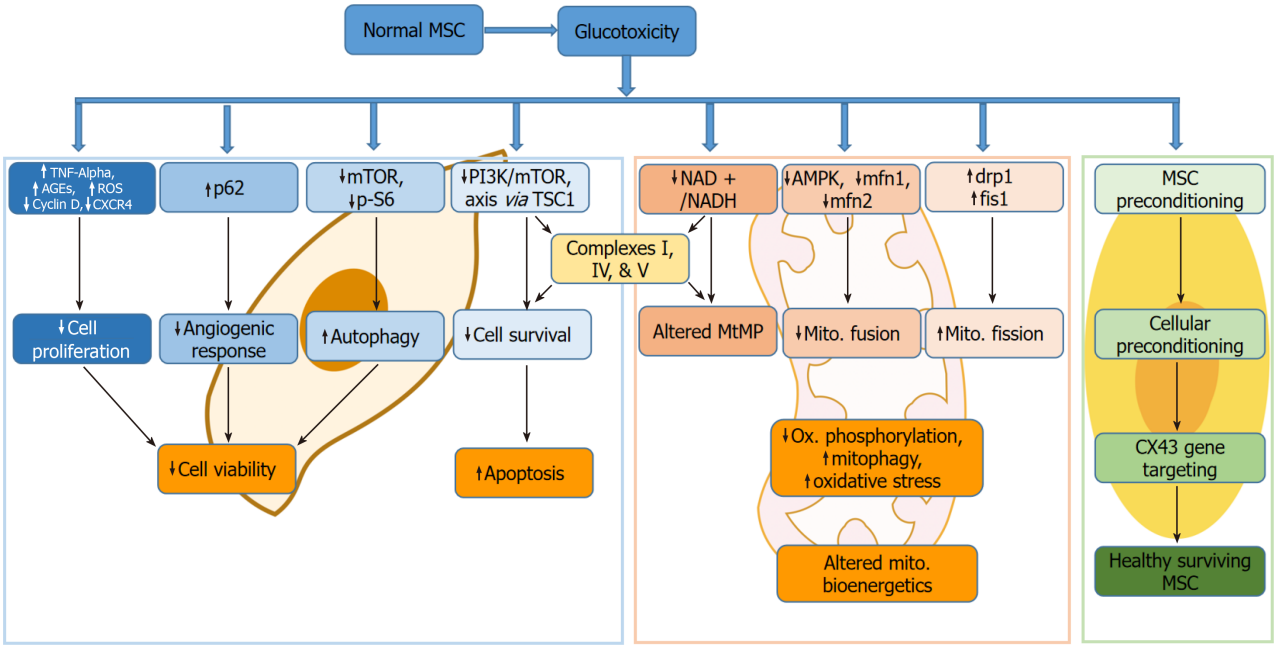

Figure 1 Glucotoxicity in mesenchymal stem cells exposed to high glucose culture conditions and hyperglycemia. AGE: Advanced glycation end product; AMPK: AMP-activated protein kinase; CXCR: C-X-C chemokine receptor type 4; drp1: Dynamin-related protein 1; fis1: Fission protein 1. mfn1: Mitofusin 1; MSC: Mesenchymal stem cell; mTOR: Mammalian target of rapamycin; PI3K: Phosphoinositide 3-kinase; ROS: Reactive oxygen species; TNF: Tumor necrosis factor; TSC1: Tuberous sclerosis 1.

ported to cause significant pathway changes during the first 4 h, with distinct clusters of genes showing altered transcriptional profiles unique to HG conditions[13]. Temporal co-expression and causal network analysis showed a relationship between type 2 diabetes mellitus and activation of growth factor signaling pathways, including signal transducer and activator of transcription 3 and nuclear factor-kappa B. On the same note, MSCs in HG culture undergo senescence mediated by Akt/mTOR dysregulation[3]. However, some studies report that for the detrimental effects of HG culture conditions, the cells may need persistent long-term exposure because they may resist short-term exposure to HG culture conditions[15]. It is interesting to note that MSCs from healthy donors had shorter doubling time under HG culture conditions compared with MSCs from diabetic donors, thus implying that the difference in their responsiveness is more a function of the pathophysiology of diabetes. On the same note, changes observed in diabetes donor-derived MSCs respiration capacity were responsible for their compromised cellular functions[6]. There is reportedly a decreased angiogenic paracrine activity, which was evident from reduced secretion of pro-angiogenic growth factors, *i.e.* vascular endothelial growth factor-A (VEGF-A), angiopoietin-1 (Ang-1), and Ang-2, and VEGF-C in the HG MSCs[7].

Chronic HG culture conditions also drive glycation reactions through the receptor for advanced glycation end products (AGEs), resulting in the formation of AGEs and endogenous inflammatory mediators[16,17]. It has been reported that stimulation with AGE-bovine serum albumin induced the generation of ROS and attenuated the proliferation and migration of MSCs *via* activation of the ROS-p38 mediated pathway[18]. Another study reported that HG reduced the regeneration ability of BM-MSCs through the activation of glycogen synthase kinase-3beta, which plays a vital role in inhibiting the proliferation of BM-MSCs *via* the inhibition of C-X-C chemokine receptor type 4[19].

Continuing their efforts to study the effects of hyperglycemia on MSC functionality, Abu-El-Rub *et al*[20] reported interesting comparative data *in vitro* by culturing human adipose tissue-derived MSCs (AD-MSCs) under low glucose and HG conditions in a parallel set of experiments. It is pertinent to mention that the authors used *in vitro* culture conditions for exposure to HG. Hence, the term "hyperglycemia" in the aims, conclusion, and elsewhere in the manuscript does not reflect the experimental design. The authors have primarily focused on three endpoints, cell viability, cell apoptosis, and mitochondrial energetics, to share their findings supported by some mechanistic studies that will be discussed in the following sections.

CELL VIABILITY AND APOPTOSIS

In addition to cellular dysfunction and suppression of proliferation, an HG microenvironment activates signaling pathways that direct MSC apoptosis. However, these signaling pathways need to be studied and established further. Change of tumor necrosis factor-α expression significantly affected MSC proliferation and death in an STZ-induced type 1 diabetic mouse model[21]. In contrast, in another interesting study, human BM-MSCs in diabetic serum showed increased cellular death and decreased angiogenic response caused by the induction of autophagy signaling with a high level of p62 expression[22].

Endoplasmic reticulum stress-induced autophagy is another mechanism contributing to the inactivation of mTOR, which was shown to reduce p-S6 (a marker of mTOR activity)[23]. Building on these data, Abu-El-Rub *et al*[20] revealed higher apoptosis in human AD-MSCs (hAD-MSCs) cultured in HG using low glucose culture as the control. Elucidating the mechanism causing poor survival of MSCs in an HG microenvironment *via* impairment of the phosphoinositide 3-kinase (PI3K)/mTOR axis, they found significantly increased tuberous sclerosis 1 (TSC1) protein. It is now well established that mTOR is an essential regulator of mitochondrial dynamics *via* generating the required mitochondrial potential to produce ATP[24]. As a part of the mechanism, TSC1 binding inactivates mTOR, while PI3K, a known activator of mTOR, is needed to remove the inhibitory effects of TSC1[25]. Furthermore, the downregulation of mTOR significantly reduced complex I, IV, and V in HG-cultured hAD-MSCs. These molecular data suggest an impact on mitochondrial oxidative phosphorylation and induction of mitophagy and massive oxidative stress[26]. Although data from the Abu-El-Rub *et al*[20] provide a better understanding of the activation of proapoptotic signaling in hAD-MSCs in the HG microenvironment, it would have been interesting to see if similar signaling was activated in MSCs from other tissue sources as well as from other species to delineate any tissue or species-specific differential responsiveness to HG culture conditions. Also, the mechanistic data would have been more convincing if the authors had used gain-of-function and loss-of-function studies to establish a causal relationship between mTOR, PI3K, Akt, and TSC1. There is no mention of TSC2, which forms a physical and functional complex *in vivo*[27]. The evidence is based on western blotting alone, showing TSC1 expression with simultaneous loss of PI3K and mTOR in HG-cultured cells. There needs to be more evidence to prove their dependence/relationship with each other. Intriguingly, the authors designed the studies for stipulated time points of 3, 7, and 14 d; they provided data only for the day 7 time point. It would have been interesting to include day 3 and day 14 data in the results or at least as supplementary data to show how early these molecular and organelle-level changes occurred and continued in the HG culture. Similarly, it would have been interesting if the cells were returned to normoglycemic conditions at each time point to observe any possible reversibility of the changes at each time point. There are better methods to observe cell viability than the trypan blue dye exclusion method to exclude researcher bias. Another mechanism suggested by the authors for MSCs' low viability was the drop in NAD+/NADH ratio in hAD-MSCs, correlated with impairment of the inner mitochondrial membrane potential (MtMP) that is discussed in the next section.

MITOCHONDRIAL CHANGES IN RESPONSE TO HYPERGLYCEMIC MICROENVIRONMENT

Before discussing the impairment of MtMP as a part of the cell's response to hyperglycemia, readers need to understand the basic functioning of mitochondria. A continual, uninterrupted energy supply is critical for cellular processes, *i.e.* growth, repair, maintenance, *etc*, for which robust intracellular mechanisms are in place[28]. Mitochondria play a crucial role in supporting these cellular functions with ATP production during normal mitochondrial bioenergetics, along with contributing to other processes such as aging, ion homeostasis, and apoptosis[29]. The mitochondrial intermembranous space houses the enzymes involved in the electron transport chain, capturing energy carried by electrons in NADH and FADH2 to generate ATP. The flux of electrons creates a stable MtMP facilitated by proton pumps, *i.e.* complexes I, III, and IV. Contingent upon the cell's energy needs, mitochondria undergo fusion or fission such that the process stimulates and inhibits ATP synthesis, respectively[30]. At the molecular level, AMPK enables mitochondrial fusion *via* mitofusin 1 (Mfn1), Mfn2, and optic atrophy 1, while dynamin-related protein 1 (Drp1) and fission protein 1 control mitochondrial fission. More recent studies have shown that mitochondrial functions go far beyond energy-producing organelle, *i.e.* cell differentiation and their regenerative potential[31-33].

HG culture conditions *in vitro* and hyperglycemia in diabetes patients cause mitochondrial dysfunction because of altered MtMP, thus lowering ATP production. A low NAD+/NADH ratio is observed in cardiac dysfunction in diabetic hearts. At the same time, it also changes mitochondrial membrane polarity and reduces mitochondrial cell mass, leading to perturbed mitochondrial homeostasis in human mononuclear cells[34,35]. Hyperglycemia also causes mitochondrial fragmentation with upregulation of Drp1 (promoting fission) or downregulation of Mfn1/2 (inhibiting fusion), thus further reducing mitochondrial ATP synthesis[35]. It creates structural and functional changes in the mitochondria, altering their bioenergetics and thus jeopardizing their survival[36-38]. There is also an increase in ROS stress in the cytosol and mitochondria[39]. Abu-El-Rub *et al*[20] have attributed reduced NAD+/NADH ratio in hAD-MSCs exposed to an HG environment as responsible for driving the cells toward apoptosis *via* dysregulation of mitochondrial complexes I, IV, and V. They have supported their findings with MtMP changes in hAD-MSCs assessed by the MtMP assay kit. All these factors confirm dysfunction in mitochondrial bioenergetics in the cells, resulting in low survival and higher apoptosis in HG culture conditions. Table 1 summarizes some of the studies from the published literature reporting the effect of HG culture conditions.

One of the main limitations of the proposed mechanism is that there needs to be an attempt to extrapolate these data *in vivo* using experimental animal models. This is important before use as a novel target to improve the survival of MSC in diabetic patients. Moreover, it would have been interesting if the authors had used cellular preconditioning using preconditioning mimetics or a subcellular preconditioning approach to stabilize the MtMP, which can enhance cell survival and reduce apoptosis in HG culture conditions[43-45]. The authors have already successfully used subcellular preconditioning for cytoprotection of donor stem cells for heart-cell therapy to enhance their post engraftment survival[46,47]. Underscoring the mechanism, the authors have shown that mito-Cx43 gene targeting was cytoprotective *via* a shift of mitochondrial Bak and Bcl-xL balance.

Table 1 Summary of some studies from the published literature reporting the effect of high glucose culture conditions

Ref.	Cell type and source	Glucose concentration used	Mechanism	Findings
Zhang *et al*[19], 2016	Rat BM-MSCs	HG: 16.5 mM *vs* NG: 5.5 mM	Activation of GSK3β and suppression of CXCR-4, β-catenin, LEF-1, and cyclin D1 under HG culture conditions	The study related HG culture with the activation of GSK3β to affect the proliferation and migration of BM-MSCs in HG culture. The proliferation and migration ability of the cells were suppressed in HG culture. HG activated GSK3β but suppressed CXCR-4, β-catenin, LEF-1, and cyclin D1. Inhibition of GSK3β by lithium chloride led to increased levels of β-catenin, LEF-1, cyclin D1, and CXCR-4 expression
Abu-El-Rub *et al*[20], 2023	hAD-MSCs	HG: 25 mM *vs* NG: 5.5 mM	Altered mitochondrial membrane potential, Low NAD+/NADH pool, reduced mTOR and PI3K	HG culture for 7 d showed reduced cell viability compared to NG cultured control. HG culture significantly reduced the mitochondrial membrane potential and NAD+/NADH ratio, showing dysregulated mitochondrial function. PI3K protein expression significantly decreased in HG-cultured cells MSCs with increased TSC1 and downregulation of mTOR protein. Mitochondrial complexes I, IV, and V were reduced in HG, leading to poor survival of MSCs in HG
Li *et al*[37], 2007	Human BM-MSCs	HG: 25 mM *vs* NG: 5.6 mM	Molecular mechanism not explored	The effect of HG culture on human MSC *in vitro* was assessed using telomerase-immortalized MSC (hMSC-TERT) and primary MSC (hMSC). HG increased hMSC-TERT proliferation in long-term studies, while it remained unchanged for hMSCs. Apoptosis was not influenced by HG in both cell types. Moreover, HG culture conditions supported osteogenic differentiation of the cells
Hankamolsiri *et al*[40], 2016	Human BM-MSCs and MSCs from gestational tissues	HG: 25 mM *vs* NG: 5.5 mM	HG-induced the expression of adipogenic gene PPARγ and LPL in BM-MSCs, as well as ADIPOQ and LPL genes in gestational tissue-derived MSCs	No change in surface markers' expression. HG reduced proliferation but enhanced adipogenic differentiation of all MSCs examined. The expression of some adipogenic genes were also upregulated when MSCs were cultured in HG. Although HG transiently reduced some osteogenic genes, its effect on the osteogenic differentiation rate of the MSCs was not demonstrated
Al-Qarakhli *et al*[41], 2019	Rat BM-MSCs	HG: 25 mM *vs* NG: 5.5 mM	HG culture conditions significantly reduced telomere length at 50 PDs and 100 PDs. Also attribute it to IGFs, TGF-β1, and BMPs	HG and NG cultured cells had similar morphology and growth characteristics. HG-cultured cells proliferated beyond 50 doublings, although with signs of senescence. The osteogenic and adipogenic differentiation rates were significantly reduced in HG-cultured cells. The effect of HG was more pronounced in advanced PDs
Khasawneh *et al*[42], 2023	Human AD-MSCs	HG: 25 mM *vs* NG: 5.5 mM	Reduced AMPK and PFK-1	Immunomodulation potential was lost in the hAD-MSCs under HG conditions and were detectable by immune cells. These changes were mediated by low IDO, IL-10, and complement factor H. AMPK and PFK-1, integral glycolysis regulators, were reduced in HG-cultured MSCs. These findings show the possibility of an immunomodulatory shift in MSCs under HG, leading to poor survival of the cells

ADIPOQ: Adiponectin; AMPK: AMP-activated protein kinase; BM: Bone marrow; BMP: Bone morphogenic proteins; CXCR4: C-X-C chemokine receptor type 4; GSK-3β: Glycogen synthase kinase-3β; hAD-MSCs: Human adipose tissue-derived mesenchymal stem cells; HG: High glucose; IDO: Indoleamine 2,3-dioxygenase; IGF: Insulin-like growth factor; IL: Interleukin; LEF-1: Lymphoid enhancer binding factor-1; LPL: Lipoprotein lipase; MSC: Mesenchymal stem cell; mTOR: Mammalian target of rapamycin; NAD: Nicotinamide adenine dinucleotide; NG: Normal glucose; PD: Population doubling; PFK-1: Phosphofructokinase-1; PI3K: Phosphoinositide 3-kinase; PPARγ: Peroxisome proliferator-activated receptor gamma; TGF-β1: Transforming growth factor-β1; TSC1: Tuberous sclerosis 1.

CONCLUSION

In conclusion, it is evident that HG conditions have detrimental effects on different cell types, including cancer cells, and may also change their normal functions, *i.e.* migration potential and invasiveness[1,2,48-50]. Hence, understanding the mechanism of apoptosis by chronic exposure to HG, both *in vitro* and *in vivo*, will help efforts to combine preconditioning strategies, especially the subcellular preconditioning approach. That will go a long way in promoting donor cell post engraftment survival in diabetes patients and *vice versa* in clinical settings wherein MSCs have already progressed to advanced phases of assessment[51,52].

FOOTNOTES

Author contributions: Alaagib N contributed to the apoptosis and supported the visual abstract; Mateen MA was involved in the mitochondrial membrane potential and visual abstract; Haider KH contributed to stem cells and overall write-up; All authors revised the manuscript.

Conflict-of-interest statement: The authors declare that they have no conflicting interests.

Country/Territory of origin: Saudi Arabia

ORCID number: Khawaja Husnain Haider 0000-0002-7907-4808.

S-Editor: Wang JJ
L-Editor: Filipodia
P-Editor: Xu ZH

REFERENCES

1 **Rajab AM**, Haider KhH. Hyperglycemia and RBCs: too sweet to survive. *Int J Diabetes Dev Countries* 2018; **38**: 357-365 [DOI: 10.1007/s13410-018-0613-6]
2 **Rajab AM**, Rahman S, Rajab TM, Haider KH. Morphology and Chromic Status of Red Blood Cells Are Significantly Influenced by Gestational Diabetes. *J Hematol* 2018; **7**: 140-148 [PMID: 32300429 DOI: 10.14740/jh449w]
3 **Zhang D**, Lu H, Chen Z, Wang Y, Lin J, Xu S, Zhang C, Wang B, Yuan Z, Feng X, Jiang X, Pan J. High glucose induces the aging of mesenchymal stem cells *via* Akt/mTOR signaling. *Mol Med Rep* 2017; **16**: 1685-1690 [PMID: 28656269 DOI: 10.3892/mmr.2017.6832]
4 **Musleh Ali AR**, Al-Kasssas W, Haider KH. Fatty Acid Escape Hypothesis: The Pathway to Type-II Diabetes. *Diabetes Res* 2019 [DOI: 10.17140/DROJ-5-140]
5 **Fadini GP**, Ferraro F, Quaini F, Asahara T, Madeddu P. Concise review: diabetes, the bone marrow niche, and impaired vascular regeneration. *Stem Cells Transl Med* 2014; **3**: 949-957 [PMID: 24944206 DOI: 10.5966/sctm.2014-0052]
6 **Nguyen LT**, Hoang DM, Nguyen KT, Bui DM, Nguyen HT, Le HTA, Hoang VT, Bui HTH, Dam PTM, Hoang XTA, Ngo ATL, Le HM, Phung NY, Vu DM, Duong TT, Nguyen TD, Ha LT, Bui HTP, Nguyen HK, Heke M, Bui AV. Type 2 diabetes mellitus duration and obesity alter the efficacy of autologously transplanted bone marrow-derived mesenchymal stem/stromal cells. *Stem Cells Transl Med* 2021; **10**: 1266-1278 [PMID: 34080789 DOI: 10.1002/sctm.20-0506]
7 **Kim H**, Han JW, Lee JY, Choi YJ, Sohn YD, Song M, Yoon YS. Diabetic Mesenchymal Stem Cells Are Ineffective for Improving Limb Ischemia Due to Their Impaired Angiogenic Capability. *Cell Transplant* 2015; **24**: 1571-1584 [PMID: 25008576 DOI: 10.3727/096368914X682792]
8 **Jin P**, Zhang X, Wu Y, Li L, Yin Q, Zheng L, Zhang H, Sun C. Streptozotocin-induced diabetic rat-derived bone marrow mesenchymal stem cells have impaired abilities in proliferation, paracrine, antiapoptosis, and myogenic differentiation. *Transplant Proc* 2010; **42**: 2745-2752 [PMID: 20832580 DOI: 10.1016/j.transproceed.2010.05.145]
9 **Liu Y**, Li Y, Nan LP, Wang F, Zhou SF, Wang JC, Feng XM, Zhang L. The effect of high glucose on the biological characteristics of nucleus pulposus-derived mesenchymal stem cells. *Cell Biochem Funct* 2020; **38**: 130-140 [PMID: 31957071 DOI: 10.1002/cbf.3441]
10 **He X**, Yang Y, Yao MW, Ren TT, Guo W, Li L, Xu X. Full title: High glucose protects mesenchymal stem cells from metformin-induced apoptosis through the AMPK-mediated mTOR pathway. *Sci Rep* 2019; **9**: 17764 [PMID: 31780804 DOI: 10.1038/s41598-019-54291-y]
11 **Hsiao CY**, Chen TH, Huang BS, Chen PH, Su CH, Shyu JF, Tsai PJ. Comparison between the therapeutic effects of differentiated and undifferentiated Wharton's jelly mesenchymal stem cells in rats with streptozotocin-induced diabetes. *World J Stem Cells* 2020; **12**: 139-151 [PMID: 32184938 DOI: 10.4252/wjsc.v12.i2.139]
12 **Ammar HI**, Shamseldeen AM, Shoukry HS, Ashour H, Kamar SS, Rashed LA, Fadel M, Srivastava A, Dhingra S. Metformin impairs homing ability and efficacy of mesenchymal stem cells for cardiac repair in streptozotocin-induced diabetic cardiomyopathy in rats. *Am J Physiol Heart Circ Physiol* 2021; **320**: H1290-H1302 [PMID: 33513084 DOI: 10.1152/ajpheart.00317.2020]
13 **Bayaraa O**, Inman CK, Thomas SA, Al Jallaf F, Alshaikh M, Idaghdour Y, Ashall L. Hyperglycemic conditions induce rapid cell dysfunction-promoting transcriptional alterations in human aortic endothelial cells. *Sci Rep* 2022; **12**: 20912 [PMID: 36463298 DOI: 10.1038/s41598-022-24999-5]
14 **Aguiari P**, Leo S, Zavan B, Vindigni V, Rimessi A, Bianchi K, Franzin C, Cortivo R, Rossato M, Vettor R, Abatangelo G, Pozzan T, Pinton P, Rizzuto R. High glucose induces adipogenic differentiation of muscle-derived stem cells. *Proc Natl Acad Sci U S A* 2008; **105**: 1226-1231 [PMID: 18212116 DOI: 10.1073/pnas.0711402105]
15 **Weil BR**, Abarbanell AM, Herrmann JL, Wang Y, Meldrum DR. High glucose concentration in cell culture medium does not acutely affect human mesenchymal stem cell growth factor production or proliferation. *Am J Physiol Regul Integr Comp Physiol* 2009; **296**: R1735-R1743 [PMID: 19386985 DOI: 10.1152/ajpregu.90876.2008]
16 **Aikawa E**, Fujita R, Asai M, Kaneda Y, Tamai K. Receptor for Advanced Glycation End Products-Mediated Signaling Impairs the Maintenance of Bone Marrow Mesenchymal Stromal Cells in Diabetic Model Mice. *Stem Cells Dev* 2016; **25**: 1721-1732 [PMID: 27539289 DOI: 10.1089/scd.2016.0067]
17 **Silva JC**, Sampaio P, Fernandes MH, Gomes PS. The Osteogenic Priming of Mesenchymal Stem Cells is Impaired in Experimental Diabetes. *J Cell Biochem* 2015; **116**: 1658-1667 [PMID: 25704854 DOI: 10.1002/jcb.25126]
18 **Yang K**, Wang XQ, He YS, Lu L, Chen QJ, Liu J, Shen WF. Advanced glycation end products induce chemokine/cytokine production *via* activation of p38 pathway and inhibit proliferation and migration of bone marrow mesenchymal stem cells. *Cardiovasc Diabetol* 2010; **9**: 66 [PMID: 20969783 DOI: 10.1186/1475-2840-9-66]
19 **Zhang B**, Liu N, Shi H, Wu H, Gao Y, He H, Gu B, Liu H. High glucose microenvironments inhibit the proliferation and migration of bone mesenchymal stem cells by activating GSK3β. *J Bone Miner Metab* 2016; **34**: 140-150 [PMID: 25840567 DOI: 10.1007/s00774-015-0662-6]

20 **Abu-El-Rub E**, Almahasneh F, Khasawneh RR, Alzu'bi A, Ghorab D, Almazari R, Magableh H, Sanajleh A, Shlool H, Mazari M, Bader NS, Al-Momani J. Human mesenchymal stem cells exhibit altered mitochondrial dynamics and poor survival in high glucose microenvironment. *World J Stem Cells* 2023; **15**: 1093-1103 [PMID: 38179215 DOI: 10.4252/wjsc.v15.i12.1093]

21 **Ko KI**, Coimbra LS, Tian C, Alblowi J, Kayal RA, Einhorn TA, Gerstenfeld LC, Pignolo RJ, Graves DT. Diabetes reduces mesenchymal stem cells in fracture healing through a TNFα-mediated mechanism. *Diabetologia* 2015; **58**: 633-642 [PMID: 25563724 DOI: 10.1007/s00125-014-3470-y]

22 **Rezabakhsh A**, Cheraghi O, Nourazarian A, Hassanpour M, Kazemi M, Ghaderi S, Faraji E, Rahbarghazi R, Avci ÇB, Bagca BG, Garjani A. Type 2 Diabetes Inhibited Human Mesenchymal Stem Cells Angiogenic Response by Over-Activity of the Autophagic Pathway. *J Cell Biochem* 2017; **118**: 1518-1530 [PMID: 27918077 DOI: 10.1002/jcb.25814]

23 **Meng Y**, Ji J, Tan W, Guo G, Xia Y, Cheng C, Gu Z, Wang Z. Involvement of autophagy in the procedure of endoplasmic reticulum stress introduced apoptosis in bone marrow mesenchymal stem cells from nonobese diabetic mice. *Cell Biochem Funct* 2016; **34**: 25-33 [PMID: 26800376 DOI: 10.1002/cbf.3161]

24 **Morita M**, Prudent J, Basu K, Goyon V, Katsumura S, Hulea L, Pearl D, Siddiqui N, Strack S, McGuirk S, St-Pierre J, Larsson O, Topisirovic I, Vali H, McBride HM, Bergeron JJ, Sonenberg N. mTOR Controls Mitochondrial Dynamics and Cell Survival *via* MTFP1. *Mol Cell* 2017; **67**: 922-935.e5 [PMID: 28918902 DOI: 10.1016/j.molcel.2017.08.013]

25 **Zhang H**, Cicchetti G, Onda H, Koon HB, Asrican K, Bajraszewski N, Vazquez F, Carpenter CL, Kwiatkowski DJ. Loss of Tsc1/Tsc2 activates mTOR and disrupts PI3K-Akt signaling through downregulation of PDGFR. *J Clin Invest* 2003; **112**: 1223-1233 [PMID: 14561707 DOI: 10.1172/JCI200317222]

26 **Guo C**, Sun L, Chen X, Zhang D. Oxidative stress, mitochondrial damage and neurodegenerative diseases. *Neural Regen Res* 2013; **8**: 2003-2014 [PMID: 25206509 DOI: 10.3969/j.issn.1673-5374.2013.21.009]

27 **Inoki K**, Li Y, Zhu T, Wu J, Guan KL. TSC2 is phosphorylated and inhibited by Akt and suppresses mTOR signalling. *Nat Cell Biol* 2002; **4**: 648-657 [PMID: 12172553 DOI: 10.1038/ncb839]

28 **Alberts B**, Johnson A, Lewis J, Raff M, Roberts K, Walter P. How cells obtain energy from food. In: Molecular Biology of the Cell. 4th ed. New York: Garland Science, 2002

29 **Chen W**, Zhao H, Li Y. Mitochondrial dynamics in health and disease: mechanisms and potential targets. *Signal Transduct Target Ther* 2023; **8**: 333 [PMID: 37669960 DOI: 10.1038/s41392-023-01547-9]

30 **Fu W**, Liu Y, Yin H. Mitochondrial Dynamics: Biogenesis, Fission, Fusion, and Mitophagy in the Regulation of Stem Cell Behaviors. *Stem Cells Int* 2019; **2019**: 9757201 [PMID: 31089338 DOI: 10.1155/2019/9757201]

31 **Wanet A**, Arnould T, Najimi M, Renard P. Connecting Mitochondria, Metabolism, and Stem Cell Fate. *Stem Cells Dev* 2015; **24**: 1957-1971 [PMID: 26134242 DOI: 10.1089/scd.2015.0117]

32 **Li Q**, Gao Z, Chen Y, Guan MX. The role of mitochondria in osteogenic, adipogenic and chondrogenic differentiation of mesenchymal stem cells. *Protein Cell* 2017; **8**: 439-445 [PMID: 28271444 DOI: 10.1007/s13238-017-0385-7]

33 **Paliwal S**, Chaudhuri R, Agrawal A, Mohanty S. Regenerative abilities of mesenchymal stem cells through mitochondrial transfer. *J Biomed Sci* 2018; **25**: 31 [PMID: 29602309 DOI: 10.1186/s12929-018-0429-1]

34 **Chiao YA**, Chakraborty AD, Light CM, Tian R, Sadoshima J, Shi X, Gu H, Lee CF. NAD(+) Redox Imbalance in the Heart Exacerbates Diabetic Cardiomyopathy. *Circ Heart Fail* 2021; **14**: e008170 [PMID: 34374300 DOI: 10.1161/CIRCHEARTFAILURE.120.008170]

35 **Zheng Y**, Luo A, Liu X. The Imbalance of Mitochondrial Fusion/Fission Drives High-Glucose-Induced Vascular Injury. *Biomolecules* 2021; **11** [PMID: 34944423 DOI: 10.3390/biom11121779]

36 **Rovira-Llopis S**, Bañuls C, Diaz-Morales N, Hernandez-Mijares A, Rocha M, Victor VM. Mitochondrial dynamics in type 2 diabetes: Pathophysiological implications. *Redox Biol* 2017; **11**: 637-645 [PMID: 28131082 DOI: 10.1016/j.redox.2017.01.013]

37 **Li YM**, Schilling T, Benisch P, Zeck S, Meissner-Weigl J, Schneider D, Limbert C, Seufert J, Kassem M, Schütze N, Jakob F, Ebert R. Effects of high glucose on mesenchymal stem cell proliferation and differentiation. *Biochem Biophys Res Commun* 2007; **363**: 209-215 [PMID: 17868648 DOI: 10.1016/j.bbrc.2007.08.161]

38 **Gong L**, Liu FQ, Wang J, Wang XP, Hou XG, Sun Y, Qin WD, Wei SJ, Zhang Y, Chen L, Zhang MX. Hyperglycemia induces apoptosis of pancreatic islet endothelial cells *via* reactive nitrogen species-mediated Jun N-terminal kinase activation. *Biochim Biophys Acta* 2011; **1813**: 1211-1219 [PMID: 21435358 DOI: 10.1016/j.bbamcr.2011.03.011]

39 **Sen S**, Domingues CC, Rouphael C, Chou C, Kim C, Yadava N. Genetic modification of human mesenchymal stem cells helps to reduce adiposity and improve glucose tolerance in an obese diabetic mouse model. *Stem Cell Res Ther* 2015; **6**: 242 [PMID: 26652025 DOI: 10.1186/s13287-015-0224-9]

40 **Hankamolsiri W**, Manochantr S, Tantrawatpan C, Tantikanlayaporn D, Tapanadechopone P, Kheolamai P. The Effects of High Glucose on Adipogenic and Osteogenic Differentiation of Gestational Tissue-Derived MSCs. *Stem Cells Int* 2016; **2016**: 9674614 [PMID: 27057179 DOI: 10.1155/2016/9674614]

41 **Al-Qarakhli AMA**, Yusop N, Waddington RJ, Moseley R. Effects of high glucose conditions on the expansion and differentiation capabilities of mesenchymal stromal cells derived from rat endosteal niche. *BMC Mol Cell Biol* 2019; **20**: 51 [PMID: 31752674 DOI: 10.1186/s12860-019-0235-y]

42 **Khasawneh RR**, Abu-El-Rub E, Almahasneh FA, Alzu'bi A, Zegallai HM, Almazari RA, Magableh H, Mazari MH, Shlool HF, Sanajleh AK. Addressing the impact of high glucose microenvironment on the immunosuppressive characteristics of human mesenchymal stem cells. *IUBMB Life* 2023 [PMID: 38014654 DOI: 10.1002/iub.2796]

43 **Ahmad N**, Wang Y, Haider KH, Wang B, Pasha Z, Uzun O, Ashraf M. Cardiac protection by mitoKATP channels is dependent on Akt translocation from cytosol to mitochondria during late preconditioning. *Am J Physiol Heart Circ Physiol* 2006; **290**: H2402-H2408 [PMID: 16687609 DOI: 10.1152/ajpheart.00737.2005]

44 **Rodríguez-Sinovas A**, Cabestrero A, López D, Torre I, Morente M, Abellán A, Miró E, Ruiz-Meana M, García-Dorado D. The modulatory effects of connexin 43 on cell death/survival beyond cell coupling. *Prog Biophys Mol Biol* 2007; **94**: 219-232 [PMID: 17462722 DOI: 10.1016/j.pbiomolbio.2007.03.003]

45 **Lu G**, Haider HKh, Porollo A, Ashraf M. Mitochondria-specific transgenic overexpression of connexin-43 simulates preconditioning-induced cytoprotection of stem cells. *Cardiovasc Res* 2010; **88**: 277-286 [PMID: 20833648 DOI: 10.1093/cvr/cvq293]

46 **Lu G**, Haider HK, Jiang S, Ashraf M. Sca-1+ stem cell survival and engraftment in the infarcted heart: dual role for preconditioning-induced connexin-43. *Circulation* 2009; **119**: 2587-2596 [PMID: 19414636 DOI: 10.1161/CIRCULATIONAHA.108.827691]

47 **Lu G**, Jiang S, Ashraf M, Haider KH. Subcellular preconditioning of stem cells: mito-Cx43 gene targeting is cytoprotective *via* shift of

mitochondrial Bak and Bcl-xL balance. *Regen Med* 2012; **7**: 323-334 [PMID: 22594326 DOI: 10.2217/rme.12.13]

48 **Su BL**, Wang LL, Zhang LY, Zhang S, Li Q, Chen GY. Potential role of microRNA-503 in Icariin-mediated prevention of high glucose-induced endoplasmic reticulum stress. *World J Diabetes* 2023; **14**: 1234-1248 [PMID: 37664468 DOI: 10.4239/wjd.v14.i8.1234]

49 **Duan XK**, Sun YX, Wang HY, Xu YY, Fan SZ, Tian JY, Yu Y, Zhao YY, Jiang YL. miR-124 is upregulated in diabetic mice and inhibits proliferation and promotes apoptosis of high-glucose-induced β-cells by targeting EZH2. *World J Diabetes* 2023; **14**: 209-221 [PMID: 37035229 DOI: 10.4239/wjd.v14.i3.209]

50 **Lin CY**, Lee CH, Huang CC, Lee ST, Guo HR, Su SB. Impact of high glucose on metastasis of colon cancer cells. *World J Gastroenterol* 2015; **21**: 2047-2057 [PMID: 25717237 DOI: 10.3748/wjg.v21.i7.2047]

51 **Al-Khani AM**, Khalifa MA, Haider KhH. Mesenchymal stem cells: How close we are to their routine clinical use? In: Haider KH. Handbook of Stem Cell Therapy. Singapore: Springer, 2022

52 **Al-Khani AM**, Kalou Y, Haider KH. Response to Letter to the Editor: Comment on Bone Marrow Mesenchymal Stem Cells for Heart Failure Treatment: A Systematic Review and Meta-Analysis. *Heart Lung Circ* 2023; **32**: e59-e60 [PMID: 37793758 DOI: 10.1016/j.hlc.2023.07.001]

World Journal of Stem Cells

Submit a Manuscript: https://www.f6publishing.com

World J Stem Cells 2024 March 26; 16(3): 245-256

DOI: 10.4252/wjsc.v16.i3.245

ISSN 1948-0210 (online)

MINIREVIEWS

How mesenchymal stem cells transform into adipocytes: Overview of the current understanding of adipogenic differentiation

Shan-Shan Liu, Xiang Fang, Xin Wen, Ji-Shan Liu, Miribangvl Alip, Tian Sun, Yuan-Yuan Wang, Hong-Wei Chen

Specialty type: Cell and tissue engineering

Provenance and peer review: Invited article; Externally peer reviewed.

Peer-review model: Single blind

Peer-review report's scientific quality classification

Grade A (Excellent): 0
Grade B (Very good): B
Grade C (Good): C
Grade D (Fair): 0
Grade E (Poor): 0

P-Reviewer: Muzes G, Hungary; Silva-Junior AJD, Brazi

Received: October 31, 2023
Peer-review started: October 31, 2023
First decision: December 19, 2023
Revised: January 15, 2024
Accepted: February 18, 2024
Article in press: February 18, 2024
Published online: March 26, 2024

Shan-Shan Liu, Xin Wen, Miribangvl Alip, Tian Sun, Hong-Wei Chen, Department of Reumatology and Immunology, Nanjing Drum Tower Hospital, The Affiliated Hospital of Medical School, Nanjing University, Nanjing 210008, Jiangsu Province, China

Xiang Fang, Department of Emergency, Nanjing Drum Tower Hospital, The Affiliated Hospital of Medical School, Nanjing University, Nanjing 210008, Jiangsu Province, China

Ji-Shan Liu, Key Laboratory for Biomechanics and Mechanobiology of Ministry of Education, School of Biological Science and Medical Engineering, Beihang University, Beijing 100191, China

Yuan-Yuan Wang, Anhui Key Laboratory of Infection and Immunity, Bengbu Medical College, Bengbu 233000, Anhui Province, China

Corresponding author: Hong-Wei Chen, PhD, Associate Professor, Department of Reumatology and Immunology, Nanjing Drum Tower Hospital, The Affiliated Hospital of Medical School, Nanjing University, No. 321 Zhongshan Road, Nanjing 210008, Jiangsu Province, China. chenhw@nju.edu.cn

Abstract

Mesenchymal stem cells (MSCs) are stem/progenitor cells capable of self-renewal and differentiation into osteoblasts, chondrocytes and adipocytes. The transformation of multipotent MSCs to adipocytes mainly involves two subsequent steps from MSCs to preadipocytes and further preadipocytes into adipocytes, in which the process MSCs are precisely controlled to commit to the adipogenic lineage and then mature into adipocytes. Previous studies have shown that the master transcription factors C/enhancer-binding protein alpha and peroxisome proliferation activator receptor gamma play vital roles in adipogenesis. However, the mechanism underlying the adipogenic differentiation of MSCs is not fully understood. Here, the current knowledge of adipogenic differentiation in MSCs is reviewed, focusing on signaling pathways, noncoding RNAs and epigenetic effects on DNA methylation and acetylation during MSC differentiation. Finally, the relationship between maladipogenic differentiation and diseases is briefly discussed. We hope that this review can broaden and deepen our understanding of how MSCs turn into adipocytes.

Key Words: Mesenchymal stem cell; Adipogenic differentiation; Signaling pathway;

Noncoding RNA; Epigenetic regulation

Core Tip: Mesenchymal stem cells (MSCs) are able to differentiate into adipocytes, while the mechanism underlying the adipogenic differentiation of MSCs is not fully understood. Here, we summarize the function of signaling pathways, noncoding RNAs and epigenetic modification in MSC differentiation, and finally discuss the relationship between maladipogenic differentiation and diseases briefly.

Citation: Liu SS, Fang X, Wen X, Liu JS, Alip M, Sun T, Wang YY, Chen HW. How mesenchymal stem cells transform into adipocytes: Overview of the current understanding of adipogenic differentiation. *World J Stem Cells* 2024; 16(3): 245-256
URL: https://www.wjgnet.com/1948-0210/full/v16/i3/245.htm
DOI: https://dx.doi.org/10.4252/wjsc.v16.i3.245

INTRODUCTION

Mesenchymal stem cells (MSCs) are multipotent stem/progenitor cells capable of self-renewal and differentiation into distinct mesodermal lineages, such as adipocytes, osteoblasts and chondrocytes. The high migratory capacity, excellent expansion potential and reduced immunogenicity of MSCs make them attractive candidates in regenerative medicine[1]. Although initially derived from bone marrow, MSCs can currently be collected from various tissues and organs, including adipose tissue, umbilical cord blood and dental pulp[2]. According to the International Society for Cellular Therapy criteria, MSCs express CD73, CD90, and CD105 but lack CD14, CD11b, CD34, CD45, CD79a or CD19 and HLA-DR expression[3]. In addition, multipotential differentiation remains the hallmark of MSC identity.

Upon differentiation, the transition of MSCs into terminal mesodermal lineages is precisely controlled by certain lineage-specific master regulators. Runx2 is well known to direct MSCs to switch into osteoblasts[4]. Sox9, an early transcription factor, regulates the expression of key genes involved in chondrogenesis[5,6]. For adipogenesis, both CAAT/enhancer-binding protein alpha (C/EBPα)[7] and peroxisome proliferation activator receptor gamma (PPARγ)[8] are vital regulators that favor adipocyte formation.

However, full adipogenic differentiation from MSCs is a long-term complex process in which multipotent MSCs gradually commit to preadipocyte differentiation and eventually differentiate into terminal adipocytes, thus resulting in an adipocytic phenotype. At each step toward adipocytes, the cell fate of MSC derivatives is precisely regulated by signaling pathways and master regulators (*e.g.*, PPARγ and C/EBPα). Moreover, other regulatory elements of noncoding RNAs and epigenetic modifications synergistically play important roles in MSC adipogenesis. Hence, this review summarizes the present knowledge of adipogenesis in MSCs, focusing on adipogenesis regulation by indispensable signaling pathways, noncoding RNAs, methylation and acetylation.

SIGNALING PATHWAYS

The lineage commitment of MSCs can be manipulated by employing various chemicals in differentiation media, which modulate key transcription factors during MSC differentiation to track adipogenesis in vitro. Typically, these components include isobutylmethylxanthine (IBMX), indomethacin, dexamethasone (Dex), and insulin. IBMX and Dex are pivotal for initiating adipogenic differentiation. IBMX inhibits phosphodiesterases, leading to an increase in intracellular cAMP levels[9], which subsequently induces changes in transcription factors through protein kinase A activation. Additionally, IBMX directly stimulates the expression of C/EBPβ. Similarly, Dex activates C/EBPδ expression by binding to intracellular glucocorticoid receptors[10]. However for indomethacin, a well-known inhibitor of COX1/2, its adipogenic activity does not stem from COX inhibition but rather from PPARγ activation[11,12]. Insulin enhances glucose uptake for triglyceride synthesis in adipocytes[13].

Under differentiation-inducing circumstances, cellular signals control MSC maturation through the adipocytic route and further promote the differentiation of preadipocytes into mature adipocytes. Preadipocytes are an intermediate state between MSCs and adipocytes. Adipocytes contain fat droplets, while preadipocytes do not necessarily have these structures (Figure 1). Currently, the molecular mechanism involved in the differentiation of preadipocytes into adipocytes is relatively clear, but the principles underlying the transformation of MSCs into preadipocytes are not well understood. Nonetheless, several cytokines and signaling pathways, including the actin, bone morphogenic protein (BMP), and transforming growth factor-beta (TGF-β)/SMAD signaling pathways, are indispensable for MSC adipogenesis.

Actin and Rho signaling

Actin, a cytoskeletal protein, is known to play a crucial role in MSC differentiation. It determines cell shape, nuclear shape, cell spreading, and cell stiffness, which eventually affects cell differentiation. MSC lineage commitment is also

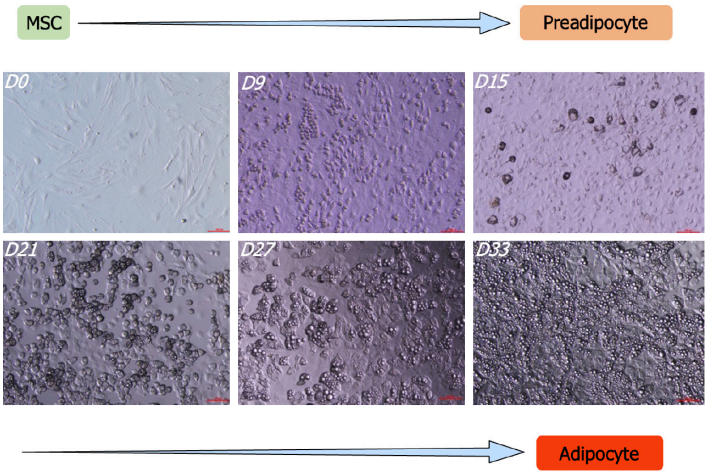

Figure 1 Morphological changes in differentiating mouse thymic mesenchymal stem cells. Schematic illustration of the adipogenic differentiation protocol and cellular morphological changes that occurred during the differentiation process 33 consecutive days after induction. Typically, mesenchymal stem cell preadipocyte commitment occurred in the first days (days 15), followed by the differentiation of preadipocytes into mature adipocytes with increasing lipid droplets. MSC: Mesenchymal stem cell.

regulated by actin cytoskeleton-mediated cell type[14], such as a flower shape during adipogenic differentiation and a star shape towards osteogenic transformation in MSCs[15-18]. The actin cytoskeleton regulates the mechanical behavior of cells through its assembly and disassembly. In undifferentiated MSCs, long and thin actin filaments line parallel to the long axis, but in adipogenic differentiation, the actin cytoskeleton reorganizes into a disorganized meshwork surrounding the oil droplet[19]. Notably, zinc finger CCCH-type containing 10 has been proven to be fundamental for adipogenic differentiation by promoting F-actin/mitochondria dynamics to safeguard proper energy metabolism and favor lipid accumulation[20]. The main regulating molecule in the actin cytoskeleton remodeling process is the Rho family of GTPase, including over 20 distinct kinds of Rho family members (RhoA, Rac1, and Cdc42, and *etc.*), which can interact with downstream effector proteins. RhoA mainly regulates the activity of myosin II to generate cellular force and tension in cells. The activation of RhoA is achieved by mechanical stress, and the inhibition of RhoA or its downstream effectors, as well as mammalian diaphanous protein kinase and Rho-associated coiled coil containing protein kinase (ROCK), leads to the reorganization of stress fibers[21]. Several studies have suggested that mechanical stress[22] and chemically induced actin depolymerization[23] favor adipogenesis. The abovementioned kinases (Rho and ROCK) may be regulators of osteoblast differentiation in MSCs[24]. These signaling pathways may play a role not only by changing the cytoskeletal organization of actin but also through the FAK, JNK, and p38 MAPK signaling pathways[25]. Moreover, biomaterials[26] and pathogens[27] induce actin remodeling during MSC differentiation.

TGF-β/SMAD signaling

Recently, the TGF-β superfamily has been shown to be crucial in controlling the adipogenesis of MSCs. In order to activate intracellular downstream SMAD family proteins, ligands implicated in TGF-β/SMAD signaling, including activin, inhibin, BMPs, growth differentiation factors (GDFs), TGF-β, Nodal, and others, attach to their cell membrane receptors. TGF-β/SMAD signaling has dual effects on the adipocyte differentiation process, specifically on the adipocyte commitment of MSCs[28]. TGF-β ligands such as TGF-β, myostatin, and GDF11 bind to cell membrane receptors in the TGF-β/SMAD signaling pathway to phosphorylate intracellular downstream SMAD2/3 (R-SMADs), and BMP ligands such as BMP2, BMP4, and BMP7 phosphorylate SMAD1/5/8 (R-SMADs). Activated R-SMADs binding with SMAD4 as a complex translocate into the nucleus to control the expression of target genes. After the genes respond to TGF-β/SMAD signaling, the R-SMAD/SMAD4 complex in the nucleus is depolymerizes and the proteins reenter the cytoplasm. TGF-β/SMAD signaling is adversely regulated by I-SMADs including SMAD6 and SMAD7. Upon transcriptional activation by TGF-β/SMAD signaling, SMAD7 shuttles from the nucleus to the cytoplasm to prevent R-SMAD phosphorylation and SMAD6 competes with SMAD1 to bind to SMAD4[28].

However, other studies have demonstrated that TGF-β signaling promotes the proliferation of MSCs and suppresses the adipocyte commitment of MSCs by inhibiting CEBPα and PPARγ expression. These discrepant results regarding adipocyte commitment may be related to the origins of the bone marrow-derived MSCs (BMSCs) isolated from different species, including mice and humans[29] as MSC origin can influence adipocyte commitment through TGF-β signaling. Notably, various clones isolated from human BMSC lines indeed exhibit different differentiation capacities. A recent study on MSC heterogeneity also suggested that different BAMBI expression levels interfere with the adipogenic capacity of cells[30]. In addition, a recent novel study reported the epigenetic mechanism of adipogenic commitment under TGF-β/SMAD signaling[31].

BMP signaling

BMP2/4/7 use SMAD1/5/8 signaling to regulate adipocyte commitment. BMP2, BMP4, and myostatin ligands affect the adipocyte commitment of MSCs. Even the differentiation of adipocyte lineage and brown adipocytes formation in MSCs

are directly induced by BMP4 signaling. Both BMP2 and BMP4 signaling activate PPARγ expression to induce adipocyte commitment.

The role of BMP4 signaling has been validated in the commitment process of MSCs. Several studies have indicated that BMP4 can induce the commitment of the pluripotent mouse embryonic fibroblast line C3H10T1/2 to the adipocyte lineage. Upon BMP4 treatment, the expression of the adipocyte markers CEBPα, PPARγ, and adipocyte protein 2 (AP2) was detected in C3H10T1/2 cells, suggesting that these cells can differentiate into adipocytes. When C3H10T1/2 cells pretreated with BMP4 were subcutaneously implanted into thymic mice, they developed into tissue undistinguishable from adipose tissue.

BMP7 also plays an important role in brown adipocyte lineage determination. This signal triggers C3H10T1/2 cells to commit to a brown adipocyte lineage with a significant increases in lipid accumulation and uncoupling protein 1 expression. BMP7 stimulates cell proliferation and differentiation in mouse and human adult MSCs. However, different dosages of BMP seem to result in distinct effects on adipogenesis in mouse BMSCs. Low concentrations of BMP7 stimulated adipocyte differentiation, whereas higher dosages inhibited adipogenesis in mice. In human BMSCs, BMP7 promoted adipogenic differentiation rather than osteogenic or chondrogenic lineage development in high-density micromass culture.

However, the role of BMP2 signaling in adipocyte commitment in MSCs has not been determined. Several studies have shown that BMP2 signaling can induce C3H10T1/2 cells to commit to the adipocyte lineage[32]. Nonetheless, adipogenesis, chondrogenesis, and osteogenesis are plastical. The addition of low-level BMP2 to C3H10T1/2 cells favored adipogenesis[32]. However, treatment with BMP2 enhanced osteoblast commitment and inhibited late adipocyte maturation in human marrow stromal precursors. Mechanistically, similar to BMP4, BMP2 activated the expression and phosphorylation of SMAD1/5/8, which formed a complex with SMAD4. Under these condition, BMP2 suppressed adipogenesis by decreasing the leptin concentration and preventing the formation of cytoplasmic lipid droplets.

NONCODING RNAS

Noncoding RNAs, especially microRNAs (miRNAs) and long-chain noncoding RNAs (lncRNAs), also participate in the adipogenic differentiation of MSCs by interfering with signaling pathways and/or transcription factors to regulate adipogenic differentiation. First, miRNAs can positively regulate adipogenesis. miR-135a-5p promotes adipogenesis in human adipose-derived MSCs (ADMSCs) by targeting LATS1 and MOB1B expression, thereby enhancing the HIPPO signaling pathway. During the process of age-related adipogenic differentiation, the levels of both miR-188 and miR-141-3p were markedly greater in aged human BMSCs. Moreover, mice with transgenic overexpression of miR-188 in osterix$^+$ osteoprogenitors had more age-associated bone loss and fat accumulation in the bone marrow than did wild-type mice [33]. However, Periyasamy-Thandavan *et al*[34] reported that human BMSCs treated with miR-141-3p exhibited decreased BMP-2 and RUNX-2 expression and increased C/BEPa2, suggesting the induction of adipocyte lineage differentiation instead of osteogenic differentiation. Interestingly, a recent study combining miRNA chip and RNA-seq data to analyze the correlation between miRNA and mRNA expression profiles during BMSC lipogenic differentiation showed that miR-140-5p may play an important role in regulating its target gene LIFR during adipogenic differentiation[6].

Other miRNAs indeed negatively regulate adipogenic differentiation in MSCs. miR-27b was the first miRNA discovered to function as a negative regulator of adipogenesis in humans[35]. The expression of miR-27b decreased during the adipogenesis of human adipose-derived stem cells (hADSCs). Further binding and luciferase reporter assays demonstrated that miR-27b directly bound to the designated miR-27b response element in the 3′ untranslated region (UTR) of human PPARγ to reduce its expression at the protein level, thus inhibiting adipogenesis. Additionally, the mutual adjustment of miR-27b and lipoprotein lipase expression can effectively regulate the adipogenic differentiation of hASCs[36]. In addition, miR27a, another family member of miR27, is inversely correlated with adipogenic markers such as PPARγ and adiponectin[37]. *In vitro* experiments showed that overexpression of miR-130a increased osteogenic differentiation and attenuated adipogenic differentiation in BMSCs. Furthermore, miR-130a promotes osteoblastic differentiation by negatively regulating Smurf2 expression and suppresses adipogenic differentiation of BMSCs by targeting PPARγ[38].

Interestingly, certain miRNAs can bidirectionally regulate osteogenic and adipogenic differentiation in BMSCs. Li *et al* [39] reported that miR-149-3p expression decreased following adipogenic differentiation but increased after osteogenic differentiation in BMSCs. Further study demonstrated that miR-149-3p manipulated alternative lineage choices between adipocytes and osteoblasts by directly targeting FTO, which is involved in adipogenesis mainly by regulating fat accumulation. Additionally, miR-21 overexpression was found to enhance osteogenic differentiation and inhibit adipogenic differentiation *via* the PI3K/AKT axis in rat BMSCs[40].

Recently, lncRNAs have also been found to be involved in regulating the adipogenic differentiation of MSCs[41]. For example, lncRNA ADINR promotes adipogenesis by binding PAl and recruiting the mll3/4 histone methyltransferase complex. In the process of fat formation, the 4-site trimethylation of the histone H3 lysine residue (H3K4me3) increases, and the H3K27me3 histone modification at the locus of the recombinant human transcription factor CCAAT enhancer binding protein reduces[42]. The lncRNA HOTAIR can affect DNA methylation changes at its binding sites to inhibit hBMSC adipogenic differentiation[43]. Huang *et al*[32] showed that the expression levels of the lncRNAs H19 and miR-675 were significantly downregulated during MSC differentiation into adipocytes, whereas adipogenesis was inhibited if H19 and miR-675 were overexpressed. The expression of another lncRNA from peroxidase, Plnc, increased during the adipose differentiation of MSCs according to microarray analysis. It was confirmed that Plncl enhanced the promoter activity of PPARγ2 by weakening the methylation state of the PPARγ2 promoter. The lncRNA ZFAS1 affects the

osteogenic and adipogenic differentiation of mouse BMSCs by sponging miR-499 and upregulating ephrin type-A receptor 5[44]. To date, there are few reports on the inhibition of MSC adipogenic differentiation by lncRNAs[45].

DNA METHYLATION

Epigenetic regulation, especially DNA methylation, plays an important role in regulating the differentiation of MSCs into adipocytes[46]. Generally, DNA methylation is carried out by three main types of methyltransferases. DNMT3a/3b catalyze *de novo* DNA methylation, and DNMT1 maintains DNA methylation in somatic cells. Knockdown of the DNA demethylase ALKBH1 was demonstrated to inhibit adipogenic differentiation *via* regulation of HIF-1 signaling in hMSCs [47,48].

Although similar global methylation profiles are normally observed in terminal adipocytes, many differences exist in the expression of DNA methylation genes in MSCs from different tissues. In pigs, the global methylation level was greater in undifferentiated BMSCs than in ADMSCs[49]. The transcription level of the DNMT1 gene increased at the beginning of adipogenesis and then decreased, while the expression levels of the DNMT3a and DNMT3b transcripts increased during differentiation. All the examined MBD genes exhibited similar expression patterns in ADMSCs and BMSCs. However, the transcript abundances of UHRF1 and CBX5 decreased in both systems. The changes in the expression patterns of these genes point to the dynamic nature of DNA methylation during porcine adipogenesis.

Further studies support the notion that tissue source determines the differentiation potential and level of DNA methylation of MSCs. In a study comprehensively characterizing the DNA methylation profiling of osteoblast and adipocyte differentiation, Hou *et al*[50] showed that MSCs from psoriatic derma have a distinguishable promoter methylation profile compared with those from normal derma. Site-specific CpG methylation in the CXCL14 promoter has been confirmed in umbilical cord-derived MSCs[51] and is associated with altered gene expression. Such changes in methylation are evident in LBW infant-derived umbilical cords and may indicate future metabolic compromise through CXCL14. Xu *et al*[52] evaluated the adipogenic differentiation potential of different MSCs and reported that BMSCs had lower adipogenic differentiation potential than ADMSCs. Furthermore, their results suggest that DNA demethylation could be involved, at least partially, in the regulation of Runx2 and PPARγ in ADMSCs and BMSCs.

How does DNA methylation dictate adipocyte differentiation in MSCs with multiple differentiation potentials? In fact, DNA methylation regulates the orientational differentiation balance through particular sequences-transposons, imprinted genes and pluripotency-associated genes. Although Marofi *et al*[53] revealed that methylation of the promoter regions of the Sox9, OCN, and PPARγ2 genes might be one of the main mechanisms adjusting gene expression during the osteoblastic differentiation of MSCs, H3K36me3, catalyzed by the histone methyltransferase SET-domain-containing 2 (SETD2), regulates the lineage commitment of BMSCs. Deletion of Setd2 in mouse BMSCs through conditional Cre expression driven by the Prx1 promoter resulted in bone loss and marrow adiposity. Loss of Setd2 in BMSCs *in vitro* facilitated the differentiation of adipocytes rather than osteoblasts. Furthermore, overexpression of lipopolysaccharide-binding protein partially rescued the lack of osteogenesis and enhanced adipogenesis resulting from the absence of Setd2 in BMSCs. In addition, DNMT3B-mediated DNA methylation of phosphatase and tensin homolog (PTEN) is a key regulator of dental pulp-derived MSC and BMSC lineage commitment. Moreover, the lysine methyltransferase G9a is needed for DNMT3B-mediated PTEN suppression, which activates AKT to promote adipogenesis and inhibit osteogenesis[54].

Zych *et al*[55] determined the effects of these epigenetic mechanisms on adipocyte differentiation in BMSCs and ADSCs using the demethylating agent 5-aza-2′-deoxycytidine (5azadC). The results showed that adipogenic differentiation decreased in a dose-dependent manner concomitant with the downregulation of the expression of the adipocyte genes PPARG and FABP4, and the expression of the antiadipocyte gene GATA2 was induced in the cultures treated with 5azadC. Additionally, the methyltransferase enhancer of zeste homology 2 (EZH2) trimethylates H3K27me3 on chromatin, and this repressive mark is removed by lysine demethylase 6A (KDM6A). Both Ezh2 and Kdm6a were shown to affect the expression of master regulatory genes involved in adipogenesis and osteogenesis and H3K27me3 on the promoters of master regulatory genes. These findings demonstrate an important epigenetic switch centered around H3K27me3, which dictates MSC lineage determination[56]. Furthermore, using methyl-DNA immunoprecipitation (MeDIP) and microarray hybridization, the potential of MSC multidirectional differentiation regulated by DNA methylation through imprinted and pluripotency-associated genes can be predicted. Empolying MeDIP methodology, Choi *et al*[57] reported that the impaired adipogenic differentiation of senescent MSCs at P15 was due to changes in CpG methylation in the LEP promoter.

ACETYLATION MODIFICATION

Acetylation and deacetylation are the key cotranslational and posttranslational modifications (PTMs) that integrate metabolic flux and physiological processes within cells, including circadian rhythm, cell cycle progression and energy production[58]. Lysine acetylation is a kind of PTM of proteins, the reactions of which are typically catalyzed by lysine acetyltransferases (KATs). KATs are classified into three families: Gcn5/PCAF (histone KAT KAT2A/2B), p300/CBP (histone KAT KAT3A/3B), and the MYST family[58,59]. Acetylation of the histone H3 N-terminal tail is catalyzed mainly by KAT Gcn5/PCAF as well as p300/CBP, and the H4 tail is predominantly acetylated by the MYST family of KATs. Adipocyte-specific genes undergo selective induction of histone hyperacetylation at their promoter regions, which leads to their upregulation during adipogenesis. Yoo *et al*[60] showed that the level of H3K9 acetylation at the promoters of

ADD1/SREBP1c, adiponectin, aP2, C/EBPa and PPARγ was markedly increased after adipogenic differentiation. These results showed that acetylation is fundamentally involved in the regulation of adipogenesis.

Acetylation

The master adipogenic transcription factor gene PPARγ is regulated by all three families of KATs. Double knockout of Gcn5/PCAF inhibits the expression of the master adipogenic transcription factor gene PPARγ, thereby preventing adipocyte differentiation[61]. Specifically, Gcn5/PCAF facilitates adipogenesis through the regulation of PPARγ and Prdm16 expression[61]. HIV-1 Tat-interacting protein 60 (Tip60) is a member of the MYST family of KATs that can positively regulate PPARγ transcriptional activity. In mature 3T3-L1 adipocytes, Tip60 interacts with PPARγ and is recruited to PPARγ target genes. Moreover, a reduction in the Tip60 protein can inhibit the differentiation of 3T3-L1 preadipocytes[62]. P300/CBP can regulate glucose and lipid metabolism by acetylating nuclear receptors, such as the bile acid receptor (farnesoid Xactivated receptor)[63], PPARγ, and cytosolic PEPCK-C[64]. Mechanistically, p300/CBP interacts with and enhances the transcriptional activity of PPARγ by acetylating nuclear receptors. Furthermore, p300 acetylates PEPCK-C, inducing its degradation and attenuating gluconeogenesis[64]. Thus, p300/CBP plays an essential role in adipocyte differentiation.

In addition to PPARγ, the acetylation of other genes is involved in adipocyte differentiation. Acetylation of malate dehydrogenase 1 and 2 (MDH1 and MDH2) promotes adipogenic differentiation by activating their enzymatic activity and increasing the intracellular levels of NADPH in 3T3-L1 preadipocytes[65,66]. Following p300 recruitment for lysine acetylation, the gene-repressive activity and function of RIP140 are enhanced as fat accumulates in differentiated adipocytes[67]. Additionally, acetylation of α-tubulin is upregulated during adipogenesis under the control of the KAT MEC-17, SIRT2 and histone deacetylase (HDAC)6, and adipocyte development is dependent on α-tubulin acetylation[68]. Additionally, cavin-1 is acetylated at lysines 291, 293, and 298 (3K) by GCN5 as an KAT to positively regulate lipolysis in 3T3-L1 and zebrafish[69].

Decetylation

Deacetylation is mainly mediated by HDACs, including sirtuins, which use NAD^+ as a coenzyme. All lysine deacetylases (KDACs) can be divided into four types: Class I KDACs (HDAC1, HDAC2, HDAC3, and HDAC8), class II KDACs (class IIa: HDAC4, HDAC5, HDAC7, and HDAC9; class IIb: HDAC6 and HDAC10), class III KDACs (Sirt1-7), and class IV KDACs (including only one member, HDAC11). HDAC activity is essential for maintaining the preadipocyte pool of the adipogenic lineage. Thus, HDAC inhibition in stem cells has the potential to block preadipocyte generation and thus overall adipogenesis[70]. Adipocyte differentiation is accompanied by decreases in the expression levels of several histone deacetylases, including HDAC1, HDAC2, and HDAC5[71]. Moreover, HDAC1 knockdown promoted adipogenesis in 3T3-L1 cells, and vice versa[60]. HDAC3 has been found to regulate mitochondrial activity and glucose or lipid metabolism in the liver, fat and muscle[72-75]. PPARα-interfered with fatty acid and lipid metabolism, and myocardial lipids accumulated in muscle-specific Hdac3-/- mice receiving a chow diet[72,74]. Furthermore, HDAC3 controls the circadian rhythm of hepatic lipid metabolism[76] and gluconeogenesis[77], which is mediated by the nuclear receptors Rev-erbAα and PPARγ. Finally, HDAC3 can be recruited to the promoter of the PPARγ gene, preventing its expression to regulate adipocyte differentiation in adipose tissue. In addition, high expression levels of HDAC5 and HDAC6 are needed for adequate adipocyte function. In contrast, HDAC9 has been reported to inhibit adipogenesis. In the case of a chronic high-fat diet, proper adipogenic differentiation is impaired, and the expression of the negative regulator of adipogenic HDAC9 is increased. Ablation of HDAC9 in mice can prevent such adverse changes, including weight gain, impaired glucose tolerance, and insulin insensitivity[78-80].

The class III sirtuin-mediated deacetylation reaction couples lysine deacetylation to NAD^+ hydrolysis[81]. Many genes related to adipocyte differentiation, such as glucose transporters type 4, AP2 and fatty acid synthase genes, are regulated by Sirt2. This coordinated regulation is attributed to the direct interaction between Sirt2 and acetylation patterns involved in controlling lipogenesis[82]. Sirt2 has also been shown to bind directly to FoxO1 and enhance insulin-stimulated FoxO1 phosphorylation/acetylation and activity[83]. Thus, Sirt2 acts as an important regulator of adipocyte differentiation. SIRT-1 facilitates the deacetylation and interaction of PPARγ and the thermogenic transcription factor PR domain containing zinc finger protein 16 (PRDM-16)[84]. Along with SIRT-1, PRDM-16 regulates the brown fat lineage. Sirt1 also promotes fat mobilization by inhibiting PPARγ in adipocytes[85]. For example, its expression can regulate lipogenesis in 3T3-L1 cells. During the process of adipocyte differentiation, Sirt1 upregulation may promote lipolysis and fat loss. Decreased Sirt1 increases the expression of the adiponectin gene through the FoxO1-C/EBPα transcription complex[85-87].

Interestingly, noncoding RNAs cooperatively interact with KDACs to regulate adipogenic processes. miR-675 can target the 3′ UTRs of HDAC4-6 transcripts, which lead to the deregulation of HDAC4-6 and fat formation. When HDACs are inhibited, the occupancy of H19 and CCCTC binding factor can be reduced, and thus, H1 can be downregulated[88]. The regulation of adipogenesis and gluconeogenesis by KDACs, KATs and noncoding RNAs is summarized in Figure 2.

ADIPOGENESIS OF MSCS AND DISEASES

MSCs are believed to exist in every organ in the body. Dysfunction or abnormal differentiation of these cells into adipocytes tends to be associated with various diseases. For example, MSCs from acute graft-*versus*-host disease patients showed reduced adipogenic differentiation in culture[89]. Even under natural physiological conditions, aging can reduce the adipogenic differentiation responses of BMSCs, myeloid-derived suppressor cells, and ASCs, with the most noticeable

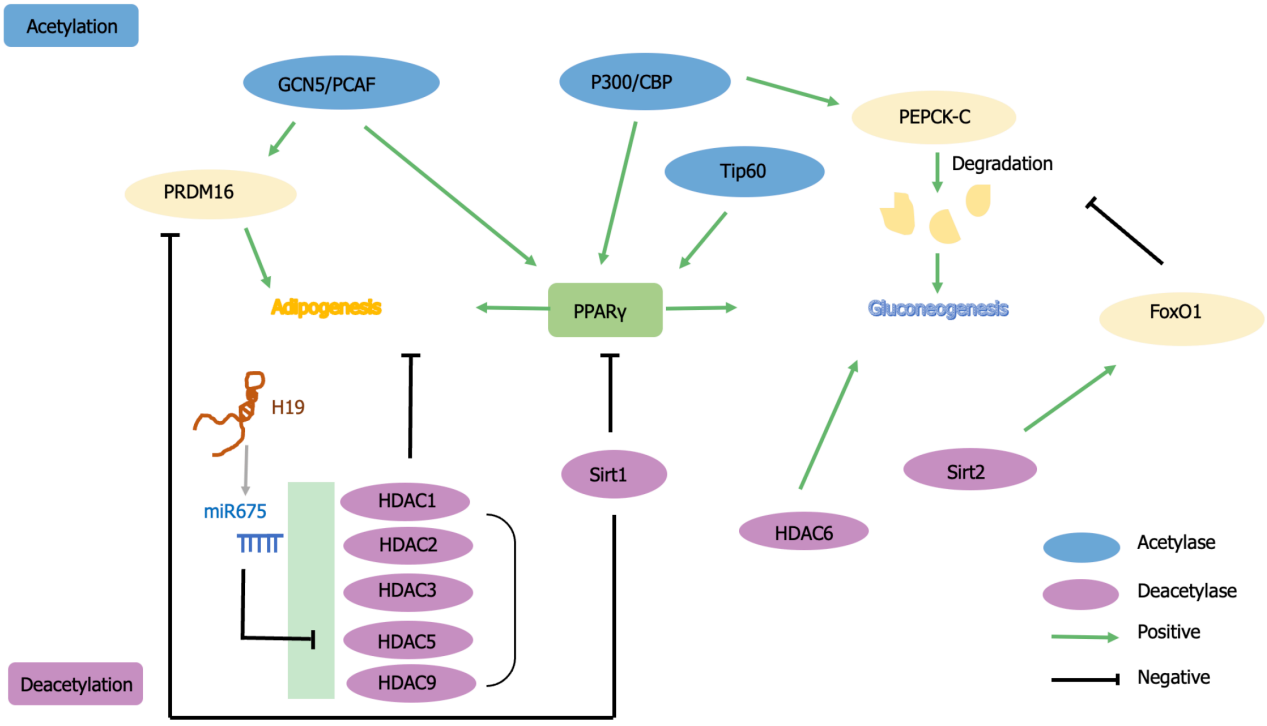

Figure 2 Regulation of adipogenesis and gluconeogenesis by lysine deacetylases, acetyltransferases and noncoding RNAs. Lysine deacetylases (KDACs) and acetyltransferases (KATs) are important regulators of adipocyte differentiation and gluconeogenesis. Peroxisome proliferation activator receptor gamma is acetylated by Gcn5/PCAF, p300/CBP and Tip60 but deacetylated by Sirt1. In addition, Gcn5/PCAF is also regulated Prdm16 expression to influence adipogenesis. Histone deacetylases (HDACs) 1, 2, 3, 5 and 9 redundantly regulate adipogenesis. Moreover, noncoding RNAs cooperatively interact with KDACs to regulate the adipogenic process. H19/miR-675 can inhibit HDAC5 expression. Hence, KDACs and KATs can regulate lipid metabolism. PEPCK-C is acetylated by p300 to induce its degradation and attenuate gluconeogenesis. Conversely, PEPCK-C is deacetylated and stabilized by Sirt2 through Sirt2 deacetylase. HDAC6 also plays an important role in gluconeogenesis regulation. PPARγ: Peroxisome proliferation activator receptor gamma; HDAC: Histone deacetylase; PRDM16: PR domain containing zinc finger protein 16.

reduction in adipogenesis occurring in ASCs[90]. Although MSC transplantation has shown beneficial effects in treating autoimmune diseases, the ability of the BAMBI^{high}MFGE8^{high} MSC subpopulation, which has limited adipogenic differentiation potential, to alleviate SLE is compromised[30].

In contrast, the adipogenic differentiation abilities of MSCs from both polycystic ovary syndrome patients and gestational diabetes mellitus patients were greater than that of MSCs from healthy controls[91,92]. Several studies suggest that pathological conditions affect MSC differentiation. In a hypoperfusion-induced abdominal aortic aneurysm model, perivascular adipose tissue plays important roles in the differentiation of MSCs into adipocytes in response to vascular hypoperfusion[93]. Additionally, abnormal adipogenic differentiation can cause disease. In a glomerulonephritis model, the early beneficial effect of MSCs in preserving damaged glomeruli and maintaining renal function was offset by long-term partial maldifferentiation of intraglomerular MSCs into adipocytes accompanied by glomerular sclerosis[94].

The adipogenic and osteogenic differentiation programs are competitively balanced in MSCs. Many hub or early-responder signaling pathways control the osteogenic and adipogenic fates of MSCs. For example, Wnt signaling upregulates Runx2 expression to promote osteoblast differentiation, which also inhibits PPARγ expression to suppress adipogenic differentiation in BMSCs[95]. In addition, HH signaling and PI3K-Akt are key active pathways involved in the early stages of cell osteogenic differentiation that simultaneously inhibit adipogenesis[96]. A decrease in the balance between the adipogenic and osteogenic potential of MSCs is also often associated with disease occurrence and/or development. In clinical osteoporosis samples, overexpression of miR-10b enhanced osteogenic differentiation and inhibited adipogenic differentiation of hADSCs *in vitro*, which was negatively correlated with the expression of the markers CEBPα, PPARγ and AP2. More recently, the lncRNA NEAT1 was shown to act as a key bone-fat switch in aged BMSCs by orchestrating mitochondrial function and BMSC multipotency[97].

However, the therapeutic potential of MSCs in cancer has been controversial. Some studies have revealed that these compounds can promote cancer pathogenesis, but others have indicated that they have suppressive effects on cancer cells. Hence, additional evidence is needed to understand the role of MSC differentiation in cancer therapy.

CONCLUSION

Much encouraging progress has recently been made in understanding how MSCs can differentiate into adipocytes through various signaling pathways, noncoding RNAs, and the epigenetic regulation of phosphorylation, methylation and acetylation. However, there is still a lack of evidence on the importance of gernerating a comprehensive map of

adipogenesis in MSCs, especially for the early commitment process from MSCs to preadipocytes. The low efficiency of adipogenic differentiation of MSCs in culture has hampered our understanding of this process. Dissecting the heterogeneity of MSCs will allow us to clearly elucidate the mechanism of adipogenic differentiation. Hopefully, these problems will be addressed with the help of fast-advancing single-cell sequencing techniques, which will shed light on the full path of MSC differentiation into adipocytes, facilitating MSC-based applications in biomedicine.

FOOTNOTES

Co-first authors: Shan-Shan Liu and Xiang Fang.

Author contributions: Liu SS and Fang X contributed equally to write the paper; Wen X, Liu JS, Alip M, Sun T, and Wang YY provided data; Chen HW designed the review and were responsible for the final proofreading; and all authors have read and approve the final manuscript.

Supported by the National Natural Science Foundation of China, No. 82271843 and 31700779; the Key Project supported by Medical Science and Technology Development Foundation, Nanjing Department of Health, No. ZKX20019; and the Natural Science Foundation of Jiangsu Province, No. BK20200137.

Conflict-of-interest statement: All the authors report no relevant conflicts of interest for this article.

Country/Territory of origin: China

ORCID number: Shan-Shan Liu 0000-0003-1220-8514; Xiang Fang 0000-0002-7407-3769; Hong-Wei Chen 0000-0002-9400-6053.

S-Editor: Wang JJ
L-Editor: A
P-Editor: Zhang XD

REFERENCES

1 **Wang D**, Li J, Zhang Y, Zhang M, Chen J, Li X, Hu X, Jiang S, Shi S, Sun L. Umbilical cord mesenchymal stem cell transplantation in active and refractory systemic lupus erythematosus: a multicenter clinical study. *Arthritis Res Ther* 2014; **16**: R79 [PMID: 24661633 DOI: 10.1186/ar4520]
2 **Ullah I**, Subbarao RB, Rho GJ. Human mesenchymal stem cells - current trends and future prospective. *Biosci Rep* 2015; **35** [PMID: 25797907 DOI: 10.1042/BSR20150025]
3 **Dominici M**, Le Blanc K, Mueller I, Slaper-Cortenbach I, Marini F, Krause D, Deans R, Keating A, Prockop Dj, Horwitz E. Minimal criteria for defining multipotent mesenchymal stromal cells. The International Society for Cellular Therapy position statement. *Cytotherapy* 2006; **8**: 315-317 [PMID: 16923606 DOI: 10.1080/14653240600855905]
4 **Komori T**. Regulation of osteoblast differentiation by transcription factors. *J Cell Biochem* 2006; **99**: 1233-1239 [PMID: 16795049 DOI: 10.1002/jcb.20958]
5 **Wang ZH**, Li XL, He XJ, Wu BJ, Xu M, Chang HM, Zhang XH, Xing Z, Jing XH, Kong DM, Kou XH, Yang YY. Delivery of the Sox9 gene promotes chondrogenic differentiation of human umbilical cord blood-derived mesenchymal stem cells in an in vitro model. *Braz J Med Biol Res* 2014; **47**: 279-286 [PMID: 24652327 DOI: 10.1590/1414-431X20133539]
6 **Yi SW**, Kim HJ, Oh HJ, Shin H, Lee JS, Park JS, Park KH. Gene expression profiling of chondrogenic differentiation by dexamethasone-conjugated polyethyleneimine with SOX trio genes in stem cells. *Stem Cell Res Ther* 2018; **9**: 341 [PMID: 30526665 DOI: 10.1186/s13287-018-0998-7]
7 **Mota de Sá P**, Richard AJ, Hang H, Stephens JM. Transcriptional Regulation of Adipogenesis. *Compr Physiol* 2017; **7**: 635-674 [PMID: 28333384 DOI: 10.1002/cphy.c160022]
8 **Zhuang H**, Zhang X, Zhu C, Tang X, Yu F, Shang GW, Cai X. Molecular Mechanisms of PPAR-γ Governing MSC Osteogenic and Adipogenic Differentiation. *Curr Stem Cell Res Ther* 2016; **11**: 255-264 [PMID: 26027680 DOI: 10.2174/1574888x10666150531173309]
9 **Dey S**, Goswami S, Eisa A, Bhattacharjee R, Brothag C, Kline D, Vijayaraghavan S. Cyclic AMP and glycogen synthase kinase 3 form a regulatory loop in spermatozoa. *J Cell Physiol* 2018; **233**: 7239-7252 [PMID: 29574946 DOI: 10.1002/jcp.26557]
10 **Mitani T**, Takaya T, Harada N, Katayama S, Yamaji R, Nakamura S, Ashida H. Theophylline suppresses interleukin-6 expression by inhibiting glucocorticoid receptor signaling in pre-adipocytes. *Arch Biochem Biophys* 2018; **646**: 98-106 [PMID: 29625124 DOI: 10.1016/j.abb.2018.04.001]
11 **Parra LG**, Erjavec LC, Casali CI, Zerpa Velazquez A, Weber K, Setton-Avruj CP, Fernández Tome MDC. Cytosolic phospholipase A(2) regulates lipid homeostasis under osmotic stress through PPARγ. *FEBS J* 2023 [PMID: 37947039 DOI: 10.1111/febs.16998]
12 **Buelvas N**, Ugarte-Vio I, Asencio-Leal L, Muñoz-Uribe M, Martin-Martin A, Rojas-Fernández A, Jara JA, Tapia JC, Arias ME, López-Muñoz RA. Indomethacin Induces Spermidine/Spermine-N(1)-Acetyltransferase-1 *via* the Nucleolin-CDK1 Axis and Synergizes with the Polyamine Oxidase Inhibitor Methoctramine in Lung Cancer Cells. *Biomolecules* 2023; **13** [PMID: 37759783 DOI: 10.3390/biom13091383]

13 **Ige S**, Alaoui K, Al-Dibouni A, Dallas ML, Cagampang FR, Sellayah D, Chantler PD, Boateng SY. Leptin-dependent differential remodeling of visceral and pericardial adipose tissue following chronic exercise and psychosocial stress. *FASEB J* 2024; **38**: e23325 [PMID: 38117486 DOI: 10.1096/fj.202300269RRR]

14 **Mishra P**, Martin DC, Androulakis IP, Moghe PV. Fluorescence Imaging of Actin Turnover Parses Early Stem Cell Lineage Divergence and Senescence. *Sci Rep* 2019; **9**: 10377 [PMID: 31316098 DOI: 10.1038/s41598-019-46682-y]

15 **Khan AU**, Qu R, Fan T, Ouyang J, Dai J. A glance on the role of actin in osteogenic and adipogenic differentiation of mesenchymal stem cells. *Stem Cell Res Ther* 2020; **11**: 283 [PMID: 32678016 DOI: 10.1186/s13287-020-01789-2]

16 **Müller P**, Langenbach A, Kaminski A, Rychly J. Modulating the actin cytoskeleton affects mechanically induced signal transduction and differentiation in mesenchymal stem cells. *PLoS One* 2013; **8**: e71283 [PMID: 23923061 DOI: 10.1371/journal.pone.0071283]

17 **Zhao Y**, Sun Q, Wang S, Huo B. Spreading Shape and Area Regulate the Osteogenesis of Mesenchymal Stem Cells. *Tissue Eng Regen Med* 2019; **16**: 573-583 [PMID: 31824820 DOI: 10.1007/s13770-019-00213-y]

18 **Kilian KA**, Bugarija B, Lahn BT, Mrksich M. Geometric cues for directing the differentiation of mesenchymal stem cells. *Proc Natl Acad Sci U S A* 2010; **107**: 4872-4877 [PMID: 20194780 DOI: 10.1073/pnas.0903269107]

19 **Rodríguez JP**, González M, Ríos S, Cambiazo V. Cytoskeletal organization of human mesenchymal stem cells (MSC) changes during their osteogenic differentiation. *J Cell Biochem* 2004; **93**: 721-731 [PMID: 15660416 DOI: 10.1002/jcb.20234]

20 **Audano M**, Pedretti S, Ligorio S, Gualdrini F, Polletti S, Russo M, Ghisletti S, Bean C, Crestani M, Caruso D, De Fabiani E, Mitro N. Zc3h10 regulates adipogenesis by controlling translation and F-actin/mitochondria interaction. *J Cell Biol* 2021; **220** [PMID: 33566069 DOI: 10.1083/jcb.202003173]

21 **Gordon WR**, Zimmerman B, He L, Miles LJ, Huang J, Tiyanont K, McArthur DG, Aster JC, Perrimon N, Loparo JJ, Blacklow SC. Mechanical Allostery: Evidence for a Force Requirement in the Proteolytic Activation of Notch. *Dev Cell* 2015; **33**: 729-736 [PMID: 26051539 DOI: 10.1016/j.devcel.2015.05.004]

22 **Lu J**, Fan Y, Gong X, Zhou X, Yi C, Zhang Y, Pan J. The Lineage Specification of Mesenchymal Stem Cells Is Directed by the Rate of Fluid Shear Stress. *J Cell Physiol* 2016; **231**: 1752-1760 [PMID: 26636289 DOI: 10.1002/jcp.25278]

23 **Samsonraj RM**, Paradise CR, Dudakovic A, Sen B, Nair AA, Dietz AB, Deyle DR, Cool SM, Rubin J, van Wijnen AJ. Validation of Osteogenic Properties of Cytochalasin D by High-Resolution RNA-Sequencing in Mesenchymal Stem Cells Derived from Bone Marrow and Adipose Tissues. *Stem Cells Dev* 2018; **27**: 1136-1145 [PMID: 29882479 DOI: 10.1089/scd.2018.0037]

24 **Prowse PD**, Elliott CG, Hutter J, Hamilton DW. Inhibition of Rac and ROCK signalling influence osteoblast adhesion, differentiation and mineralization on titanium topographies. *PLoS One* 2013; **8**: e58898 [PMID: 23505566 DOI: 10.1371/journal.pone.0058898]

25 **Sun B**, Qu R, Fan T, Yang Y, Jiang X, Khan AU, Zhou Z, Zhang J, Wei K, Ouyang J, Dai J. Actin polymerization state regulates osteogenic differentiation in human adipose-derived stem cells. *Cell Mol Biol Lett* 2021; **26**: 15 [PMID: 33858321 DOI: 10.1186/s11658-021-00259-8]

26 **Di Cio S**, Iskratsch T, Connelly JT, Gautrot JE. Contractile myosin rings and cofilin-mediated actin disassembly orchestrate ECM nanotopography sensing. *Biomaterials* 2020; **232**: 119683 [PMID: 31927180 DOI: 10.1016/j.biomaterials.2019.119683]

27 **Sultana H**, Neelakanta G, Kantor FS, Malawista SE, Fish D, Montgomery RR, Fikrig E. Anaplasma phagocytophilum induces actin phosphorylation to selectively regulate gene transcription in Ixodes scapularis ticks. *J Exp Med* 2010; **207**: 1727-1743 [PMID: 20660616 DOI: 10.1084/jem.20100276]

28 **Li SN**, Wu JF. TGF-β/SMAD signaling regulation of mesenchymal stem cells in adipocyte commitment. *Stem Cell Res Ther* 2020; **11**: 41 [PMID: 31996252 DOI: 10.1186/s13287-020-1552-y]

29 **Elsafadi M**, Manikandan M, Atteya M, Abu Dawud R, Almalki S, Ali Kaimkhani Z, Aldahmash A, Alajez NM, Alfayez M, Kassem M, Mahmood A. SERPINB2 is a novel TGFβ-responsive lineage fate determinant of human bone marrow stromal cells. *Sci Rep* 2017; **7**: 10797 [PMID: 28883483 DOI: 10.1038/s41598-017-10983-x]

30 **Chen H**, Wen X, Liu S, Sun T, Song H, Wang F, Xu J, Zhang Y, Zhao Y, Yu J, Sun L. Dissecting Heterogeneity Reveals a Unique BAMBI(high) MFGE8(high) Subpopulation of Human UC-MSCs. *Adv Sci (Weinh)* 2022; **10**: e2202510 [PMID: 36373720 DOI: 10.1002/advs.202202510]

31 **Elsafadi M**, Shinwari T, Al-Malki S, Manikandan M, Mahmood A, Aldahmash A, Alfayez M, Kassem M, Alajez NM. Convergence of TGFβ and BMP signaling in regulating human bone marrow stromal cell differentiation. *Sci Rep* 2019; **9**: 4977 [PMID: 30899078 DOI: 10.1038/s41598-019-41543-0]

32 **Huang HY**, Hu LL, Song TJ, Li X, He Q, Sun X, Li YM, Lu HJ, Yang PY, Tang QQ. Involvement of cytoskeleton-associated proteins in the commitment of C3H10T1/2 pluripotent stem cells to adipocyte lineage induced by BMP2/4. *Mol Cell Proteomics* 2011; **10**: M110.002691 [PMID: 20713452 DOI: 10.1074/mcp.M110.002691]

33 **Li CJ**, Cheng P, Liang MK, Chen YS, Lu Q, Wang JY, Xia ZY, Zhou HD, Cao X, Xie H, Liao EY, Luo XH. MicroRNA-188 regulates age-related switch between osteoblast and adipocyte differentiation. *J Clin Invest* 2015; **125**: 1509-1522 [PMID: 25751060 DOI: 10.1172/JCI77716]

34 **Periyasamy-Thandavan S**, Burke J, Mendhe B, Kondrikova G, Kolhe R, Hunter M, Isales CM, Hamrick MW, Hill WD, Fulzele S. MicroRNA-141-3p Negatively Modulates SDF-1 Expression in Age-Dependent Pathophysiology of Human and Murine Bone Marrow Stromal Cells. *J Gerontol A Biol Sci Med Sci* 2019; **74**: 1368-1374 [PMID: 31505568 DOI: 10.1093/gerona/gly186]

35 **Karbiener M**, Fischer C, Nowitsch S, Opriessnig P, Papak C, Ailhaud G, Dani C, Amri EZ, Scheideler M. microRNA miR-27b impairs human adipocyte differentiation and targets PPARgamma. *Biochem Biophys Res Commun* 2009; **390**: 247-251 [PMID: 19800867 DOI: 10.1016/j.bbrc.2009.09.098]

36 **Hu X**, Tang J, Hu X, Bao P, Pan J, Chen Z, Xian J. MiR-27b Impairs Adipocyte Differentiation of Human Adipose Tissue-Derived Mesenchymal Stem Cells by Targeting LPL. *Cell Physiol Biochem* 2018; **47**: 545-555 [PMID: 29794473 DOI: 10.1159/000489988]

37 **Kim SY**, Kim AY, Lee HW, Son YH, Lee GY, Lee JW, Lee YS, Kim JB. miR-27a is a negative regulator of adipocyte differentiation *via* suppressing PPARgamma expression. *Biochem Biophys Res Commun* 2010; **392**: 323-328 [PMID: 20060380 DOI: 10.1016/j.bbrc.2010.01.012]

38 **Lin Z**, He H, Wang M, Liang J. MicroRNA-130a controls bone marrow mesenchymal stem cell differentiation towards the osteoblastic and adipogenic fate. *Cell Prolif* 2019; **52**: e12688 [PMID: 31557368 DOI: 10.1111/cpr.12688]

39 **Li Y**, Yang F, Gao M, Gong R, Jin M, Liu T, Sun Y, Fu Y, Huang Q, Zhang W, Liu S, Yu M, Yan G, Feng C, He M, Zhang L, Ding F, Ma W, Bi Z, Xu C, Yuan Y, Cai B, Yang L. miR-149-3p Regulates the Switch between Adipogenic and Osteogenic Differentiation of BMSCs by Targeting FTO. *Mol Ther Nucleic Acids* 2019; **17**: 590-600 [PMID: 31382190 DOI: 10.1016/j.omtn.2019.06.023]

40 **Wu PY**, Chen W, Huang H, Tang W, Liang J. Morinda officinalis polysaccharide regulates rat bone mesenchymal stem cell osteogenic-

adipogenic differentiation in osteoporosis by upregulating miR-21 and activating the PI3K/AKT pathway. *Kaohsiung J Med Sci* 2022; **38**: 675-685 [PMID: 35593324 DOI: 10.1002/kjm2.12544]

41 **Li CJ**, Xiao Y, Yang M, Su T, Sun X, Guo Q, Huang Y, Luo XH. Long noncoding RNA Bmncr regulates mesenchymal stem cell fate during skeletal aging. *J Clin Invest* 2018; **128**: 5251-5266 [PMID: 30352426 DOI: 10.1172/JCI99044]

42 **Zhu E**, Zhang J, Li Y, Yuan H, Zhou J, Wang B. Long noncoding RNA Plnc1 controls adipocyte differentiation by regulating peroxisome proliferator-activated receptor γ. *FASEB J* 2019; **33**: 2396-2408 [PMID: 30277818 DOI: 10.1096/fj.201800739RRR]

43 **Kalwa M**, Hänzelmann S, Otto S, Kuo CC, Franzen J, Joussen S, Fernandez-Rebollo E, Rath B, Koch C, Hofmann A, Lee SH, Teschendorff AE, Denecke B, Lin Q, Widschwendter M, Weinhold E, Costa IG, Wagner W. The lncRNA HOTAIR impacts on mesenchymal stem cells *via* triple helix formation. *Nucleic Acids Res* 2016; **44**: 10631-10643 [PMID: 27634931 DOI: 10.1093/nar/gkw802]

44 **Wu J**, Lin T, Gao Y, Li X, Yang C, Zhang K, Wang C, Zhou X. Long noncoding RNA ZFAS1 suppresses osteogenic differentiation of bone marrow-derived mesenchymal stem cells by upregulating miR-499-EPHA5 axis. *Mol Cell Endocrinol* 2022; **539**: 111490 [PMID: 34655661 DOI: 10.1016/j.mce.2021.111490]

45 **Hu K**, Jiang W, Sun H, Li Z, Rong G, Yin Z. Long noncoding RNA ZBED3-AS1 induces the differentiation of mesenchymal stem cells and enhances bone regeneration by repressing IL-1β *via* Wnt/β-catenin signaling pathway. *J Cell Physiol* 2019; **234**: 17863-17875 [PMID: 30919957 DOI: 10.1002/jcp.28416]

46 **Liu J**, Gan L, Ma B, He S, Wu P, Li H, Xiong J. Alterations in chromatin accessibility during osteoblast and adipocyte differentiation in human mesenchymal stem cells. *BMC Med Genomics* 2022; **15**: 17 [PMID: 35101056 DOI: 10.1186/s12920-022-01168-1]

47 **Liu Y**, Chen Y, Wang Y, Jiang S, Lin W, Wu Y, Li Q, Guo Y, Liu W, Yuan Q. DNA demethylase ALKBH1 promotes adipogenic differentiation *via* regulation of HIF-1 signaling. *J Biol Chem* 2022; **298**: 101499 [PMID: 34922943 DOI: 10.1016/j.jbc.2021.101499]

48 **Cai GP**, Liu YL, Luo LP, Xiao Y, Jiang TJ, Yuan J, Wang M. Alkbh1-mediated DNA N6-methyladenine modification regulates bone marrow mesenchymal stem cell fate during skeletal aging. *Cell Prolif* 2022; **55**: e13178 [PMID: 35018683 DOI: 10.1111/cpr.13178]

49 **Stachecka J**, Lemanska W, Noak M, Szczerbal I. Expression of key genes involved in DNA methylation during in vitro differentiation of porcine mesenchymal stem cells (MSCs) into adipocytes. *Biochem Biophys Res Commun* 2020; **522**: 811-818 [PMID: 31791576 DOI: 10.1016/j.bbrc.2019.11.175]

50 **Hou R**, Yin G, An P, Wang C, Liu R, Yang Y, Yan X, Li J, Li X, Zhang K. DNA methylation of dermal MSCs in psoriasis: identification of epigenetically dysregulated genes. *J Dermatol Sci* 2013; **72**: 103-109 [PMID: 23916410 DOI: 10.1016/j.jdermsci.2013.07.002]

51 **Cheong CY**, Chng K, Lim MK, Amrithraj AI, Joseph R, Sukarieh R, Chee Tan Y, Chan L, Tan JH, Chen L, Pan H, Holbrook JD, Meaney MJ, Seng Chong Y, Gluckman PD, Stünkel W. Alterations to DNA methylation and expression of CXCL14 are associated with suboptimal birth outcomes. *J Hum Genet* 2014; **59**: 504-511 [PMID: 25102097 DOI: 10.1038/jhg.2014.63]

52 **Xu L**, Liu Y, Sun Y, Wang B, Xiong Y, Lin W, Wei Q, Wang H, He W, Li G. Tissue source determines the differentiation potentials of mesenchymal stem cells: a comparative study of human mesenchymal stem cells from bone marrow and adipose tissue. *Stem Cell Res Ther* 2017; **8**: 275 [PMID: 29208029 DOI: 10.1186/s13287-017-0716-x]

53 **Marofi F**, Hassanzadeh A, Solali S, Vahedi G, Mousavi Ardehaie R, Salarinasab S, Aliparasti MR, Ghaebi M, Farshdousti Hagh M. Epigenetic mechanisms are behind the regulation of the key genes associated with the osteoblastic differentiation of the mesenchymal stem cells: The role of zoledronic acid on tuning the epigenetic changes. *J Cell Physiol* 2019; **234**: 15108-15122 [PMID: 30652308 DOI: 10.1002/jcp.28152]

54 **Shen WC**, Lai YC, Li LH, Liao K, Lai HC, Kao SY, Wang J, Chuong CM, Hung SC. Methylation and PTEN activation in dental pulp mesenchymal stem cells promotes osteogenesis and reduces oncogenesis. *Nat Commun* 2019; **10**: 2226 [PMID: 31110221 DOI: 10.1038/s41467-019-10197-x]

55 **Zych J**, Stimamiglio MA, Senegaglia AC, Brofman PR, Dallagiovanna B, Goldenberg S, Correa A. The epigenetic modifiers 5-aza-2'-deoxycytidine and trichostatin A influence adipocyte differentiation in human mesenchymal stem cells. *Braz J Med Biol Res* 2013; **46**: 405-416 [PMID: 23797495 DOI: 10.1590/1414-431X20132893]

56 **Hemming S**, Cakouros D, Isenmann S, Cooper L, Menicanin D, Zannettino A, Gronthos S. EZH2 and KDM6A act as an epigenetic switch to regulate mesenchymal stem cell lineage specification. *Stem Cells* 2014; **32**: 802-815 [PMID: 24123378 DOI: 10.1002/stem.1573]

57 **Choi MR**, In YH, Park J, Park T, Jung KH, Chai JC, Chung MK, Lee YS, Chai YG. Genome-scale DNA methylation pattern profiling of human bone marrow mesenchymal stem cells in long-term culture. *Exp Mol Med* 2012; **44**: 503-512 [PMID: 22684242 DOI: 10.3858/emm.2012.44.8.057]

58 **Menzies KJ**, Zhang H, Katsyuba E, Auwerx J. Protein acetylation in metabolism - metabolites and cofactors. *Nat Rev Endocrinol* 2016; **12**: 43-60 [PMID: 26503676 DOI: 10.1038/nrendo.2015.181]

59 **Drazic A**, Myklebust LM, Ree R, Arnesen T. The world of protein acetylation. *Biochim Biophys Acta* 2016; **1864**: 1372-1401 [PMID: 27296530 DOI: 10.1016/j.bbapap.2016.06.007]

60 **Yoo EJ**, Chung JJ, Choe SS, Kim KH, Kim JB. Down-regulation of histone deacetylases stimulates adipocyte differentiation. *J Biol Chem* 2006; **281**: 6608-6615 [PMID: 16407282 DOI: 10.1074/jbc.M508982200]

61 **Jin Q**, Wang C, Kuang X, Feng X, Sartorelli V, Ying H, Ge K, Dent SY. Gcn5 and PCAF regulate PPARγ and Prdm16 expression to facilitate brown adipogenesis. *Mol Cell Biol* 2014; **34**: 3746-3753 [PMID: 25071153 DOI: 10.1128/MCB.00622-14]

62 **van Beekum O**, Brenkman AB, Grøntved L, Hamers N, van den Broek NJ, Berger R, Mandrup S, Kalkhoven E. The adipogenic acetyltransferase Tip60 targets activation function 1 of peroxisome proliferator-activated receptor gamma. *Endocrinology* 2008; **149**: 1840-1849 [PMID: 18096664 DOI: 10.1210/en.2007-0977]

63 **Kemper JK**, Xiao Z, Ponugoti B, Miao J, Fang S, Kanamaluru D, Tsang S, Wu SY, Chiang CM, Veenstra TD. FXR acetylation is normally dynamically regulated by p300 and SIRT1 but constitutively elevated in metabolic disease states. *Cell Metab* 2009; **10**: 392-404 [PMID: 19883617 DOI: 10.1016/j.cmet.2009.09.009]

64 **Jiang W**, Wang S, Xiao M, Lin Y, Zhou L, Lei Q, Xiong Y, Guan KL, Zhao S. Acetylation regulates gluconeogenesis by promoting PEPCK1 degradation *via* recruiting the UBR5 ubiquitin ligase. *Mol Cell* 2011; **43**: 33-44 [PMID: 21726808 DOI: 10.1016/j.molcel.2011.04.028]

65 **Kim EY**, Han BS, Kim WK, Lee SC, Bae KH. Acceleration of adipogenic differentiation *via* acetylation of malate dehydrogenase 2. *Biochem Biophys Res Commun* 2013; **441**: 77-82 [PMID: 24134846 DOI: 10.1016/j.bbrc.2013.10.016]

66 **Kim EY**, Kim WK, Kang HJ, Kim JH, Chung SJ, Seo YS, Park SG, Lee SC, Bae KH. Acetylation of malate dehydrogenase 1 promotes adipogenic differentiation *via* activating its enzymatic activity. *J Lipid Res* 2012; **53**: 1864-1876 [PMID: 22693256 DOI: 10.1194/jlr.M026567]

67 **Ho PC**, Gupta P, Tsui YC, Ha SG, Huq M, Wei LN. Modulation of lysine acetylation-stimulated repressive activity by Erk2-mediated phosphorylation of RIP140 in adipocyte differentiation. *Cell Signal* 2008; **20**: 1911-1919 [PMID: 18655826 DOI: 10.1016/j.cellsig.2008.07.001]

68 **Yang W**, Guo X, Thein S, Xu F, Sugii S, Baas PW, Radda GK, Han W. Regulation of adipogenesis by cytoskeleton remodelling is facilitated by acetyltransferase MEC-17-dependent acetylation of α-tubulin. *Biochem J* 2013; **449**: 605-612 [PMID: 23126280 DOI: 10.1042/BJ20121121]

69 **Zhou SR**, Guo L, Wang X, Liu Y, Peng WQ, Wei XB, Dou X, Ding M, Lei QY, Qian SW, Li X, Tang QQ. Acetylation of Cavin-1 Promotes Lipolysis in White Adipose Tissue. *Mol Cell Biol* 2017; **37** [PMID: 28559430 DOI: 10.1128/MCB.00058-17]

70 **Saidi N**, Ghalavand M, Hashemzadeh MS, Dorostkar R, Mohammadi H, Mahdian-Shakib A. Dynamic changes of epigenetic signatures during chondrogenic and adipogenic differentiation of mesenchymal stem cells. *Biomed Pharmacother* 2017; **89**: 719-731 [PMID: 28273634 DOI: 10.1016/j.biopha.2017.02.093]

71 **Haberland M**, Carrer M, Mokalled MH, Montgomery RL, Olson EN. Redundant control of adipogenesis by histone deacetylases 1 and 2. *J Biol Chem* 2010; **285**: 14663-14670 [PMID: 20190228 DOI: 10.1074/jbc.M109.081679]

72 **Sun Z**, Singh N, Mullican SE, Everett LJ, Li L, Yuan L, Liu X, Epstein JA, Lazar MA. Diet-induced lethality due to deletion of the Hdac3 gene in heart and skeletal muscle. *J Biol Chem* 2011; **286**: 33301-33309 [PMID: 21808063 DOI: 10.1074/jbc.M111.277707]

73 **Fajas L**, Egler V, Reiter R, Hansen J, Kristiansen K, Debril MB, Miard S, Auwerx J. The retinoblastoma-histone deacetylase 3 complex inhibits PPARgamma and adipocyte differentiation. *Dev Cell* 2002; **3**: 903-910 [PMID: 12479814 DOI: 10.1016/s1534-5807(02)00360-x]

74 **Montgomery RL**, Potthoff MJ, Haberland M, Qi X, Matsuzaki S, Humphries KM, Richardson JA, Bassel-Duby R, Olson EN. Maintenance of cardiac energy metabolism by histone deacetylase 3 in mice. *J Clin Invest* 2008; **118**: 3588-3597 [PMID: 18830415 DOI: 10.1172/JCI35847]

75 **Grégoire S**, Xiao L, Nie J, Zhang X, Xu M, Li J, Wong J, Seto E, Yang XJ. Histone deacetylase 3 interacts with and deacetylates myocyte enhancer factor 2. *Mol Cell Biol* 2007; **27**: 1280-1295 [PMID: 17158926 DOI: 10.1128/MCB.00882-06]

76 **Feng D**, Liu T, Sun Z, Bugge A, Mullican SE, Alenghat T, Liu XS, Lazar MA. A circadian rhythm orchestrated by histone deacetylase 3 controls hepatic lipid metabolism. *Science* 2011; **331**: 1315-1319 [PMID: 21393543 DOI: 10.1126/science.1198125]

77 **Sun Z**, Miller RA, Patel RT, Chen J, Dhir R, Wang H, Zhang D, Graham MJ, Unterman TG, Shulman GI, Sztalryd C, Bennett MJ, Ahima RS, Birnbaum MJ, Lazar MA. Hepatic Hdac3 promotes gluconeogenesis by repressing lipid synthesis and sequestration. *Nat Med* 2012; **18**: 934-942 [PMID: 22561686 DOI: 10.1038/nm.2744]

78 **Chatterjee TK**, Basford JE, Knoll E, Tong WS, Blanco V, Blomkalns AL, Rudich S, Lentsch AB, Hui DY, Weintraub NL. HDAC9 knockout mice are protected from adipose tissue dysfunction and systemic metabolic disease during high-fat feeding. *Diabetes* 2014; **63**: 176-187 [PMID: 24101673 DOI: 10.2337/db13-1148]

79 **Chatterjee TK**, Idelman G, Blanco V, Blomkalns AL, Piegore MG Jr, Weintraub DS, Kumar S, Rajsheker S, Manka D, Rudich SM, Tang Y, Hui DY, Bassel-Duby R, Olson EN, Lingrel JB, Ho SM, Weintraub NL. Histone deacetylase 9 is a negative regulator of adipogenic differentiation. *J Biol Chem* 2011; **286**: 27836-27847 [PMID: 21680747 DOI: 10.1074/jbc.M111.262964]

80 **Farmer SR**. Transcriptional control of adipocyte formation. *Cell Metab* 2006; **4**: 263-273 [PMID: 17011499 DOI: 10.1016/j.cmet.2006.07.001]

81 **Klein MA**, Denu JM. Biological and catalytic functions of sirtuin 6 as targets for small-molecule modulators. *J Biol Chem* 2020; **295**: 11021-11041 [PMID: 32518153 DOI: 10.1074/jbc.REV120.011438]

82 **Wang F**, Tong Q. SIRT2 suppresses adipocyte differentiation by deacetylating FOXO1 and enhancing FOXO1's repressive interaction with PPARgamma. *Mol Biol Cell* 2009; **20**: 801-808 [PMID: 19037106 DOI: 10.1091/mbc.E08-06-0647]

83 **Jing E**, Gesta S, Kahn CR. SIRT2 regulates adipocyte differentiation through FoxO1 acetylation/deacetylation. *Cell Metab* 2007; **6**: 105-114 [PMID: 17681146 DOI: 10.1016/j.cmet.2007.07.003]

84 **Baskaran P**, Krishnan V, Fettel K, Gao P, Zhu Z, Ren J, Thyagarajan B. TRPV1 activation counters diet-induced obesity through sirtuin-1 activation and PRDM-16 deacetylation in brown adipose tissue. *Int J Obes (Lond)* 2017; **41**: 739-749 [PMID: 28104916 DOI: 10.1038/ijo.2017.16]

85 **Qiang L**, Wang L, Kon N, Zhao W, Lee S, Zhang Y, Rosenbaum M, Zhao Y, Gu W, Farmer SR, Accili D. Brown remodeling of white adipose tissue by SirT1-dependent deacetylation of Pparγ. *Cell* 2012; **150**: 620-632 [PMID: 22863012 DOI: 10.1016/j.cell.2012.06.027]

86 **Puri N**, Sodhi K, Haarstad M, Kim DH, Bohinc S, Foglio E, Favero G, Abraham NG. Heme induced oxidative stress attenuates sirtuin1 and enhances adipogenesis in mesenchymal stem cells and mouse pre-adipocytes. *J Cell Biochem* 2012; **113**: 1926-1935 [PMID: 22234917 DOI: 10.1002/jcb.24061]

87 **Qu P**, Wang L, Min Y, McKennett L, Keller JR, Lin PC. Vav1 Regulates Mesenchymal Stem Cell Differentiation Decision Between Adipocyte and Chondrocyte *via* Sirt1. *Stem Cells* 2016; **34**: 1934-1946 [PMID: 26990002 DOI: 10.1002/stem.2365]

88 **Xiao T**, Liu L, Li H, Sun Y, Luo H, Li T, Wang S, Dalton S, Zhao RC, Chen R. Long Noncoding RNA ADINR Regulates Adipogenesis by Transcriptionally Activating C/EBPα. *Stem Cell Reports* 2015; **5**: 856-865 [PMID: 26489893 DOI: 10.1016/j.stemcr.2015.09.007]

89 **Ding L**, Ning HM, Li PL, Yan HM, Han DM, Zheng XL, Liu J, Zhu L, Xue M, Mao N, Guo ZK, Zhu H, Wang HX. Tumor necrosis factor α in aGVHD patients contributed to the impairment of recipient bone marrow MSC stemness and deficiency of their hematopoiesis-promotion capacity. *Stem Cell Res Ther* 2020; **11**: 119 [PMID: 32183881 DOI: 10.1186/s13287-020-01615-9]

90 **Beane OS**, Fonseca VC, Cooper LL, Koren G, Darling EM. Impact of aging on the regenerative properties of bone marrow-, muscle-, and adipose-derived mesenchymal stem/stromal cells. *PLoS One* 2014; **9**: e115963 [PMID: 25541697 DOI: 10.1371/journal.pone.0115963]

91 **Fisch SC**, Nikou AF, Wright EA, Phan JD, Leung KL, Grogan TR, Abbott DH, Chazenbalk GD, Dumesic DA. Precocious subcutaneous abdominal stem cell development to adipocytes in normal-weight women with polycystic ovary syndrome. *Fertil Steril* 2018; **110**: 1367-1376 [PMID: 30503136 DOI: 10.1016/j.fertnstert.2018.08.042]

92 **Chen L**, Merkhan MM, Forsyth NR, Wu P. Chorionic and amniotic membrane-derived stem cells have distinct, and gestational diabetes mellitus independent, proliferative, differentiation, and immunomodulatory capacities. *Stem Cell Res* 2019; **40**: 101537 [PMID: 31422237 DOI: 10.1016/j.scr.2019.101537]

93 **Kugo H**, Moriyama T, Zaima N. The role of perivascular adipose tissue in the appearance of ectopic adipocytes in the abdominal aortic aneurysmal wall. *Adipocyte* 2019; **8**: 229-239 [PMID: 31250691 DOI: 10.1080/21623945.2019.1636625]

94 **Kunter U**, Rong S, Boor P, Eitner F, Müller-Newen G, Djuric Z, van Roeyen CR, Konieczny A, Ostendorf T, Villa L, Milovanceva-Popovska M, Kerjaschki D, Floege J. Mesenchymal stem cells prevent progressive experimental renal failure but maldifferentiate into glomerular adipocytes. *J Am Soc Nephrol* 2007; **18**: 1754-1764 [PMID: 17460140 DOI: 10.1681/ASN.2007010044]

95 **Dhinekaran A**, Lakshmi M, Graceline H, Dey A, Adhikari S, Ramalingam S, Ramachandran I, Bisgin A, Boga I, Pathak S, Banerjee A. Regulation of mesenchymal stem cell differentiation by key cell signaling pathways. In: Pathak S, Banerjee A. Stem Cells and Signaling Pathways. Amsterdam: Elsevier, 2024: 1-25

96 **Wu J**, Cai P, Lu Z, Zhang Z, He X, Zhu B, Zheng L, Zhao J. Identification of potential specific biomarkers and key signaling pathways

between osteogenic and adipogenic differentiation of hBMSCs for osteoporosis therapy. *J Orthop Surg Res* 2020; **15**: 437 [PMID: 32967719 DOI: 10.1186/s13018-020-01965-3]

97 **Zhang H**, Xu R, Li B, Xin Z, Ling Z, Zhu W, Li X, Zhang P, Fu Y, Chen J, Liu L, Cheng J, Jiang H. LncRNA NEAT1 controls the lineage fates of BMSCs during skeletal aging by impairing mitochondrial function and pluripotency maintenance. *Cell Death Differ* 2022; **29**: 351-365 [PMID: 34497381 DOI: 10.1038/s41418-021-00858-0]

World Journal of Stem Cells

Submit a Manuscript: https://www.f6publishing.com

World J Stem Cells 2024 March 26; 16(3): 257-266

DOI: 10.4252/wjsc.v16.i3.257

ISSN 1948-0210 (online)

ORIGINAL ARTICLE

Retrospective Study

Long-term outcome of stem cell transplantation with and without anti-tumor necrotic factor therapy in perianal fistula with Crohn's disease

Min Young Park, Yong Sik Yoon, Jae Ha Park, Jong Lyul Lee, Chang Sik Yu

Specialty type: Cell and tissue engineering

Provenance and peer review: Invited article; Externally peer reviewed.

Peer-review model: Single blind

Peer-review report's scientific quality classification

Grade A (Excellent): 0
Grade B (Very good): B
Grade C (Good): C
Grade D (Fair): 0
Grade E (Poor): 0

P-Reviewer: Li SC, United States; Zheng H, China

Received: October 13, 2023
Peer-review started: October 13, 2023
First decision: December 11, 2023
Revised: December 25, 2023
Accepted: February 18, 2024
Article in press: February 18, 2024
Published online: March 26, 2024

Min Young Park, Division of Colon and Rectal Surgery, Department of Surgery, Yonsei University College of Medicine, Seoul 03722, South Korea

Yong Sik Yoon, Jae Ha Park, Jong Lyul Lee, Chang Sik Yu, Division of Colon and Rectal Surgery, Department of Surgery, University of Ulsan College of Medicine, Asan Medical Center, Seoul 05505, South Korea

Corresponding author: Yong Sik Yoon, MD, PhD, Professor, Division of Colon and Rectal Surgery, Department of Surgery, University of Ulsan College of Medicine, Asan Medical Center, 88 Olympic-ro 43-gil, Songpa-gu, Seoul 05505, South Korea. yoonys@amc.seoul.kr

Abstract

BACKGROUND

Stem cell transplantation is a promising therapeutic option for curing perianal fistula in Crohn's disease (CD). Anti-tumor necrotic factor (TNF) therapy combined with drainage procedure is effective as well. However, previous studies are limited to proving whether the combination treatment of biologics and stem cell transplantation improves the effect of fistula closure.

AIM

This study aimed to evaluate the long-term outcomes of stem cell transplantation and compare Crohn's perianal fistula (CPF) closure rates after stem cell transplantation with and without anti-TNF therapy, and to identify the factors affecting CPF closure and recurrence.

METHODS

The patients with CD who underwent stem cell transplantation for treating perianal fistula in our institution between Jun 2014 and December 2022 were enrolled. Clinical data were compared according to anti-TNF therapy and CPF closure.

RESULTS

A total of 65 patients were included. The median age of females was 26 years (range: 21-31) and that of males was 29 (44.6%). The mean follow-up duration was 65.88 ± 32.65 months, and complete closure was observed in 50 (76.9%) patients. The closure rates were similar after stem cell transplantation with and without

anti-TNF therapy (66.7% *vs* 81.6% at 3 year, P = 0.098). The patients with fistula closure had short fistulous tract and infrequent proctitis and anorectal stricture (P = 0.027, 0.002, and 0.008, respectively). Clinical factors such as complexity, number of fistulas, presence of concurrent abscess, and medication were not significant for closure. The cumulative 1-, 2-, and 3-year closure rates were 66.2%, 73.8%, and 75.4%, respectively.

CONCLUSION

Anti-TNF therapy does not increase CPF closure rates in patients with stem cell transplantation. However, both refractory and non-refractory CPF have similar closure rates after additional anti-TNF therapy. Fistulous tract length, proctitis, and anal stricture are risk factors for non-closure in patients with CPF after stem cell transplantation.

Key Words: Crohn's disease; Anus; Fistula; Stem cell transplantation; Tumor necrosis factor-alpha inhibitors; Infliximab

Core Tip: This study examined the closure rates of Crohn's perianal fistula (CPF) in patients undergoing stem cell transplantation for treatment. The complete closure was observed in 76.9% of cases, with similar closure rates after stem cell transplantation with and without anti-tumor necrotic factor (TNF) therapy. Factors associated with higher closure rates included shorter fistulous tracts and the absence of proctitis and anorectal stricture. Clinical factors such as complexity, number of fistulas, concurrent abscess presence, and medication did not significantly affect closure. The cumulative 1-, 2-, and 3-year closure rates were 66.2%, 73.8%, and 75.4%, respectively, suggesting that anti-TNF therapy did not increase CPF closure rates.

Citation: Park MY, Yoon YS, Park JH, Lee JL, Yu CS. Long-term outcome of stem cell transplantation with and without anti-tumor necrotic factor therapy in perianal fistula with Crohn's disease. *World J Stem Cells* 2024; 16(3): 257-266
URL: https://www.wjgnet.com/1948-0210/full/v16/i3/257.htm
DOI: https://dx.doi.org/10.4252/wjsc.v16.i3.257

INTRODUCTION

A perianal fistula is an abnormal connection between the rectal or anal canal and external perianal or ischioanal skin[1] and one of the most common complications in Crohn's disease (CD), with a 14%-38% lifetime risk[2]. The incidence of perianal complications in East Asia is higher than that in the West, ranging from 30.3% to 58.8%[3]. Currently, the number of patients with CD in Asia is increasing, and perianal fistula has been detected in a high proportion of patients in Korea. Based on the recently reported epidemiological study of patients with CD in the Songpa-Kangdong district of Seoul, Korea, perianal fistula/abscess was present in 43.3% of cases before or at CD diagnosis[4].

Antibiotics are commonly used as a first-line therapy for fistula treatment, but not effective in treating Crohn's perianal fistula (CPF)[5]. A meta-analysis of five studies found a response in 54% patients treated with azathioprine or 6-mercaptopurine, but this meta-analysis did not review well-designed prospective clinical studies and the response was assessed based on different criteria with complete closure or reduced discharge as secondary endpoints[6]. Currently, biological agents such as anti-tumor necrosis factor (TNF)-α are increasingly being used to treat CPF[7,8]. In the ACCENT II trial, the fistula closure rate at weeks 14 and 54 were 63% and 36%, respectively[8]. Overall, the currently available treatments for CPF are not satisfactory as they do not achieve complete closure and recurrence reduction.

Owing to the problems of CPF and unmet medical needs, studies have focused on stem cell transplantation. Autologous or allogenic adipose tissue-derived stem cells (ASCs) have been studied for CPF treatment and could be considered effective and safe therapeutic tools[9,10]. Several studies in South Korea have showed the favorable results of using autologous ASCs[11,12]. However, few studies have focused on the long-term outcomes of stem cell transplantation and the risk factors affecting them.

Infliximab is a well-established agent for treating CD and CPF[13]. Moreover, autologous ASC transplantation is safe and effective for treating CPF[11,14]. Furthermore, according to the previous systematic review article, the combination of medication and surgery was more effective than single therapy, with 52% (37%-79%) and 43% (24%-67%) complete healing rates, respectively[15]. The study reported a closure rate of 18%-80% in the surgical treatment alone group and 45%-80% in the surgical and medical combined treatment group[16]. Another study reported a closure rate of 20%-65% in the surgical treatment alone group and 18%-85% in the surgical and medical combined treatment group[17]. However, there is a limitation in proving the effectiveness of the combined therapy of anti-TNF agents and stem cell transplantation because stem cell transplantation was not included in the studies as a treatment option.

This study aimed to evaluate the long-term outcomes of stem cell transplantation and compare the closure rates associated with stem cell transplantation with and without anti-TNF therapy. Additionally, the risk factors for therapeutic failure and CPF recurrence after stem cell transplantation were identified.

MATERIALS AND METHODS

Patients and clinical variables

Data of patients with CD who underwent stem cell transplantation for perianal fistula at the Asan Medical Center, Seoul, Korea from June 2014 to December 2022 were reviewed retrospectively. CD was diagnosed by gastroenterologists based on clinical, endoscopic, radiological, and histopathologic criteria according to the diagnostic guidelines for CD in Korea [16]. Patients with insufficient medical records and those lost to follow-up were excluded. Patient characteristics including age, sex, smoking status, and subclass of the Montreal classification[17] were compared. Fistula evaluation included fistula type (simple *vs* complex, single *vs* multiple), perioperative CD medication (immunomodulators or steroids) including biologics, the presence of proctitis or stricture, and the presence of perianal abscess. Autologous adipose tissue-derived mesenchymal stem cells (Cupistem®, Anterogen, South Korea) were used in this study. Cupistem® was approved by the Korea Ministry of Food and Drug Safety in 2012 (advanced therapy medicinal product). Cupistem® manufacturing process was validated and standardized during product development and critical process parameters have been established to ensure product quality. Prior to release, Cupistem® has been tested for cell appearance, cell contents, cell viability, cell surface marker, and impurity in addition to adventitious agents including mycoplasma and bacteria, fungi, and endotoxin[20]. Moreover, anti-TNF agents used in this study were infliximab (Remicade®, Janssen Biotech, Inc., Horsham, PA, United States) and adalimumab (Humira®, AbbVie, Inc., North Chicago, IL, United States). The study protocol was approved by the Institutional Review Board of Asan Medical Center (No. 2020-1059).

Fistula types

Fistulas were classified according to Park's classification criteria[18]. Intersphincteric fistulas are formed when the tract penetrates the internal sphincter and courses through the intersphincteric space to the perianal skin. Transsphincteric fistulas penetrate both the internal and external sphincter. Suprasphincteric fistulas cross the internal sphincter, spread upward in the intersphincteric space, and cross the levator ani muscle downward before reaching the perianal skin. Extra-sphincteric fistulas originate from the rectal wall and course downward through the levator ani muscle lateral to the external sphincter to reach the perianal skin without penetrating the anal sphincter complex.

Autologous ASC preparation

Autologous ASCs were isolated from the subcutaneous fat tissues of patients using lipo-aspirates. The lipo-aspirates were washed with phosphate buffered saline (PBS) and digested in an equal volume of PBS containing 1% bovine serum albumin and 0.025% collagenase type I for 80 min at 37 °C with intermittent shaking. The stromal vascular fraction isolated from the fat tissue was cultured in Dulbecco's modified Eagle's medium (DMEM) with 10% fetal bovine serum and 1 ng/mL human basic fibroblast growth factor to obtain the required number of ASCs for injection. Residual animal products were removed through a washing process of ASCs. During the development of manufacturing method of Cupistem®, washing validation and risk assessment for residuals were conducted to ensure product quality and safety. The risk of residual substances such as fetal bovine serum was evaluated based on "Points to Consider in the Characterization of Cell Lines Used to Produce Biologicals (1993)" and 21CFR610.15. The cells were harvested *via* trypsinization, suspended in DMEM, and packaged into single-use vials containing 3×10^7 cells/mL. All manufacturing procedures were carried out according to the Good Manufacturing Practices authorized by the Korean Food and Drug Administration. Stem cells were sufficiently generated from autologous fat cells evacuated from a patient's buttocks in 4 to 5 wk[19].

Surgical procedures, anti-TNF agents, and postoperative management

Stem cell transplantation: Before stem cell transplantation, all candidates with CPF underwent seton placement to control inflammation around the fistula. Stem cell transplantation was performed in patients without active inflammation after seton drainage. The tract was curetted to remove the inflamed and fibrotic surrounding tissue, which prevents the penetration of transplanted stem cells. The tract was cleaned with isotonic saline and the previous seton was removed. The internal opening of the tract on the rectal or anal canal was closed using direct Vicryl suture ligation. Then, 3×10^7 autologous adipose tissue-derived mesenchymal stem cells/mL (Cupistem®, Anterogen, South Korea) were injected into the submucosa around the internal opening and fistula tract. The opened fistula tract was also filled with fibrin glue-mixed stem cells. The ASC dose was determined based on fistula length and diameter, which were measured using a probe before injection. When the fistula diameter was < 1 cm, approximately 3×10^7 cells were injected per cm. When the fistula diameter was between 1 and 2 cm, approximately 6×10^7 cells were injected per cm. All patients included in this study received only one stem cell transplantation.

Anti-TNF agents: The initiation of anti-TNF treatment was determined by a gastroenterologist according to the patients' clinical factors such as the extent of intestinal inflammation and the patient's response to previous therapeutic drugs. The dosage for infliximab was 5 mg/kg per infusion. Infliximab was administered 2 and 6 wk after the first dose, and every 8 wk after the third dose. Adalimumab was administered every 2 wk after the first dose. Adalimumab was administered at 100 mg for the first dose, 80 mg at the second week, and subsequently 40 mg every 2 wk. The adjustment of the dosage was also determined by a gastroenterologist. The medication was administered according to the protocol unless there were absolute contraindications such as the risk of infection.

Postoperative management: The patients were admitted on the day of operation and discharged the next day. Follow-up was done at an outpatient clinic every 1 or 2 mo. Fistula closure was confirmed through physical examination at the outpatient clinic, where the absence of inflammation or discharge was observed.

Study groups

Patients treated with anti-TNF agents at least once from 3 months before surgery to 3 months after surgery were defined as the "anti-TNF group" regardless of the interval between the initiation of anti-TNF treatment and stem cell transplantation. And the other patient treated without anti-TNF agents from 3 months before surgery to 3 months after surgery were defined as the "without anti-TNF group".

Outcomes

Primary outcomes of the present study were evaluating the closure rate of patients who underwent stem cell transplantation and comparing closure rates between patients who underwent stem cell transplantation with and without biologics. Fistula tract closure was defined as no discharge, swelling, or pain. Recurrence was defined as relapse of discharge and perianal symptoms, including pain and swelling, after closure of the fistulous tract without discharge.

Statistics

Categorical and continuous variables were compared by χ^2 and Student's *t*-tests, respectively. Continuous variables are expressed as the median with inter-quadrant range or the mean with standard deviation, and discrete variables are expressed as numbers with percentages. Statistical analyses were performed using SPSS for Windows, ver. 25.0 (SPSS Inc., Chicago, IL, United States). $P < 0.05$ was considered statistically significant. The cumulative probability of the event was estimated using the life-table method for 3 years at 3-months intervals. The difference in cumulative probability (closure minus recurrence) was calculated for each time period.

RESULTS

Totally 65 patients underwent stem cell transplantation to treat CPF between June 2014 and December 2022. Among them, 26 were treated with preoperative anti-TNF agents. The mean follow-up duration of all patients was 66.09 ± 32.37 months. Complete closure of perianal fistula occurred in 50 (76.9%) patients, of whom 18 (36.0%) were treated with postoperative anti-TNF agents.

The mean age, sex ratio, fistula characteristics, mean CD duration, and mean number of previous operations for CPF were similar between patients treated with and without anti-TNF agents. However, more immunomodulators were used in the patients without anti-TNF treatment (40.7% *vs* 73.7%, $P = 0.008$) and the number of patients with ileocolic involvement (L3) was higher in the patients with anti-TNF treatment (88.9% *vs* 60.5%, $P = 0.025$) (Table 1).

During the follow-up, closure rate after stem cell transplantation was 76.9%. The mean duration from stem cell transplantation to fistula closure was 6.94 ± 9.68 months. Moreover, the recurrence rate in patients experiencing fistula closure was 14.0%, with the mean period from fistula closure to recurrence being 16.57 ± 19.38 months. All recurrences were detected in 3 years. The patients who received anti-TNF treatment experienced fistula closure within 2 years. The closure rates at 1 year and 2 years for the patients who received anti-TNF treatment were 63.0% and 66.7%, respectively. The 1-, 2-, and 3-year closure rates for the patients without anti-TNF treatment were 68.4%, 78.9%, and 81.6%, respectively. Only one patient without anti-TNF treatment experienced fistula closure after 3 years. The closure and recurrence rates were not significantly different according to anti-TNF agent use (66.7% *vs* 84.2%, $P = 0.098$; Table 2, Figure 1). The final cumulative closure rate excluding those who had recurrence was about 66.1% (Figure 2).

Mean age, sex ratio, fistula type or number, mean disease duration, or surgical history for CPF were similar between the patients with and without fistula closure. Fistulas longer than 7 cm (40.0% *vs* 14.0%, $P = 0.027$), proctitis (66.7% *vs* 30.0%, $P = 0.002$), and rectal stricture (26.7% *vs* 8.0%, $P = 0.008$) were significantly less in the patients with fistula closure (Table 3). The Crohn's Disease Activity Index score was higher in the patients with anti-TNF treatment (101.87 ± 55.69 *vs* 80.79 ± 47.47, $P = 0.111$) but not significant, and did not affect closure.

DISCUSSION

Recently, various pharmacological and surgical treatments for CD fistula have been developed and studied[20,21]. Moreover, various studies have proven that stem cell transplantation is effective[10,22]. Biological agents such as anti-TNF-α are increasingly being used as pharmacological treatments to treat CD fistula[7]. Despite extensive research, therapy for CD-derived fistula was inadequate. This study analyzed whether combining these treatment modalities increases the effectiveness and showed that stem cell transplantation in combination with anti-TNF treatment did not increase the fistula closure rate.

The safety and efficacy of autologous MSCs have been studied through multiple phases I, II, and III clinical trials. A phase I trial on five patients with CD fistula showed complete closure of the external opening and an absence of abscess in 75% of patients[22]. A phase II study on complex perianal fistulas reported fistula healing and closure in 71% and 56% of patients receiving autologous ASC treatment, respectively[10]. A phase III trial evaluating ASC efficacy in complex fistulas reported approximately 40% and 50% fistula healing rates at 6 months and 1 year, respectively[23]. Moreover, previous studies using the same ASCs used in this study have shown that the 1- and 2-year closure rates were 88% and 75%, respectively[11,14].

The overall closure rate of patients with stem cell transplantation was 76.9%. Two patients treated with anti-TNF agent only after stem cell transplantation experienced fistula closure. Among them, one patient was treated with anti-TNF due

Table 1 Patient characteristics and clinical variables between anti-tumor necrotic factor and without anti-tumor necrotic factor groups, *n* (%)

	Anti-TNF (*n* = 27)	Without anti-TNF (*n* = 38)	*P* value
Age, median (IQR) (yr)	26 (23.00-32.00)	26 (20.00-31.25)	0.378
Sex			0.596
Male	11 (40.7)	18 (47.4)	
Female	16 (59.3)	20 (52.6)	
Montreal classification			
Age at onset			0.772
A1 (≤ 16 yr)	5 (18.5)	6 (15.8)	
A2 (17-40 yr)	22 (81.5)	32 (84.2)	
A3 (≥ 41 yr)	0 (0.0)	0 (0.0)	
Location			0.025
L1 (Ileum)	3 (11.1)	9 (23.7)	
L2 (Colon)	0 (0.0)	6 (15.8)	
L3 (Ileocolon)	24 (88.9)	23 (60.5)	
Behavior			0.850
B1 (non-stricturing, non-penetrating)	17 (63.0)	26 (68.4)	
B2 (stricturing)	5 (18.5)	8 (21.1)	
B3 (penetrating)	5 (18.5)	4 (10.5)	
Fistula type			0.915
Simple	4 (14.8)	6 (15.8)	
Complex	23 (85.2)	32 (84.2)	
Multiple fistula	9 (33.3)	13 (46.4)	0.941
Fistula length > 7 cm	8 (29.6)	5 (13.2)	0.102
CDAI, (mean ± SD)	101.87 ± 55.69	80.79 ± 47.47	0.111
Proctitis	10 (37.0)	12 (31.6)	0.647
Stricture	3 (11.1)	3 (7.9)	0.659
Abscess	3 (11.1)	2 (5.3)	0.383
Recto-vaginal fistula	3 (11.1)	2 (5.3)	0.383
Medical treatment			
Immunomodulators	11 (40.7)	28 (73.7)	0.008
Smoking	1 (3.7)	1 (2.6)	0.217
Previous fistula OP	27 (100.0)	38 (100.0)	1.000
No. previous fistula OP, mean ± SD (times)	3.30 ± 2.55	2.45 ± 3.29	0.266
Disease duration, mean ± SD (yr)	7.15 ± 4.74	5.87 ± 5.28	0.310
Follow-up, mean ± SD (months)	70.52 ± 31.74	62.58 ± 33.31	0.338

TNF: Tumor necrotic factor; IQR: Interquartile range; CDAI: Crohn's Disease Activity Index; OP: Operation.

to bowel inflammation 1 months after stem cell transplantation, and the other was treated with anti-TNF for unclosed fistula until 1 year after stem cell transplantation. During the follow-up period of approximately 5 years, 14.0% of patients with fistula closure experienced recurrence. Previous studies have reported the recurrence rate at 1 and 2 years after stem cell transplantation as 11% and 16%, respectively[11,14], which is consistent with the recurrence rate of this study. The closure rate was slightly lower in patients treated with anti-TNF agents, although it was not statistically significant. This result is possibly because ASCs initiate or enhance tissue regeneration by two different mechanisms: Differentiating into

Table 2 Fistula closure and recurrence, *n* (%)

	Total	Anti-TNF (*n* = 27)	Without anti-TNF (*n* = 38)	*P* value
Cumulative closure rate	50/65 (76.9%)	18/27 (66.7%)	32/38 (84.2%)	0.098
1-yr	43 (66.2)	17 (63.0)	26 (68.4)	
2-yr	48 (73.8)	18 (66.7)	30 (78.9)	
3-yr	49 (75.4)	-	31 (81.6)	
Closure time (months)	6.94 ± 9.68	4.56 ± 4.37	8.28 ± 11.52	0.195
Cumulative recurrence rate	7/50 (14.0)	3/18 (16.7)	4/32 (12.5)	0.684
1-yr	4 (8.0)	2 (11.1)	2 (6.3)	
2-yr	5 (10.0)	3 (16.7)	2 (6.3)	
3-yr	7 (14.0)	-	4 (12.5)	
Recurrence time (months)	16.57 ± 19.38	7.33 ± 7.77	23.50 ± 23.70	0.316

TNF: Tumor necrotic factor.

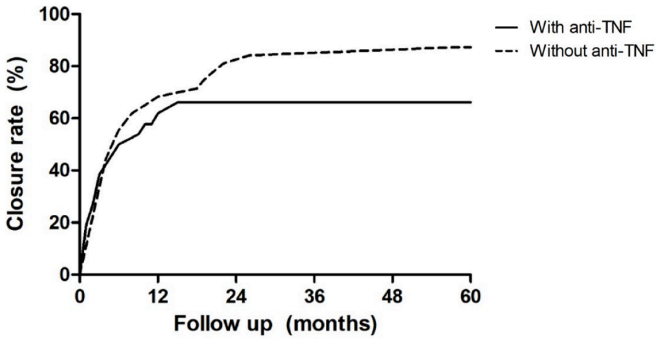

Figure 1 Closure rate with and without anti-tumor necrosis factor agents. The patients who received anti-tumor necrosis factor (TNF) treatment experienced fistula closure within 2 years and the closure rates at 1 year and 2 years were 63.0% and 66.7%, respectively. The 1-, 2-, and 3-year closure rates for the patients without anti-TNF treatment were 68.4%, 78.9%, and 81.6%, respectively. The 5-year closure rates were not significantly different according to anti-TNF agent use (66.7% *vs* 84.2%, *P* = 0.098). The anti-TNF agents used in this study were infliximab (Remicade®, Janssen Biotech, Inc., Horsham, PA, United States) and adalimumab (Humira®, AbbVie, Inc., North Chicago, IL, United States). TNF: Tumor necrosis factor.

skin cells or secreting paracrine factors that initiate the healing process through recruiting endogenous stem cells and endothelial cells or downregulating the inflammatory response. Thus, the anti-inflammatory response of stem cell transplantation, which is a local treatment for CPF, is strong among patients, and prolongs and minimizes the effect of systemic treatment with anti-TNF[24]. Additionally, more refractory CPF was included in the anti-TNF treatment group as the patients treated with anti-TNF agents had a prolonged disease duration and previous surgeries for CPF might affect the result. Furthermore, our study showed that proctitis, stricture, and long fistulous tract reduced the closure rate, and biologics did not affect the closure and recurrence. The actual cumulative fistula closure rate, excluding those with recurrence, was approximately 66.1%.

This study has several limitations. First, its retrospective design may have caused patient selection bias. To minimize the selection bias, we enrolled all patients who underwent stem cell transplantation during the study period. Second, because the surgical procedure, like stem cell transplantation, was determined subjectively by each operator depending on the severity of inflammation in the fistula, it may have affected the high closure rate of stem cell transplantation. Moreover, the actual healing rate after treatment was not evaluated through imaging studies such as magnetic resonance imaging (MRI) because only four patients underwent MRI for other reasons not for fistula, as MRI for diagnosing perianal fistula is not covered by insurance in Korea.

CONCLUSION

Concludingly, stem cell transplantation is one of the feasible treatment options for CPF. Anti-TNF agents do not increase the fistula closure rate after stem cell transplantation in CPF patients. Furthermore, selecting appropriate patients considering factors such as clinical features like proctitis or stricture, as well as the length of the fistulous tract may influence the prognosis of fistula closure according to this study results. Therefore, if stem cell transplantation is

Table 3 Patient characteristics and clinical variables between closure and non-closure groups, *n* (%)

	No closure (*n* = 15)	Closure (*n* = 50)	*P* value
Age, median (IQR) (yr)	28.0 (23.0-33.0)	26.0 (20.8-31.0)	0.433
Sex			0.316
Male	5 (33.3)	24 (48.0)	
Female	10 (66.7)	26 (52.0)	
Montreal classification			
Age at onset			0.227
A1 (≤ 16 yr)	1 (6.7)	10 (20.0)	
A2 (17-40 yr)	14 (93.3)	40 (80.0)	
A3 (≥ 41 yr)	0 (0.0)	0 (0.0)	
Location			0.285
L1 (Ileum)	4 (26.7)	8 (16.0)	
L2 (Colon)	0 (0.0)	6 (12.0)	
L3 (Ileocolon)	11 (73.3)	36 (72.0)	
Behavior			0.998
B1 (non-stricturing, non-penetrating)	10 (66.7)	33 (66.0)	
B2 (stricturing)	3 (20.0)	10 (20.0)	
B3 (penetrating)	2 (13.3)	7 (14.0)	
Fistula type			0.572
Simple	3 (20.0)	7 (14.0)	
Complex	12 (80.0)	43 (86.0)	
Multiple fistula	8 (53.3)	14 (28.0)	0.069
Fistula length > 7 cm	6 (40.0)	7 (14.0)	0.027
CDAI, mean ± SD	98.84 ± 54.62	87.01 ± 51.16	0.444
Proctitis	10 (66.7)	15 (30.0)	0.002
Stricture	4 (26.7)	2 (8.0)	0.008
Abscess	2 (13.3)	3 (6.0)	0.350
Recto-vaginal fistula	1 (6.7)	4 (8.0)	0.865
Medical treatment			
Immunomodulators	8 (53.3)	31 (62.0)	0.548
Biologics	9 (60.0)	18 (36.0)	0.098
Smoking	0 (0.0)	2 (4.0)	0.733
Previous fistula OP	15 (100.0)	33 (100.0)	1.000
No. previous fistula OP, mean ± SD (times)	4.27 ± 5.06	2.36 ± 1.91	0.173
Disease duration, mean ± SD (yr)	5.53 ± 4.24	6.66 ± 5.29	0.454
Follow-up, mean ± SD (months)	63.87 ± 40.12	66.48 ± 30.52	0.788

IQR: Interquartile range; CDAI: Crohn's Disease Activity Index; OP: Operation.

performed in appropriate patients, regardless of the use of anti-TNF agents, favorable outcomes can be expected. However, since most patients enrolled in this study were taking anti-TNF agents for the treatment of bowel inflammation rather than perianal fistula, further research should be considered to determine whether combining stem cell transplantation and anti-TNF solely for perianal fistula treatment is effective. This study was conducted at a single center, and due to the limited number of patients, we believe that further research is needed with a larger cohort from multi-centers to investigate the long-term outcomes and prognostic factors of stem cell transplantation in patients with CPF.

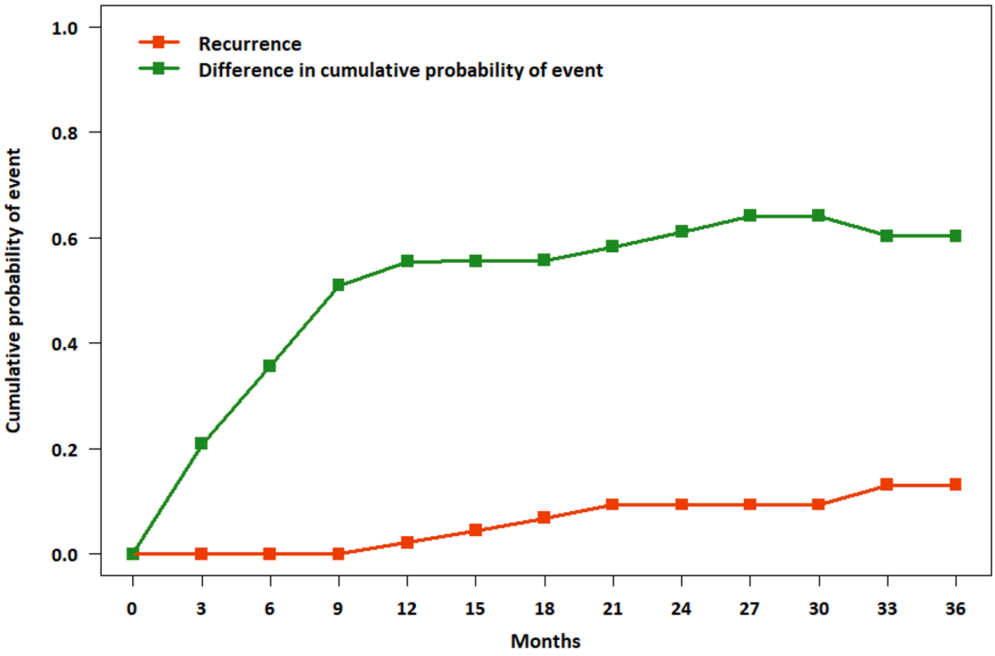

Figure 2 Cumulative closure and recurrence rates after stem cell transplantation. All recurrences were detected in 3 years during the 5-year follow-up period after stem cell transplantation. The final cumulative closure rate (green line) excluding those who had recurrence (red line) was about 66.1% after stem cell transplantation regardless of the anti-tumor necrosis factor (TNF) therapy. The anti-TNF agents used in this study were infliximab (Remicade®, Janssen Biotech, Inc., Horsham, PA, United States) and adalimumab (Humira®, AbbVie, Inc., North Chicago, IL, United States).

ARTICLE HIGHLIGHTS

Research background

Perianal fistulas are a common complication in Crohn's disease, with a higher incidence in East Asia. Stem cell transplantation, specifically using autologous adipose tissue-derived stem cells (ASCs), has been explored as a potential effective and safe therapeutic approach, with favorable results reported in South Korean studies.

Research motivation

While the combination of medication and surgery has shown promise, the effectiveness of combining biologics such as anti-tumor necrosis factor (TNF) agents with stem cell transplantation remains an unproven area in improving fistula closure outcomes.

Research objectives

The study focused on assessing the long-term outcomes of stem cell transplantation, comparing closure rates with and without anti-TNF therapy, and evaluating risk factors for therapeutic failure and recurrence in Crohn's perianal fistula (CPF) after stem cell transplantation.

Research methods

This retrospective study, conducted at Asan Medical Center in Seoul, Korea, aimed to evaluate the long-term outcomes of stem cell transplantation in patients with CPF. Data from patients who underwent stem cell transplantation from June 2014 to December 2022 were reviewed, considering clinical variables such as age, sex, smoking status, and Montreal classification subclass. Autologous ASCs were used, and the study also included information on surgical procedures, anti-TNF agents (infliximab and adalimumab) used, and postoperative management. The study focused on comparing closure rates between patients who underwent stem cell transplantation with and without biologics, defining closure as the absence of discharge, swelling, or pain, and recurrence as the relapse of symptoms after the closure of the fistulous tract. Statistical analyses were performed to assess differences in outcomes.

Research results

Between June 2014 and December 2022, a total of 65 patients underwent stem cell transplantation for the treatment of CPF, with 26 receiving preoperative anti-TNF agents. The mean follow-up duration was 66.09 ± 32.37 months. Among all patients, 76.9% achieved complete closure of perianal fistula, and the recurrence rate after closure was 14.0%. The closure rates at 1 and 2 years for patients with anti-TNF treatment were 63.0% and 66.7%, respectively, while for those without anti-TNF treatment, the rates were 68.4%, 78.9%, and 81.6% at 1, 2, and 3 years, respectively. Fistula closure was less likely in patients with longer fistulas (> 7 cm), proctitis, and rectal stricture. The cumulative closure rate, excluding those with recurrence, was approximately 66.1%. The use of anti-TNF agents did not significantly impact closure and

recurrence rates.

Research conclusions

In conclusion, stem cell transplantation emerges as a viable treatment option for CPF, with favorable outcomes expected in appropriate patients regardless of the use of anti-TNF agents. This study suggests that selecting patients based on clinical features such as proctitis or stricture, along with considering the length of the fistulous tract, plays an important role in influencing the prognosis of fistula closure.

Research perspectives

The study, conducted at a single center with a limited number of patients, underscores the need for further research involving a larger multi-center cohort to thoroughly investigate the long-term outcomes and prognostic factors associated with stem cell transplantation in patients with CPF.

FOOTNOTES

Author contributions: Park MY designed and performed the research and wrote the paper; Yoon YS designed the research and supervised the report; Park JH contributed to the analysis; Lee JL and Yu CS provided clinical advice and supervised the report.

Supported by the grants from the Asan Institute for Life Sciences, Asan Medical Center, Seoul, Korea, No. 2019IF0593 and No. 2020IP0039.

Institutional review board statement: This study was reviewed and approved by the Institutional Review Board of Asan Medical Center (No. 2020-1059).

Informed consent statement: This is a retrospective study that used anonymous data, and the Institutional Review Board of Asan Medical Center approved the study and waived informed consent.

Conflict-of-interest statement: All the authors report no relevant conflicts of interest for this article.

Data sharing statement: No additional data are available.

Country/Territory of origin: South Korea

ORCID number: Min Young Park 0000-0002-7444-5075; Yong Sik Yoon 0000-0002-3196-8423; Jae Ha Park 0009-0007-1292-5755; Jong Lyul Lee 0000-0002-5878-8000; Chang Sik Yu 0000-0001-9401-9981.

S-Editor: Wang JJ
L-Editor: Wang TQ
P-Editor: Zhang XD

REFERENCES

1 **Steinhart AH**, Panaccione R, Targownik L, Bressler B, Khanna R, Marshall JK, Afif W, Bernstein CN, Bitton A, Borgaonkar M, Chauhan U, Halloran B, Jones J, Kennedy E, Leontiadis GI, Loftus EV Jr, Meddings J, Moayyedi P, Murthy S, Plamondon S, Rosenfeld G, Schwartz D, Seow CH, Williams C. Clinical Practice Guideline for the Medical Management of Perianal Fistulizing Crohn's Disease: The Toronto Consensus. *Inflamm Bowel Dis* 2019; **25**: 1-13 [PMID: 30099529 DOI: 10.1093/ibd/izy247]

2 **Williams DR**, Coller JA, Corman ML, Nugent FW, Veidenheimer MC. Anal complications in Crohn's disease. *Dis Colon Rectum* 1981; **24**: 22-24 [PMID: 7472097 DOI: 10.1007/BF02603444]

3 **Im JP**. Adalimumab or infliximab: which is better for perianal fistula in Crohn's disease? *Intest Res* 2017; **15**: 147-148 [PMID: 28522942 DOI: 10.5217/ir.2017.15.2.147]

4 **Park SH**, Kim YJ, Rhee KH, Kim YH, Hong SN, Kim KH, Seo SI, Cha JM, Park SY, Jeong SK, Lee JH, Park H, Kim JS, Im JP, Yoon H, Kim SH, Jang J, Kim JH, Suh SO, Kim YK, Ye BD, Yang SK; Songpa-Kangdong Inflammatory Bowel Disease [SK-IBD] Study Group. A 30-year Trend Analysis in the Epidemiology of Inflammatory Bowel Disease in the Songpa-Kangdong District of Seoul, Korea in 1986-2015. *J Crohns Colitis* 2019; **13**: 1410-1417 [PMID: 30989166 DOI: 10.1093/ecco-jcc/jjz081]

5 **Present DH**. Crohn's fistula: current concepts in management. *Gastroenterology* 2003; **124**: 1629-1635 [PMID: 12761721 DOI: 10.1016/s0016-5085(03)00392-5]

6 **Pearson DC**, May GR, Fick GH, Sutherland LR. Azathioprine and 6-mercaptopurine in Crohn disease. A meta-analysis. *Ann Intern Med* 1995; **123**: 132-142 [PMID: 7778826 DOI: 10.7326/0003-4819-123-2-199507150-00009]

7 **Gecse KB**, Bemelman W, Kamm MA, Stoker J, Khanna R, Ng SC, Panés J, van Assche G, Liu Z, Hart A, Levesque BG, D'Haens G; World

Gastroenterology Organization, International Organisation for Inflammatory Bowel Diseases IOIBD, European Society of Coloproctology and Robarts Clinical Trials; World Gastroenterology Organization International Organisation for Inflammatory Bowel Diseases IOIBD European Society of Coloproctology and Robarts Clinical Trials. A global consensus on the classification, diagnosis and multidisciplinary treatment of perianal fistulising Crohn's disease. *Gut* 2014; **63**: 1381-1392 [PMID: 24951257 DOI: 10.1136/gutjnl-2013-306709]

8 **Sands BE**, Anderson FH, Bernstein CN, Chey WY, Feagan BG, Fedorak RN, Kamm MA, Korzenik JR, Lashner BA, Onken JE, Rachmilewitz D, Rutgeerts P, Wild G, Wolf DC, Marsters PA, Travers SB, Blank MA, van Deventer SJ. Infliximab maintenance therapy for fistulizing Crohn's disease. *N Engl J Med* 2004; **350**: 876-885 [PMID: 14985485 DOI: 10.1056/NEJMoa030815]

9 **García-Olmo D**, García-Arranz M, García LG, Cuellar ES, Blanco IF, Prianes LA, Montes JA, Pinto FL, Marcos DH, García-Sancho L. Autologous stem cell transplantation for treatment of rectovaginal fistula in perianal Crohn's disease: a new cell-based therapy. *Int J Colorectal Dis* 2003; **18**: 451-454 [PMID: 12756590 DOI: 10.1007/s00384-003-0490-3]

10 **Garcia-Olmo D**, Herreros D, Pascual I, Pascual JA, Del-Valle E, Zorrilla J, De-La-Quintana P, Garcia-Arranz M, Pascual M. Expanded adipose-derived stem cells for the treatment of complex perianal fistula: a phase II clinical trial. *Dis Colon Rectum* 2009; **52**: 79-86 [PMID: 19273960 DOI: 10.1007/DCR.0b013e3181973487]

11 **Cho YB**, Park KJ, Yoon SN, Song KH, Kim DS, Jung SH, Kim M, Jeong HY, Yu CS. Long-term results of adipose-derived stem cell therapy for the treatment of Crohn's fistula. *Stem Cells Transl Med* 2015; **4**: 532-537 [PMID: 25829404 DOI: 10.5966/sctm.2014-0199]

12 **Park KJ**, Ryoo SB, Kim JS, Kim TI, Baik SH, Kim HJ, Lee KY, Kim M, Kim WH. Allogeneic adipose-derived stem cells for the treatment of perianal fistula in Crohn's disease: a pilot clinical trial. *Colorectal Dis* 2016; **18**: 468-476 [PMID: 26603576 DOI: 10.1111/codi.13223]

13 **Targan SR**, Hanauer SB, van Deventer SJ, Mayer L, Present DH, Braakman T, DeWoody KL, Schaible TF, Rutgeerts PJ. A short-term study of chimeric monoclonal antibody cA2 to tumor necrosis factor alpha for Crohn's disease. Crohn's Disease cA2 Study Group. *N Engl J Med* 1997; **337**: 1029-1035 [PMID: 9321530 DOI: 10.1056/NEJM199710093371502]

14 **Lee WY**, Park KJ, Cho YB, Yoon SN, Song KH, Kim DS, Jung SH, Kim M, Yoo HW, Kim I, Ha H, Yu CS. Autologous adipose tissue-derived stem cells treatment demonstrated favorable and sustainable therapeutic effect for Crohn's fistula. *Stem Cells* 2013; **31**: 2575-2581 [PMID: 23404825 DOI: 10.1002/stem.1357]

15 **Yassin NA**, Askari A, Warusavitarne J, Faiz OD, Athanasiou T, Phillips RK, Hart AL. Systematic review: the combined surgical and medical treatment of fistulising perianal Crohn's disease. *Aliment Pharmacol Ther* 2014; **40**: 741-749 [PMID: 25115149 DOI: 10.1111/apt.12906]

16 **Lennard-Jones JE**. Classification of inflammatory bowel disease. *Scand J Gastroenterol Suppl* 1989; **170**: 2-6; discussion 16 [PMID: 2617184 DOI: 10.3109/00365528909091339]

17 **Silverberg MS**, Satsangi J, Ahmad T, Arnott ID, Bernstein CN, Brant SR, Caprilli R, Colombel JF, Gasche C, Geboes K, Jewell DP, Karban A, Loftus EV Jr, Peña AS, Riddell RH, Sachar DB, Schreiber S, Steinhart AH, Targan SR, Vermeire S, Warren BF. Toward an integrated clinical, molecular and serological classification of inflammatory bowel disease: report of a Working Party of the 2005 Montreal World Congress of Gastroenterology. *Can J Gastroenterol* 2005; **19** Suppl A: 5A-36A [PMID: 16151544 DOI: 10.1155/2005/269076]

18 **Parks AG**, Gordon PH, Hardcastle JD. A classification of fistula-in-ano. *Br J Surg* 1976; **63**: 1-12 [PMID: 1267867 DOI: 10.1002/bjs.1800630102]

19 **Park MY**, Yoon YS, Lee JL, Park SH, Ye BD, Yang SK, Yu CS. Comparative perianal fistula closure rates following autologous adipose tissue-derived stem cell transplantation or treatment with anti-tumor necrosis factor agents after seton placement in patients with Crohn's disease: a retrospective observational study. *Stem Cell Res Ther* 2021; **12**: 401 [PMID: 34256838 DOI: 10.1186/s13287-021-02484-6]

20 **Bouguen G**, Siproudhis L, Gizard E, Wallenhorst T, Billioud V, Bretagne JF, Bigard MA, Peyrin-Biroulet L. Long-term outcome of perianal fistulizing Crohn's disease treated with infliximab. *Clin Gastroenterol Hepatol* 2013; **11**: 975-81.e1 [PMID: 23376316 DOI: 10.1016/j.cgh.2012.12.042]

21 **Gaertner WB**, Decanini A, Mellgren A, Lowry AC, Goldberg SM, Madoff RD, Spencer MP. Does infliximab infusion impact results of operative treatment for Crohn's perianal fistulas? *Dis Colon Rectum* 2007; **50**: 1754-1760 [PMID: 17899271 DOI: 10.1007/s10350-007-9077-3]

22 **García-Olmo D**, García-Arranz M, Herreros D, Pascual I, Peiro C, Rodríguez-Montes JA. A phase I clinical trial of the treatment of Crohn's fistula by adipose mesenchymal stem cell transplantation. *Dis Colon Rectum* 2005; **48**: 1416-1423 [PMID: 15933795 DOI: 10.1007/s10350-005-0052-6]

23 **Garcia-Olmo D**, Guadalajara H, Rubio-Perez I, Herreros MD, de-la-Quintana P, Garcia-Arranz M. Recurrent anal fistulae: limited surgery supported by stem cells. *World J Gastroenterol* 2015; **21**: 3330-3336 [PMID: 25805941 DOI: 10.3748/wjg.v21.i11.3330]

24 **Hassan WU**, Greiser U, Wang W. Role of adipose-derived stem cells in wound healing. *Wound Repair Regen* 2014; **22**: 313-325 [PMID: 24844331 DOI: 10.1111/wrr.12173]

World Journal of Stem Cells

Submit a Manuscript: https://www.f6publishing.com

World J Stem Cells 2024 March 26; 16(3): 267-286

DOI: 10.4252/wjsc.v16.i3.267

ISSN 1948-0210 (online)

ORIGINAL ARTICLE

Basic Study

Low-intensity pulsed ultrasound reduces alveolar bone resorption during orthodontic treatment *via* Lamin A/C-Yes-associated protein axis in stem cells

Tong Wu, Fu Zheng, Hong-Yi Tang, Hua-Zhi Li, Xin-Yu Cui, Shuai Ding, Duo Liu, Cui-Ying Li, Jiu-Hui Jiang, Rui-Li Yang

Specialty type: Cell and tissue engineering

Provenance and peer review: Unsolicited article; Externally peer reviewed.

Peer-review model: Single blind

Peer-review report's scientific quality classification

Grade A (Excellent): 0
Grade B (Very good): B
Grade C (Good): 0
Grade D (Fair): 0
Grade E (Poor): 0

P-Reviewer: Li SC, United States; Roomi AB, Iraq

Received: October 26, 2023
Peer-review started: October 26, 2023
First decision: December 17, 2023
Revised: December 30, 2023
Accepted: February 1, 2024
Article in press: February 1, 2024
Published online: March 26, 2024

Tong Wu, Fu Zheng, Hong-Yi Tang, Hua-Zhi Li, Xin-Yu Cui, Shuai Ding, Duo Liu, Jiu-Hui Jiang, Rui-Li Yang, Department of Orthodontics, Peking University School and Hospital of Stomatology, National Engineering Laboratory for Digital and Material Technology of Stomatology, Beijing Key Laboratory of Digital Stomatology, Beijing 100081, China

Cui-Ying Li, Department of Central Laboratory, Peking University School and Hospital of Stomatology, National Clinical Research Center for Oral Diseases & National Engineering Laboratory for Digital and Material Technology of Stomatology, Beijing Key Laboratory of Digital Stomatology, Beijing 100081, China

Corresponding author: Rui-Li Yang, PhD, Professor, Department of Orthodontics, Peking University School and Hospital of Stomatology, National Engineering Laboratory for Digital and Material Technology of Stomatology, Beijing Key Laboratory of Digital Stomatology, No. 22 Zhongguancun South Avenue, Beijing 100081, China. ruiliyangabc@163.com

Abstract

BACKGROUND

The bone remodeling during orthodontic treatment for malocclusion often requires a long duration of around two to three years, which also may lead to some complications such as alveolar bone resorption or tooth root resorption. Low-intensity pulsed ultrasound (LIPUS), a noninvasive physical therapy, has been shown to promote bone fracture healing. It is also reported that LIPUS could reduce the duration of orthodontic treatment; however, how LIPUS regulates the bone metabolism during the orthodontic treatment process is still unclear.

AIM

To investigate the effects of LIPUS on bone remodeling in an orthodontic tooth movement (OTM) model and explore the underlying mechanisms.

METHODS

A rat model of OTM was established, and alveolar bone remodeling and tooth movement rate were evaluated *via* micro-computed tomography and staining of tissue sections. *In vitro*, human bone marrow mesenchymal stem cells (hBMSCs) were isolated to detect their osteogenic differentiation potential under compre-

ssion and LIPUS stimulation by quantitative reverse transcription-polymerase chain reaction, Western blot, alkaline phosphatase (ALP) staining, and Alizarin red staining. The expression of Yes-associated protein (YAP1), the actin cytoskeleton, and the Lamin A/C nucleoskeleton were detected with or without YAP1 small interfering RNA (siRNA) application *via* immunofluorescence.

RESULTS

The force treatment inhibited the osteogenic differentiation potential of hBMSCs; moreover, the expression of osteogenesis markers, such as type 1 collagen (COL1), runt-related transcription factor 2, ALP, and osteocalcin (OCN), decreased. LIPUS could rescue the osteogenic differentiation of hBMSCs with increased expression of osteogenic marker inhibited by force. Mechanically, the expression of LaminA/C, F-actin, and YAP1 was downregulated after force treatment, which could be rescued by LIPUS. Moreover, the osteogenic differentiation of hBMSCs increased by LIPUS could be attenuated by YAP siRNA treatment. Consistently, LIPUS increased alveolar bone density and decreased vertical bone absorption *in vivo*. The decreased expression of COL1, OCN, and YAP1 on the compression side of the alveolar bone was partially rescued by LIPUS.

CONCLUSION

LIPUS can accelerate tooth movement and reduce alveolar bone resorption by modulating the cytoskeleton-Lamin A/C-YAP axis, which may be a promising strategy to reduce the orthodontic treatment process.

Key Words: Low-intensity pulsed ultrasound; Bone resorption; Osteogenesis; Cytoskeleton-Lamin A/C-Yes-associated protein axis; Bone marrow mesenchymal stem cells; Orthodontic tooth movement

Core Tip: Low-intensity pulsed ultrasound can promote local alveolar bone remodeling and reduce vertical alveolar bone resorption and consequent gingival recession by regulating the osteogenic ability of bone marrow mesenchymal stem cells by upregulating the expression and nuclear translocation of Yes-associated protein decreased by mechanical stress *via* affecting the cytoskeleton and nuclear skeleton.

Citation: Wu T, Zheng F, Tang HY, Li HZ, Cui XY, Ding S, Liu D, Li CY, Jiang JH, Yang RL. Low-intensity pulsed ultrasound reduces alveolar bone resorption during orthodontic treatment *via* Lamin A/C-Yes-associated protein axis in stem cells. *World J Stem Cells* 2024; 16(3): 267-286

URL: https://www.wjgnet.com/1948-0210/full/v16/i3/267.htm

DOI: https://dx.doi.org/10.4252/wjsc.v16.i3.267

INTRODUCTION

Orthodontic treatment for malocclusion usually lasts 2-3 years, which brings great challenges to patient compliance and increases the risk of many complications, such as alveolar bone resorption, gingivitis, and other destructive diseases of the periodontal supporting tissue[1]. The alveolar bone loss caused by long-term orthodontic treatment may be due to imbalanced osteogenic and osteoclast activity.

Low-intensity pulsed ultrasound (LIPUS) usually refers to a pulse-emitted ultrasonic wave with an intensity between 30 and 100 mW/cm^2, which is a noninvasive physical mechanical energy source[2]. It is delivered in the form of an acoustic wave and applied to tissue and cells to regulate biochemical functions[3]. As revealed by several clinical trials and animal experiments *in vivo*, LIPUS can reduce the fracture healing time[4] and effectively treat delayed fracture union [5] and bone nonunion[6], and is safer and noninvasive than other treatments.

LIPUS has also gained attention in the field of orthodontics. *In vivo*, LIPUS can increase the distance of the teeth movement[7]; a retrospective clinical study also showed that LIPUS reduced the duration of invisible treatment by an average of 49%[8]. In a clinical study, buccal alveolar bone thickness and height did not respond to LIPUS during maxillary arch expansion[9]. In a tooth movement model in rats, LIPUS application increased the number of osteoclasts on the compression side[10]. The increased osteoclasts may lead to alveolar bone resorption and periodontal supporting tissue destruction. It is unclear whether LIPUS regulates alveolar bone remodeling.

Bone marrow mesenchymal stem cells (BMSCs), as bone marrow-derived stem cells, exhibit self-renewal capacity and multiple differentiation potential and can differentiate into multiple types of cells, tissues, and organs under proper conditions[11]. LIPUS could regulate MSC growth[12] and promote chondrogenesis of MSCs seeded on three-dimensionally (3D) printed scaffolds[13]. Besides, MSCs encapsulated in hydrogels of certain stiffness show enhanced osteogenesis ability under LIPUS[14]. Few studies have reported the effect of LIPUS on cells loaded in compression. Whether LIPUS could regulate the property of MSCs under compression force to control the alveolar bone remodeling during orthodontic treatment and the underlying mechanism need to be investigated.

Here, we show that LIPUS could accelerate the orthodontic tooth movement (OTM) and increase alveolar bone density and decreased vertical bone absorption *via* the Lamin A/C-Yes-associated protein (YAP) axis, suggesting that LIPUS is a promising strategy to accelerate the orthodontic treatment with little side effects.

MATERIALS AND METHODS

Cell culture

The human jawbone tissue sampling protocol gained approval from the Ethical Guidelines of Hospital of Stomatology, Peking University (No. PKUSSIRB-202385020) and was carried out after informed consent was obtained. BMSCs were isolated and cultured following the previously reported protocol[15]. Briefly, we obtained a small piece of cortical bone located above the tooth crown, which required removal during the extraction of the donor's impacted third molars. The bone was carefully sectioned using a scalpel and subsequently digested using collagenase type I (2 mg/mL; Worthington Biochem, Lakewood, NJ, United States) and dispase II (4 mg/mL; Roche Diagnostic, Indianapolis, IN, United States) for an hour at 37 °C. Single-cell suspensions from the jaw bone were subsequently acquired using 70-μm cell strainers (BD Bioscience, United States). Then, single cells were seeded onto 100-mm dishes at 1 to 1.5 × 10^6 cells/mL. BMSCs were isolated and cultured following the previously reported protocol[15]. BMSCs were cultivated in Minimum Essential Medium α (VivaCell, Shanghai, China) supplemented with 15% fetal bovine serum (Gibco, Grand Island, NY, United States) and 1% penicillin-streptomycin solution (Cytiva, Shanghai, China) at 37 °C with 5% CO_2, and the medium was changed at 3-d intervals. The expression of stem cell surface markers in BMSCs was characterized by flow cytometry according to the manufacturer's protocol (BD Bioscience).

Transfection of small interfering RNA

Before transfection, the cell culture medium was changed to standard conditions without penicillin-streptomycin solution. The cells were then transfected with control small interfering RNA (siRNA) or YAP1 siRNA (Ribobio, Guangzhou, China) *via* a ribo*FECT*™ CP Transfection Kit (Ribobio) in accordance with the manufacturer's instructions. Quantitative reverse transcription-polymerase chain reaction (qRT-PCR), Western blotting, and immunofluorescence staining were subsequently performed to measure the knockdown rate.

Osteogenic differentiation, alkaline phosphatase activity, and alizarin red staining

BMSCs (1 × 10^5/mL) were seeded onto 6-well plates and cultured until the cell confluence reached 70%-80% before the medium was changed to osteogenic differentiation medium supplemented with L-ascorbic acid (50 μg/mL; Sigma, Missouri, United States), β-glycerophosphate (10 mmol/L; Sigma), and dexamethasone (0.1 μM; Sigma). During osteogenic induction of stem cells, the induction differentiation medium was changed every 3 d.

After induction for 14 d, alkaline phosphatase (ALP) staining (Beyotime, Shanghai, China) were conducted in accordance with the protocol, and so did alizarin red staining (Sigma) after induction for 21 d. For the quantification of mineralization, we dissolved red matrix sediment in 10% cetyl-pyridinium chloride (Macklin, Shanghai, China), and the absorbance of the solution was measured to determine the degree of mineralization quantitatively[16].

Application of a compression force

Compression force was applied to the BMSCs to mimic stress during orthodontic movement[17]. Briefly, a rounded glass sheet (30 mm in diameter) was placed over cell layers close to confluence in a 6-well plate. Stainless steel beads were placed above the glass sheet to adjust the static pressure to 1 g/cm^2. The cells were under static compression for 24 h.

LIPUS treatment

In this study, the LIPUS device was obtained from the Institute of Acoustics (Chinese Academy of Sciences, Beijing, China). The device has circular transducers with an area of 9.07 cm^2 to match the area of a well in a 6-well plate. The cells were stimulated with LIPUS following the following specifications: 1.5 MHz frequency, 0.2 pulse duration ratio, 30 mW/cm^2 incident intensity, and 1.0 kHz repetition rate. Stimulation was applied for 20 min every day *in vivo* and *in vitro* until the rats and cells were harvested, and the control group and force group were treated by pseudo-LIPUS. *In vivo*, the rats under anesthesia were placed at a constant location, after which the transducer was pressed against the side of the cheek closest to the maxillary first molar. *In vitro*, we attached the transducer to the bottom of the plate corresponding to the well[18].

qRT-PCR

After 7 d of osteogenic induction, we utilized TRIzol reagent (Invitrogen, California, United States) to extract total cellular RNA following the previous protocol[19]. Table 1 displays all the primers used. cDNA synthesis kits (Takara Bio, Tokyo, Japan) were used to prepare first-strand cDNA from RNA through reverse transcription in accordance with the protocol. A Viia™ 7 Real-time PCR System (Applied Biosystems, Washington, Rhode Island, United States) was used for qRT-PCR, which was carried out in triplicate.

Western blot analysis

After 7 d of osteogenic induction, RIPA buffer containing 1 mM phenylmethanesulfonyl fluoride (Solarbio, Beijing, China) was added for cell lysis, followed by centrifugation at 12000 × *g* for 20 min at 4 °C. Thereafter, the supernatant was

Table 1 Primer sequences for quantitative reverse transcription-polymerase chain reaction

Gene	Primer sequence	
GAPDH	Forward	TCATTGACCTCAACTACATG
	Reverse	TCGCTCCTGGAAGATGGTGAT
RUNX2	Forward	TGGTTACTGTCATGGCGGGTA
	Reverse	TCTCAGATCGTTGAACCTTGCTA
ALP	Forward	ACTGGTACTCAGACAACGAGAT
	Reverse	ACGTCAATGTCCCTGATGTTATG
COL1a1	Forward	GTGCGATGACGTGATCTGTGA
	Reverse	CGGTGGTTTCTTGGTCGGT
OCN	Forward	CACTCCTCGCCCTATTGGC
	Reverse	CAGCAGAGCGACACCCTAGAC
YAP1	Forward	AGAATCAGTCAGAGTGCTCCAGTG
	Reverse	CGCAGCCTCTCCTTCTCCATC

ALP: Alkaline phosphatase; RUNX2: Runt-related transcription factor 2; COL: Collagen; OCN: Osteocalcin; YAP1: Yes-associated protein.

quantified with a BCA assay (Beyotime). Total protein was added to loading buffer, and the mixture was subsequently boiled for 10 min at 100 °C. Thereafter, the samples were stored at -20 °C. Equal amounts of total protein (30 μg) were loaded on sodium dodecyl sulfate-polyacrylamide gels and separated prior to electroblotting onto polyvinylidene difluoride membranes (Millipore, Billerica, Massachusetts, United States). After blocking with 5% bovine serum albumin, the membranes were incubated overnight on a shaker at 4 °C. The primary antibodies used were rabbit anti-type 1 collagen (COL1) and anti-osteocalcin (OCN) (1:500; Abcam, Cambridge, Massachusetts, United States), rabbit anti-ALP (1:500; Invitrogen), and mouse anti-GAPDH (1:1000; ProteinTech, Cook, Illinois, United States). Finally, HRP-labeled secondary antibodies (Zsgb-Bio, Beijing, China) were added for another 1-h incubation, followed by visualization *via* enhanced chemiluminescence (NCM Biotech, Suzhou, China). ImageJ software was used for band intensity analysis.

Immunofluorescence staining

After 7 d of osteogenic induction, 4% paraformaldehyde (PFA) was added for 15 min to fix the cells, after which the cells were rinsed with phosphate buffered saline (PBS) three times prior to 10 min of permeabilization with 0.5% Triton X-100 and washing with PBS. Thereafter, 5% BSA was added to the block cells for an hour before they were incubated with primary antibodies (1:200; Abcam) against YAP1, Lamin A/C, and F-actin at 4 °C overnight. The cells were washed with PBS before further incubation with Alexa Fluor 488- and Alexa Fluor 594-labeled antibodies (1:200; Invitrogen) for one hour. Finally, medium containing DAPI was added to the mount cells after washing. Images were captured with an inverted confocal microscope (Olympus, Tokyo, Japan).

Rat model of OTM

Male SD rats (6 wk old) weighing 200 ± 20 g were obtained from Beijing Vital River Laboratory Animal Technology Co., Ltd. (Beijing, China) and housed under laboratory conditions (12 h light/dark cycle, 21 ± 2 °C, 50% humidity, *ad libitum* access to food and water). All animal protocols utilized in the present work were approved by the Ethics Committee for Animal Experiments at Peking University Health Science Center (No. LA2022288) and were designed to minimize animal pain or discomfort.

In total, 27 male rats were randomized to control (n = 3), force (day 7 and day 14) (n = 6 per group), or force + LIPUS group (day 7 and day 14) (n = 6 per group). Before establishing the experimental OTM model, each rat was administered pentobarbital sodium (40 mg/kg of body weight) for anesthesia. In those latter two groups, the OTM model was established as described in our previous study[20]. A stainless steel ligation wire (0.025 mm in diameter; Tomy International, Inc., Tokyo, Japan) was used to ligate a closed-coil spring (Tomy International, Inc., Tokyo, Japan) to the maxillary first molar and incisor neck. The spring offers 50 g of force to move the maxillary first molar mesially. To enhance the retaining force and prevent the device from falling off, a 0.5 mm deep groove was made by a slow speed mill near the gingival margin of the maxillary incisor to accommodate the ligature wire, which was subsequently filled with flowing resin (3 M, Minnesota, United States). All animals were sacrificed with an overdose of pentobarbital sodium (150 mg/kg) for tissue collection.

Micro-computed tomography imaging and measurements

A microcomputed tomography scanner was used to scan maxillary samples at 8.82 μm resolution, 500 μA tube current, 60 kV tube voltage, and 1500 ms exposure time. Inveon Research Workplace software (Siemens, Munich, Germany) together with Mimics Research 21.0 software (Materialise, Leuven, Belgium) was used for raw data reconstruction. With respect to

the reconstructed 3D model, the shortest distance from the first to second molar crown was considered the tooth movement distance (Figure 1B). A straight plane was made at the cementum-enamel boundary (CEJ) on the first molar's distal buccal side, and the farthest distance between it and the parallel line tangent to alveolar crest resorption was measured to assess the reduction in alveolar bone height. In addition, Inveon Research Workplace software was used to evaluate the BV/TV, Tb.Th, Tb.N, Tb.Sp, and BS/BV in the chosen regions of interest (ROIs) (Figure 1C) by the reviewer, who was blinded to the groupings. All the samples were analyzed thrice to obtain the means.

Tissue processing

We set the experimental period at 7 and 14 d following the establishment of the tooth movement device. The rats were sacrificed with an overdose of pentobarbital sodium, after which the maxilla was dissected and immersed in 4% paraformaladehyde. For hematoxylin and eosin (HE), tartrate-resistant acid phosphatase (TRAP), and immunohistochemical staining, the trimmed tissues were decalcified with 5% ethylenediaminetetraacetic acid disodium for 15 d, followed by ethanol dehydration and paraffin embedding. Thereafter, the samples were cut into 5-μm vertical serial sections with a rotary microtome (RM2125RT, Leica, Heidelberger, Germany).

HE, TRAP, and immunohistochemical staining

Sections were stained with an HE staining kit (Sigma, Missouri, United States) or a TRAP staining kit (Solarbio, Beijing, China) following the protocols. Immunohistochemical staining was performed as follows. After xylene deparaffinization and ethanol rehydration, 0.125% trypsin and 20 μg/mL proteinase K solution were added to the sections, which were incubated at 37 °C for a 30-min period. Endogenous peroxidase activity was blocked with 3% H_2O_2 for a 30-min period at room temperature. The sections were subsequently washed with PBS, blocked with 5% BSA for an hour, and incubated with polyclonal anti-rabbit COL1 and OCN antibodies (1:200; Abcam) overnight at 4 °C, followed by another 1-h incubation with HRP-labeled secondary goat anti-rabbit IgG (Zsgb-Bio, Beijing, China) at room temperature. Diaminobenzidine (Zsgb-Bio) was used for visualization in accordance with the protocol. After hematoxylin counterstaining, gradient ethanol, and xylene dehydration, the sections were mounted using neutral resins.

Statistical analysis

The data are presented as the mean ± SD and were analyzed with GraphPad Prism 7 software (GraphPad, Inc., La Jolla, CA, United States). Every assay was carried out thrice. Student's *t* test was used to evaluate intergroup differences, while one-way analysis of variance (ANOVA) with multiple comparisons was used to evaluate differences among multiple groups. $P < 0.05$ indicated statistical significance.

RESULTS

Orthodontic force treatment decreases alveolar bone height on the compression side

We detected the movement distance of the maxillary first molars on the 7th d and 14th d after force application and found that the movement distance increased with time under the effect of 50 g of force ($P < 0.01$, $n = 3$) (Figure 1A), suggesting that the rat OTM model was successfully constructed. Moreover, the distance between the alveolar crest and CEJ significantly increased on day 7 and day 14, showing that orthodontic force led to vertical resorption of alveolar bone beginning on day 7 (Figure 1B). We selected the alveolar bone mesial to the medial 1/3 of the first molar's distal buccal root with a certain thickness as the ROI (Figure 1C). Micro-computed tomography results showed that at 7 and 14 d of tooth movement, the alveolar bone BV/TV and Tb.Th decreased after force application, while the BS/BV and Tb.Sp increased after force application (Figure 1C). This result showed that the bone density decreased on the compression side after orthodontic force treatment. HE staining and immunohistochemical staining revealed a decreased number of cells positive for the osteogenic markers COL1 and OCN in alveolar bone on the pressure side (Figure 1D and E), with a greater number of TRAP-positive cells on the pressure side near the alveolar bone edge (Figure 1F).

Osteogenic differentiation of BMSCs is inhibited by force treatment

Static pressure was used *in vitro* to simulate alveolar bone on the pressurized side. Compared to those in the control group, the osteogenic differentiation of the BMSCs in the force group was decreased, as evidenced by the ALP and alizarin red staining results (Supplementary Figure 1 and Figure 2A-D). Correspondingly, the expression levels of the osteogenesis-related markers ALP, COL1, runt-related transcription factor 2 (RUNX2), and OCN in the force group significantly decreased (Figure 2E and F) compared to the control ones, as detected by qRT-PCR and Western blot.

LIPUS induces osteogenic differentiation of BMSCs

The force treatment decreased the osteogenic differentiation of BMSCs, while LIPUS could rescue the impaired osteogenic differentiation of BMSCs caused by force treatment (Figure 3A-D), as shown by ALP and alizarin red staining. Moreover, the expression of ALP, COL1, RUNX2, and OCN was accordingly increased after LIPUS treatment compared with the force group, as assessed by qRT-PCR (Figure 3E) and Western blot (Figure 3F).

LIPUS decreases alveolar bone resorption in vivo

The movement distance of the first molar in the force + LIPUS group was greater than that of the force group on the 7th and 14th d after force application ($P < 0.05$) (Figure 4A-D). Moreover, the height of alveolar bone resorption was also

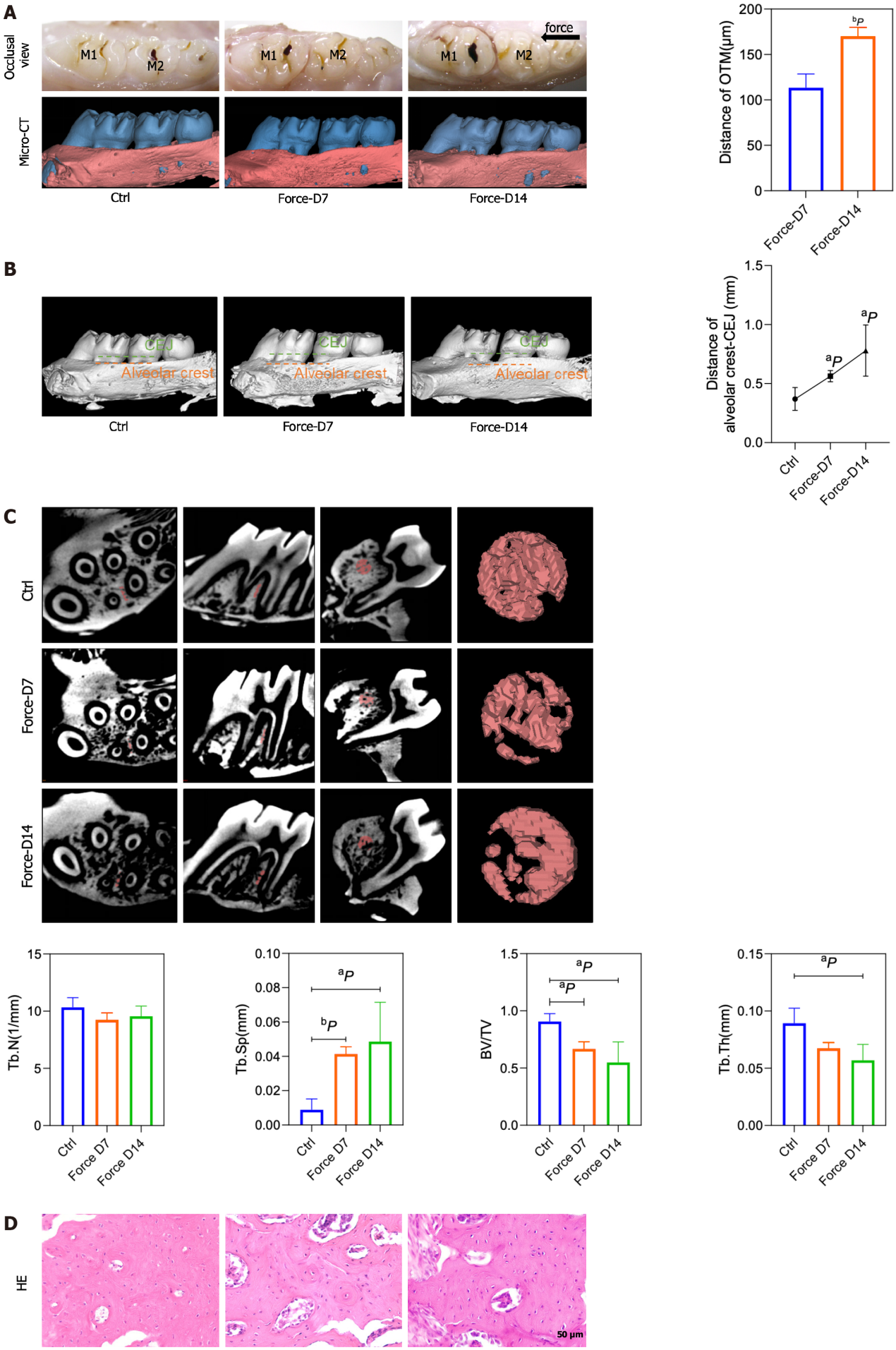
A
Occlusal view
Micro-CT
M1
M2
force
Ctrl
Force-D7
Force-D14
Distance of OTM(μm)
B
CEJ
Alveolar crest
Distance of alveolar crest-CEJ (mm)
C
Ctrl
Force-D7
Force-D14
Tb.N(1/mm)
Tb.Sp(mm)
BV/TV
Tb.Th(mm)
Force D7
Force D14
D
HE
50 μm

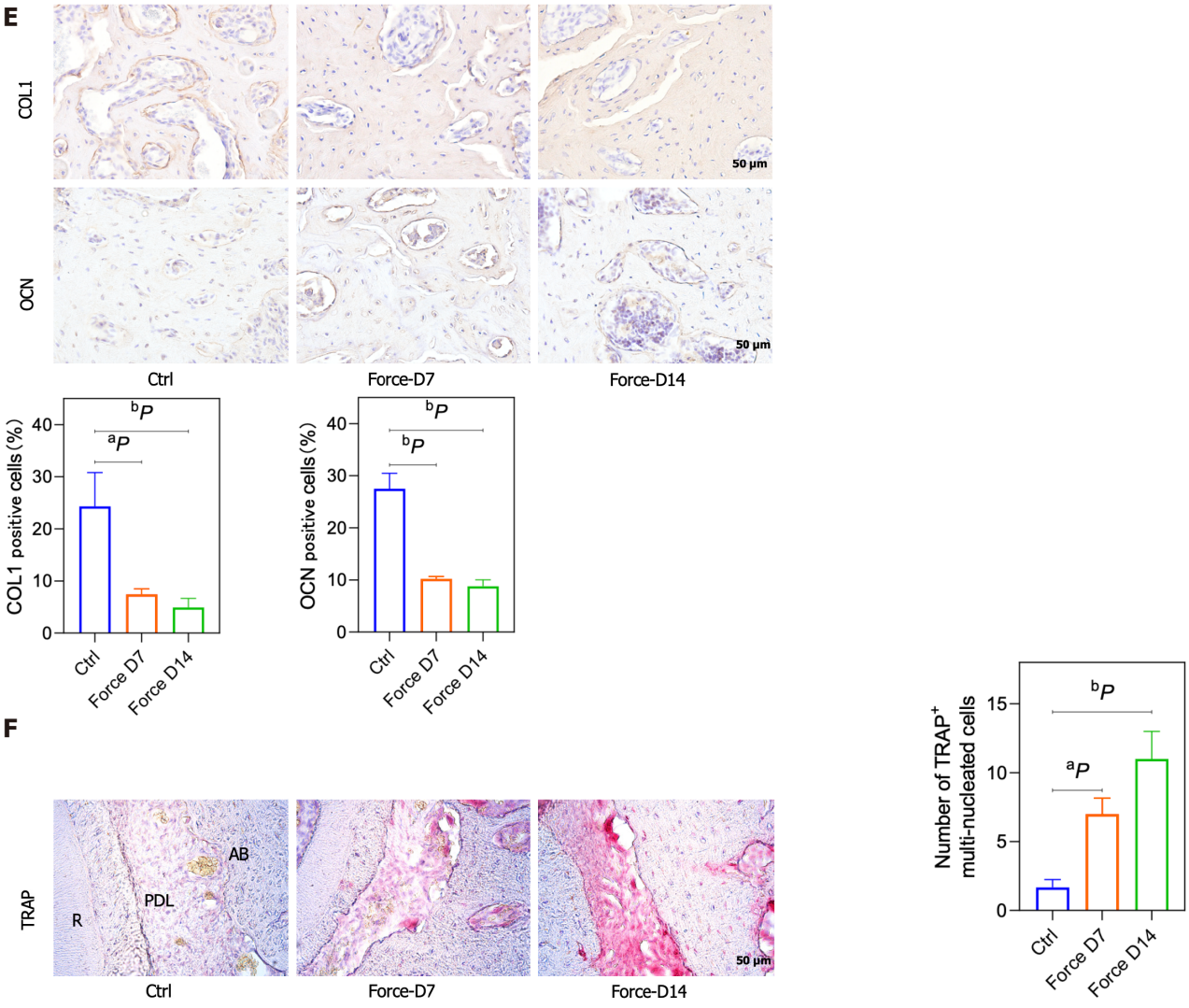

Figure 1 The bone density decreased, and the alveolar bone height decreased on the compression side. A: Representative pictures of the rat tooth movement model and 3D model images reconstructed with Mimics software (left) and the statistical diagram of the tooth movement distance (right); B: Representative images of 3D models reconstructed from micro-computed tomography images showing the distance from the alveolar crest to the cemento-enamel junction (left) and the corresponding statistical analysis (right); C: Representative region of interest (ROI) selection diagrams (left) and statistical analysis (right). A certain volume of alveolar bone on the compressed side of the middle 1/2 root of the distal buccal root of the first molar was selected for subsequent analysis. The statistical analysis of the BV/TV, Tb.Th, Tb.N, Tb.Sp and BS/BV values of the ROI region was performed with Siemens software; D: Representative images of hematoxylin and eosin staining; E: Representative images of immunohistochemical staining for type 1 collagen and osteocalcin (left) and quantitative analyses (right); F: Representative images of tartrate-resistant acid phosphatase (TRAP) staining (left) and counting of TRAP-positive multinuclear (> 3 nuclei) cells (right). $^{a}P < 0.05$ *vs* control group, $^{b}P < 0.01$ *vs* control group. CEJ: Cementum-enamel boundary; HE: Hematoxylin and eosin; TRAP: Tartrate-resistant acid phosphatase; COL1: Type 1 collagen; OCN: Osteocalcin; CT: Computed tomography.

reduced in the LIPUS treatment group ($P < 0.05$) (Figure 4E and F). ROI measurements of the corresponding sites indicated that the BV/TV and Tb.Th of the force + LIPUS group were higher than those of the force group, while the BS/BV and Tb.Sp were decreased ($P < 0.05$, $n = 3$) (Figure 4G-I), indicating that LIPUS promoted alveolar bone formation. Furthermore, the expression of COL1 and OCN was increased on the compressed side in the LIPUS treatment group compared with the force group (Figure 5A-D). However, no significant differences in TRAP-positive cell numbers were observed between the force group and the force + LIPUS group (Figure 5B and E).

LIPUS activates YAP1 signaling via Lamin A/C

To explore the role of LIPUS in regulating the cytoskeleton in BMSCs, we performed F-actin and Lamin A/C immunofluorescence co-staining *in vitro*. The results showed that the compressive force treatment downregulated the expression of F-actin, disrupted the cytoskeleton, and inhibited the Lamin A/C ratio in BMSCs, while LIPUS effectively reversed these changes (Figure 6A). Lamin A/C was reported to mediate the YAP1 nuclear localization by regulating nuclear stiffness[21,22]. Next, we analyzed the expression of YAP1. The results showed that the expression of YAP1 was decreased by force treatment, whereas LIPUS restored the expression of YAP1 and increased the nuclear localization of YAP1, as shown by immunofluorescence staining and Western blot (Figure 6B and C). Consistently, the expression of YAP1 was decreased in the force group, while its expression was increased in the LIPUS treatment group *in vivo*, *as*

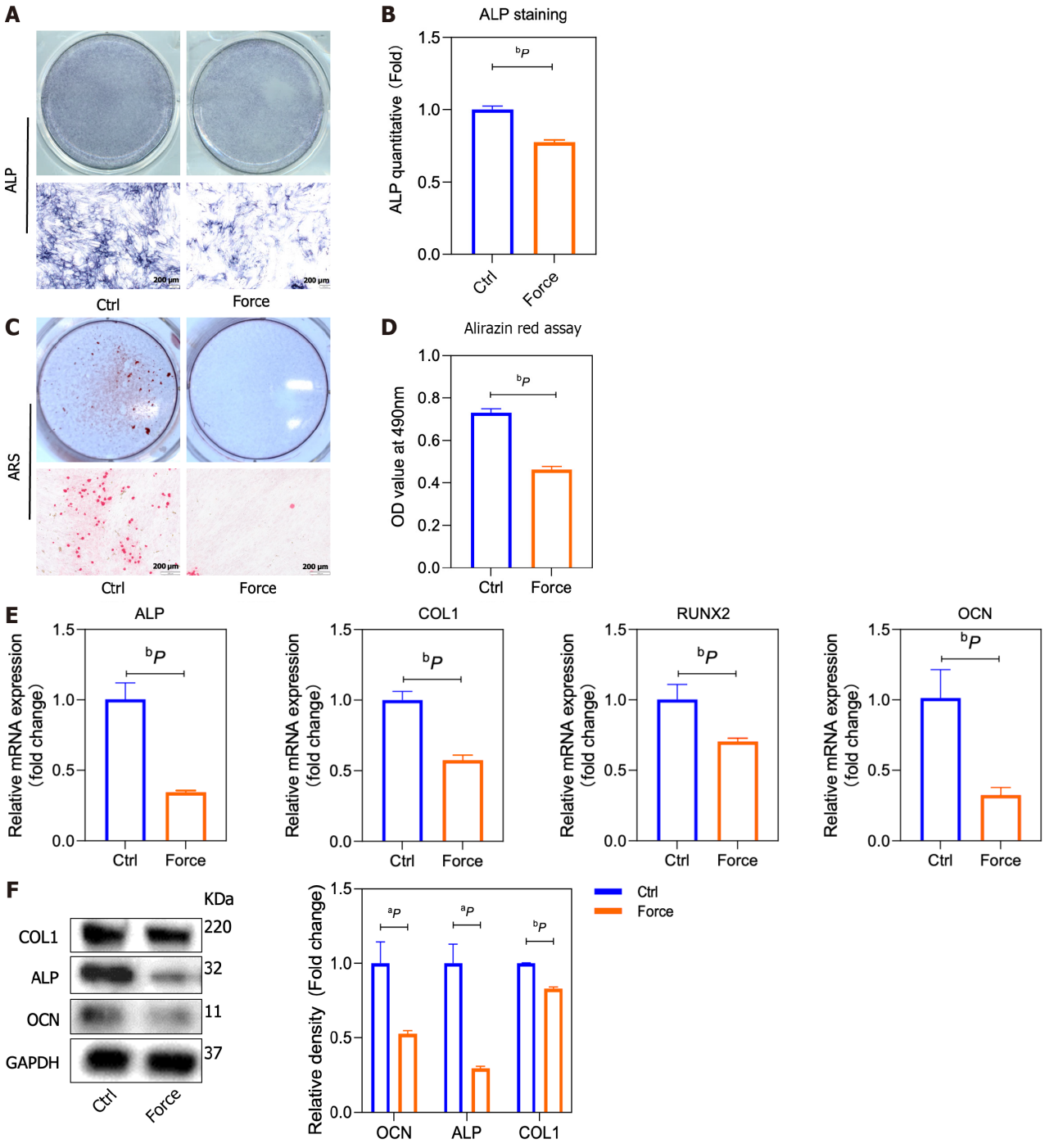

Figure 2 Static pressure inhibits the osteogenic differentiation of bone marrow mesenchymal stem cells *in vitro*. A and B: Representative alkaline phosphatase (ALP) staining images and statistical analysis; C and D: Representative alizarin red staining images and quantitative data from the alirazin red assay; E: mRNA expression of ALP, type 1 collagen (COL1), runt-related transcription factor 2, and osteocalcin (OCN) folded to control group by quantitative reverse transcription-polymerase chain reaction; F: COL1, ALP, and OCN protein expression in bone marrow mesenchymal stem cells analyzed by Western blotting (left), and the band intensities measured with ImageJ software (right). $^{a}P < 0.05$ *vs* control group, $^{b}P < 0.01$ *vs* control group. ALP: Alkaline phosphatase; RUNX2: Runt-related transcription factor 2; COL1: Type 1 collagen; OCN: Osteocalcin; ARS: Alizarin red staining.

analyzed by immunochemical staining (Figure 6D).

Knockdown of YAP1 blocks osteogenic differentiation of BMSCs induced by LIPUS

To verify the role of YAP1 on the property of BMSCs, we used YAP1 siRNA to treat BMSCs (Figure 7A), and the results showed that the expression of osteogenic differentiation-related markers ALP, COL1, RUNX2 and OCN increased by LIPUS treatment could be blocked by YAP1 siRNA treatment (Figure 7B and C). The osteogenic differentiation of BMSCs increased by LIPUS treatment could also be inhibited by YAP1 siRNA treatment, as assessed by ALP and alizarin red staining (Figure 7D and E). Our results demonstrated that LIPUS can accelerate tooth movement and reduce alveolar bone resorption by modulating the cytoskeleton-Lamin A/C-YAP axis (Figure 8).

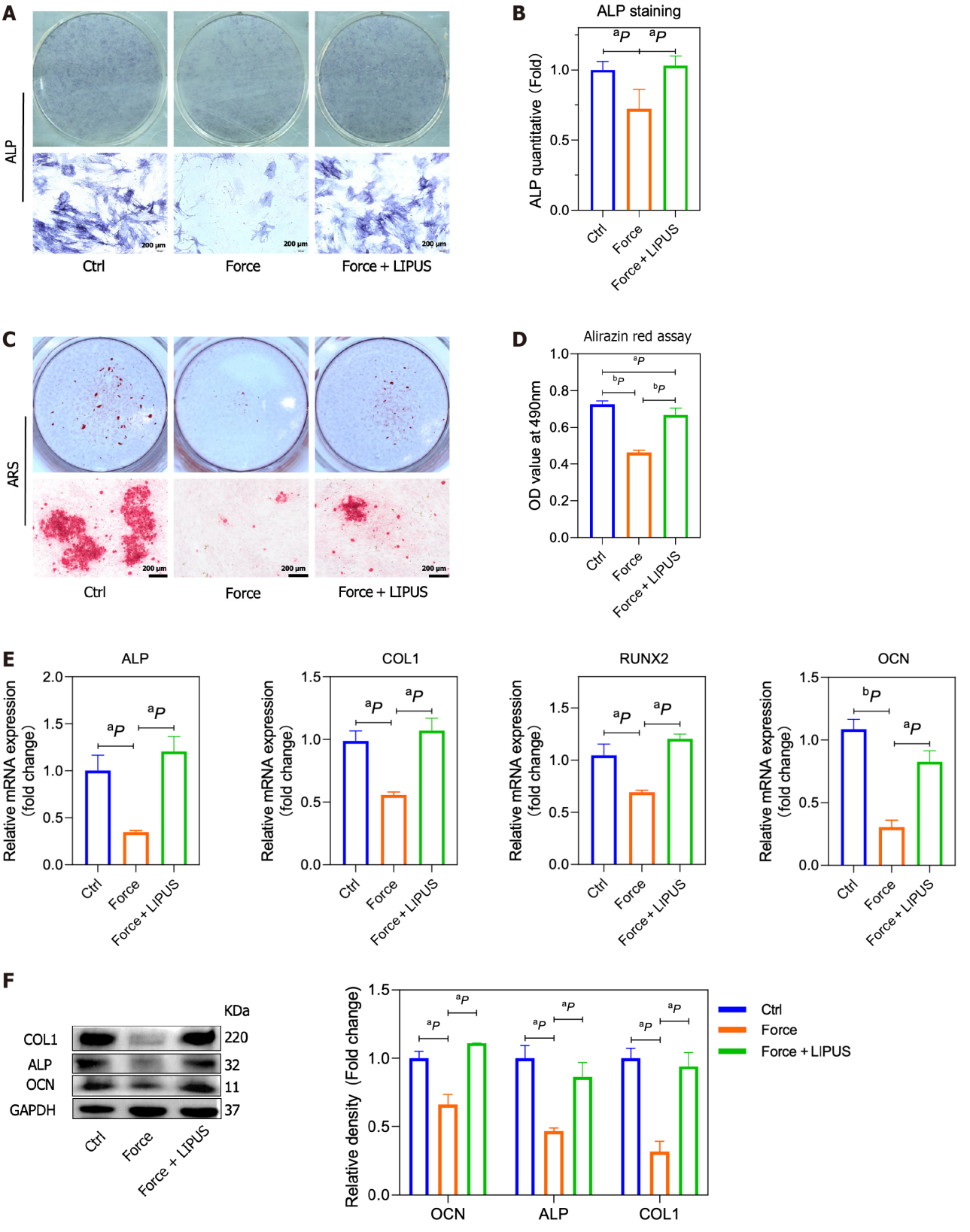

Figure 3 Low-intensity pulsed ultrasound promotes the osteogenesis of bone marrow mesenchymal stem cells. A and B: Representative alkaline phosphatase (ALP) staining images and statistical analysis; C and D: Representative alizarin red staining images and quantitative data from the alirazin red assay; E: mRNA expression of ALP, type 1 collagen (COL1), runt-related transcription factor 2, and osteocalcin (OCN) folded to control group by quantitative reverse transcription-polymerase chain reaction; F: COL1, ALP, and OCN protein expression in rat alveolar bone tissues analyzed *via* Western blotting (left), and the band intensities measured *via* ImageJ software (right). $^{a}P < 0.05$ *vs* control group, $^{b}P < 0.01$ *vs* control group. ALP: Alkaline phosphatase; RUNX2: Runt-related transcription factor 2; COL1: Type 1 collagen; OCN: Osteocalcin; LIPUS: Low-intensity pulsed ultrasound; ARS: Alizarin red staining.

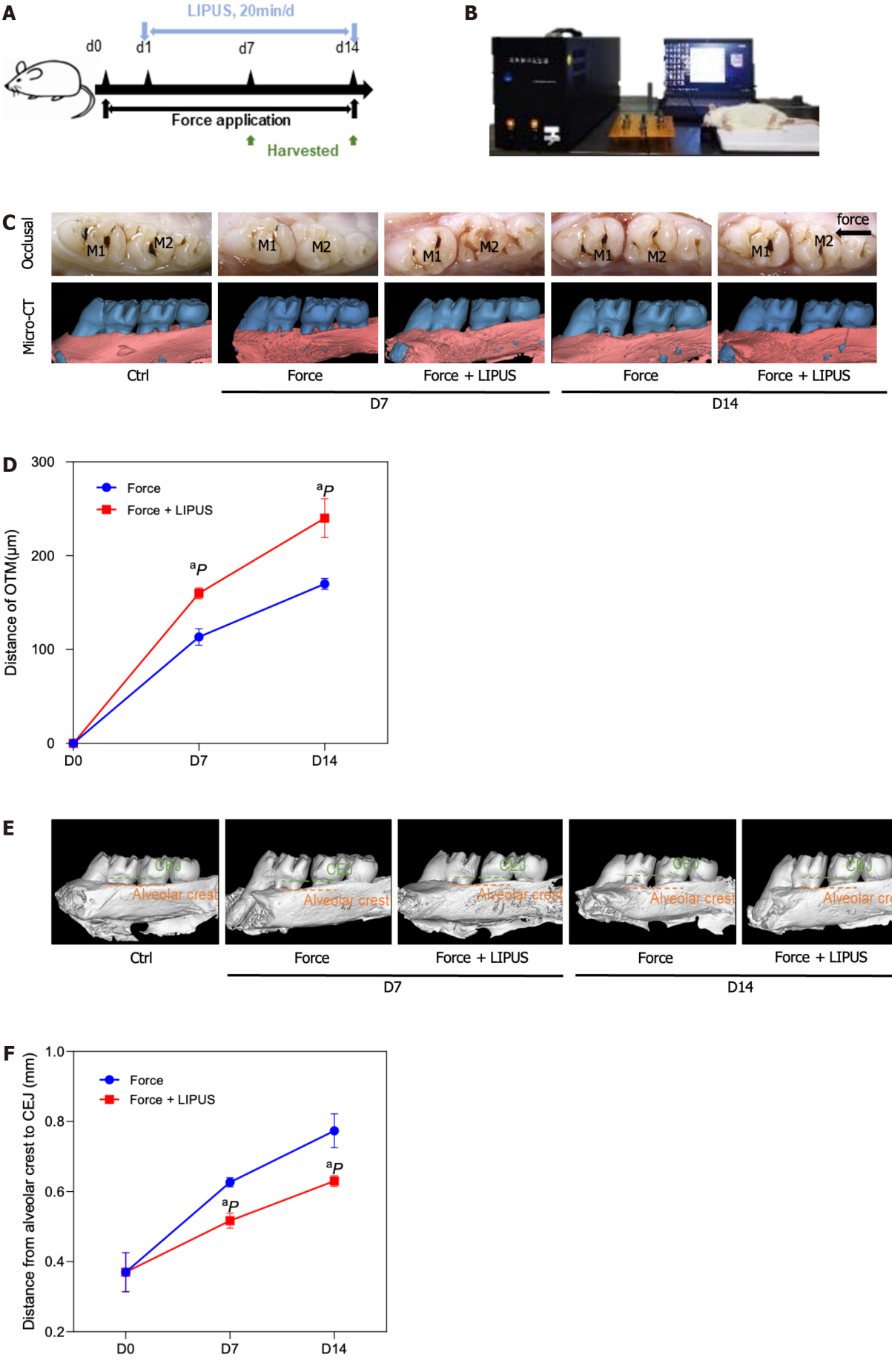
A
LIPUS, 20min/d
d0
d1
d7
d14
Force application
Harvested
B
C
Occlusal
Micro-CT
M1
M2
force
Ctrl
Force
Force + LIPUS
Force
Force + LIPUS
D7
D14
D
Distance of OTM(μm)
300
200
100
0
Force
Force + LIPUS
aP
aP
D0
D7
D14
E
CEJ
Alveolar crest
Ctrl
Force
Force + LIPUS
Force
Force + LIPUS
D7
D14
F
Distance from alveolar crest to CEJ (mm)
1.0
0.8
0.6
0.4
0.2
Force
Force + LIPUS
aP
aP
D0
D7
D14

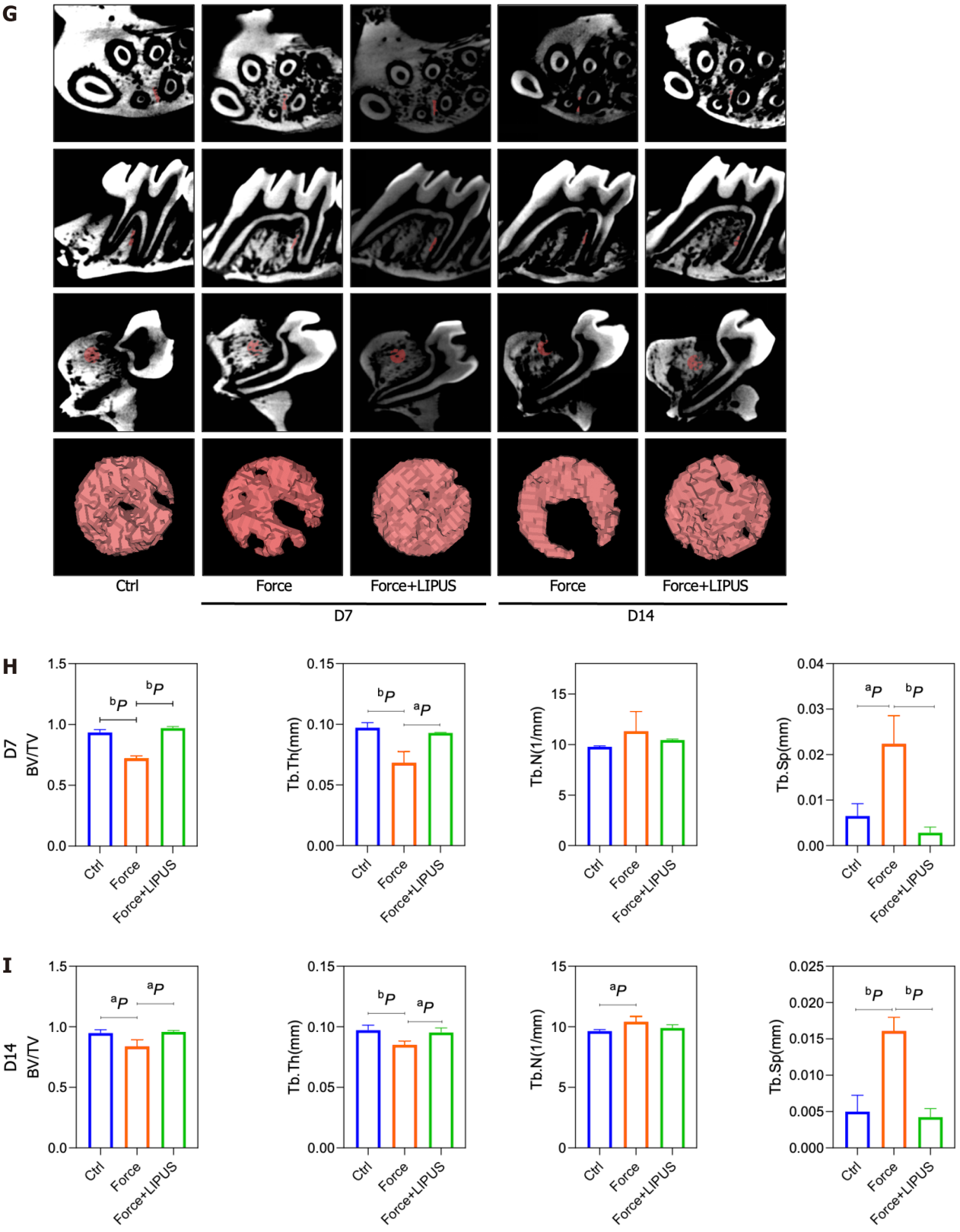

Figure 4 Low-intensity pulsed ultrasound accelerates tooth movement, inhibits alveolar bone resorption, and promotes bone formation. A: Schematic diagram of the animal experiment procedure. The orthodontic tooth movement model was established on day 0. From day 1 to the end point, the force + low-intensity pulsed ultrasound (LIPUS) group was stimulated with LIPUS for 20 min every day until the samples were harvested on days 7 and 14; B: Schematic representation of LIPUS stimulating the maxillary first molar at the corresponding position on the buccal side; C-F: Representative images (C) and 3D reconstructed model images (E). Tooth movement distances (D) and distances from the alveolar crest to the cementum-enamel boundary (F) were measured with Mimics software; G-I: Representative region of interest (ROI) region selection diagrams and statistical analysis of the BV/TV, Tb.Th, Tb.N, Tb.Sp, and BS/BV values of the ROI. ^{a}P < 0.05 *vs* control group, ^{b}P < 0.01 *vs* control group. CT: Computed tomography; LIPUS: Low-intensity pulsed ultrasound.

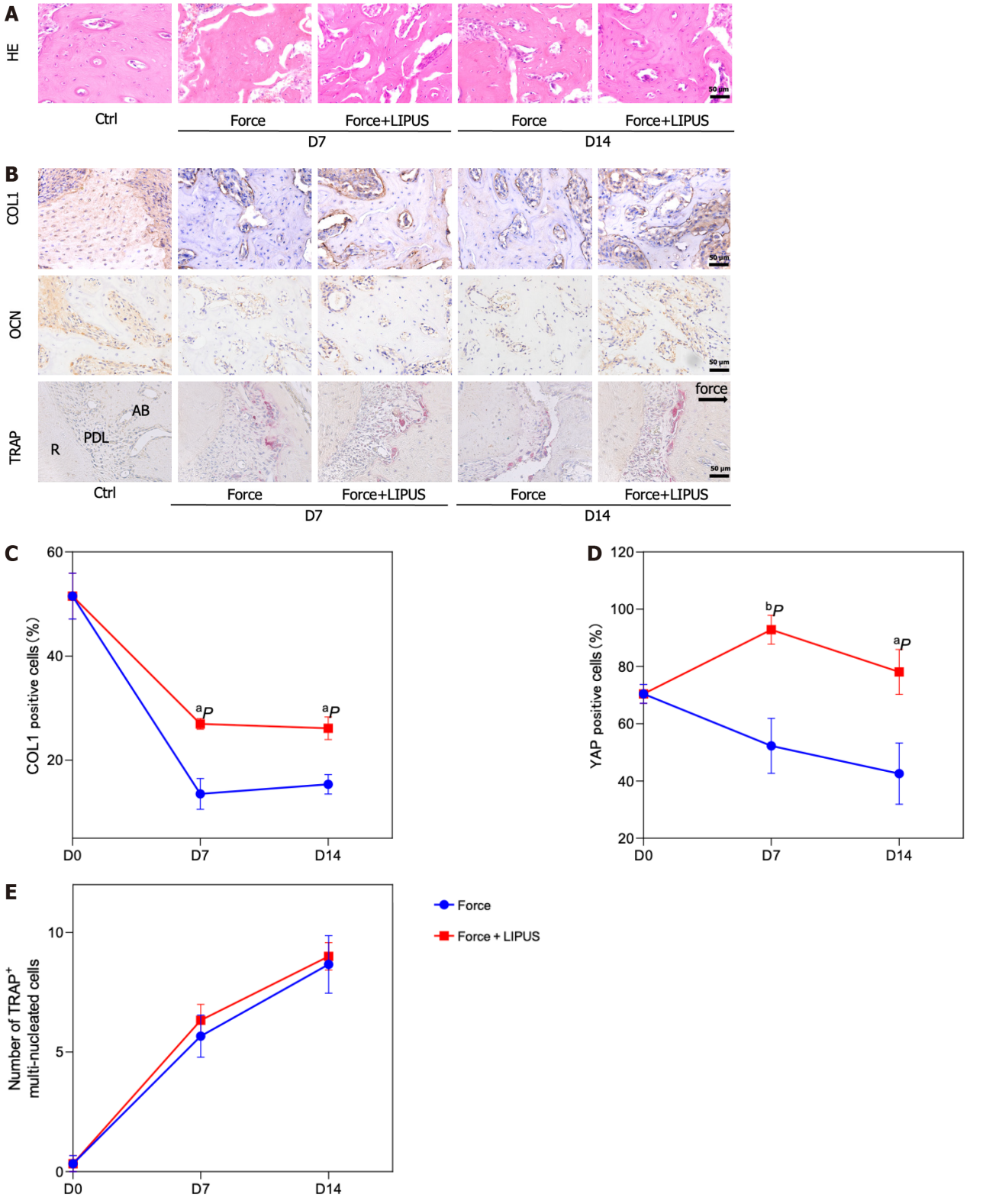

Figure 5 Low-intensity pulsed ultrasound promotes bone formation. A: Representative images of hematoxylin and eosin staining; B: Representative images of immunohistochemical staining for type 1 collagen and osteocalcin and tartrate-resistant acid phosphatase staining (TRAP); C-E: Statistical analyses of the immunohistochemical staining and TRAP staining results. $^{a}P < 0.05$ *vs* control group, $^{b}P < 0.01$ *vs* control group. HE: Hematoxylin and eosin; TRAP: Tartrate-resistant acid phosphatase; COL1: Type 1 collagen; OCN: Osteocalcin; LIPUS: Low-intensity pulsed ultrasound.

DISCUSSION

The process of orthodontic treatment is a bone remodeling process. The force applied to drive tooth movement in some extent led to some adverse reactions, such as root resorption and bone mineral density decline. LIPUS has been reported to alleviate chondrocyte damage in temporomandibular disorders[23], reduce root resorption[24], and enhance bone

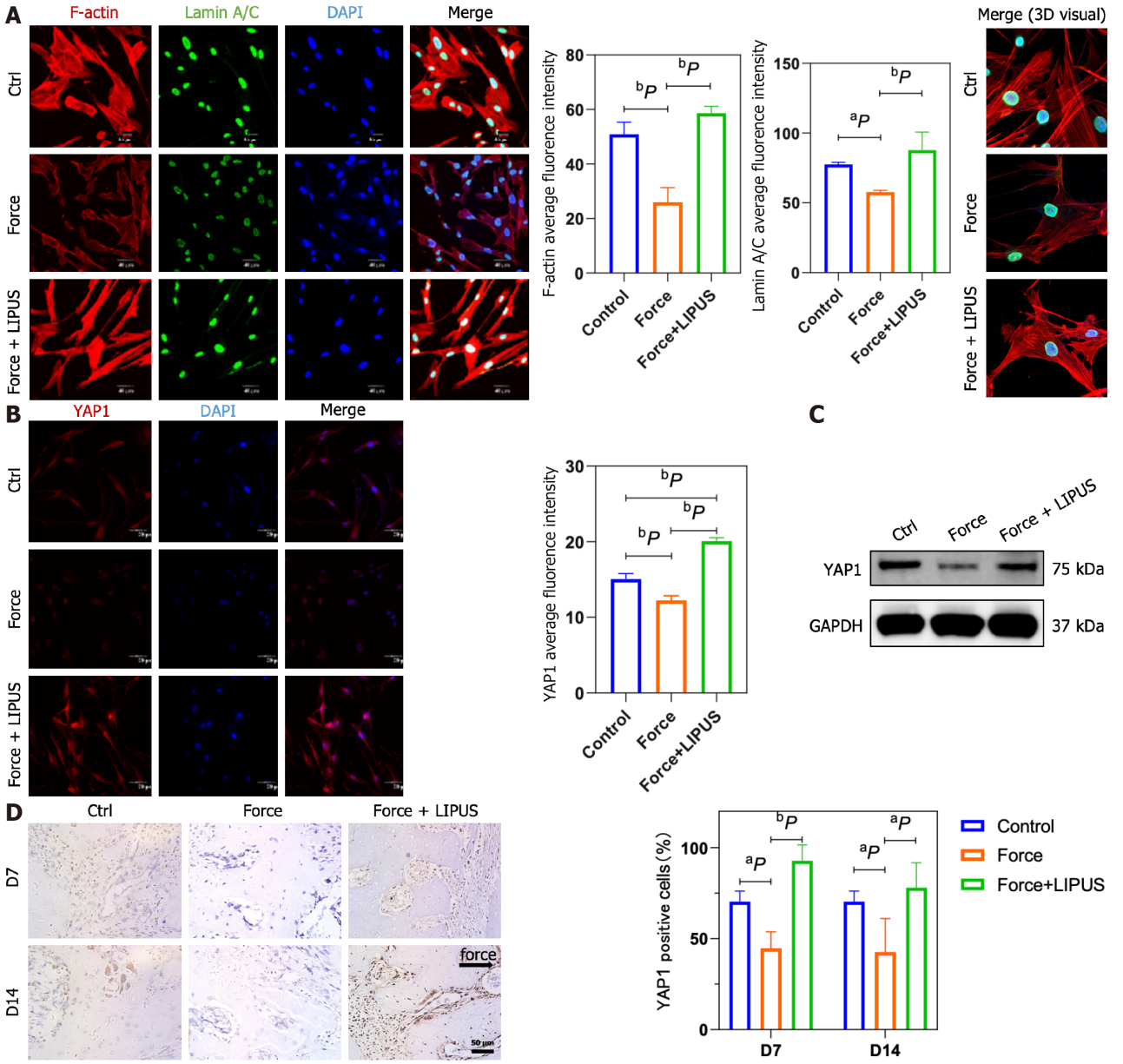

Figure 6 Low-intensity pulsed ultrasound reverses the stress-induced decrease in LaminA/C, F-actin, and Yes-associated protein expression. A: Representative immunofluorescence images of F-actin (red), LaminA/C (green), and DAPI (blue) staining (left) and statistical analyses (middle), as well as representative 3D merged images constructed with Imaris software (right); B: Representative immunofluorescence images of Yes-associated protein (YAP1) (red) and DAPI (blue) staining (left) and statistical analyses (right); C: YAP1 protein expression analyzed by Western blotting; D: Representative images of immunohistochemical staining for YAP1 (left) and statistical analysis (right). $^{a}P < 0.05$ *vs* control group, $^{b}P < 0.01$ *vs* control group. LIPUS: Low-intensity pulsed ultrasound; YAP1: Yes-associated protein.

remodeling[10]. However, there is a lack of research on the effect of LIPUS on the aesthetic problem of gingival recession due to the loss of alveolar bone height during orthodontic treatment. Changes in alveolar bone morphology affect the aesthetic effect, safety, and stability[25] of orthodontic treatment. Clinical studies have shown that alveolar bone height loss often leads to insufficient periodontal supporting tissue, decreased dental stability, and aesthetic problems in the anterior teeth[26]. Our experiments showed that LIPUS could effectively ameliorate the aesthetic and health problems caused by alveolar bone height loss by reducing vertical alveolar bone resorption and improving the morphology of alveolar bone remodeling, and filled the research gap in the relevant field.

Clinical studies have used cone beam computed tomography to assess changes in periodontal bone mineral density during orthodontic treatment. On average, the alveolar bone mineral density decreases by 24% after 7 mo of orthodontic treatment, while the region with the largest reduction in bone mineral density seems to be related to the direction of tooth movement[27,28]. Consistently, in the present study, we found that bone mineral density decreased at 7 and 14 d after stress. Mechanical stress can modulate osteoclasts and osteoblasts, thereby promoting bone reconstruction[29,30]. Excessive compressive force can cause stem cell apoptosis[31], aggravate mitochondrial dysfunction, ATP consumption, and oxidative stress in stem cells[32], and inhibit the proliferation, colony formation, and migration of stem cells[33]. Bone mineral density is positively correlated with OCN protein level[34]. In our study, static pressure on BMSCs

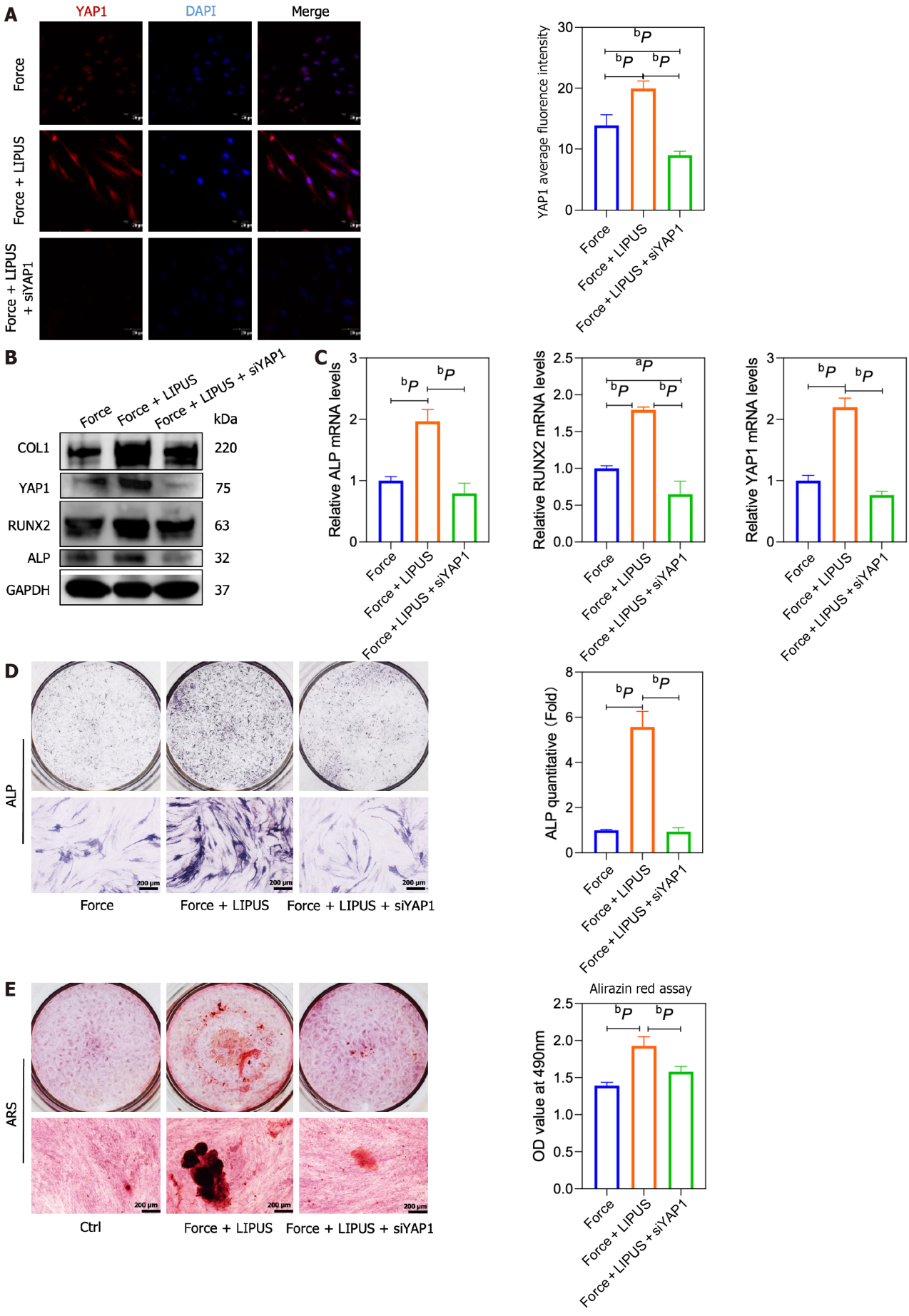

Figure 7 siYAP1 blocks the effect of low-intensity pulsed ultrasound-induced osteogenic differentiation of bone marrow mesenchymal

stem cells. A: Representative immunofluorescence images of Yes-associated protein (YAP1) (red) and DAPI (blue) staining (left) and statistical analyses (right); B: Western blotting results for type 1 collagen, YAP1, runt-related transcription factor 2 (RUNX2), and alkaline phosphatase (ALP); C: mRNA expression of ALP, RUNX2, and YAP1 in the force group by quantitative reverse transcription-polymerase chain reaction; D and E: Representative ALP and alizarin red staining staining images and statistical analysis. [a]*P* < 0.05 *vs* control group, [b]*P* < 0.01 *vs* control group. ALP: Alkaline phosphatase; COL1: Type 1 collagen; LIPUS: Low-intensity pulsed ultrasound; RUNX2: Runt-related transcription factor 2; YAP1: Yes-associated protein; ARS: Alizarin red staining.

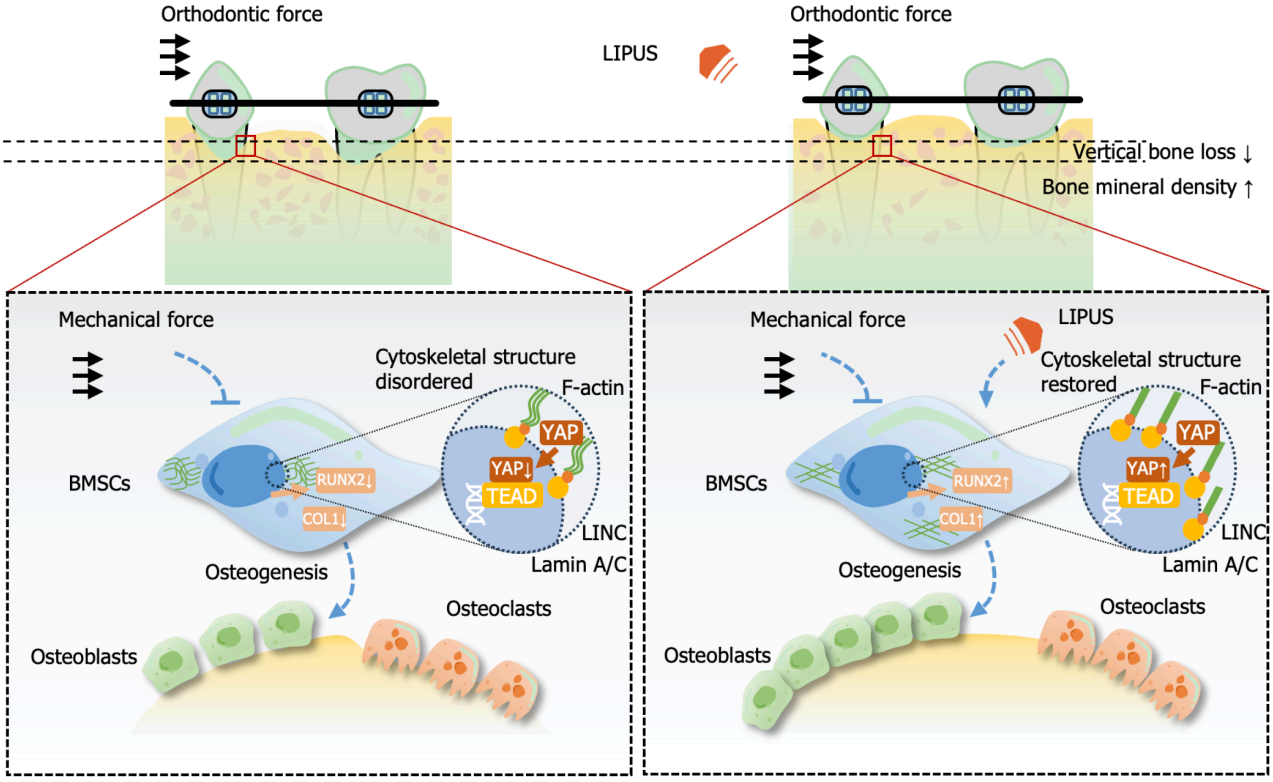

Figure 8 Putative mechanism of the effect of low-intensity pulsed ultrasound on alveolar bone during orthodontic treatment. Low-intensity pulsed ultrasound has little effect on osteoclast differentiation but may rescue osteogenic gene expression suppressed by static force and promote osteoblastic differentiation by reordering the cytoskeleton, upregulating the expression of F-actin and Lamin A/C, and increasing the nuclear translocation of Yes-associated protein 1, thereby contributing to alveolar bone homeostasis and morphology while accelerating tooth movement during orthodontic treatment. COL1: Type 1 collagen; LIPUS: Low-intensity pulsed ultrasound; RUNX2: Runt-related transcription factor 2; BMSC: Bone marrow mesenchymal stem cell; YAP1: Yes-associated protein.

inhibited the mRNA and protein expression of osteogenic differentiation markers such as COL1 and OCN, which partly explained the reduction in alveolar bone mineral density around moving teeth under orthodontic force.

Previous studies have shown that LIPUS plays a role in bone metabolism and remodeling by regulating osteogenic and osteoclast activity[35-37]. In our study, on day 7 and day 14, the number of osteoclasts in the force group was not significantly different from that in the force + LIPUS group, indicating that LIPUS may promote bone remodeling by promoting osteoclast activity but not by increasing the number of osteoclasts. As shown in numerous clinical trials and animal studies, LIPUS promotes osteogenesis, resulting in improved and quicker fracture healing[38,39]. It can also stimulate condylar growth and increase mandibular ramus height in rabbits[40,41]. LIPUS is effective in various cell processes, such as growth, differentiation[42,43], extracellular matrix formation, and mineralization of osteoblasts[44], and involves multiple signaling pathways, such as the hedgehog and TRPM7 pathways[45,46]. In addition to osteoblasts, LIPUS can promote the differentiation of adipose-derived stromal cells[47], mesenchymal stem cells[48], periodontal ligament stem cells[49], and rat osteosarcoma cell lines[50] and increase the expression of RUNX2 and COL1. LIPUS stimulation of BMSCs can enhance cell activity, promote osteogenic differentiation, and increase COL1 and OCN gene expression[51]. To date, few reports have focused on the role of LIPUS in cellular functions under loading conditions. In our study, LIPUS increased COL1, RUNX2, and OCN expression at the mRNA and protein levels, and rescued the inhibitory effect of compression force on the osteoblastic differentiation of BMSCs, demonstrating a positive effect on alveolar bone remodeling during orthodontic processing at the cellular level.

The way that mechanical signals can be transmitted from the plasma membrane to the nucleus directly *via* the cytoskeleton is considered to be an important mechanical signal transduction pathway[52]. The nucleus is considered a key mechanoreceptor that can directly influence chromatin organization, epigenetic modifications, and gene expression [53]. Lamin A/C, as LMNA-encoded Lamin proteins, participate in nuclear mechanics[54] and the transduction of mechanical signals[55,56], thereby regulating the fate of stem cells. The lincRNAs (linkers of cytoskeleton and nucleo-

skeleton) complex links Lamin A/C to the cytoskeleton, thereby mediating the transmission of mechanical signals from the cytoskeleton to the nucleus[57]. The Lamin A level is known to increase during osteogenic differentiation of MSCs but decrease during adipogenic differentiation[58,59]. In our study, Lamin A/C and F-actin were consistently downregulated after compression force application, and the cytoskeleton was more disordered under compression. To our knowledge, our study is the first to show that LIPUS increases Lamin A/C and F-actin expression and reorders the cytoskeleton under compression, thus reversing the decrease in osteogenesis of BMSCs induced by static force.

As a transcriptional coactivator protein, YAP1 is closely associated with changes in the mechanical state of cellular microenvironments[60]. YAP1 can relocate to the nucleus from the cytoplasm, interact with the TEA domain[61], and promote transcription. In mechanical transduction, it is also a downstream signal for the assembly and contraction of actin filaments[62]. Pressure can promote F-actin depolymerization and lead to cytoplasmic translocation of YAP1[63]. YAP1 was found to participate in multiple cellular activities. For example, YAP1 was reported to be activated during inflammation in endothelial cells induced by lipopolysaccharide[64] and was essential for epithelial cell proliferation[65]. In the inflammatory microenvironment in periodontitis, YAP1 expression and nuclear translocation are decreased[66]. In the force group, the YAP1 level decreased, while in the force + LIPUS group, the YAP1 level increased both *in vitro* and *in vivo*, suggesting that YAP1 exerts a crucial effect on the regulation of BMSC osteogenesis by mechanical force and LIPUS and might be a downstream effector of the cytoskeleton and nuclear skeleton.

This study has some limitations. Osteoblasts and osteoclasts jointly participate in the process of bone metabolism. This study mainly focused on the effect of LIPUS on the osteogenic function of stem cells, and whether LIPUS could regulate the crosstalk of osteoclasts and osteoblasts is unclear, which needs further investigation. In addition, the underlying mechanism of how LIPUS controls cytoskeleton changes remains unclear.

CONCLUSION

In summary, LIPUS can promote local alveolar bone remodeling, increase bone mineral density, and reduce vertical alveolar bone resorption and consequent gingival recession by regulating the osteogenic ability of BMSCs. In terms of mechanism, LIPUS upregulates the expression and nuclear translocation of YAP, which is decreased by mechanical stress through effects on the cytoskeleton and nuclear skeleton, thereby affecting the osteogenic differentiation of BMSCs.

ARTICLE HIGHLIGHTS

Research background

The bone remodeling during orthodontic treatment for malocclusion often requires a long duration, which also may lead to some complications such as alveolar bone resorption. Low-intensity pulsed ultrasound (LIPUS), a noninvasive physical therapy, has been shown to promote bone fracture healing and reduce the duration of orthodontic treatment; however, how LIPUS regulates the bone metabolism during the orthodontic treatment process is still unclear.

Research motivation

How to shorten the orthodontic treatment duration and reduce the side effects caused by orthodontic treatment such as alveolar bone resorption has become a very important clinical problem. LIPUS, as a non-invasive physical therapy, has been reported to promote the fracture healing process, and may also play a good role in orthodontic treatment.

Research objectives

This study was to investigate the effects of LIPUS on bone remodeling in an orthodontic tooth movement (OTM) model and explore the underlying mechanisms.

Research methods

We established a rat model of OTM, and alveolar bone remodeling and tooth movement rate were evaluated *via* micro-computed tomography and staining of tissue sections. *In vitro*, human bone marrow mesenchymal stem cells (hBMSCs) were isolated to detect their osteogenic differentiation potential under compression and LIPUS stimulation and to investigate the underlying mechanisms.

Research results

The force treatment inhibited the expression of osteogenesis markers and osteogenic differentiation potential of hBMSCs, which could be rescued by LIPUS treatment. Mechanically, the expression of LaminA/C, F-actin, and Yes-associated protein (YAP1) was downregulated after force application, which could be rescued by LIPUS treatment. Moreover, the osteogenic differentiation of MSCs increased by LIPUS treatment could be attenuated by YAP small interfering RNA treatment. Consistently, LIPUS increased alveolar bone density and decreased vertical bone absorption *in vivo*. The decreased expression of type 1 collagen, osteocalcin, and YAP1 on the compression side of the alveolar bone was partially rescued by the LIPUS treatment.

Research conclusions

By regulating the cytoskeleton-Lamin A/C-YAP axis, LIPUS can effectively accelerate tooth movement and reduce bone resorption. Therefore, LIPUS can be used as an effective auxiliary method for orthodontic treatment.

Research perspectives

These results may provide an adjunctive treatment strategy for orthodontic treatment and enrich the theoretical basis for LIPUS application.

FOOTNOTES

Co-first authors: Tong Wu and Fu Zheng.

Co-corresponding authors: Jiu-Hui Jiang and Rui-Li Yang.

Author contributions: Li CY, Jiang JH, and Yang RL were responsible for the study design and conduction; Jiang JH and Yang RL made equal contributions to the determination of study directions and the design of experimental methods, and they are the co-corresponding authors of this paper; Wu T and Zheng F contributed to the experimental implementation, data analysis, and manuscript writing equally; Tang HY, Li HZ, Cui XY, Ding S, and Liu D participated in some of the experiments; all authors approved the final version for submission.

Supported by the National Science and Technology Major Project of the Ministry of Science and Technology of China, No. 2022YFA1105800; the National Natural Science Foundation of China, No. 81970940.

Institutional review board statement: The study was approved by Ethical Guidelines of Hospital of Stomatology, Peking University (Approval No. PKUSSIRB-202385020).

Institutional animal care and use committee statement: All procedures involving animals were reviewed and approved by the Ethics Committee for Animal Experiments at Peking University Health Science Center (IACUC protocol number No. LA2022288).

Conflict-of-interest statement: All the authors report no relevant conflicts of interest for this article.

Data sharing statement: No additional data are available.

ARRIVE guidelines statement: The authors have read the ARRIVE guidelines, and the manuscript was prepared and revised according to the ARRIVE guidelines.

Country/Territory of origin: China

ORCID number: Cui-Ying Li 0000-0002-5536-5432; Jiu-Hui Jiang 0000-0003-4881-5949; Rui-Li Yang 0000-0002-3283-9893.

S-Editor: Wang JJ
L-Editor: Wang TQ
P-Editor: Zhang XD

REFERENCES

1 **Kirschneck C**, Fanghänel J, Wahlmann U, Wolf M, Roldán JC, Proff P. Interactive effects of periodontitis and orthodontic tooth movement on dental root resorption, tooth movement velocity and alveolar bone loss in a rat model. *Ann Anat* 2017; **210**: 32-43 [PMID: 27838559 DOI: 10.1016/j.aanat.2016.10.004]

2 **Hu B**, Zhang Y, Zhou J, Li J, Deng F, Wang Z, Song J. Low-intensity pulsed ultrasound stimulation facilitates osteogenic differentiation of human periodontal ligament cells. *PLoS One* 2014; **9**: e95168 [PMID: 24743551 DOI: 10.1371/journal.pone.0095168]

3 **Liu Z**, Xu J, E L, Wang D. Ultrasound enhances the healing of orthodontically induced root resorption in rats. *Angle Orthod* 2012; **82**: 48-55 [PMID: 21787199 DOI: 10.2319/030711-164.1]

4 **Chung SL**, Pounder NM, de Ana FJ, Qin L, Sui Leung K, Cheung WH. Fracture healing enhancement with low intensity pulsed ultrasound at a critical application angle. *Ultrasound Med Biol* 2011; **37**: 1120-1133 [PMID: 21640476 DOI: 10.1016/j.ultrasmedbio.2011.04.017]

5 **Naruse K**, Uchino M, Hirakawa N, Toyama M, Miyajima G, Mukai M, Urabe K, Uchida K, Itoman M. 4. The Low-Intensity Pulsed Ultrasound (LIPUS) Mechanism and the Effect of Teriparatide on Fracture Healing. *J Orthop Trauma* 2016; **30**: S3 [PMID: 27441765 DOI: 10.1097/01.bot.0000489989.28108.21]

6 **Zura R**, Della Rocca GJ, Mehta S, Harrison A, Brodie C, Jones J, Steen RG. Treatment of chronic (>1 year) fracture nonunion: heal rate in a cohort of 767 patients treated with low-intensity pulsed ultrasound (LIPUS). *Injury* 2015; **46**: 2036-2041 [PMID: 26052056 DOI:

10.1016/j.injury.2015.05.042]
7 **Alazzawi MMJ**, Husein A, Alam MK, Hassan R, Shaari R, Azlina A, Salzihan MS. Effect of low level laser and low intensity pulsed ultrasound therapy on bone remodeling during orthodontic tooth movement in rats. *Prog Orthod* 2018; **19**: 10 [PMID: 29658096 DOI: 10.1186/s40510-018-0208-2]
8 **Kaur H**, El-Bialy T. Shortening of Overall Orthodontic Treatment Duration with Low-Intensity Pulsed Ultrasound (LIPUS). *J Clin Med* 2020; **9** [PMID: 32370099 DOI: 10.3390/jcm9051303]
9 **Bahammam M**, El-Bialy T. Effect of Low-Intensity Pulsed Ultrasound (LIPUS) on Alveolar Bone during Maxillary Expansion Using Clear Aligners. *Biomed Res Int* 2022; **2022**: 4505063 [PMID: 35528174 DOI: 10.1155/2022/4505063]
10 **Arai C**, Kawai N, Nomura Y, Tsuge A, Nakamura Y, Tanaka E. Low-intensity pulsed ultrasound enhances the rate of lateral tooth movement and compensatory bone formation in rats. *Am J Orthod Dentofacial Orthop* 2020; **157**: 59-66 [PMID: 31901282 DOI: 10.1016/j.ajodo.2019.01.027]
11 **Berebichez-Fridman R**, Montero-Olvera PR. Sources and Clinical Applications of Mesenchymal Stem Cells: State-of-the-art review. *Sultan Qaboos Univ Med J* 2018; **18**: e264-e277 [PMID: 30607265 DOI: 10.18295/squmj.2018.18.03.002]
12 **Xie S**, Jiang X, Wang R, Xie S, Hua Y, Zhou S, Yang Y, Zhang J. Low-intensity pulsed ultrasound promotes the proliferation of human bone mesenchymal stem cells by activating PI3K/AKt signaling pathways. *J Cell Biochem* 2019; **120**: 15823-15833 [PMID: 31090943 DOI: 10.1002/jcb.28853]
13 **Aliabouzar M**, Lee SJ, Zhou X, Zhang GL, Sarkar K. Effects of scaffold microstructure and low intensity pulsed ultrasound on chondrogenic differentiation of human mesenchymal stem cells. *Biotechnol Bioeng* 2018; **115**: 495-506 [PMID: 29064570 DOI: 10.1002/bit.26480]
14 **Assanah F**, Grassie K, Anderson H, Xin X, Rowe D, Khan Y. Ultrasound-derived mechanical stimulation of cell-laden collagen hydrogels for bone repair. *J Biomed Mater Res A* 2023; **111**: 1200-1215 [PMID: 36728346 DOI: 10.1002/jbm.a.37508]
15 **Pettersson LF**, Kingham PJ, Wiberg M, Kelk P. In Vitro Osteogenic Differentiation of Human Mesenchymal Stem Cells from Jawbone Compared with Dental Tissue. *Tissue Eng Regen Med* 2017; **14**: 763-774 [PMID: 30603526 DOI: 10.1007/s13770-017-0071-0]
16 **Zhan X**, Li S, Cui Y, Tao A, Wang C, Li H, Zhang L, Yu H, Jiang J, Li C. Comparison of the osteoblastic activity of low elastic modulus Ti-24Nb-4Zr-8Sn alloy and pure titanium modified by physical and chemical methods. *Mater Sci Eng C Mater Biol Appl* 2020; **113**: 111018 [PMID: 32487417 DOI: 10.1016/j.msec.2020.111018]
17 **Wang J**, Jiao D, Huang X, Bai Y. Osteoclastic effects of mBMMSCs under compressive pressure during orthodontic tooth movement. *Stem Cell Res Ther* 2021; **12**: 148 [PMID: 33632323 DOI: 10.1186/s13287-021-02220-0]
18 **Zhou J**, Zhu Y, Ai D, Zhou M, Li H, Fu Y, Song J. Low-intensity pulsed ultrasound regulates osteoblast-osteoclast crosstalk *via* EphrinB2/EphB4 signaling for orthodontic alveolar bone remodeling. *Front Bioeng Biotechnol* 2023; **11**: 1192720 [PMID: 37425367 DOI: 10.3389/fbioe.2023.1192720]
19 **Sun Y**, Wang H, Li Y, Liu S, Chen J, Ying H. miR-24 and miR-122 Negatively Regulate the Transforming Growth Factor-β/Smad Signaling Pathway in Skeletal Muscle Fibrosis. *Mol Ther Nucleic Acids* 2018; **11**: 528-537 [PMID: 29858088 DOI: 10.1016/j.omtn.2018.04.005]
20 **Xin J**, Zhan X, Zheng F, Li H, Wang Y, Li C, Jiang J. The effect of low-frequency high-intensity ultrasound combined with aspirin on tooth movement in rats. *BMC Oral Health* 2023; **23**: 642 [PMID: 37670292 DOI: 10.1186/s12903-023-03359-3]
21 **Koushki N**, Ghagre A, Srivastava LK, Molter C, Ehrlicher AJ. Nuclear compression regulates YAP spatiotemporal fluctuations in living cells. *Proc Natl Acad Sci U S A* 2023; **120(28)** e2301285120. [PMID: 37399392 DOI: 10.1073/pnas.2301285120]
22 **Elosegui-Artola A**, Andreu I, Beedle AEM, Lezamiz A, Uroz M, Kosmalska AJ, Oria R, Kechagia JZ, Rico-Lastres P, Le Roux AL, Shanahan CM, Trepat X, Navajas D, Garcia-Manyes S, Roca-Cusachs P. Force Triggers YAP Nuclear Entry by Regulating Transport across Nuclear Pores. *Cell* 2017; **171**: 1397-1410.e14 [PMID: 29107331 DOI: 10.1016/j.cell.2017.10.008]
23 **Yang T**, Liang C, Chen L, Li J, Geng W. Low-Intensity Pulsed Ultrasound Alleviates Hypoxia-Induced Chondrocyte Damage in Temporomandibular Disorders by Modulating the Hypoxia-Inducible Factor Pathway. *Front Pharmacol* 2020; **11**: 689 [PMID: 32477144 DOI: 10.3389/fphar.2020.00689]
24 **El-Bialy T**, Farouk K, Carlyle TD, Wiltshire W, Drummond R, Dumore T, Knowlton K, Tompson B. Effect of Low Intensity Pulsed Ultrasound (LIPUS) on Tooth Movement and Root Resorption: A Prospective Multi-Center Randomized Controlled Trial. *J Clin Med* 2020; **9** [PMID: 32188053 DOI: 10.3390/jcm9030804]
25 **Ahn HW**, Moon SC, Baek SH. Morphometric evaluation of changes in the alveolar bone and roots of the maxillary anterior teeth before and after en masse retraction using cone-beam computed tomography. *Angle Orthod* 2013; **83**: 212-221 [PMID: 23066654 DOI: 10.2319/041812-325.1]
26 **Zheng Y**, Zhu C, Zhu M, Lei L. Difference in the alveolar bone remodeling between the adolescents and adults during upper incisor retraction: a retrospective study. *Sci Rep* 2022; **12**: 9161 [PMID: 35650260 DOI: 10.1038/s41598-022-12967-y]
27 **Chang HW**, Huang HL, Yu JH, Hsu JT, Li YF, Wu YF. Effects of orthodontic tooth movement on alveolar bone density. *Clin Oral Investig* 2012; **16**: 679-688 [PMID: 21519883 DOI: 10.1007/s00784-011-0552-9]
28 **Hsu JT**, Chang HW, Huang HL, Yu JH, Li YF, Tu MG. Bone density changes around teeth during orthodontic treatment. *Clin Oral Investig* 2011; **15**: 511-519 [PMID: 20393863 DOI: 10.1007/s00784-010-0410-1]
29 **Carter DR**. Mechanical loading histories and cortical bone remodeling. *Calcif Tissue Int* 1984; **36** Suppl 1: S19-S24 [PMID: 6430518 DOI: 10.1007/bf02406129]
30 **Nomura S**, Takano-Yamamoto T. Molecular events caused by mechanical stress in bone. *Matrix Biol* 2000; **19**: 91-96 [PMID: 10842092 DOI: 10.1016/s0945-053x(00)00050-0]
31 **Hu Y**, Huang L, Shen M, Liu Y, Liu G, Wu Y, Ding F, Ma K, Wang W, Zhang Y, Shao Z, Cai X, Xiong L. Pioglitazone Protects Compression-Mediated Apoptosis in Nucleus Pulposus Mesenchymal Stem Cells by Suppressing Oxidative Stress. *Oxid Med Cell Longev* 2019; **2019**: 4764071 [PMID: 31885796 DOI: 10.1155/2019/4764071]
32 **Li Z**, Chen S, Ma K, Lv X, Lin H, Hu B, He R, Shao Z. CsA attenuates compression-induced nucleus pulposus mesenchymal stem cells apoptosis *via* alleviating mitochondrial dysfunction and oxidative stress. *Life Sci* 2018; **205**: 26-37 [PMID: 29746847 DOI: 10.1016/j.lfs.2018.05.014]
33 **Liang H**, Chen S, Huang D, Deng X, Ma K, Shao Z. Effect of Compression Loading on Human Nucleus Pulposus-Derived Mesenchymal Stem Cells. *Stem Cells Int* 2018; **2018**: 1481243 [PMID: 30402107 DOI: 10.1155/2018/1481243]
34 **Roomi AB**, Mahdi Salih AH, Noori SD, Nori W, Tariq S. Evaluation of Bone Mineral Density, Serum Osteocalcin, and Osteopontin Levels in Postmenopausal Women with Type 2 Diabetes Mellitus, with/without Osteoporosis. *J Osteoporos* 2022; **2022**: 1437061 [PMID: 35198139 DOI: 10.1155/2022/1437061]

35 **Sasaki K**, Takeshita N, Fukunaga T, Seiryu M, Sakamoto M, Oyanagi T, Maeda T, Takano-Yamamoto T. Vibration accelerates orthodontic tooth movement by inducing osteoclastogenesis *via* transforming growth factor-β signalling in osteocytes. *Eur J Orthod* 2022; **44**: 698-704 [PMID: 36111523 DOI: 10.1093/ejo/cjac036]

36 **Feres MFN**, Kucharski C, Diar-Bakirly S, El-Bialy T. Effect of low-intensity pulsed ultrasound on the activity of osteoclasts: An in vitro study. *Arch Oral Biol* 2016; **70**: 73-78 [PMID: 27341458 DOI: 10.1016/j.archoralbio.2016.06.007]

37 **Rauner M**, Sipos W, Pietschmann P. Osteoimmunology. *Int Arch Allergy Immunol* 2007; **143**: 31-48 [PMID: 17191007 DOI: 10.1159/000098223]

38 **Berber R**, Aziz S, Simkins J, Lin SS, Mangwani J. Low Intensity Pulsed Ultrasound Therapy (LIPUS): A review of evidence and potential applications in diabetics. *J Clin Orthop Trauma* 2020; **11**: S500-S505 [PMID: 32774018 DOI: 10.1016/j.jcot.2020.03.009]

39 **He R**, Zhou W, Zhang Y, Hu S, Yu H, Luo Y, Liu B, Ran J, Wu J, Wang Y, Chen W. Combination of low-intensity pulsed ultrasound and C3H10T1/2 cells promotes bone-defect healing. *Int Orthop* 2015; **39**: 2181-2189 [PMID: 26169839 DOI: 10.1007/s00264-015-2898-0]

40 **El-Bialy T**, El-Shamy I, Graber TM. Growth modification of the rabbit mandible using therapeutic ultrasound: is it possible to enhance functional appliance results? *Angle Orthod* 2003; **73**: 631-639 [PMID: 14719726 DOI: 10.1043/0003-3219(2003)073<0631:GMOTRM>2.0.CO;2]

41 **Erdogan O**, Esen E, Ustün Y, Kürkçü M, Akova T, Gönlüşen G, Uysal H, Cevlik F. Effects of low-intensity pulsed ultrasound on healing of mandibular fractures: an experimental study in rabbits. *J Oral Maxillofac Surg* 2006; **64**: 180-188 [PMID: 16413888 DOI: 10.1016/j.joms.2005.10.027]

42 **Li L**, Yang Z, Zhang H, Chen W, Chen M, Zhu Z. Low-intensity pulsed ultrasound regulates proliferation and differentiation of osteoblasts through osteocytes. *Biochem Biophys Res Commun* 2012; **418**: 296-300 [PMID: 22266313 DOI: 10.1016/j.bbrc.2012.01.014]

43 **Man J**, Shelton RM, Cooper PR, Landini G, Scheven BA. Low intensity ultrasound stimulates osteoblast migration at different frequencies. *J Bone Miner Metab* 2012; **30**: 602-607 [PMID: 22752127 DOI: 10.1007/s00774-012-0368-y]

44 **Tassinary JAF**, Lunardelli A, Basso BS, Dias HB, Catarina AV, Stülp S, Haute GV, Martha BA, Melo DADS, Nunes FB, Donadio MVF, Oliveira JR. Low-intensity pulsed ultrasound (LIPUS) stimulates mineralization of MC3T3-E1 cells through calcium and phosphate uptake. *Ultrasonics* 2018; **84**: 290-295 [PMID: 29182945 DOI: 10.1016/j.ultras.2017.11.011]

45 **Matsumoto K**, Shimo T, Kurio N, Okui T, Ibaragi S, Kunisada Y, Obata K, Masui M, Pai P, Horikiri Y, Yamanaka N, Takigawa M, Sasaki A. Low-intensity pulsed ultrasound stimulation promotes osteoblast differentiation through hedgehog signaling. *J Cell Biochem* 2018; **119**: 4352-4360 [PMID: 28981158 DOI: 10.1002/jcb.26418]

46 **Yao H**, Zhang L, Yan S, He Y, Zhu H, Li Y, Wang D, Yang K. Low-intensity pulsed ultrasound/nanomechanical force generators enhance osteogenesis of BMSCs through microfilaments and TRPM7. *J Nanobiotechnology* 2022; **20**: 378 [PMID: 35964037 DOI: 10.1186/s12951-022-01587-3]

47 **Chen C**, Zhang T, Liu F, Qu J, Chen Y, Fan S, Chen H, Sun L, Zhao C, Hu J, Lu H. Effect of Low-Intensity Pulsed Ultrasound After Autologous Adipose-Derived Stromal Cell Transplantation for Bone-Tendon Healing in a Rabbit Model. *Am J Sports Med* 2019; **47**: 942-953 [PMID: 30870031 DOI: 10.1177/0363546518820324]

48 **Costa V**, Carina V, Fontana S, De Luca A, Monteleone F, Pagani S, Sartori M, Setti S, Faldini C, Alessandro R, Fini M, Giavaresi G. Osteogenic commitment and differentiation of human mesenchymal stem cells by low-intensity pulsed ultrasound stimulation. *J Cell Physiol* 2018; **233**: 1558-1573 [PMID: 28621452 DOI: 10.1002/jcp.26058]

49 **Li H**, Deng Y, Tan M, Feng G, Kuang Y, Li J, Song J. Low-intensity pulsed ultrasound upregulates osteogenesis under inflammatory conditions in periodontal ligament stem cells through unfolded protein response. *Stem Cell Res Ther* 2020; **11**: 215 [PMID: 32493507 DOI: 10.1186/s13287-020-01732-5]

50 **Takayama T**, Suzuki N, Ikeda K, Shimada T, Suzuki A, Maeno M, Otsuka K, Ito K. Low-intensity pulsed ultrasound stimulates osteogenic differentiation in ROS 17/2.8 cells. *Life Sci* 2007; **80**: 965-971 [PMID: 17174343 DOI: 10.1016/j.lfs.2006.11.037]

51 **Lim K**, Kim J, Seonwoo H, Park SH, Choung PH, Chung JH. In vitro effects of low-intensity pulsed ultrasound stimulation on the osteogenic differentiation of human alveolar bone-derived mesenchymal stem cells for tooth tissue engineering. *Biomed Res Int* 2013; **2013**: 269724 [PMID: 24195067 DOI: 10.1155/2013/269724]

52 **Zhang B**, Yang Y, Keyimu R, Hao J, Zhao Z, Ye R. The role of lamin A/C in mesenchymal stem cell differentiation. *J Physiol Biochem* 2019; **75**: 11-18 [PMID: 30706289 DOI: 10.1007/s13105-019-00661-z]

53 **Killaars AR**, Walker CJ, Anseth KS. Nuclear mechanosensing controls MSC osteogenic potential through HDAC epigenetic remodeling. *Proc Natl Acad Sci U S A* 2020; **117**: 21258-21266 [PMID: 32817542 DOI: 10.1073/pnas.2006765117]

54 **Dahl KN**, Kalinowski A. Nucleoskeleton mechanics at a glance. *J Cell Sci* 2011; **124**: 675-678 [PMID: 21321324 DOI: 10.1242/jcs.069096]

55 **Philip JT**, Dahl KN. Nuclear mechanotransduction: response of the lamina to extracellular stress with implications in aging. *J Biomech* 2008; **41**: 3164-3170 [PMID: 18945430 DOI: 10.1016/j.jbiomech.2008.08.024]

56 **Martino F**, Perestrelo AR, Vinarský V, Pagliari S, Forte G. Cellular Mechanotransduction: From Tension to Function. *Front Physiol* 2018; **9**: 824 [PMID: 30026699 DOI: 10.3389/fphys.2018.00824]

57 **Stroud MJ**. Linker of nucleoskeleton and cytoskeleton complex proteins in cardiomyopathy. *Biophys Rev* 2018; **10**: 1033-1051 [PMID: 29869195 DOI: 10.1007/s12551-018-0431-6]

58 **Swift J**, Ivanovska IL, Buxboim A, Harada T, Dingal PC, Pinter J, Pajerowski JD, Spinler KR, Shin JW, Tewari M, Rehfeldt F, Speicher DW, Discher DE. Nuclear lamin-A scales with tissue stiffness and enhances matrix-directed differentiation. *Science* 2013; **341**: 1240104 [PMID: 23990565 DOI: 10.1126/science.1240104]

59 **Bermeo S**, Vidal C, Zhou H, Duque G. Lamin A/C Acts as an Essential Factor in Mesenchymal Stem Cell Differentiation Through the Regulation of the Dynamics of the Wnt/β-Catenin Pathway. *J Cell Biochem* 2015; **116**: 2344-2353 [PMID: 25846419 DOI: 10.1002/jcb.25185]

60 **La Verde G**, Artiola V, Pugliese M, La Commara M, Arrichiello C, Muto P, Netti PA, Fusco S, Panzetta V. Radiation therapy affects YAP expression and intracellular localization by modulating lamin A/C levels in breast cancer. *Front Bioeng Biotechnol* 2022; **10**: 969004 [PMID: 36091449 DOI: 10.3389/fbioe.2022.969004]

61 **Piccolo S**, Dupont S, Cordenonsi M. The biology of YAP/TAZ: hippo signaling and beyond. *Physiol Rev* 2014; **94**: 1287-1312 [PMID: 25287865 DOI: 10.1152/physrev.00005.2014]

62 **Dupont S**, Morsut L, Aragona M, Enzo E, Giulitti S, Cordenonsi M, Zanconato F, Le Digabel J, Forcato M, Bicciato S, Elvassore N, Piccolo S. Role of YAP/TAZ in mechanotransduction. *Nature* 2011; **474**: 179-183 [PMID: 21654799 DOI: 10.1038/nature10137]

63 **Gao J**, He L, Zhou L, Jing Y, Wang F, Shi Y, Cai M, Sun J, Xu H, Jiang J, Zhang L, Wang H. Mechanical force regulation of YAP by F-actin

and GPCR revealed by super-resolution imaging. *Nanoscale* 2020; **12**: 2703-2714 [PMID: 31950964 DOI: 10.1039/c9nr09452k]

64 **Pavel M**, Renna M, Park SJ, Menzies FM, Ricketts T, Füllgrabe J, Ashkenazi A, Frake RA, Lombarte AC, Bento CF, Franze K, Rubinsztein DC. Contact inhibition controls cell survival and proliferation *via* YAP/TAZ-autophagy axis. *Nat Commun* 2018; **9**: 2961 [PMID: 30054475 DOI: 10.1038/s41467-018-05388-x]

65 **Lin C**, Yao E, Zhang K, Jiang X, Croll S, Thompson-Peer K, Chuang PT. YAP is essential for mechanical force production and epithelial cell proliferation during lung branching morphogenesis. *Elife* 2017; **6** [PMID: 28323616 DOI: 10.7554/eLife.21130]

World Journal of Stem Cells

Submit a Manuscript: https://www.f6publishing.com

World J Stem Cells 2024 March 26; 16(3): 287-304

DOI: 10.4252/wjsc.v16.i3.287

ISSN 1948-0210 (online)

ORIGINAL ARTICLE

Basic Study

Self-assembly of differentiated dental pulp stem cells facilitates spheroid human dental organoid formation and prevascularization

Fei Liu, Jing Xiao, Lei-Hui Chen, Yu-Yue Pan, Jun-Zhang Tian, Zhi-Ren Zhang, Xiao-Chun Bai

Specialty type: Cell and tissue engineering

Provenance and peer review: Unsolicited article; Externally peer reviewed.

Peer-review model: Single blind

Peer-review report's scientific quality classification

Grade A (Excellent): A
Grade B (Very good): B
Grade C (Good): 0
Grade D (Fair): 0
Grade E (Poor): 0

P-Reviewer: Cordelier P, France; Li SC, United States

Received: December 19, 2023
Peer-review started: December 19, 2023
First decision: January 12, 2024
Revised: January 21, 2024
Accepted: February 28, 2024
Article in press: February 28, 2024
Published online: March 26, 2024

Fei Liu, School of Basic Medical Sciences, Southern Medical University, Guangzhou 510515, Guangdong Province, China

Fei Liu, Jun-Zhang Tian, Department of Health Management, Guangdong Second Provincial General Hospital, Guangzhou 510317, Guangdong Province, China

Jing Xiao, Guangdong Provincial Key Laboratory of Tumor Interventional Diagnosis and Treatment, Zhuhai People's Hospital Affiliated with Jinan University, Zhuhai 519000, Guangdong Province, China

Jing Xiao, Centre of Reproduction, Development and Aging, Faculty of Health Sciences, University of Macau, Macau 999078, China

Lei-Hui Chen, Yu-Yue Pan, Department of Stomatology, Guangdong Second Provincial General Hospital, Guangzhou 510317, Guangdong Province, China

Zhi-Ren Zhang, Zhuhai Institute of Translational Medicine, Zhuhai Hospital Affiliated with Jinan University, Zhuhai 519000, Guangdong Province, China

Xiao-Chun Bai, Department of Cell Biology, School of Basic Medical Sciences, Southern Medical University, Guangzhou 510515, Guangdong Province, China

Corresponding author: Xiao-Chun Bai, PhD, Professor, Department of Cell Biology, School of Basic Medical Sciences, Southern Medical University, No. 1023-1063 Shatai South Road, Baiyun District, Guangzhou 510515, Guangdong Province, China. baixc15@smu.edu.cn

Abstract

BACKGROUND

The self-assembly of solid organs from stem cells has the potential to greatly expand the applicability of regenerative medicine. Stem cells can self-organise into microsized organ units, partially modelling tissue function and regeneration. Dental pulp organoids have been used to recapitulate the processes of tooth development and related diseases. However, the lack of vasculature limits the utility of dental pulp organoids.

AIM

To improve survival and aid in recovery after stem cell transplantation, we demonstrated the three-dimensional (3D) self-assembly of adult stem cell-human dental pulp stem cells (hDPSCs) and endothelial cells (ECs) into a novel type of

spheroid-shaped dental pulp organoid *in vitro* under hypoxia and conditioned medium (CM).

METHODS

During culture, primary hDPSCs were induced to differentiate into ECs by exposing them to a hypoxic environment and CM. The hypoxic pretreated hDPSCs were then mixed with ECs at specific ratios and conditioned in a 3D environment to produce prevascularized dental pulp organoids. The biological characteristics of the organoids were analysed, and the regulatory pathways associated with angiogenesis were studied.

RESULTS

The combination of these two agents resulted in prevascularized human dental pulp organoids (Vorganoids) that more closely resembled dental pulp tissue in terms of morphology and function. Single-cell RNA sequencing of dental pulp tissue and RNA sequencing of Vorganoids were integrated to analyse key regulatory pathways associated with angiogenesis. The biomarkers forkhead box protein O1 and fibroblast growth factor 2 were identified to be involved in the regulation of Vorganoids.

CONCLUSION

In this innovative study, we effectively established an *in vitro* model of Vorganoids and used it to elucidate new mechanisms of angiogenesis during regeneration, facilitating the development of clinical treatment strategies.

Key Words: Human dental pulp stem cells; Prevascularized organoids; Integrated analyses; Angiogenesis; Forkhead box protein O1

Core Tip: We demonstrated the three-dimensional self-assembly of adult stem cell-human dermal papilla cells and endothelial cells into a novel type of spheroid-shaped dental pulp organoid *in vitro* under hypoxia and conditioned medium. These organoids have been constructed to be morphologically and functionally closer to dental pulp tissue. Through the integration and analysis of single-cell RNA sequencing and RNA sequencing data, forkhead box protein O1 and fibroblast growth factor 2 were identified as crucial markers involved in the regulation of organoid angiogenesis. In this innovative study, we effectively established an *in vitro* model of prevascularized dental pulp organoids and used it to elucidate new mechanisms of angiogenesis during regeneration, facilitating the development of clinical treatment strategies.

Citation: Liu F, Xiao J, Chen LH, Pan YY, Tian JZ, Zhang ZR, Bai XC. Self-assembly of differentiated dental pulp stem cells facilitates spheroid human dental organoid formation and prevascularization. *World J Stem Cells* 2024; 16(3): 287-304
URL: https://www.wjgnet.com/1948-0210/full/v16/i3/287.htm
DOI: https://dx.doi.org/10.4252/wjsc.v16.i3.287

INTRODUCTION

The main experimental tool and goal of tissue regeneration engineering is the implantation of specific stem cells into diseased environments to repair and compensate for the dysfunction of damaged tissues and organs. However, the complexity and variability of the tissue microenvironment at the site of injury, such as hypoxic lethality, the inflammatory response, immune resistance and inadequate blood supply, leads to low survival rates (success rates of approximately 1%-3%) and poor maturation rates of directed differentiation after stem cell transplantation, all of which limit the clinical application and promotion of stem cells[1,2]. Therefore, it is critical for stem cells to form additional microvessels after implantation to quickly connect to the host's circulatory system and form functional blood vessels to ensure nutrient and oxygen delivery after implantation.

Organoids are constructed *in vitro* following an *in vivo* developmental programme that allows cells to grow, migrate, differentiate and function in three-dimensional (3D). A variety of organoids are currently constructed *in vitro*[3,4]. Compared to traditional 2D culture methods, 3D culture facilitates cell access to bio-factors and reduces intercellular shear force, which promotes the proliferation and differentiation of dental pulp stem cells. With the advent of 3D pulp culture technology, great progress has been made in regenerative endodontic procedures[5-7]. Although the construction of organoid models has outstanding advantages in terms of clinical application, it still faces a major challenge, namely, the lack of model nourishment due to the absence of angiogenesis, which is the main dilemma for the *in vitro* application of such models. In recent years, numerous studies have investigated the relationship between angiogenesis and pulp regeneration[7,8]. Several researchers have proposed that the addition of high concentrations of nutrients and their controlled and sustained release from scaffolds are important strategies for optimising angiogenesis during pulp regeneration[9]. A hydrogel scaffold was used in combination with conditioned media to release bio-factors in a controlled manner, which subsequently promoted blood vessel and nerve formation and dental tissue repair[10].

Our previous study revealed that hypoxia-activated phosphatidylinositol 3 kinase/protein kinase B (PI3K/Akt) inhibits oxidative stress in human dental pulp stem cells (hDPSCs) by regulating reactive oxygen species[11], thereby maintaining stem cell stemness during *in vitro* expansion. In addition, a number of signalling pathways associated with angiogenesis are activated, and the expression of regulatory factors associated with angiogenesis is altered. Does using hypoxic hDPSCs in *in vitro* organoid cultures better induce angiogenesis? How can prevascularized organoids be constructed to address current challenges in stem cell applications? Is angiogenesis regulated by the same mechanisms in dental pulp and prevascularized dental pulp organoids (Vorganoids)?

We induced endothelial cells (ECs) and hDPSCs in culture and subsequently fused the two cell types to obtain Vorganoids, which are morphologically and functionally more similar to dental pulp tissue. Single-cell RNA sequencing (scRNA-seq) of dental pulp tissue and RNA-seq of Vorganoids were subsequently integrated to analyse key regulatory pathways associated with angiogenesis in dental pulp tissue. Vascular endothelial growth factor A (VEGFA), a key signalling pathway regulating the differentiation of vascular ECs in dental pulp tissue, was also significantly enriched in the development of Vorganoids. The biomarkers forkhead box protein O1 (FOXO1) and fibroblast growth factor 2 (FGF2) were identified to be involved in the regulation of Vorganoids. In this innovative study, we effectively established an *in vitro* model of prevascularized dental pulp organoids and used it to elucidate new mechanisms of angiogenesis during regeneration, facilitating the development of clinical treatment strategies.

MATERIALS AND METHODS

Single-cell data download and preprocessing

We downloaded the GSE161266 dataset from the Gene Expression Omnibus database[12] and performed the following analyses: (1) Quality control and selection of cells for further analysis; (2) Background correction; (3) Selection of high-variability features (identification of high-variability markers in single-cell populations as candidate regulatory genes); (4) Dimensionality reduction (principal component analysis, linear dimensionality reduction, and determination of the appropriate "dimensionality" of the dataset); (5) Clustering of cell populations based on principal component analysis; and (6) Nonlinear dimensionality reduction by the UMAP/tSNE algorithm. Identification of differentially expressed genes (DEGs) in cell subpopulations. Dataset quality control was performed by removing cells with < 200 expressed genes, low-quality/dying cells, and empty droplets (cells with a mitochondrial genome accounting for > 5% of the total genome were selected)[13-15]. Subsequently, global scaling normalisation of overall expression was performed for the cells included in the analyses, and the expression levels were log-transformed. To reduce the noise in the data, Seurat's nonlinear dimensionality reduction algorithm was used to extract the principal components of the core data regarding the "meta-features" of the clustered dataset. Based on the similarity of the cell expression profiles, cells were grouped into highly related subpopulations and clusters using the KNN algorithm[13,15].

Cell cluster definition and pseudotime-series analysis

Cell clusters were reannotated by the SingleR and scCATCH algorithms[14]. For the cell clusters with inconsistent annotation results, cell markers were visualised for analysis and determination of the cell subpopulation. Pseudotime-series analysis was performed on the entire cell population and core cell subpopulations. The Monocle algorithm was used to analyse the serial changes in gene expression experienced by each cell during the process of cell-state transition; this algorithm reveals the overall "trajectory" of gene expression changes and defines the appropriate regulatory point of each cell in the trajectory[16]. Based on the Monocle algorithm, cells were arranged in 2D space according to their global expression profiles, and the cell state trajectory was plotted. Subsequently, DEGs with kinetic correlations were identified by differential expression analysis based on the pseudotime values[13,15].

Functional enrichment analysis of the core cell subpopulations identified by pseudotime-series analysis

Based on the above analyses, core cell subpopulations were selected, and DEGs with kinetic correlations were subjected to pathway enrichment analysis: (1) The clusterProfiler package was used for Gene Ontology (GO) enrichment analysis (biological process, molecular function, and cellular component)[17]; and (2) GSVA was used to calculate the enrichment scores of pathways[18]: (1) Cell expression profiles were obtained from the preparation of samples for calculation of gene expression; (2) In preparation of the gene set, the core pathway gene list was downloaded from the MSIGDB database (https://www.gsea-msigdb.org/gsea/msigdb/index.jsp); and (3) The gene set was introduced into the algorithm, the pathways were scored by the GSVA algorithm for each sample, and the pathway scores were subjected to relative quantification.

RNA-seq analysis

The RNA-seq data units corresponding to the FPKM values of the samples were included. Differential gene expression analysis was performed on the samples from the two clusters with the most significant difference in survival. The DESeq algorithm was used to normalise the gene expression profiles and filter out genes with low expression[19]. The criteria for selecting DEGs were as follows: Log2-fold change ≥ 1.5 and Benjamini-Hochberg (B-H) adjusted *P* value < 0.05. Through unsupervised cluster analysis, the identified DEGs were clustered according to the sample group, and GO enrichment analysis of these genes was subsequently performed to explore their potential biological functions through the ToppGene Suite (https://toppgene.cchmc.org)[20].

Gene functional enrichment analysis

Gene set enrichment analysis (GSEA) was performed to identify the core pathways and regulatory genes whose expression significantly changed. Further clustering and quantitative analysis of the core pathways and involved genes were performed using GSVA and the Ternary Cluster. Finally, regulatory genes related to pathological progression in the core cell subpopulations were obtained.

Cell culture and identification

The hDPSCs were collected from pulp tissues of extracted third molars from patients aged 18 to 25 years (12 males and 8 females). Cells from the first to fifth passages were used in this study. All patients were informed, agreed to participate in this study, and signed an informed consent. The study protocol was approved by the Ethics Committee of Guangdong Second Provincial General Hospital. Multiple differentiation assays for hDPSCs were performed according to a previously described procedure. Once the cells had reached 70%-80% confluence, the hDPSCs were allowed to differentiate in osteogenic, chondrogenic, or adipogenic induction media. The induction medium was changed every 2 d until the differentiated cells were harvested.

Analysis of cell surface markers

The hDPSCs were washed and resuspended in phosphate buffered saline (containing 1% foetal bovine serum) and then labelled with monoclonal anti-human CD146-PE, CD90-APC, CD34-PerCP and CD45-APC (Chemicon, Temecula, CA) for 30 min. The cells were washed twice, resuspended in staining buffer and analysed by flow cytometry.

Strategies for the construction of a model for the study of vascularized human dental pulp-like organs

Preconditioning: Primary hDPSC cultures were incubated under 3% hypoxia beginning at passage 1. When the cells had expanded to passage 3, vasculogenic conditioned medium 1 (CM1) was added, and the culture was continued under hypoxic conditions for 7 d. CM1: EGM2 + 10% foetal bovine serum + 50 ng/mL VEGF 165 rh.

Aggregate formation: Hypoxic cells were then mixed with conditionally induced cells at a 2:8 ratio (total 5 × 10^4 cells) in a 96-well low-attachment plate containing 150 μL of CM2 per well. CM2: CM1 + 50 μM Y27632 + 5 μL Matrigel. After 1 d of 3D culture, the medium was changed to CM1, and the incubation continued for 6 d.

Analysis: The medium was changed to normal medium, and the experimental application phase of the Vorganoids experimental model was started (Figure 1). The standard experimental procedures for[5] identifying the organoids were performed according to previous methods.

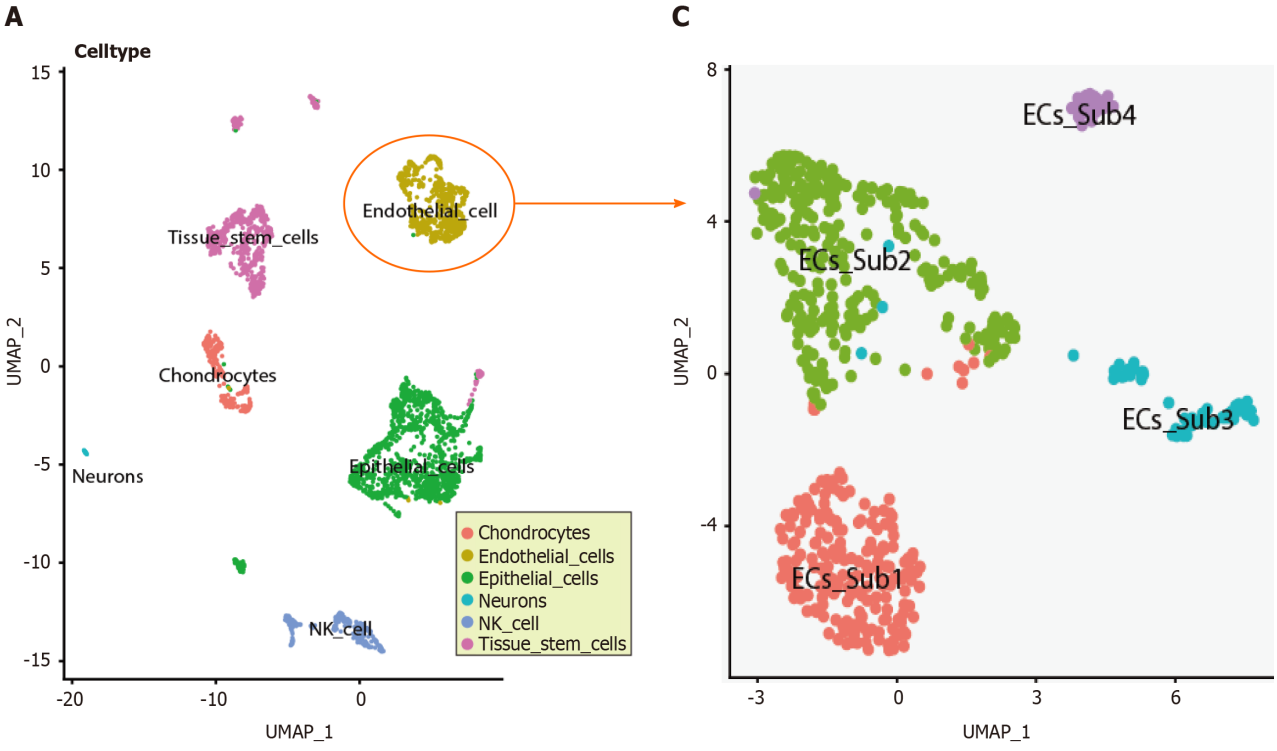

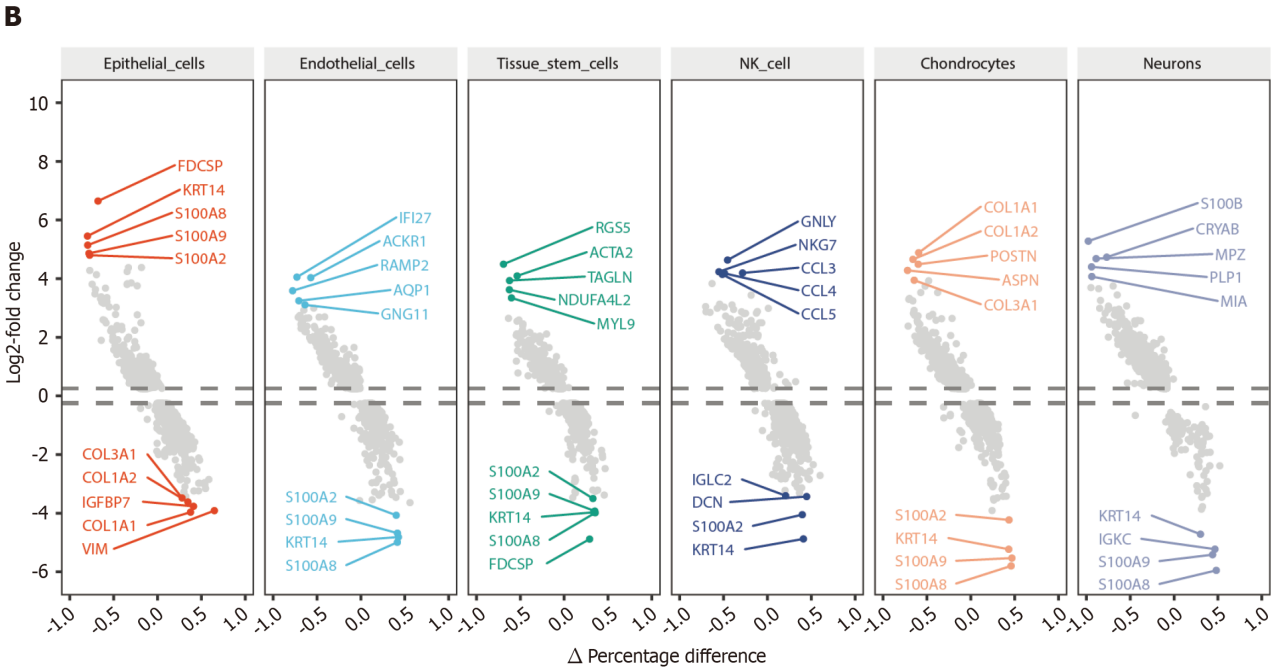
B
Epithelial_cells
Endothelial_cells
Tissue_stem_cells
NK_cell
Chondrocytes
Neurons
Log2-fold change
FDCSP
KRT14
S100A8
S100A9
S100A2
COL3A1
COL1A2
IGFBP7
COL1A1
VIM
IFI27
ACKR1
RAMP2
AQP1
GNG11
RGS5
ACTA2
TAGLN
NDUFA4L2
MYL9
GNLY
NKG7
CCL3
CCL4
CCL5
IGLC2
DCN
COL1A1
COL1A2
POSTN
ASPN
COL3A1
S100B
CRYAB
MPZ
PLP1
MIA
IGKC
Δ Percentage difference

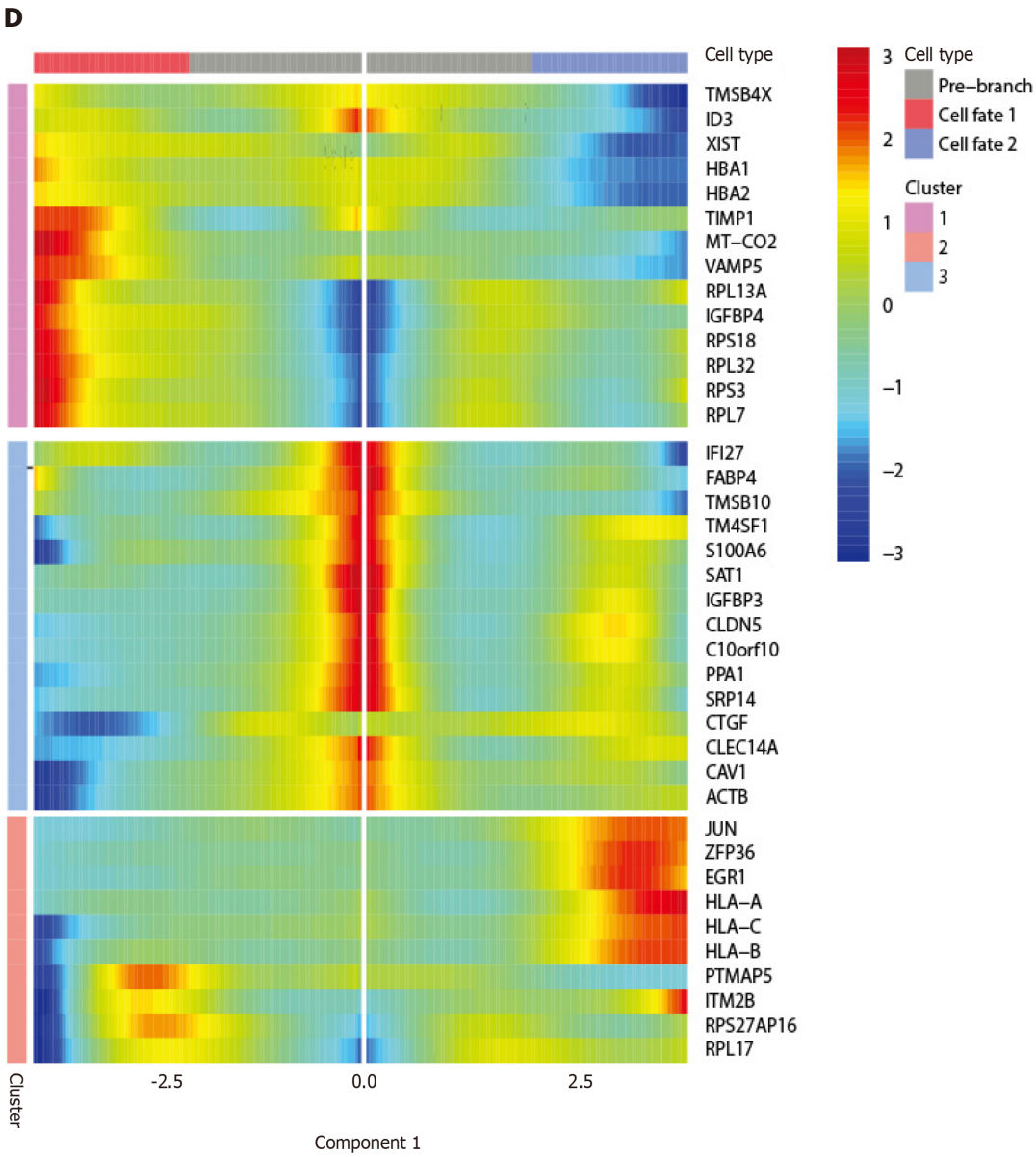
D
Cell type
Pre–branch
Cell fate 1
Cell fate 2
Cluster
TMSB4X
ID3
XIST
HBA1
HBA2
TIMP1
MT–CO2
VAMP5
RPL13A
IGFBP4
RPS18
RPL32
RPS3
RPL7
IFI27
FABP4
TMSB10
TM4SF1
S100A6
SAT1
IGFBP3
CLDN5
C10orf10
PPA1
SRP14
CTGF
CLEC14A
CAV1
ACTB
JUN
ZFP36
EGR1
HLA–A
HLA–C
HLA–B
PTMAP5
ITM2B
RPS27AP16
RPL17
-2.5
0.0
2.5
Component 1

E

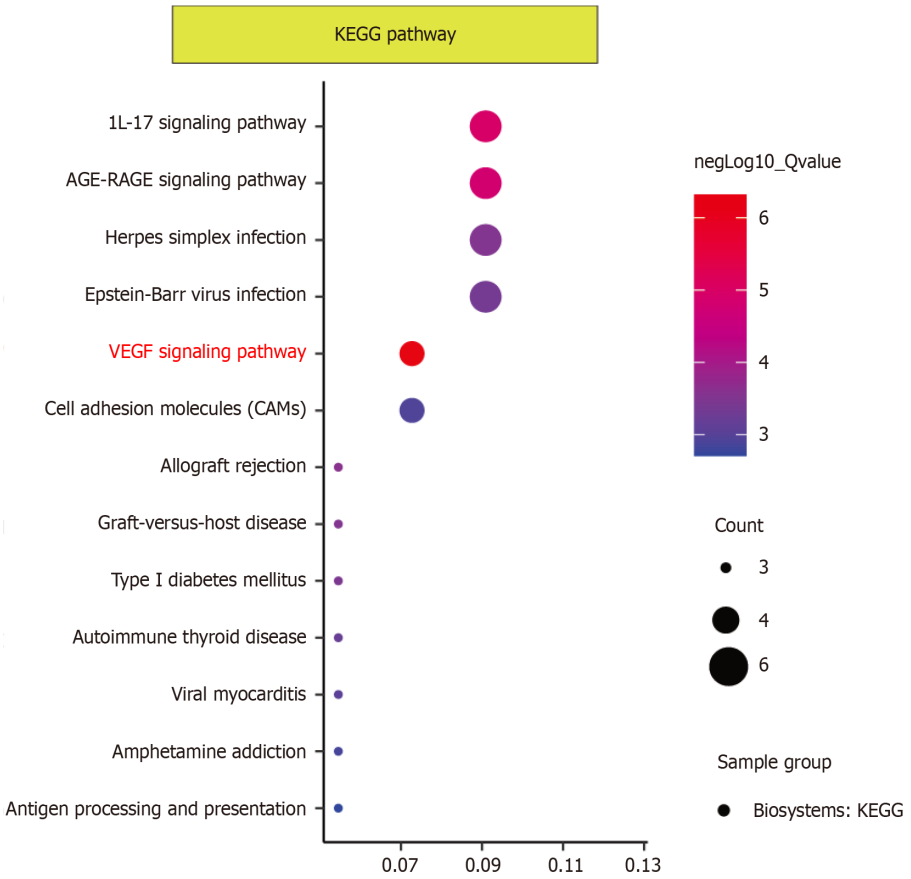
KEGG pathway
1L-17 signaling pathway
AGE-RAGE signaling pathway
Herpes simplex infection
Epstein-Barr virus infection
VEGF signaling pathway
Cell adhesion molecules (CAMs)
Allograft rejection
Graft-versus-host disease
Type I diabetes mellitus
Autoimmune thyroid disease
Viral myocarditis
Amphetamine addiction
Antigen processing and presentation
0.07
0.09
0.11
0.13
negLog10_Qvalue
6
5
4
3
Count
3
4
6
Sample group
Biosystems: KEGG

F

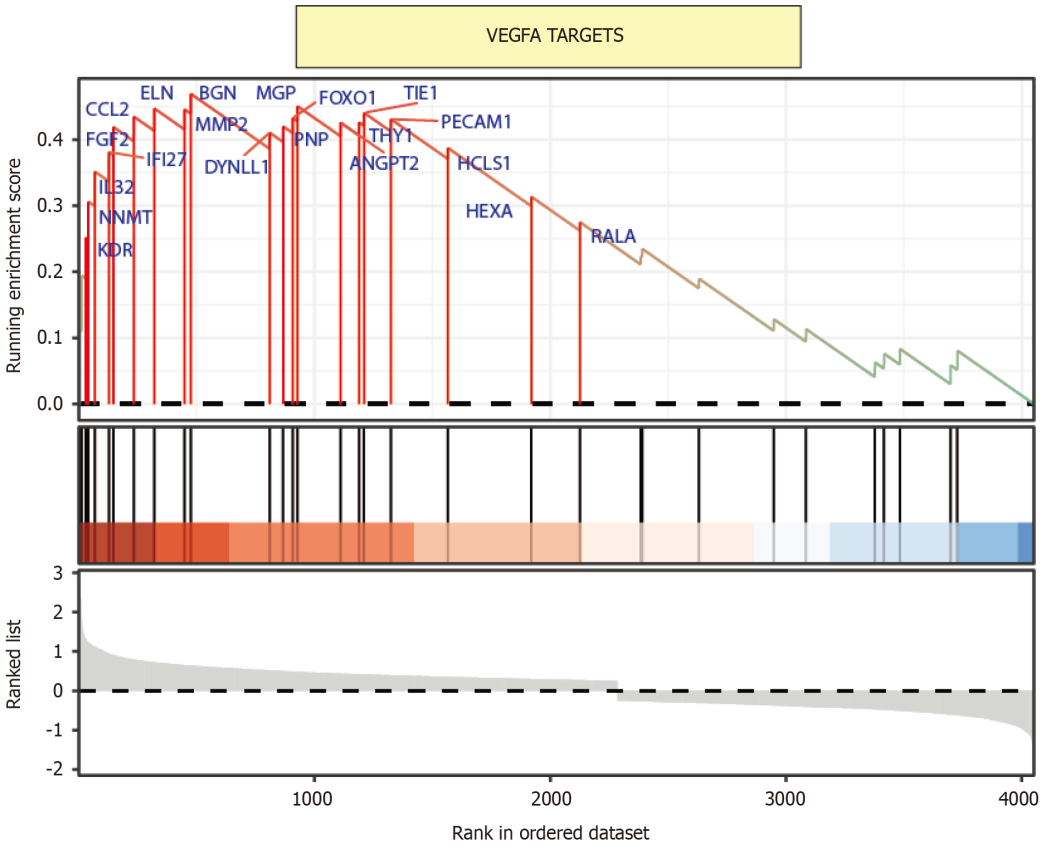
VEGFA TARGETS
CCL2
ELN
BGN
MGP
FOXO1
TIE1
FGF2
MMP2
PNP
THY1
PECAM1
IFI27
DYNLL1
ANGPT2
HCLS1
IL32
HEXA
NNMT
RALA
KDR
Running enrichment score
0.0
0.1
0.2
0.3
0.4
Ranked list
3
2
1
0
-1
-2
1000
2000
3000
4000
Rank in ordered dataset

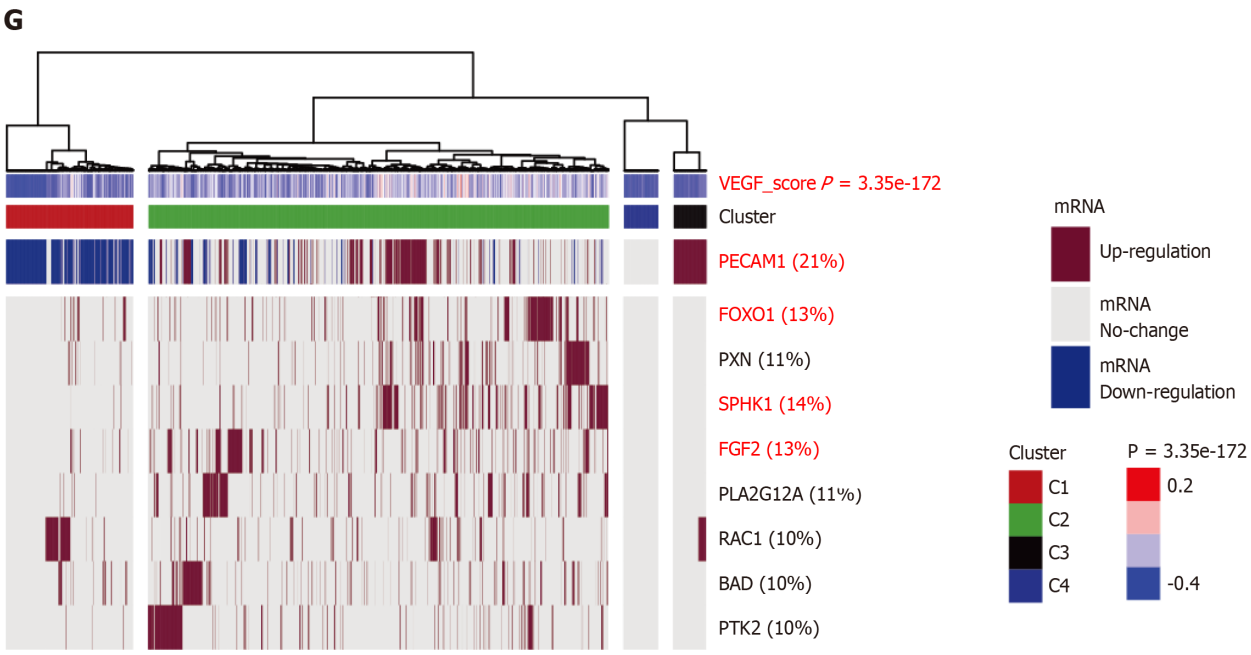

Figure 1 The single-cell atlas of human teeth. A: Single-cell RNA sequencing data from human teeth were projected onto the UMAP map. Annotation-cell and nonannotation clusters are presented on the same UMAP plot; B: The top 5 upregulated and downregulated differentially expressed genes (DEGs) were subsequently detected in each cell cluster; C: The UMAP map shows all the endothelial cell subsets; D: Heatmap of DEGs associated with endothelial cell subset development according to pseudotime trajectory analysis. The prebranch, cell fate1, and cell fate2 subsets of endothelial cells exhibit distinct fates; E: Vascular endothelial growth factor A targets identified by gene set enrichment analysis for pseudotime trajectory-related DEGs; F: GSVA and Ternary Cluster analyses revealed a significant difference in the vascular endothelial growth factor signalling pathway among the dental pulp endothelial cells; G: The GSVA and Ternary Cluster analyses showed a significant difference in vascular endothelial growth factor signaling pathway among dental pulp endothelial cells. VEGFA: Vascular endothelial growth factor A; IL: Interleukin; KEGG: Kyoto Encyclopedia of Genes and Genomes.

Hematoxylin-eosin staining

Various tissues were placed in 4% paraformaldehyde for histological examination. The tissues were dehydrated, embedded in paraffin, cut into 4 μm thick slices, and baked in an oven at 60 °C for 3 h. Paraffin was removed for hematoxylin-eosin (HE) staining, and the sections were observed and photographed under a microscope (Nikon, Tokyo, Japan).

Transmission electron microscopy imaging

For morphological analysis, the samples were then fixed with 2.5% glutaraldehyde for 12 h at room temperature. The samples were dehydrated in a graded series of ethanol (50%-100%), permeabilized with propylene oxide, and embedded in a poly/bed 812 kit (Polysciences, Washington, PA, United States). After embedding and polymerising the pure fresh resin in an electron microscope oven (DOSAKA) for 24 h, the initial sections were cut at approximately 50-200 nm, stained with toluidine blue (Sigma), and examined *via* light microscopy. Sections of approximately 70 nm were double stained with 6% uranyl acetate and lead citrate (Thermo Fisher Scientific, Waltham, MA, United States) for comparison. These sections were cut using a Leica EM UC-7 (Leica Microsystems, Tokyo, Japan) instrument equipped with a diamond knife (Diatome, Hatfield, PA, United States) and then transferred to copper and nickel grids. A transmission electron microscope (JEOL) with an acceleration voltage of 80 kV was used to observe all thin sections.

Immunofluorescence staining

Samples from each group were fixed with 4% paraformaldehyde for 24 h and subsequently incubated with 0.5% Triton-X for 10 min. Bovine serum albumin (1%) was used to block the cells for 1 h. Samples were dehydrated in sections after paraffin embedding. After blocking with 5% goat serum (Life Technologies, New York, NY, United States) for 1 h at 20 °C, the specimens were then treated with rabbit anti-CD31 (Cell Signaling Technology, Boston, United States), anti-VE-cadherin (Cell Signaling Technology, Boston, United States), FGF2 (Ab208687-40, Abcame, Shanghai, United States), anti-FOXO1 (Cell Signaling Technology, Boston, United States), or anti-p-AKT (Cell Signaling Technology, Boston, United States) antibodies for 12 h at 4 °C. Alexa Fluor 594-conjugated goat anti-rabbit secondary antibody (GB25303; Sevicebio, Wuhan, China) was added, and the cells were incubated for 2 h at room temperature. The nuclei were stained with 4′,6-diamidino-2-phenylindole. CD31, VE-cadherin, FGF2, FOXO1, and p-AKT expression was observed under a fluorescence microscope (Nikon Eclipse, Tokyo, Japan). Statistical analysis was performed using GraphPad Prism 7 Software (San Diego, CA, United States).

Adenosine triphosphate

To quantify the metabolic activity of Vorganoids formed at different stages. RIPA buffer was added to lyse the

Vorganoids, which were subsequently centrifuged at 4 °C for 5 min at 12000 rpm, after which the supernatant was removed for adenosine triphosphate (ATP) determination. The ATP assay working solution was prepared according to the kit instructions (S0026, Beyotime, China), and an ATP standard curve was constructed. The ATP working solution (100 μL) was added to the test wells and allowed to stand for 3-5 min at room temperature to eliminate background effects. Then, an appropriate amount of sample or standard was added and mixed well. The relative light unit value was measured using a chemiluminescence metre.

Lactate dehydrogenase assay

To quantify the degree of cell death at Vorganoids that formed at different stages, the culture supernatants were changed to serum-free DMEM 24 h before the culture medium was aspirated from each well, and the sediment was removed by centrifugation at 1000 rpm for 5 min according to the manufacturer's protocol. A kit was used to measure the lactate dehydrogenase (LDH) concentration in each group of cultures according to the manufacturer's instructions (C0017, Beyotime, China).

Enzyme-linked immunosorbent assay

To quantify the expression of inflammatory markers in VOrganoids that formed at different stages, the levels of interleukin (IL)-6, IL-8, IL-10, IL-1β, and tumour necrosis factor-α in culture supernatants were assayed *via* enzyme-linked immunosorbent assay (BioLegend) according to the manufacturer's instructions.

Statistical analysis

The data were analysed using IBM SPSS Statistics 22.0 and Image-Pro Plus 6.0, and the normality and variance of the data distribution were analysed using the Kolmogorov-Smirnov test and Levene's test, respectively. Means were compared between two groups by *t* tests, and means were compared between multiple groups by one-way ANOVA with Bonferroni correction for two-way comparisons. Differences were considered statistically significant when $P < 0.05$.

RESULTS

scRNA-seq analysis

After quality control, we found no differences in the cell cycle distribution between the single-cell subpopulations. Cell clustering by UMAP resulted in 13 cell subpopulations in two spatial dimensions, which were annotated and divided into six classes: Chondrocytes, ECs, epithelial cells, neurons, natural killer cells, and tissue stem cells (Figure 1A). Among the DEGs, *FDCSP*, *KRT14*, *S100A8*, *S100A9*, and *S100A2* were the most common upregulated DEGs, while *COL3A1*, *COL1A2*, *IGFBP7*, *COL1A1*, and *VIM* were the most common. For ECs, the upregulated DEGs were *IFI27*, *ACKR1*, *RAMP2*, *AQP1*, and *GNG11*, and the downregulated DEGs were *S100A2*, *S100A9*, *KRT14*, and *S100A8*. For chondrocytes, *COL1A1*, *COL1A2*, *POSTN*, *ASPN*, and *COL3A1* were upregulated DEGs, while *S100A2*, *KRT14*, *S100A9*, and *S100A8* were downregulated DEGs (Figure 1B).

Reclustering analysis of core cell subpopulations

ECs were re-extracted and reclustered. The 2D cell distribution determined by UMAP was used to analyse the cell spatial clustering, and four subpopulations were obtained (Figure 1C). Pseudotime-series analysis revealed that the cell population could be divided into three developmental stages, and hub regulators are also presented (Figure 1D). GO analysis of development-related genes revealed that the primary regulatory pathways were closely related to ribonucleoprotein complex biogenesis, proteasomal protein catabolic process, and RNA splicing.

EC pseudotime series and functional enrichment analyses

Pseudotime-series analysis of ECs revealed that *CRIP1*, *IFITM1*, and *B2M* were expressed at high levels in fate2 ECs, while *TMSB4X*, *ID3*, and *XIST* were expressed at low levels. In fate1 cells, *MT-ND4*, *TIMP1*, and *MT-CO2* were highly expressed, while *PTMAP5*, *ITM2B*, and *RPS27AP16* were expressed at low levels. In differentiating cells, *MT-RNR1*, *MT-RNR2*, and *DNASE1L3* were expressed at low levels, while *IFI27*, *FABP4*, and *TMSB10* were highly expressed (Figure 1D). Kyoto Encyclopedia of Genes and Genomes pathway analysis revealed that the VEGF signalling pathway (B-H adjusted *P* value = 4.63E-06, gene count = 4), the IL-17 signalling pathway (B-H adjusted *P* value = 1.18E-05, gene count = 5), and the AGE-RAGE signalling pathway in diabetic complications (B-H adjusted *P* value= 1.60E-05, gene count = 5) were the predominant pathways enriched (Figure 1E).

GSEA of core pathways

GSEA showed that WESTON-VEGFA TARGETS (enrichment score = 0.47, normalised enrichment score = 2.11, and B-H adjusted *P* value = 0.018) was associated with endodontium differentiation and progression. *BGN*, *ELN*, *FOXO1*, *TIE1*, and *PECAM1*, which had relatively high running enrichment scores, were considered key regulators of dental pulp development (Figure 1F). In addition, GSVA and ternary cluster analyses revealed a significant difference in the VEGF signalling pathway among the dental pulp ECs ($P = 3.35e-172$). *PECAM1* (21%), *FGF2* (13%), *FOXO1* (13%), and *SPHK1* (14%) were the core genes with high variability (Figure 1G).

Derivation of human dermal papilla cells from mesenchymal tissue with multipotential differentiation potential

To investigate the multidirectional differentiation potential of hDPSCs, we first established hDPSCs from pulp tissues extracted from third molars (patient age: 15 to 25 years). Cell surface marker identification experiments showed that the hDPSCs were derived from mesenchymal tissue and expressed mesenchymal-specific surface markers (Figure 2A). Multidirectional differentiation experiments revealed that hDPSCs could differentiate into osteogenic cells, cartilage cells, and adipocytes and express their corresponding specific markers (Figure 2B). Collectively, these data proved that hDPSCs exhibit multidirectional differentiation potential.

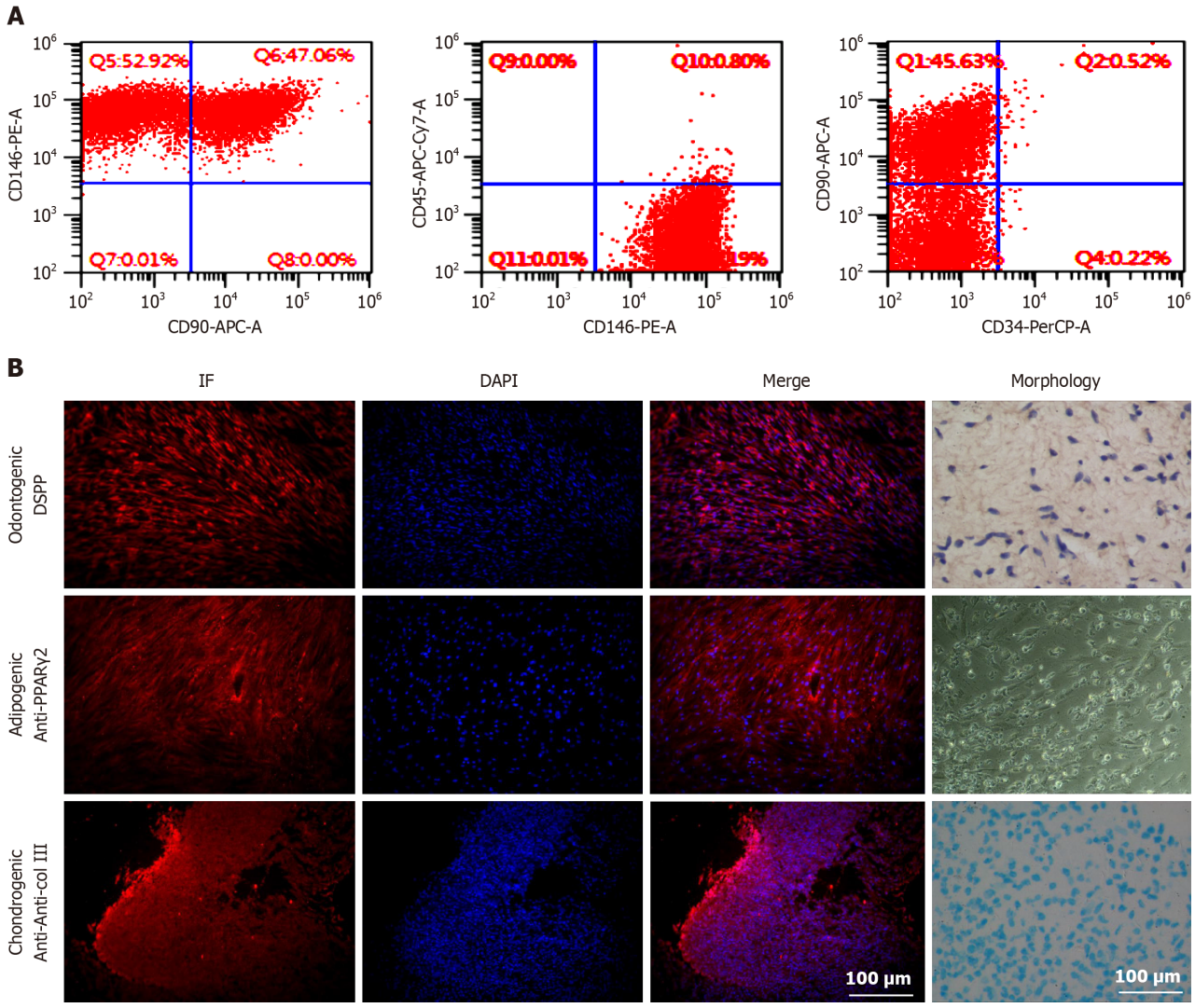

Figure 2 Human dental pulp stem cell culture and identification of multilineage differentiation ability. A: Human dental pulp stem cell surface marker identification; B: Immunofluorescence staining for dentin sialophosphoprotein, peroxisome proliferator-activated receptor γ2, and collagen type III. Osteogenic, adipogenic, and chondrogenic differentiation were examined by assessing mineralised nodule formation, oil red O staining, and alcian blue staining, respectively, *via* pellet culture (morphology). Scale bar = 100 μm. DSPP: Dentin sialophosphoprotein; PPARγ2: Peroxisome proliferator-activated receptor γ2; col III: Collagen type III; IF: Immunofluorescence; DAPI: 4',6-diamidino-2-phenylindole.

Morphological and functional identification of vascularized human dental pulp organoids

The cells began to aggregate into clusters at approximately 6 h and formed a single spherical morphology after approximately 1 d. The final diameter of the Vorganoid was approximately 400-600 μm. After the addition of 0.3% Triton X to permeabilize the Vorganoids for 30 min, the cells were unevenly distributed within the Vorganoids, and flocculent and irregularly distributed within the Vorganoids were observed. Long-term cultures of Vorganoids showed irregular cell proliferation and hyaline stroma at the edges, and Vorganoids were cultured continuously for more than 42 d *in vitro* (Figure 3A). HE staining and transmission electron microscopy revealed that the cells at the edge of the Vorganoids were arranged in a spindle row complex with normal intracellular organelles and fewer necrotic cells. In contrast, lysosome-like vesicles, which are polygonal in shape and tend to be compressed, appear in central cells. Compared to those in organoid culture, Vorganoids in culture had a greater proportion of Matrigel, a looser cell density and internal structure, fewer necrotic cells, and a greater distribution density and morphology similar to those of dental pulp tissue (Figure 3B).

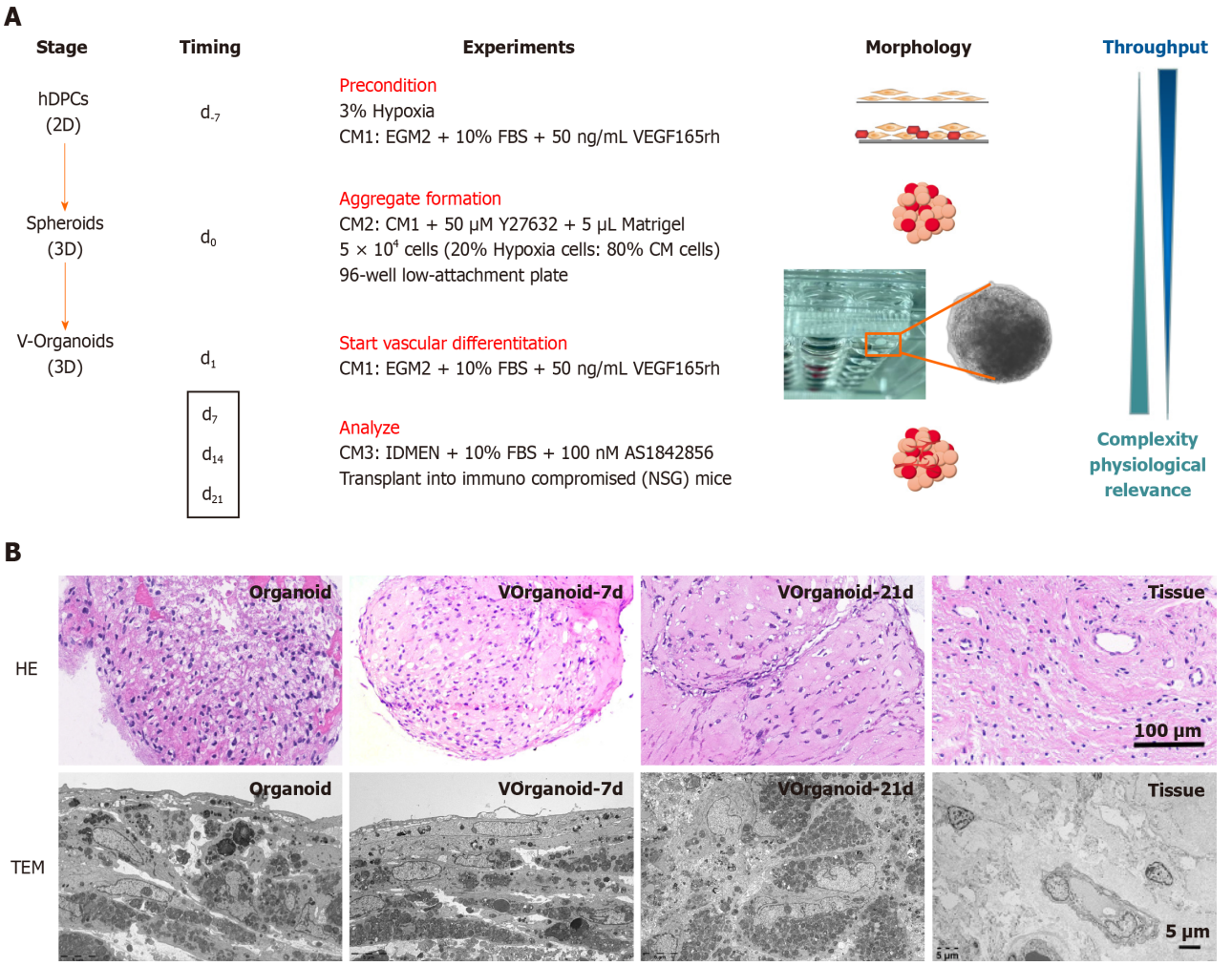

Figure 3 Strategies for the construction of a model for the study of prevascularized dental pulp organoids (Vorganoids). A: Schematic diagram of the timeline for generating Vorganoids from human dental pulp stem cells; B: Morphological differences between normal tissues, organoids, and vorganoids. Scale bar for hematoxylin-eosin staining = 100 μm and for transchromatic electron microscope = 5 μm. CM: Condition medium; HE: Hematoxylin-eosin; TEM: Transchromatic electron microscope; hDPCs: Human dental pulp stem cells; VEGF: Vascular endothelial growth factor; CM: Conditioned medium; FBS: Foetal bovine serum.

Differences in the expression of the angiogenic markers CD31 and VE were compared in three different tissues. CD31 was weakly expressed in pulp tissue, and VE was less expressed; CD31 was weakly expressed in organoids, while VE was not expressed; and the fluorescence intensities of CD31 and VE were greater in Vorganoid than in pulp tissue and organoids (Figure 4A). CD31 expression increased in the early stages of culture, reaching a peak at 14 d, with a subsequent decrease in expression (Figure 4B). The Vorganoids maintained a morphology similar to that of dental pulp for the first 21 d of *in vitro* culture, but when the culture time was extended to 28 d, loose dissociation occurred within the Vorganoid masses (Figure 4C). The ATP concentration decreased with increasing culture time, and the LDH concentration increased with increasing culture time (Figure 4D and E). The expression of IL-6 and IL-8 increased (Figure 4F), but there were no statistically significant differences in the expression of the other inflammatory factors. This finding suggested that the optimal period for using Vorganoids as a model for *in vitro* cell studies is within approximately 21 d.

RNA-Seq analysis of dentin-pulp-like organoid development

By sample clustering analysis, we found that the pulp cells were well differentiated between the 2D/3D culture and normal groups (Figure 5A). Compared with control, organoid showed 4171 and 2598 up- and downregulated genes, respectively, and Vorganoid showed 5227 and 3355 up- and downregulated genes, respectively (Figure 5B and C). GSEA showed that the DEGs in the VEGFA pathway were significantly enriched in the organoid and Vorganoid groups relative to the control group (organoid *vs* control: Enrichment score = 0.61, NES = 1.22, *P*.adjust = 0.0082; Vorganoid *vs* control: Enrichment Score = 0.64, NES = 1.63, *P*.adjust = 0.0058) (Figure 5D and E).

Target gene identification and validation

The above analyses revealed that the VEGFA TARGETS pathway may be the major pathway associated with the progression of and changes in the organoid and Vorganoid pathways compared to those in the control group. The enrich-

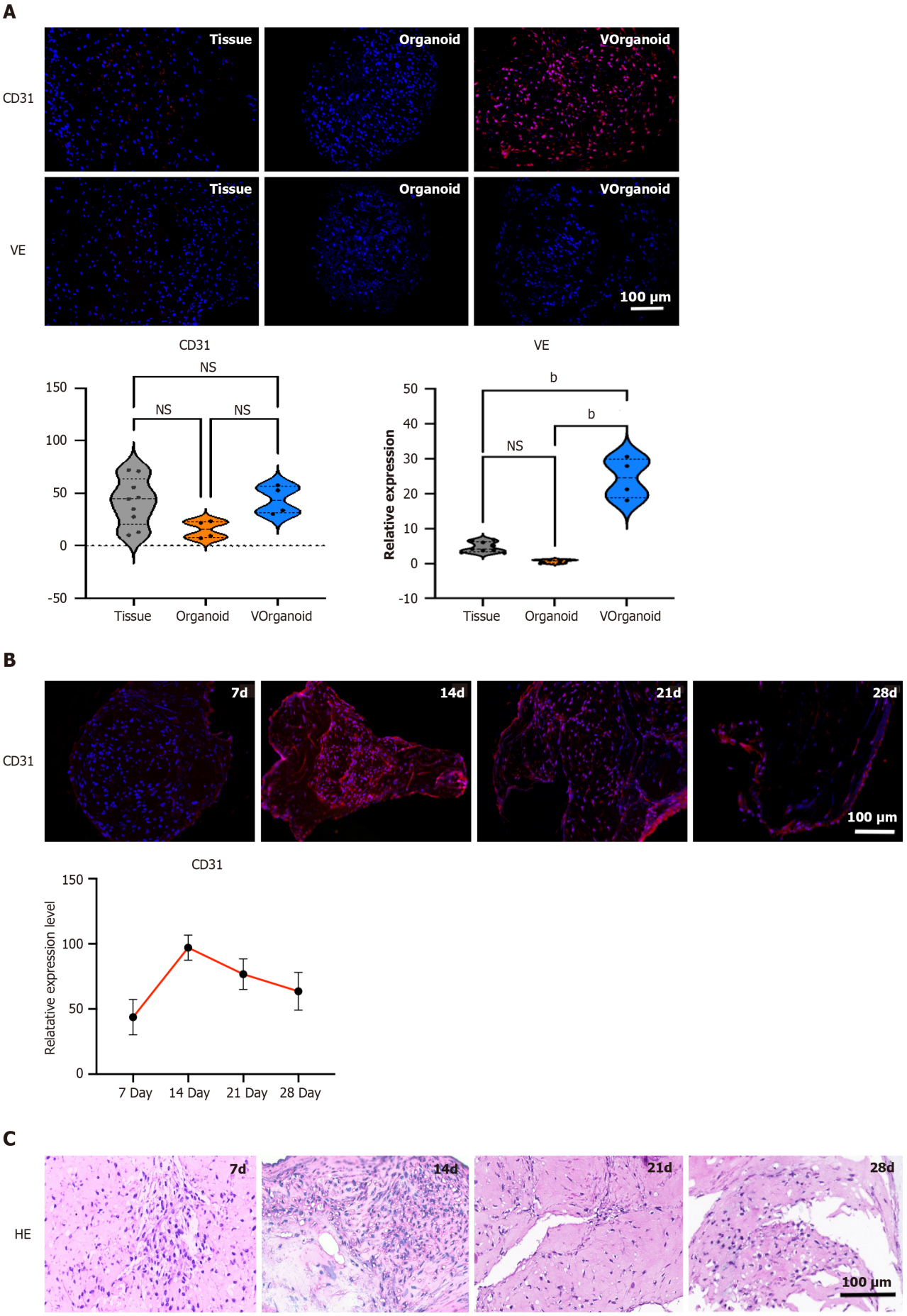
A
CD31
VE
Tissue
Organoid
VOrganoid
100 μm
CD31
VE
NS
NS
NS
b
b
NS
Relative expression
150
100
50
0
-50
50
40
30
20
10
0
-10
Tissue
Organoid
VOrganoid
B
CD31
7d
14d
21d
28d
100 μm
CD31
Relatative expression level
150
100
50
0
7 Day
14 Day
21 Day
28 Day
C
HE
7d
14d
21d
28d
100 μm

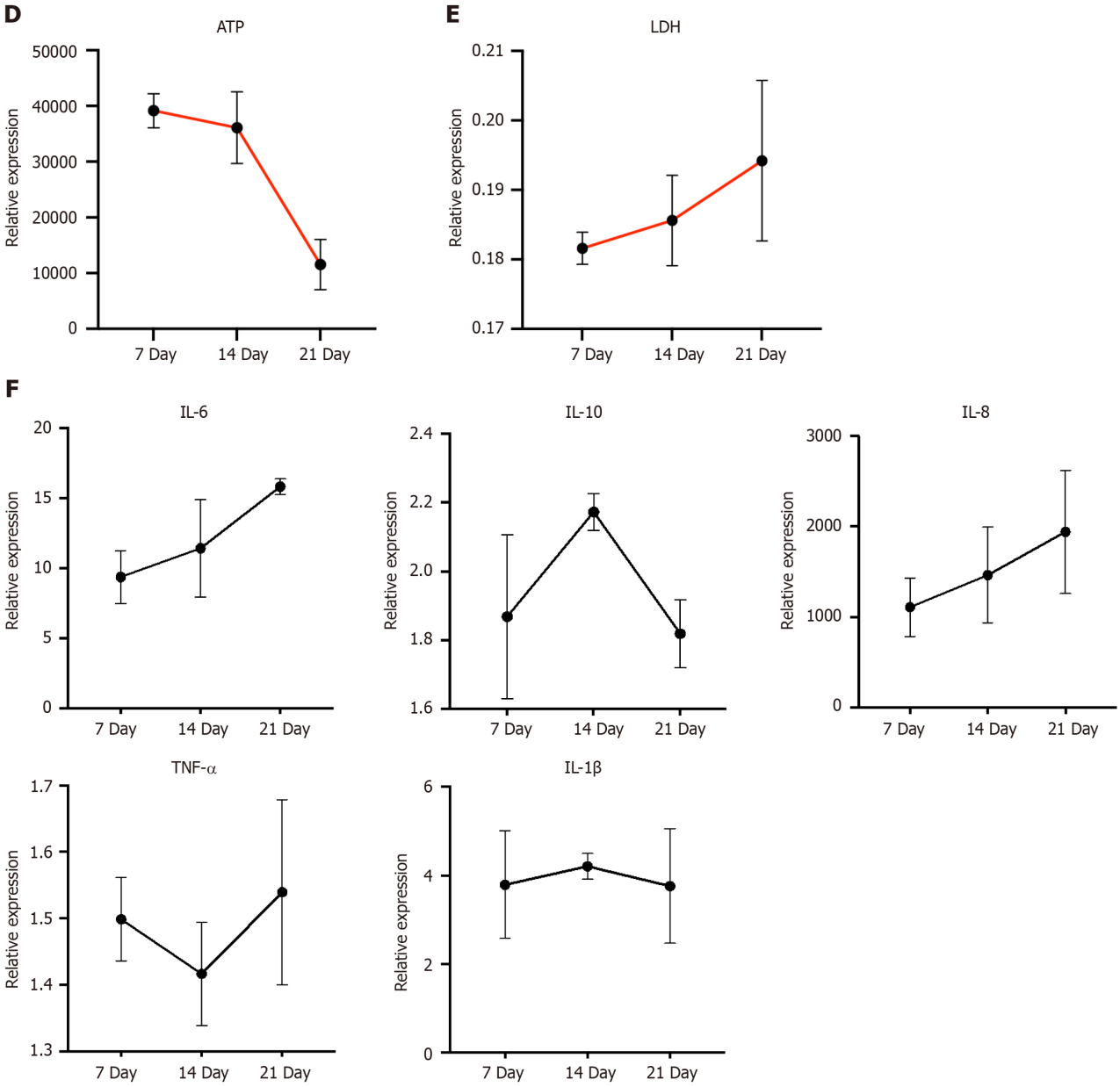

Figure 4 Morphological and functional identification of Vorganoids. A: Immunofluorescence staining for vasculogenesis-related markers; B: CD31 expression pattern in Vorganoid cells during different culture durations; C: Morphological changes in Vorganoid cells during different culture durations; D and E: Analysis of adenosine triphosphate (D) and lactate dehydrogenase (E) levels in Vorganoids during different culture durations; F: Expression patterns of inflammatory markers in Vorganoids analysed *via* enzyme-linked immunosorbent assay. Significant difference between the groups, $^{b}P < 0.01$, Scale bar = 100 μm. HE: Hematoxylin-eosin; ATP: Adenosine triphosphate; LDH: Lactate dehydrogenase; IL: Interleukin; TNF: Tumour necrosis factor; NS: Not significant.

ment analysis revealed that the DEGs intersected with the DEGs identified by pseudotime series and single-cell RNA-seq analysis to identify three common DEGs: PECAM1 (21%), FGF2 (13%) and FOXO1 (13%) (Figure 5D).

Immunofluorescence staining revealed that the increase in FOXO1 and FGF2 expression was significantly greater in the Vorganoids group ($P < 0.05$) (Figure 6A). After 7 d of addition of the FOXO1 inhibitor AS1842856 to the Vorganoid medium, a decrease in CD31 expression and an increase in FGF2 expression were observed, as was a decrease in the ratio of p-AKT/FOXO1 expression, with no significant change in VE expression (Figure 6B).

DISCUSSION

Revascularization plays an important role in tissue engineering. In this study, first, prevascularized human pulp organoids were constructed, and the vascularized organoids were found to be more similar to normal pulp tissue in terms of function and morphology (Figure 7). hDPSCs have stem cell properties and can differentiate into different cell types for clinical restorative applications. High expression of CD105, CD133 and CD146 has been shown to indicate subpopulations of cells with high angiogenic potential[21]. Selected CD105-positive dental pulp cells encapsulated in collagen scaffolds

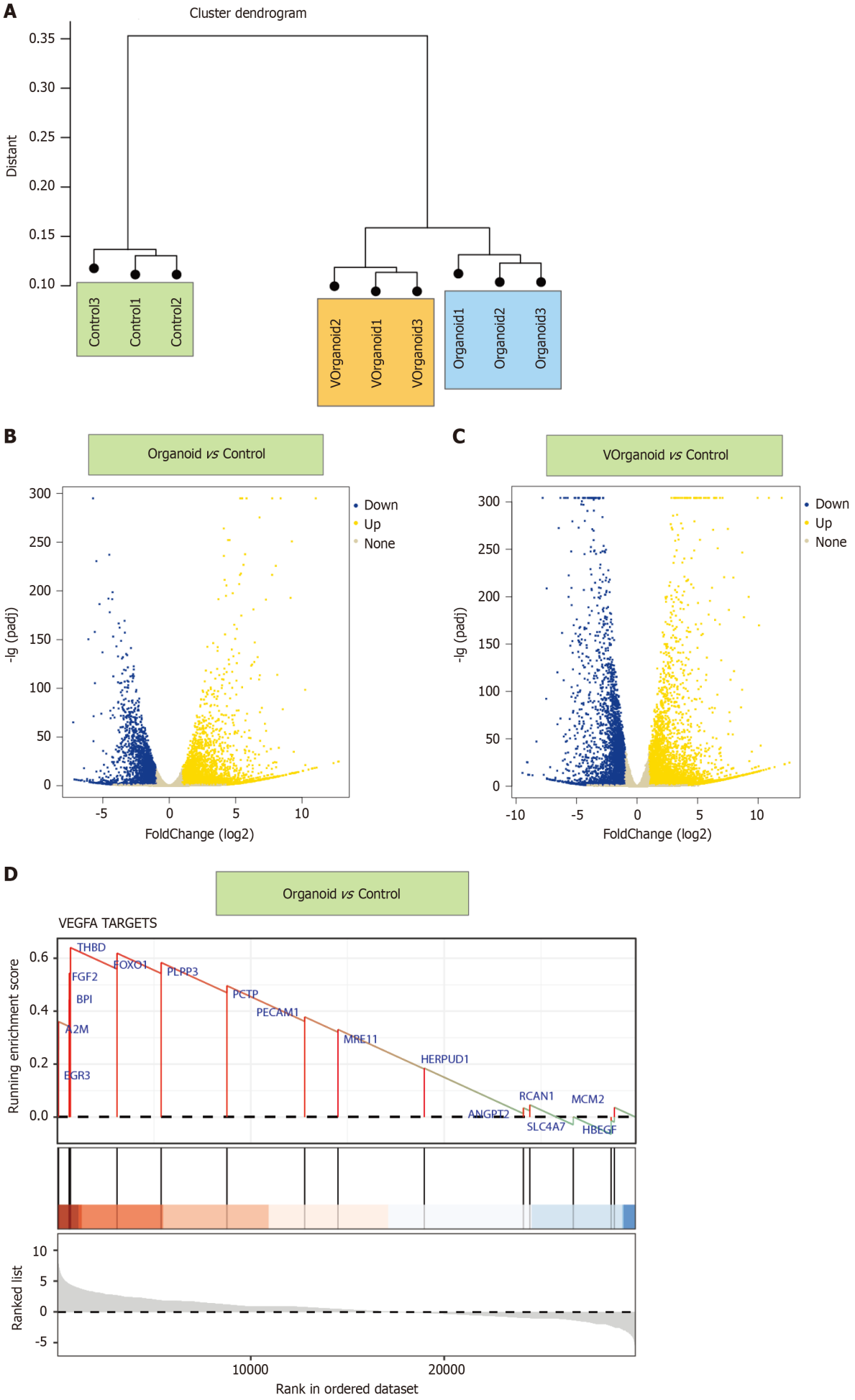
A
Cluster dendrogram
Distant
0.35
0.30
0.25
0.20
0.15
0.10
Control3
Control1
Control2
VOrganoid2
VOrganoid1
VOrganoid3
Organoid1
Organoid2
Organoid3
B
Organoid vs Control
-lg (padj)
FoldChange (log2)
Down
Up
None
C
VOrganoid vs Control
-lg (padj)
FoldChange (log2)
Down
Up
None
D
Organoid vs Control
VEGFA TARGETS
Running enrichment score
THBD
FOXO1
FGF2
PLPP3
BPI
PCTP
PECAM1
A2M
MRE11
EGR3
HERPUD1
RCAN1
MCM2
ANGPT2
SLC4A7
HBEGF
Ranked list
Rank in ordered dataset

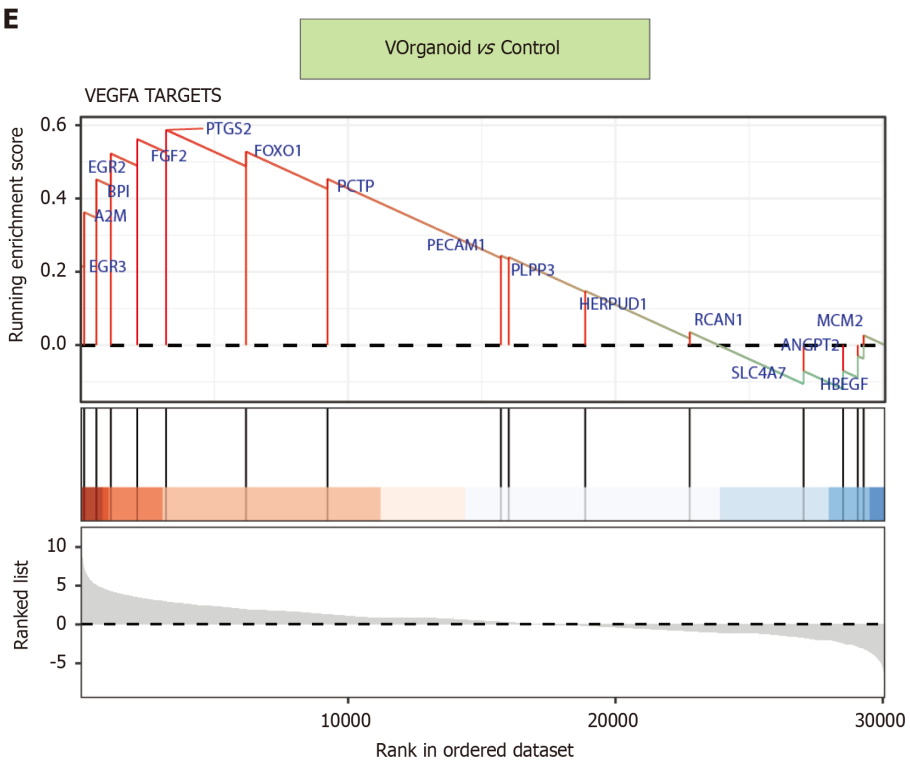

Figure 5 Functional enrichment analysis results for differentially expressed genes in the organoid *vs* control and Vorganoid *vs* control comparisons. A: The sample cluster dendrogram of different states of dentin-pulp-like organoid development; B and C: Volcano map showing the differentially expressed genes identified *via* differential comparison of the organoid *vs* control (B) and Vorganoid *vs* control (C) groups; D and E: The vascular endothelial growth factor A targets identified by gene set enrichment analysis enrichment analysis in the organoid *vs* control (D) and Vorganoid *vs* control (E) groups. VEGFA: Vascular endothelial growth factor A.

and stromal cell-derived factor 1α and transplanted into root canals were able to form tissue with vascular-like structures [22]. In addition, the angiogenic capacities of different cell types differ; interactions between cells enhance angiogenic capacity, and an appropriate cell mixing ratio can significantly enhance angiogenesis[21,23-25]. In this study, the stemness of hDPSCs was maintained by 3% hypoxia treatment, vascularisation medium was added to promote the differentiation of pulp cells into ECs, Matrigel scaffolds provided attachment sites and growth space for the cells to maintain a suitable biomechanical microenvironment, and 3D coculture with unconditioned pulp cells was subsequently performed to promote organoid prevascularisation (Figures 5A and 7). Depending on the diffusional supply of nutrients and oxygen [26], the diameter of the Vorganoids remains within 500 μm. To promote organoid vascularisa-tion, four elements, namely, cells, oxygen levels, scaffolding and signalling factors, work synergistically. The morphological and functional tests indicate that the Vorganoid partially. It should be noted that Vorganoids differ from tightly controlled structures *in vivo*. The use of *in vitro* models is limited in terms of representing the cell composition and structure of the *in vivo* counterpart, which can make them less reproducible.

To more thoroughly analyse the mechanisms involved in pulp tissue angiogenesis, we extracted single-cell sequencing data from public databases, further analysed the key regulatory pathways linking EC subpopulations in the tissue to angiogenesis, and performed a temporal analysis of key genes at different temporal and spatial nodes[27]. ECs were dominant in Vorganoid culture, and the proportion of ECs in the cell population was quite high in Vorganoid culture. Combined with the RNA-seq results, these findings revealed that the pathways associated with VEGFA targets were significantly enriched in the development of Vorganoids. Among the regulatory factors, the FOXO1 and FGF2 biomarkers were found to be involved in the regulation of Vorganoids.

FOXO1 is a key transcription factor involved in a wide range of biological functions. It is widely expressed in vascular ECs, and vascular cell adhesion molecule 1, intercellular adhesion molecule 1 and E-selectin have been reported to be downstream regulators of vascular ECs[28,29]. Systematic knockout of the *FOXO1* gene impaired angiogenesis and killed embryos, but specific knockout of the *FOXO1* gene in the adult mouse myocardium did not affect cardiac function[30,31]. Previous experiments showed that FOXO1 transcript expression was reduced in hypoxic culture but increased when the culture environment was changed to conditional induction culture or 3D organoid formation (Figure 7). Thus, FOXO1 may regulate different gene transcripts that act at different stages of angiogenesis, particularly during embryonic development. Therefore, we investigated the role of FOXO1 in the different stages of angiogenic differentiation in hDPSCs; however, it is unclear whether it plays a synergistic role between its antioxidant and angiogenic effects. This topic is worth investigating further.

The ability of cellular grafts to repair damaged tissues is limited, and the introduction of vascularized grafts brings them closer to the function and maturation of the corresponding tissues. This technique has the potential to overcome the limitations of many other models, such as maintaining *in vitro* accessibility and scalability, but significant improvements

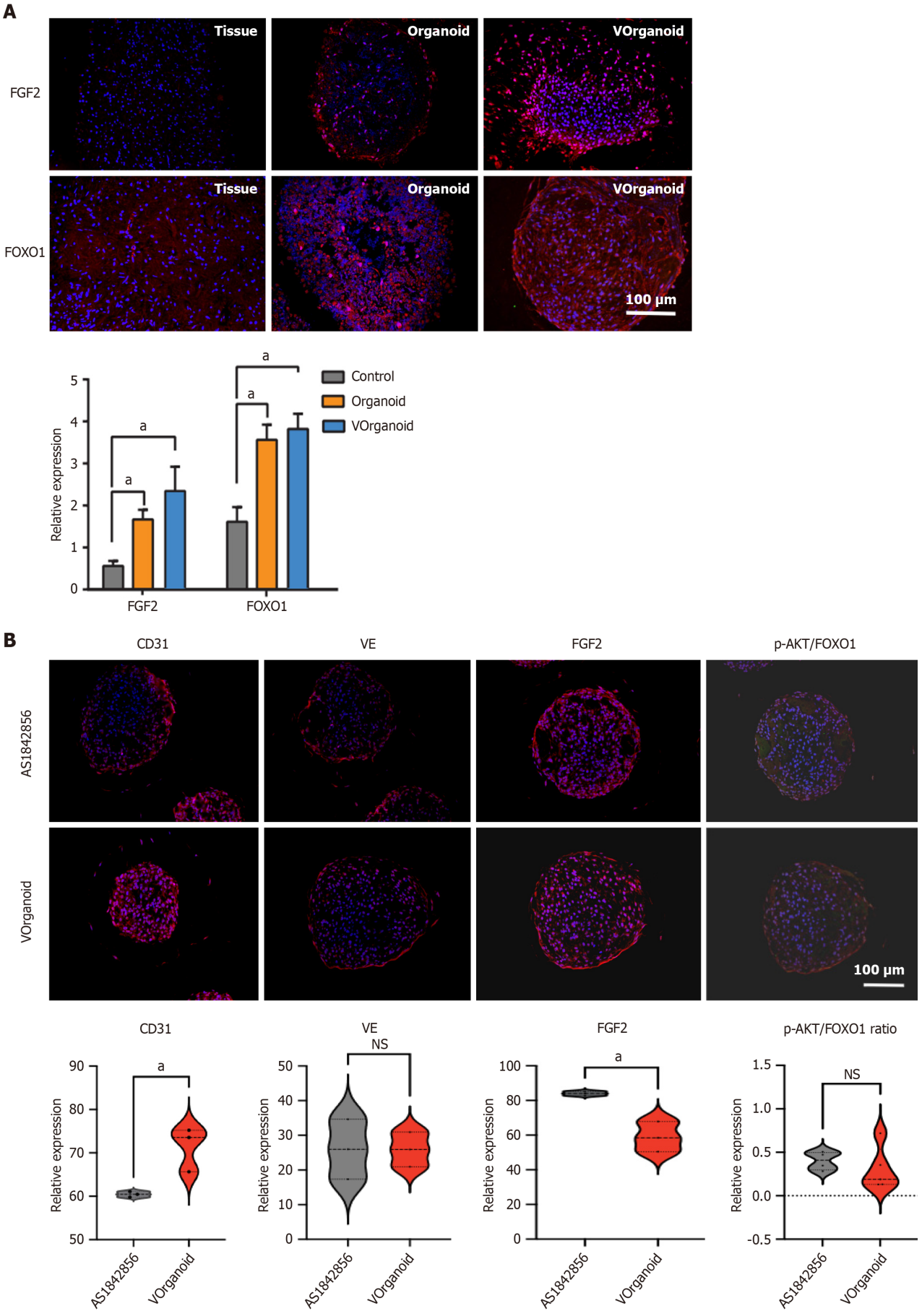

Figure 6 Target gene identification and validation. A and B: Immunofluorescence staining and quantification. Significant difference between the groups, $^{a}P < 0.05$. Scale bar = 100 μm. FGF2: Fibroblast growth factor 2; FOXO1: Forkhead box protein O1; NS: Not significant.

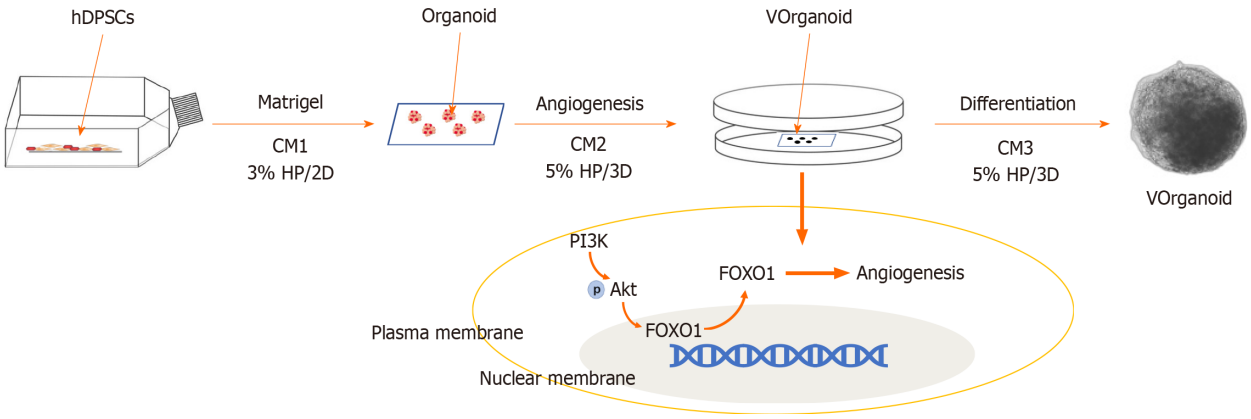

Figure 7 Generation of Vorganoids through differentiated human dental pulp stem cell assembly. hDPSCs: Human dental pulp stem cells; CM: Conditioned medium; FOXO1: Forkhead box protein O1.

are still needed. In conclusion, the finding of this study suggested that this new model could be applied in the field, which may pave the way for future dental regeneration prospects. In addition, vascularized organoids are more biologically similar to normal tissue. In addition to tissue regeneration and repair, Vorganoids can also be used for disease modelling, toxicity testing and drug screening. The use of human 3D organoids, along with other advances in single-cell technology, has revealed unprecedented insights into human biology and disease mechanisms.

CONCLUSION

Current organoid models do not fully replicate all cell types, levels of cell maturation, and physiological functions of their respective organs. They only exhibit some of the organ's functions. In this study, we effectively established an *in vitro* model of prevascularized dental pulp organoids and used it to elucidate new mechanisms of angiogenesis. Our results suggest that the biomarkers FOXO1 and FGF2 confirm the angiogenic regulatory role of Vorganoids. However, to understand the mechanisms by which organoids interact between structure and function, further investigation is required. Additionally, the use of organoids in simulating inflammation in clinically relevant diseases and the immunogenicity of dental materials should be studied.

ARTICLE HIGHLIGHTS

Research background

Stem cells can self-organise into microsized organ units, which can partially model tissue function and regeneration. Dental pulp organoids have been used to replicate the processes of tooth development and related diseases. However, the lack of vasculature limits the usefulness of dental pulp organo.

Research motivation

The survival of stem cell transplants should be promoted, thereby improving the repair ability of the cells.

Research objectives

Three-dimensional (3D) self-assembly of a novel vascularised dental pulp-like organoid *in vitro* by hypoxia and conditioned media.

Research methods

Human dental pulp stem cells were induced from endothelial cells (ECs) through exposure to a hypoxic environment and conditioned medium. The resulting cells were then mixed with ECs at specific ratios and conditioned in a 3D environment to produce Vorganoids. The biological characteristics of the Vorganoids were analysed, and the regulatory pathways associated with angiogenesis were studied.

Research results

Vorganoids are similar in morphology and function to dental pulp tissue. Single-cell RNA sequencing of dental pulp tissue and RNA sequencing of Vorganoids were performed to identify the involvement of the biomarkers forkhead box protein O1 (FOXO1) and fibroblast growth factor 2 (FGF2) in key regulatory pathways associated with Vorganoid angiogenesis.

Research conclusions

In this study, we effectively established an *in vitro* model of prevascularized dental pulp organoids and used it to elucidate novel mechanisms of angiogenesis during dental regeneration. The biomarkers FOXO1 and FGF2 confirmed the angiogenesis-regulating role of angiopoietins.

Research perspectives

This innovative study has effectively established an *in vitro* model of prevascularized dental pulp organoids and used it to elucidate new mechanisms of angiogenesis during regeneration, facilitating the development of clinical treatment strategies.

FOOTNOTES

Co-first authors: Fei Liu and Jing Xiao.

Co-corresponding authors: Zhi-Ren Zhang and Chun-Xiao Bai.

Author contributions: Liu F, Xiao J, Tian JZ, Zhang ZR, and Bai XC designed the research; Liu F and Xiao J performed the research and analyzed the data; Chen LH and Pan YY contributed human dental pulp tissue; Liu F wrote the paper. Liu F and Xiao J contributed to the work equally and should be regarded as co-first authors. Bai XC and Zhang ZR contributed to the work equally and should be regarded as co-corresponding author.

Supported by the Science and Technology Programme of Guangzhou City, No. 202201020341.

Institutional review board statement: This study was approved by the Ethics Committee of Guangdong Second Provincial General Hospital.

Conflict-of-interest statement: All the authors report no relevant conflicts of interest for this article.

Data sharing statement: Technical appendix, statistical code, and dataset available from the corresponding author at kqliufei@126.com. Participants gave informed consent for data sharing.

Country/Territory of origin: China

ORCID number: Fei Liu 0000-0002-5186-7661; Jun-Zhang Tian 0000-0002-4832-3648; Zhi-Ren Zhang 0000-0001-6780-4079; Xiao-Chun Bai 0000-0001-9631-4781.

S-Editor: Wang JJ
L-Editor: A
P-Editor: Zhao YQ

REFERENCES

1 **Roche ET**, Hastings CL, Lewin SA, Shvartsman D, Brudno Y, Vasilyev NV, O'Brien FJ, Walsh CJ, Duffy GP, Mooney DJ. Comparison of biomaterial delivery vehicles for improving acute retention of stem cells in the infarcted heart. *Biomaterials* 2014; **35**: 6850-6858 [PMID: 24862441 DOI: 10.1016/j.biomaterials.2014.04.114]

2 **Karp JM**, Leng Teo GS. Mesenchymal stem cell homing: the devil is in the details. *Cell Stem Cell* 2009; **4**: 206-216 [PMID: 19265660 DOI: 10.1016/j.stem.2009.02.001]

3 **Corsini NS**, Knoblich JA. Human organoids: New strategies and methods for analyzing human development and disease. *Cell* 2022; **185**: 2756-2769 [PMID: 35868278 DOI: 10.1016/j.cell.2022.06.051]

4 **Wimmer RA**, Leopoldi A, Aichinger M, Kerjaschki D, Penninger JM. Generation of blood vessel organoids from human pluripotent stem cells. *Nat Protoc* 2019; **14**: 3082-3100 [PMID: 31554955 DOI: 10.1038/s41596-019-0213-z]

5 **Jeong SY**, Lee S, Choi WH, Jee JH, Kim HR, Yoo J. Fabrication of Dentin-Pulp-Like Organoids Using Dental-Pulp Stem Cells. *Cells* 2020; **9** [PMID: 32155898 DOI: 10.3390/cells9030642]

6 **Hemeryck L**, Hermans F, Chappell J, Kobayashi H, Lambrechts D, Lambrichts I, Bronckaers A, Vankelecom H. Organoids from human tooth showing epithelial stemness phenotype and differentiation potential. *Cell Mol Life Sci* 2022; **79**: 153 [PMID: 35217915 DOI: 10.1007/s00018-022-04183-8]

7 **Katata C**, Sasaki JI, Li A, Abe GL, Nör JE, Hayashi M, Imazato S. Fabrication of Vascularized DPSC Constructs for Efficient Pulp Regeneration. *J Dent Res* 2021; **100**: 1351-1358 [PMID: 33913364 DOI: 10.1177/00220345211007427]

8 **Stegen S**, van Gastel N, Eelen G, Ghesquière B, D'Anna F, Thienpont B, Goveia J, Torrekens S, Van Looveren R, Luyten FP, Maxwell PH, Wielockx B, Lambrechts D, Fendt SM, Carmeliet P, Carmeliet G. HIF-1α Promotes Glutamine-Mediated Redox Homeostasis and Glycogen-

Dependent Bioenergetics to Support Postimplantation Bone Cell Survival. *Cell Metab* 2016; **23**: 265-279 [PMID: 26863487 DOI: 10.1016/j.cmet.2016.01.002]

9 **Bertassoni LE**. Progress and Challenges in Microengineering the Dental Pulp Vascular Microenvironment. *J Endod* 2020; **46**: S90-S100 [PMID: 32950200 DOI: 10.1016/j.joen.2020.06.033]

10 **Carvalho GL**, Sarra G, Schröter GT, Silva LSRG, Ariga SKK, Gonçalves F, Caballero-Flores HV, Moreira MS. Pro-angiogenic potential of a functionalized hydrogel scaffold as a secretome delivery platform: An innovative strategy for cell homing-based dental pulp tissue engineering. *J Tissue Eng Regen Med* 2022; **16**: 472-483 [PMID: 35244346 DOI: 10.1002/term.3294]

11 **Liu F**, Huang X, Luo Z, He J, Haider F, Song C, Peng L, Chen T, Wu B. Hypoxia-Activated PI3K/Akt Inhibits Oxidative Stress *via* the Regulation of Reactive Oxygen Species in Human Dental Pulp Cells. *Oxid Med Cell Longev* 2019; **2019**: 6595189 [PMID: 30728888 DOI: 10.1155/2019/6595189]

12 **Clough E**, Barrett T. The Gene Expression Omnibus Database. *Methods Mol Biol* 2016; **1418**: 93-110 [PMID: 27008011 DOI: 10.1007/978-1-4939-3578-9_5]

13 **Hafemeister C**, Satija R. Normalization and variance stabilization of single-cell RNA-seq data using regularized negative binomial regression. *Genome Biol* 2019; **20**: 296 [PMID: 31870423 DOI: 10.1186/s13059-019-1874-1]

14 **Butler A**, Hoffman P, Smibert P, Papalexi E, Satija R. Integrating single-cell transcriptomic data across different conditions, technologies, and species. *Nat Biotechnol* 2018; **36**: 411-420 [PMID: 29608179 DOI: 10.1038/nbt.4096]

15 **Sinha D**, Sinha P, Saha R, Bandyopadhyay S, Sengupta D. Improved dropClust R package with integrative analysis support for scRNA-seq data. *Bioinformatics* 2019 [PMID: 31693086 DOI: 10.1093/bioinformatics/btz823]

16 **Slovin S**, Carissimo A, Panariello F, Grimaldi A, Bouché V, Gambardella G, Cacchiarelli D. Single-Cell RNA Sequencing Analysis: A Step-by-Step Overview. *Methods Mol Biol* 2021; **2284**: 343-365 [PMID: 33835452 DOI: 10.1007/978-1-0716-1307-8_19]

17 **Wu T**, Hu E, Xu S, Chen M, Guo P, Dai Z, Feng T, Zhou L, Tang W, Zhan L, Fu X, Liu S, Bo X, Yu G. clusterProfiler 4.0: A universal enrichment tool for interpreting omics data. *Innovation (Camb)* 2021; **2**: 100141 [PMID: 34557778 DOI: 10.1016/j.xinn.2021.100141]

18 **Hänzelmann S**, Castelo R, Guinney J. GSVA: gene set variation analysis for microarray and RNA-seq data. *BMC Bioinformatics* 2013; **14**: 7 [PMID: 23323831 DOI: 10.1186/1471-2105-14-7]

19 **Anders S**, Huber W. Differential expression analysis for sequence count data. *Genome Biol* 2010; **11**: R106 [PMID: 20979621 DOI: 10.1186/gb-2010-11-10-r106]

20 **Chen J**, Bardes EE, Aronow BJ, Jegga AG. ToppGene Suite for gene list enrichment analysis and candidate gene prioritization. *Nucleic Acids Res* 2009; **37**: W305-W311 [PMID: 19465376 DOI: 10.1093/nar/gkp427]

21 **Gandia C**, Armiñan A, García-Verdugo JM, Lledó E, Ruiz A, Miñana MD, Sanchez-Torrijos J, Payá R, Mirabet V, Carbonell-Uberos F, Llop M, Montero JA, Sepúlveda P. Human dental pulp stem cells improve left ventricular function, induce angiogenesis, and reduce infarct size in rats with acute myocardial infarction. *Stem Cells* 2008; **26**: 638-645 [PMID: 18079433 DOI: 10.1634/stemcells.2007-0484]

22 **Iohara K**, Imabayashi K, Ishizaka R, Watanabe A, Nabekura J, Ito M, Matsushita K, Nakamura H, Nakashima M. Complete pulp regeneration after pulpectomy by transplantation of CD105+ stem cells with stromal cell-derived factor-1. *Tissue Eng Part A* 2011; **17**: 1911-1920 [PMID: 21417716 DOI: 10.1089/ten.TEA.2010.0615]

23 **Dissanayaka WL**, Zhan X, Zhang C, Hargreaves KM, Jin L, Tong EH. Coculture of dental pulp stem cells with endothelial cells enhances osteo-/odontogenic and angiogenic potential in vitro. *J Endod* 2012; **38**: 454-463 [PMID: 22414829 DOI: 10.1016/j.joen.2011.12.024]

24 **Dissanayaka WL**, Hargreaves KM, Jin L, Samaranayake LP, Zhang C. The interplay of dental pulp stem cells and endothelial cells in an injectable peptide hydrogel on angiogenesis and pulp regeneration in vivo. *Tissue Eng Part A* 2015; **21**: 550-563 [PMID: 25203774 DOI: 10.1089/ten.TEA.2014.0154]

25 **Xu X**, Li Z, Ai X, Tang Y, Yang D, Dou L. Human three-dimensional dental pulp organoid model for toxicity screening of dental materials on dental pulp cells and tissue. *Int Endod J* 2022; **55**: 79-88 [PMID: 34587308 DOI: 10.1111/iej.13641]

26 **Wörsdörfer P**, Ergün S. The Impact of Oxygen Availability and Multilineage Communication on Organoid Maturation. *Antioxid Redox Signal* 2021; **35**: 217-233 [PMID: 33334234 DOI: 10.1089/ars.2020.8195]

27 **Vargas-Valderrama A**, Messina A, Mitjavila-Garcia MT, Guenou H. The endothelium, a key actor in organ development and hPSC-derived organoid vascularization. *J Biomed Sci* 2020; **27**: 67 [PMID: 32443983 DOI: 10.1186/s12929-020-00661-y]

28 **Wang S**, Shi M, Li J, Zhang Y, Wang W, Xu P, Li Y. Endothelial cell-derived exosomal circHIPK3 promotes the proliferation of vascular smooth muscle cells induced by high glucose *via* the miR-106a-5p/Foxo1/Vcam1 pathway. *Aging (Albany NY)* 2021; **13**: 25241-25255 [PMID: 34887361 DOI: 10.18632/aging.203742]

29 **Zhuang T**, Liu J, Chen X, Zhang L, Pi J, Sun H, Li L, Bauer R, Wang H, Yu Z, Zhang Q, Tomlinson B, Chan P, Zheng X, Morrisey E, Liu Z, Reilly M, Zhang Y. Endothelial Foxp1 Suppresses Atherosclerosis *via* Modulation of Nlrp3 Inflammasome Activation. *Circ Res* 2019; **125**: 590-605 [PMID: 31318658 DOI: 10.1161/CIRCRESAHA.118.314402]

30 **Hariharan N**, Maejima Y, Nakae J, Paik J, Depinho RA, Sadoshima J. Deacetylation of FoxO by Sirt1 Plays an Essential Role in Mediating Starvation-Induced Autophagy in Cardiac Myocytes. *Circ Res* 2010; **107**: 1470-1482 [PMID: 20947830 DOI: 10.1161/CIRCRESAHA.110.227371]

31 **Qi Y**, Zhu Q, Zhang K, Thomas C, Wu Y, Kumar R, Baker KM, Xu Z, Chen S, Guo S. Activation of Foxo1 by insulin resistance promotes cardiac dysfunction and β-myosin heavy chain gene expression. *Circ Heart Fail* 2015; **8**: 198-208 [PMID: 25477432 DOI: 10.1161/CIRCHEARTFAILURE.114.001457]

World Journal of Stem Cells

Submit a Manuscript: https://www.f6publishing.com

World J Stem Cells 2024 March 26; 16(3): 305-323

DOI: 10.4252/wjsc.v16.i3.305

ISSN 1948-0210 (online)

ORIGINAL ARTICLE

Basic Study

Evaluation of genetic response of mesenchymal stem cells to nanosecond pulsed electric fields by whole transcriptome sequencing

Jian-Jing Lin, Tong Ning, Shi-Cheng Jia, Ke-Jia Li, Yong-Can Huang, Qiang Liu, Jian-Hao Lin, Xin-Tao Zhang

Specialty type: Cell and tissue engineering

Provenance and peer review: Invited article; Externally peer reviewed.

Peer-review model: Single blind

Peer-review report's scientific quality classification

Grade A (Excellent): 0
Grade B (Very good): B, B
Grade C (Good): C
Grade D (Fair): 0
Grade E (Poor): 0

P-Reviewer: Delben PB, Brazil; Mohammadzadeh I, Iran; Soltani R, Iran

Received: December 13, 2023
Peer-review started: December 13, 2023
First decision: January 24, 2024
Revised: January 31, 2024
Accepted: February 28, 2024
Article in press: February 28, 2024
Published online: March 26, 2024

Jian-Jing Lin, Shi-Cheng Jia, Xin-Tao Zhang, Department of Sports Medicine and Rehabilitation, Peking University Shenzhen Hospital, Shenzhen 518036, Guangdong Province, China

Tong Ning, Institute of Medical Science, The Second Hospital, Cheeloo College of Medicine, Shandong University, Jinan 250033, Shandong Province, China

Ke-Jia Li, Department of Biomedical Engineering, Institute of Future Technology, Peking University, Beijing 100871, China

Yong-Can Huang, Shenzhen Engineering Laboratory of Orthopaedic Regenerative Technologies, Peking University Shenzhen Hospital, Shenzhen 518036, Guangdong Province, China

Qiang Liu, Jian-Hao Lin, Arthritis Clinical and Research Center, Peking University People's Hospital, Beijing 100044, China

Corresponding author: Xin-Tao Zhang, PhD, Chief Physician, Department of Sports Medicine and Rehabilitation, Peking University Shenzhen Hospital, No. 1120 Lianhua Road, Futian District, Shenzhen 518036, Guangdong Province, China. zhangxintao@sina.com

Abstract

BACKGROUND

Mesenchymal stem cells (MSCs) modulated by various exogenous signals have been applied extensively in regenerative medicine research. Notably, nanosecond pulsed electric fields (nsPEFs), characterized by short duration and high strength, significantly influence cell phenotypes and regulate MSCs differentiation *via* multiple pathways. Consequently, we used transcriptomics to study changes in messenger RNA (mRNA), long noncoding RNA (lncRNA), microRNA (miRNA), and circular RNA expression during nsPEFs application.

AIM

To explore gene expression profiles and potential transcriptional regulatory mechanisms in MSCs pretreated with nsPEFs.

METHODS

The impact of nsPEFs on the MSCs transcriptome was investigated through whole

transcriptome sequencing. MSCs were pretreated with 5-pulse nsPEFs (100 ns at 10 kV/cm, 1 Hz), followed by total RNA isolation. Each transcript was normalized by fragments per kilobase per million. Fold change and difference significance were applied to screen the differentially expressed genes (DEGs). Gene Ontology and Kyoto Encyclopedia of Genes and Genomes analyses were performed to elucidate gene functions, complemented by quantitative polymerase chain reaction verification.

RESULTS

In total, 263 DEGs were discovered, with 92 upregulated and 171 downregulated. DEGs were predominantly enriched in epithelial cell proliferation, osteoblast differentiation, mesenchymal cell differentiation, nuclear division, and wound healing. Regarding cellular components, DEGs are primarily involved in condensed chromosome, chromosomal region, actin cytoskeleton, and kinetochore. From aspect of molecular functions, DEGs are mainly involved in glycosaminoglycan binding, integrin binding, nuclear steroid receptor activity, cytoskeletal motor activity, and steroid binding. Quantitative real-time polymerase chain reaction confirmed targeted transcript regulation.

CONCLUSION

Our systematic investigation of the wide-ranging transcriptional pattern modulated by nsPEFs revealed the differential expression of 263 mRNAs, 2 miRNAs, and 65 lncRNAs. Our study demonstrates that nsPEFs may affect stem cells through several signaling pathways, which are involved in vesicular transport, calcium ion transport, cytoskeleton, and cell differentiation.

Key Words: Nanosecond pulsed electric fields; Whole transcriptome sequencing; Mesenchymal stem cells; Genetic response; Stem cell engineering

Core Tip: Nanosecond pulsed electric fields (nsPEFs) have been found to regulate the osteogenic, chondrogenic, and adipogenic differentiation of mesenchymal stem cells (MSCs). We hypothesized that several key factors may be regulated by nsPEFs, thereby influencing the biological functions of MSCs. Following exposure of MSCs to nsPEFs, we identified the differential expression of 263 messenger RNAs, 65 long noncoding RNAs, and 2 microRNAs. Verification by quantitative polymerase chain reaction and Gene Ontology and Kyoko Encyclopedia of Genes and Genomes enrichment analyses demonstrated the involvement of chromosome, cytoskeleton, and calcium signaling pathways following nsPEFs pretreatment. These results may be very meaningful for the further application of nsPEFs in MSCs.

Citation: Lin JJ, Ning T, Jia SC, Li KJ, Huang YC, Liu Q, Lin JH, Zhang XT. Evaluation of genetic response of mesenchymal stem cells to nanosecond pulsed electric fields by whole transcriptome sequencing. *World J Stem Cells* 2024; 16(3): 305-323
URL: https://www.wjgnet.com/1948-0210/full/v16/i3/305.htm
DOI: https://dx.doi.org/10.4252/wjsc.v16.i3.305

INTRODUCTION

Mesenchymal stem cells (MSCs), as seed cells in regenerative repair, have been extensively applied in preclinical and clinical research in regenerative medicine, such as osteoarthritis[1], cartilage defects[2], and bone defects[3]. The differentiation and function of MSCs can be modulated by various exogenous signals, including biological factors[4], drug formulations[5], and physical signals[6]. The quest for an appropriate exogenous signal to regulate the functions and differentiation of stem cells remains a dynamic area of investigation for numerous researchers.

Pulsed electric fields (PEFs), as a crucial biophysical signal, can induce changes in cell membranes and alterations in intracellular calcium ion concentrations. Under specific conditions, PEFs can significantly influence cell phenotypes and regulate stem cell differentiation through multiple pathways[7,8]. However, the biological effects of traditional PEFs are relatively weak, and the time required for the emergence of a differentiating response can often range from hours to days [9]. This may be attributed to the fact that the pulse width of traditional PEFs is in the microsecond range or higher, exceeding the intrinsic charging and discharging time of cell membranes (in the range of hundreds of nanoseconds). As a result, traditional PEFs face difficulties in deeply penetrating the cell interior due to the shielding effect of the cell membrane[10]. In contrast, nanosecond PEFs (nsPEFs) represent nanosecond-duration, high-strength electric fields, with a shorter pulse width than the charging and discharging time of the cell membrane. Furthermore, nsPEFs can deeply penetrate into cellular organelles and exhibit significant biological effects[11]. In our previous research, it was found that nsPEFs can influence the osteogenic, adipogenic, and chondrogenic differentiation of MSCs by regulating DNA methylation and the MAPK signaling pathway[12]. Although nsPEFs show strong regulatory effects on MSCs differentiation, previous studies have mainly focused on specific molecules or pathways, and a comprehensive exploration of the

mechanisms by which nsPEFs regulate MSCs has not been conducted.

Transcriptomics analysis, by examining messenger RNA (mRNA), long noncoding RNA (lncRNA), microRNA (miRNA), and circular RNA (circRNA), allows for a comprehensive understanding of changes in gene expression. It also holds significant importance in unraveling alterations in biological processes. In this study, we first utilized high-throughput transcriptomics sequencing to detect the changes of mRNA, miRNA, lncRNA, and circRNA expression in MSCs after nsPEFs treatment. Additionally, we carried out Gene Ontology (GO) and Kyoto Encyclopedia of Genes and Genomes (KEGG) analyses to explore the biological processes and signaling pathways associated with differentially expressed target genes. Furthermore, we validated their expression levels using quantitative real-time polymerase chain reaction, providing further support for the application of nsPEFs in MSCs.

MATERIALS AND METHODS

Cell isolation and culture

All animal experiments were approved by the Institutional Animal Care and Use Committee of Peking University (COE-GeZ-7). Rat bone marrow MSCs (rMSCs) were harvested from 8-wk-old Sprague-Dawley rats according to our previous study[13]. MSCs were cultured in expansion medium composed of Dulbecco's modified Eagle's medium (DMEM, Hyclone) supplemented with 10% (v/v) fetal bovine serum (Gibco) and 1% penicillin/streptomycin (Amresco), in a humidified incubator at 37 °C with 5% CO_2. Cells were trypsinized with 0.25% (w/v) trypsin (Invitrogen, Carlsbad, CA, United States) upon reaching 85% confluence. MSCs at passage 5 were used for subsequent experiments.

Application of nsPEFs

We previously found that nsPEFs (100 ns, 10 kV/cm, 1 Hz, 5 pulses) can improve the stemness of porcine bone marrow MSCs, human bone marrow MSCs, and rMSCs, and promote osteochondral defect repair in rats[12-14]. In this study, nsPEFs with the same parameters were applied to regulate MSCs performance. According to our previous study[12-14], one million MSCs were suspended in 1 mL of DMEM within a 0.4-cm gap cuvette (Bio-Rad, 165-2088, United States) and stimulated by 5 pulses of nsPEFs (100 ns at 10 kV/cm, 1 Hz), and the time interval between two pulses was 1 s. The cells were then subjected to nsPEFs with a duration of 100 ns, as previously described. Five pulses were applied at 1-s intervals between each pulse. MSCs without nsPEFs stimulation served as the control group.

RNA isolation

Total RNA was isolated from the cells 24 h after exposure with the miRNA extraction kit (Cat#TR205-200, Tanmo). Qualified total RNA was further purified with the RNAClean XP Kit (Cat#A63987, Beckman Coulter, Inc.Kraemer Boulevard Brea, CA, United States) and the RNase-Free DNase Set (Cat#79254, QIAGEN, GmBH, Germany). RNA quantity was assessed by UV spectrometry at 260 nm/280 nm absorbance on a spectropchotometer (NanoDrop Technologies, Wilmington, DE, United States).

RNA-seq and differentially expressed gene analysis

The filtered clean reads were mapped to the reference genome database. Each transcript was normalized by fragments per kilobase per million to eliminate the influence of gene length and sequencing depth. The counts of each sample were mapped to the annotated genome after standardization and normalization. Finally, fold change (FC) and difference significance were used to screen the differentially expressed genes (DEGs). Each group of cells was sequenced with three independent biological replicates.

GO and KEGG enrichment analysis

GO term and KEGG pathway enrichment analyses were performed using the tool for Function Annotation in DAVID (https://david.ncifcrf.gov/). The KEGG pathway maps were obtained from the KEGG database (http://www.kegg.jp/).

Expression validation using quantitative polymerase chain reaction

Total RNA was extracted from 1 × 10^6 cells treated with 1 mL TRIzol. RNA purity and concentration were determined by a NanoDrop 2000 spectropchotometer (Thermo Fisher Scientific). cDNA was synthesized with the ReverTra Ace qPCR Kit (TOYOBO, FSQ-101) and then subjected to quantitative polymerase chain reaction using Power SYBR Green PCR Master Mix (ABI, 4368708). The mRNA levels were determined using 50 ng of cDNA on an Applied Biosystems 7300. All template amplifications were conducted in triplicate with a three-step polymerase chain reaction process. Using Actin expression as a normalization control, the relative expression was calculated using the $2^{-\Delta\Delta Ct}$ method. The primer sequences are provided in Table 1.

Statistical analysis

All numerical data from quantitative polymerase chain reaction are presented as the mean ± SD. Comparisons between groups were performed by the independent sample *t*-test. Results are presented as the mean ± SD. The Student's *t*-test was used to evaluate the difference between the two groups using Prism 8.21 software (GraphPad). The statistical significance level was set at $P < 0.05$.

Table 1 Primer sequences used in the study

Primer	Primer sequence (5' to 3')
Actg2-F	CTCTCTCCACCTTCCAGCAAA
Actg2-R	AGGGCCCCGCTTCATC
Nek2-F	TGGAGGGCCTGACAATCTG
Nek2-R	CCACCACACTGAGTTTCTGGTTT
Cenpf-F	GGAGAGCCTGTGTGCATGTG
Cenpf-R	ACGTGAGCAGGAGGTTATGAAAC
Scin-F	TGGCCGAAGATGATGTCATG
Scin-R	CTTTGCCAATCCAAATGAAGATC
Kif20b-F	TGTGCCACACCAGTCACAATT
Kif20b-R	ACCTCGCCACTCTTCCTCTTC
Nog-F	CGAGGGTTTTCAATGAACTTTTTT
Nog-R	AGTGCATTACATGAACCAGAAAGC
Ereg-F	GGGTTGCCACAAGTCTGAACA
Ereg-R	GCATGCTGCACATCCTTGTC
Asic3-F	GCCTGCTTACCATCCTTGAGA
Asic3-R	CCCCAGGACTCTGTCTTGGA
Aldh3a1-F	TCCCACCGCCGCTCTT
Aldh3a1-R	GCCTTGTGAGCTTCTTCATTCA
Tubb2b-F	GGCGAGGATGAGGCTTGA
Tubb2b-R	TTCACCTCAGCTTTCCCTAACC
Cryba4-F	CGTGCTGGAGAGCGATCA
Cryba4-R	AGCCCCACTCCCTGAAGTG
Nr3c2-F	CGCACAGCAATATGAAAACCA
Nr3c2-R	GCCCCTTTCCCCCAGAA
Stxbp5l-F	AAGCCTCAGCAGGAAAAGCA
Stxbp5l-R	TGCCCGGTCCAGGAATG
Actin-F	TCTGTGTGGATTGGTGGCTCTA
Actin-R	CTGCTTGCTGATCCACATCTG

RESULTS

Identification of DEGs

Differentially expressed lncRNAs and mRNAs (n = 4) are displayed using Volcano plots (Figure 1) and heat maps (Figure 2). The top 20 differentially expressed lncRNAs and mRNAs in the nsPEFs-treated group compared to the control group are listed in Tables 2 and 3, respectively.

In total, 263 DEGs were identified in the PRJNA931816 dataset, of which 92 and 171 were significantly ($|\log2FC| > 0.585$ and $q < 0.05$) upregulated and downregulated, respectively (Figures 1A and 2A). Of these DEGs, 65 were lncRNAs, of which 36 and 19 were significantly ($|\log2FC| > 1$ and $q < 0.05$) upregulated and downregulated, respectively (Figures 1B and 2B); 0 were circRNAs (Figure 1C); and 2 were miRNAs, both of which were significantly upregulated (Figure 1D).

Enrichment analysis of DEGs

To investigate the biological functions and pathways of DEGs, KEGG and GO analyses were conducted for the 263 DEGs. Figure 3 demonstrates the mainly enriched functional annotations from three aspects, including biological processes, cellular components (CC), and molecular functions (MF). From the perspective of biological processes, DEGs were mainly enriched in epithelial cell proliferation, osteoblast differentiation, mesenchymal cell differentiation, nuclear division, and wound healing. From the perspective of CC, DEGs are mainly involved in condensed chromosome, chromosomal region, actin cytoskeleton, and the kinetochore. From the perspective of MF, DEGs are mainly involved in glycosaminoglycan

Table 2 Top 20 differentially expressed long noncoding RNAs

LncRNA_ID	Locus	Log2FC	*Q* value
NONRATT027355.2	7:143840739-143841394	6.223946	0.038374
NONRATT014734.2	19:44137444-44139463	6.103516	0.001285
NONRATT000391.2	1:78818388-78818948	6.035452	0.008784
NONRATT030693.2	X:115351001-115352258	5.611966	0.011922
MSTRG.1686.44	1:180852586-181353774	5.574714	0.004533
NONRATT029722.2	9:113936538-113936864	5.563687	0.013263
MSTRG.1686.24	1:180804226-181295177	5.546189	0.000326
NONRATT024954.2	6:50889024-50923726	5.468331	7.04E-05
NONRATT010080.2	14:83648401-83660792	5.356187	0.021489
NONRATT021215.2	4:29083076-29092661	-5.06373	0.022244
NONRATT015697.2	2:211078318-211078606	-5.08835	0.01522
NONRATT002358.2	1:80335470-80336633	-5.27782	0.011922
NONRATT015446.2	2:188562082-188565332	-5.7896	7.11E-08
NONRATT026659.2	7:30291089-30293287	-5.84278	0.001419
NONRATT017622.2	20:7219444-7220293	-5.89986	4.44E-16
NONRATT031234.2	X:116752819-116754309	-5.9906	0.021489
NONRATT024688.2	6:136358084-136363672	-6.06997	0.018677
NONRATT024848.2	6:25912732-26051235	-7.01177	0.000482
NONRATT005942.2	10:84682448-84688899	-7.27093	0.016558
NONRATT002900.2	X:157319040-157323878	-11.8256	3.16E-09

LncRNA: Long noncoding RNA; FC: Fold change.

binding, integrin binding, nuclear steroid receptor activity, cytoskeletal motor activity, and steroid binding. When the upregulated mRNAs were enriched, 12 mRNAs were found to be involved in chromosome segregation (biological process). For example, among the 12 mRNAs, Top2a is a conserved regulator of chromatin topology which plays an important role in catalyzing reversible DNA double-strand breaks[15]. From the perspective of CC, upregulated mRNAs were mainly enriched in the chromosome, centromeric region, kinetochore, and midbody. From the perspective of MF, upregulated mRNAs were mainly enriched in integrin binding. When the downregulated mRNAs were enriched, they are involved in the extracellular space (CC). Among the 12 mRNAs, *Wnt11* encodes a protein that plays an important role in regulating extracellular matrix (ECM) organization[16], and *Smoc1* encodes an extracellular glycoprotein that is a critical regulator of cell attachment to the ECM by binding to calcium[17]. From the perspective of GO, downregulated mRNAs were mainly enriched in the positive regulation of gene expression, cell differentiation, and ventricular septum morphogenesis (Figures 3A and C). The detailed relationship between DEGs and GO are shown by the Chord diagram of GO (Figure 3E). GO analysis classified genes heavily involved in epithelial cell proliferation and osteoblast differentiation, among others.

Moreover, KEGG analysis shown in Figures 3B, D, and F demonstrated that DEGs mainly participate in the calcium signaling pathway, ECM-receptor interaction, focal adhesion, and vascular smooth muscle contraction. A Waterfall plot was generated to reveal the potential effects of nsPEFs on signaling pathways (Figure 3F). Other related signaling pathways such as the regulation of actin cytoskeleton, PI3K-Akt signaling pathway, Rap1 signaling pathway, cGMP-PKG signaling pathway, and Hippo signaling pathway-multiple species may also contribute to completing the reaction process of MSCs to nsPEFs. The term cluster showed that nsPEFs may stimulate the cells through the calcium signaling pathway, *etc.*

Enrichment analysis of differentially expressed lncRNA and miRNAs

The GO enrichment analysis results for the differentially expressed lncRNAs, miRNAs, and mRNAs are shown in Figure 4. Based on the target genes of differentially expressed lncRNAs, the most significantly enriched biological processes were regulation of endothelial cell migration, and ribonucleoprotein complex subunit organization. The most significantly enriched CC were the oligosaccharyltransferase complex, endoplasmic reticulum protein-containing complex, chromosome, and centromeric region. The most significantly enriched MF were tubulin binding, nuclear retinoid X receptor binding, and nuclear retinoic acid receptor binding (Figure 4A). Moreover, in Figure 4B, KEGG

Table 3 Top 20 differentially expressed messenger RNAs

Gene ID	Gene name	Log2FC	*Q* value
ENSRNOG00000017609	*Cnga4*	4.049502	0.041927
ENSRNOG00000005883	*Nek10*	3.164517	0.001515
ENSRNOG00000051612	*AABR07044570.1*	3.006014	0.020392
ENSRNOG00000003891	*Porf1*	2.826433	0.000369
ENSRNOG00000042070	*Ticam2*	2.821013	0.00501
ENSRNOG00000046566	*Tub*	2.803217	0.006364
ENSRNOG00000032973	*Il13ra2*	2.661856	1.68E-08
ENSRNOG00000025261	*AABR07050407.1*	2.232324	0.00943
ENSRNOG00000001959	*Mx1*	2.073926	0.049836
ENSRNOG00000031598	*Atp8b4*	2.055746	0.024695
ENSRNOG00000003283	*Rcsd1*	-2.09387	0.018919
ENSRNOG00000010454	*Ccno*	-2.1785	0.011229
ENSRNOG00000002456	*Hlf*	-2.44194	0.021066
ENSRNOG00000052129	*Nwd1*	-2.45693	0.032717
ENSRNOG00000014424	*RGD1563354*	-2.46926	0.016841
ENSRNOG00000049115	*Ccr5*	-2.73203	0.01083
ENSRNOG00000055401	*Kcnc1*	-3.13004	0.021817
ENSRNOG00000055318	*AABR07068030.1*	-3.34625	0.000321
ENSRNOG00000014556	*Cdh20*	-3.47543	0.025307
ENSRNOG00000054723	*AABR07058174.1*	-3.5912	0.047547
ENSRNOG00000011946	*Ptn*	-3.6805	0.000634

FC: Fold change.

analysis shows that differentially expressed lncRNAs mainly participate in the glycerophospholipid metabolism signaling pathway.

Based on the target genes of differentially expressed miRNAs, the most significantly enriched biological processes were the flavonoid metabolic process, cellular glucuronidation, vesicle fusion to plasma membrane, and animal organ regeneration. The most significantly enriched CC were the intrinsic component of organelle membrane, the integral component of organelle membrane, and the peroxisome. The most significantly enriched MF were glucuronosyltransferase activity, hexosyltransferase activity, and MAP kinase activity (Figure 4C). In addition, KEGG analysis in Figure 4D shows that differentially expressed miRNAs mainly participate in porphyrin metabolism, ascorbate and aldarate metabolism, biosynthesis of cofactors, and the pentose and glucuronate interconversions signaling pathway.

Validation of mRNA expression using quantitative polymerase chain reaction

We confirmed the accuracy of sequencing data for selected mRNAs, and the mRNA validation results were consistent with the RNA-seq data (Figure 5). According to the related signaling pathway, we selected seven upregulated mRNAs, aldehyde dehydrogenase 3 family member A1 (*Aldh3a1*), centromere protein F (*Cenpf*), kinesin family member 20B (*Kif20b*), epiregulin (*Ereg*), *Nek2*, nuclear receptor subfamily 3 group C member 2 (*Nr3c2*), and scinderin (*Scin*). The expression of these seven genes was found to be increased 2.02-fold, 1.8-fold, 2.11-fold, 2.12-fold, 1.66-fold, 2.01-fold, and 2.19-fold, respectively, in nsPEFs-treated cells. We selected six downregulated mRNAs, *Actg2, Asic3, Crybat4, Nog, Stxbp5 L*, and *Tubb2b*. The expression of these genes was found to be decreased in nsPEFs-treated cells, indicating that the mRNA validation results were consistent with the RNA-seq data.

DISCUSSION

In this study, nsPEFs-treated rMSCs were evaluated by whole transcriptome sequencing in terms of mRNA, lncRNA, circRNA, and miRNA expression. Previous studies have shown that nsPEFs can regulate the expression levels of some mRNAs in MSCs and upregulate the differentiation potential of MSCs[12]. nsPEFs can regulate the chondrogenic differ-

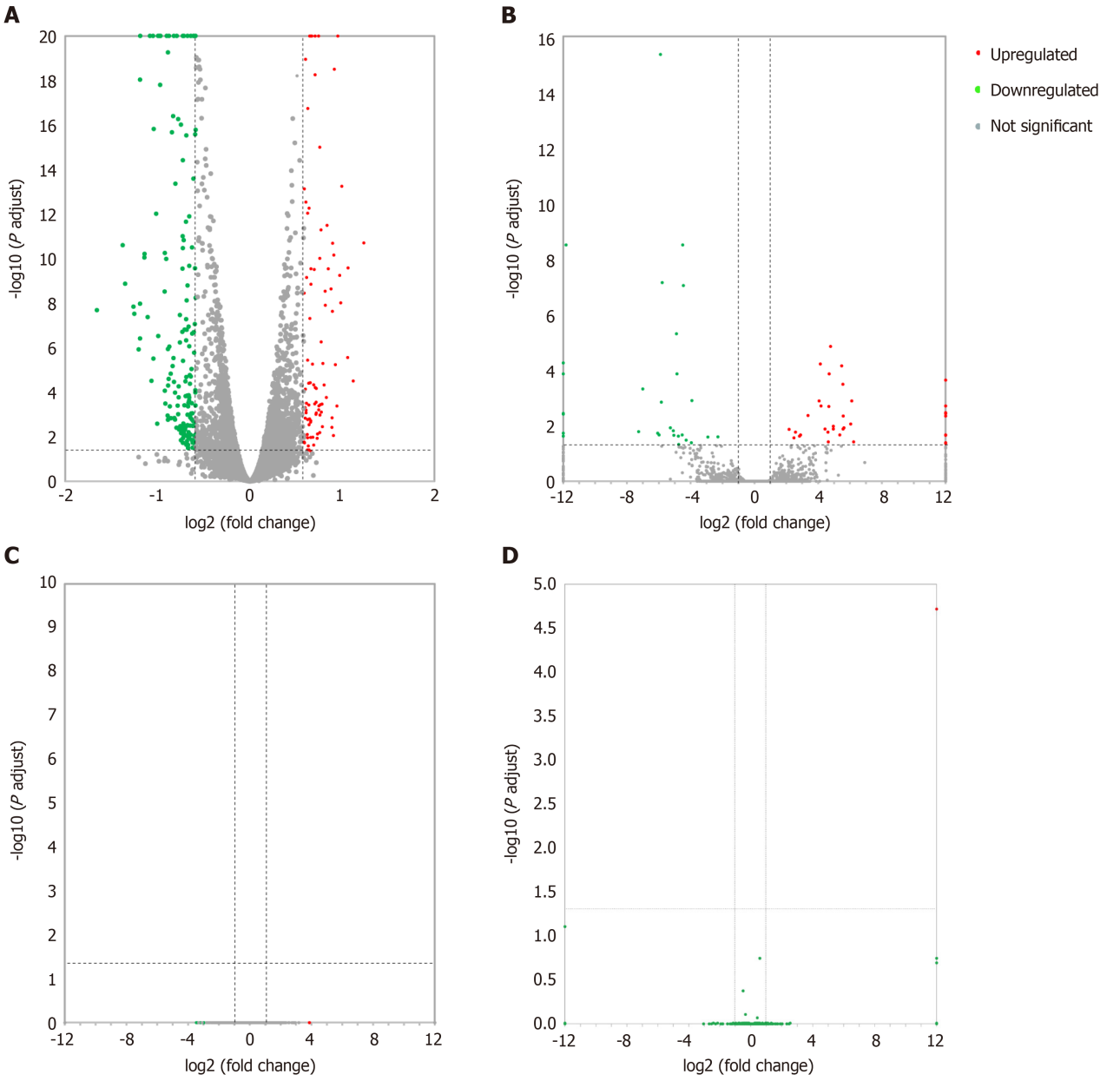

Figure 1 Volcano plots illustrating comparisons of differentially expressed messenger RNAs, long noncoding RNAs, circular RNAs, and microRNAs between each nanosecond pulsed electric field-treated group and the control group. A: Differentially expressed messenger RNAs; B: Differentially expressed long noncoding RNAs; C: Differentially expressed circular RNAs; D: Differentially expressed microRNAs.

entiation of MSCs through phosphorylation of molecules of the MAPK signaling pathways[14]. nsPEFs can also regulate the differentiation potential of MSCs through demethylation of stemness genes[12], and can induce nodule formation in osteoblasts[18]. However, the lack of a systematic study hinders further application of nsPEFs in stem cell differentiation.

Using whole transcriptome sequencing, 263 differentially expressed mRNAs ($q < 0.05$, $|\log2FC| > 0.585$), 2 differentially expressed miRNAs, and 65 differentially expressed lncRNAs were identified, which are involved in stem cell differentiation, calcium ions, plasma membrane, cell skeleton, chromatin, cell adhesion, *etc.* Our previous study found that nsPEFs (100 ns, 10kV/cm) with specific parameter combinations could promote the chondrogenic, osteoblastic, and adipogenic differentiation of stem cells, but did not induce apoptosis under these parameters[13,15]. Therefore, a combination of 100 ns and 10 kV/cm was selected to conduct electrical stimulation treatment on rMSCs to determine their effects on the gene expression profile. mRNA analysis indicated that nsPEFs may affect cell differentiation, calcium ions, plasma membrane, and other aspects. The expression levels of *Scin, Ereg, Kif20b, Aldh3a1, Nr3c2*, and *Cenpf* were upregulated. To better understand the universal effects of nsPEFs on mammalian cells, we compared the gene expression profiles between rMSCs (our data), TM3 cells, Jurkat cells, and U937 cells based on publicly available data[19,20]. We found that the gene expression levels of 23 genes were co-upregulated in rMSCs and TM3 cells, including *Kif20b*, which indicated that nsPEFs may cause common effects (Supplementary Figure 1). Compared with rMSCs, we found more common DEGs in TM3 cells (23 genes) than in Jurkat cells (3 genes) and U937 cells (6 genes). The reason for this may be that TM3 and rMSCs are adherent cells, and they are from mice or rats, while U937 and Jurkat cells are suspension cells, and are from humans. The 23 common DEGs are involved in the ECM-receptor interaction signaling pathway. Electric

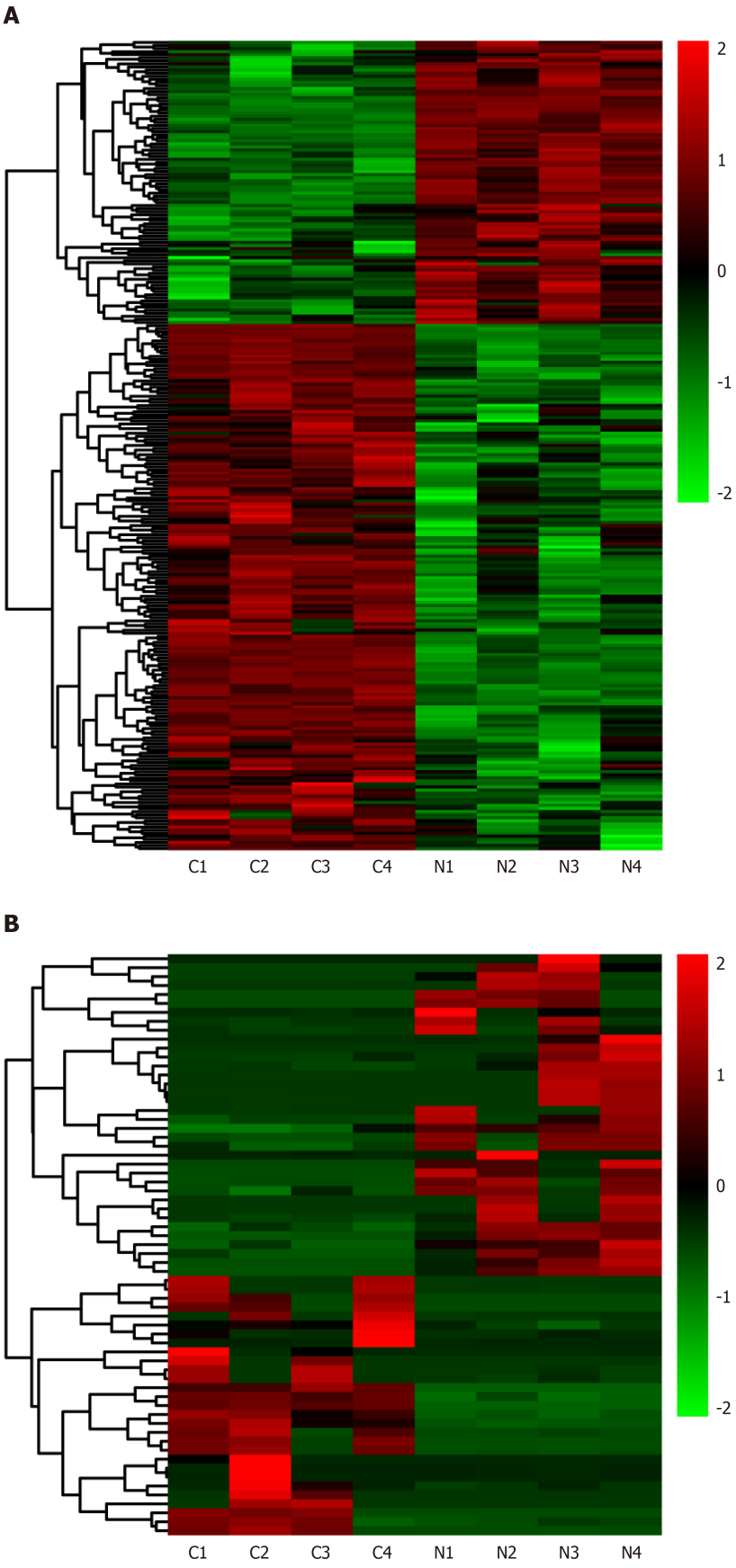

Figure 2 Heat maps displaying the hierarchical clustering of differentially expressed messenger RNAs and long noncoding RNAs. A: Differentially expressed messenger RNAs, B: Differentially expressed long noncoding RNAs. Red indicates up-regulation and green indicates down-regulation.

A

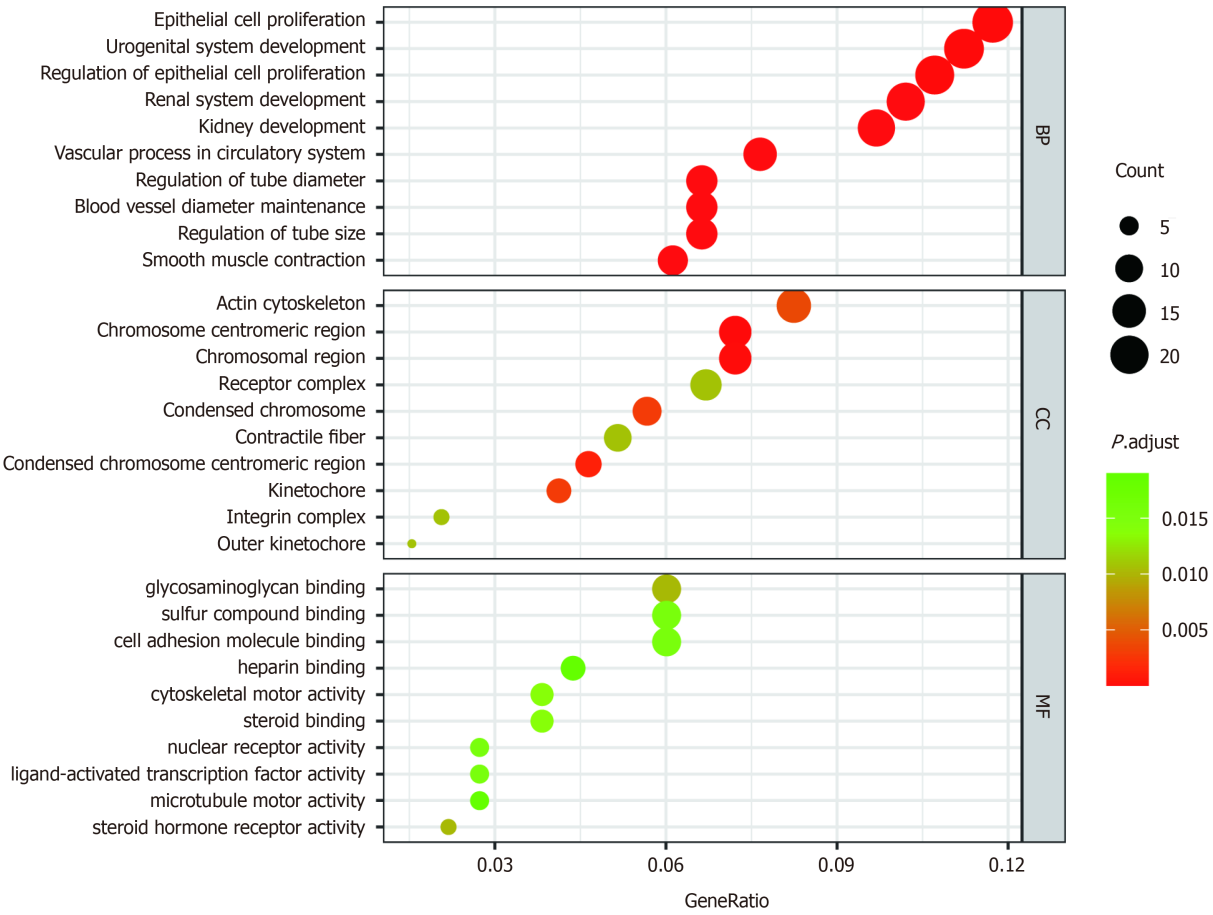
Epithelial cell proliferation
Urogenital system development
Regulation of epithelial cell proliferation
Renal system development
Kidney development
Vascular process in circulatory system
Regulation of tube diameter
Blood vessel diameter maintenance
Regulation of tube size
Smooth muscle contraction
Actin cytoskeleton
Chromosome centromeric region
Chromosomal region
Receptor complex
Condensed chromosome
Contractile fiber
Condensed chromosome centromeric region
Kinetochore
Integrin complex
Outer kinetochore
glycosaminoglycan binding
sulfur compound binding
cell adhesion molecule binding
heparin binding
cytoskeletal motor activity
steroid binding
nuclear receptor activity
ligand-activated transcription factor activity
microtubule motor activity
steroid hormone receptor activity
BP
CC
MF
0.03
0.06
0.09
0.12
GeneRatio
Count
5
10
15
20
P.adjust
0.015
0.010
0.005

B

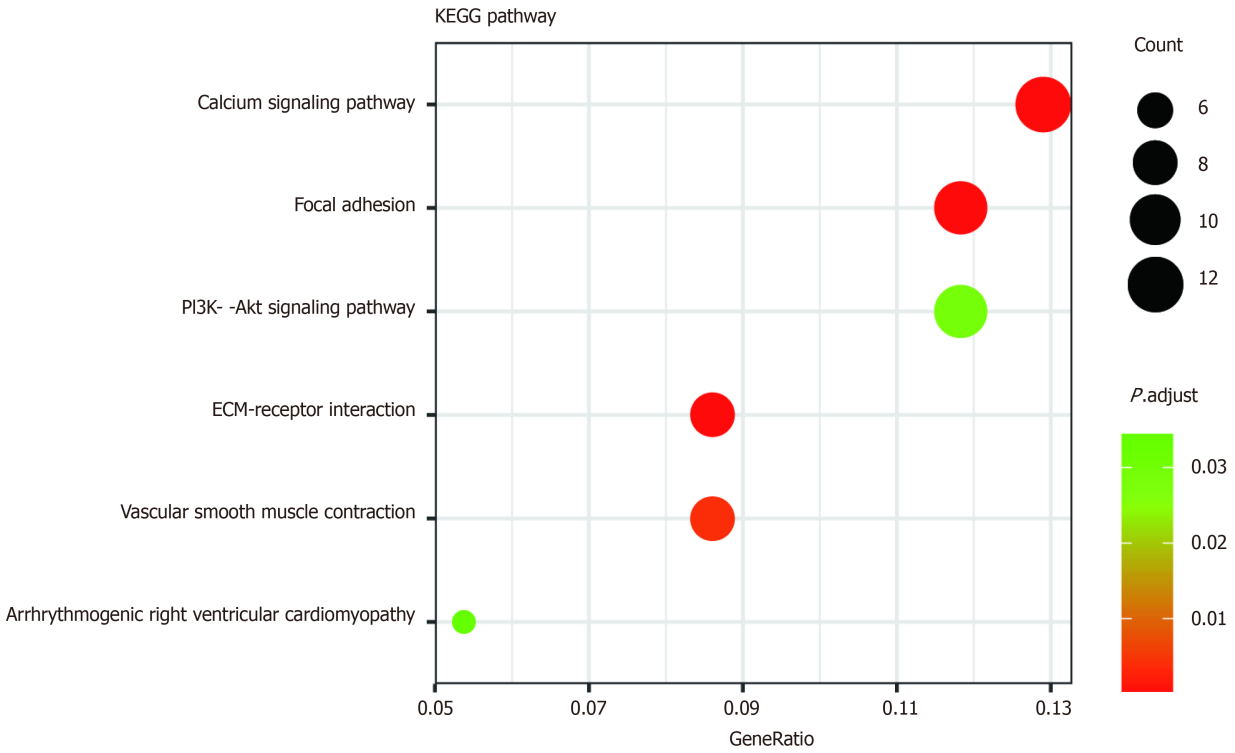
KEGG pathway
Calcium signaling pathway
Focal adhesion
PI3K- -Akt signaling pathway
ECM-receptor interaction
Vascular smooth muscle contraction
Arrhythmogenic right ventricular cardiomyopathy
0.05
0.07
0.09
0.11
0.13
GeneRatio
Count
6
8
10
12
P.adjust
0.03
0.02
0.01

C

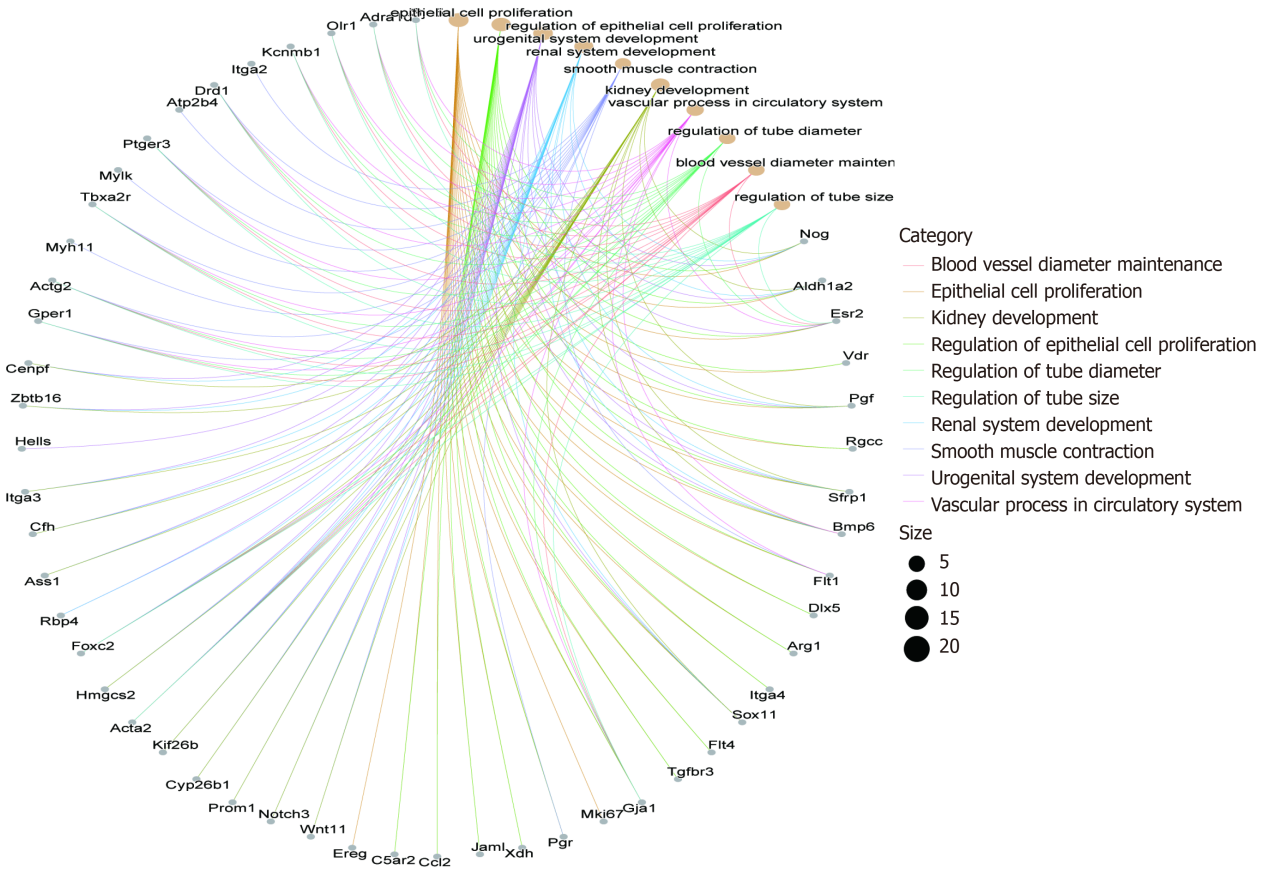
epithelial cell proliferation
regulation of epithelial cell proliferation
urogenital system development
renal system development
smooth muscle contraction
kidney development
vascular process in circulatory system
regulation of tube diameter
blood vessel diameter mainten
regulation of tube size
Olr1
Kcnmb1
Itga2
Drd1
Atp2b4
Ptger3
Mylk
Tbxa2r
Myh11
Actg2
Gper1
Cenpf
Zbtb16
Hells
Itga3
Cfh
Ass1
Rbp4
Foxc2
Hmgcs2
Acta2
Kif26b
Cyp26b1
Prom1
Notch3
Wnt11
Ereg
C5ar2
Ccl2
Jaml
Xdh
Pgr
Mki67
Gja1
Tgfbr3
Flt4
Sox11
Itga4
Arg1
Dlx5
Flt1
Bmp6
Sfrp1
Rgcc
Pgf
Vdr
Esr2
Aldh1a2
Nog
Category
Blood vessel diameter maintenance
Epithelial cell proliferation
Kidney development
Regulation of epithelial cell proliferation
Regulation of tube diameter
Regulation of tube size
Renal system development
Smooth muscle contraction
Urogenital system development
Vascular process in circulatory system
Size
5
10
15
20

D

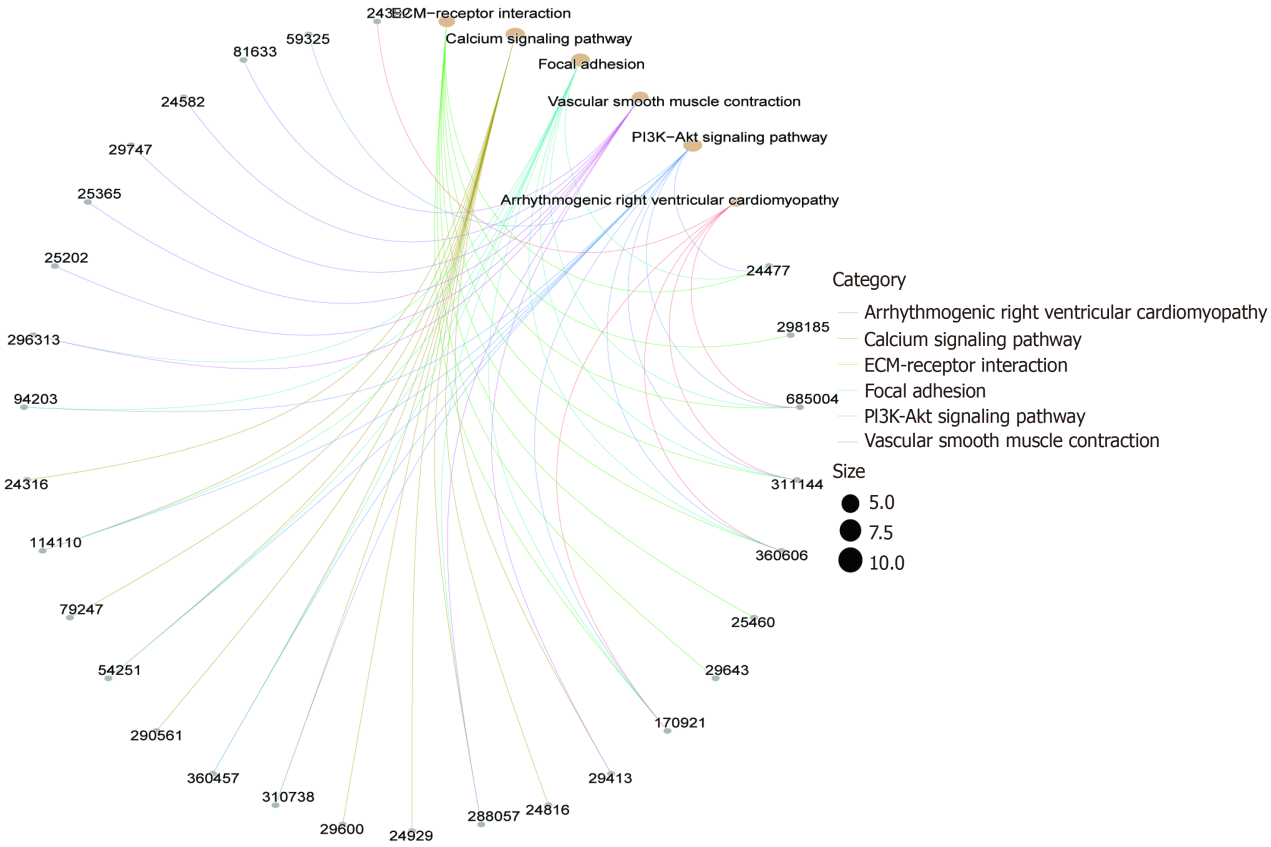
ECM-receptor interaction
Calcium signaling pathway
Focal adhesion
Vascular smooth muscle contraction
PI3K-Akt signaling pathway
Arrhythmogenic right ventricular cardiomyopathy
24316
59325
81633
24582
29747
25365
25202
296313
94203
24316
114110
79247
54251
290561
360457
310738
29600
24929
288057
24816
29413
170921
29643
25460
360606
311144
685004
298185
24477
Category
Arrhythmogenic right ventricular cardiomyopathy
Calcium signaling pathway
ECM-receptor interaction
Focal adhesion
PI3K-Akt signaling pathway
Vascular smooth muscle contraction
Size
5.0
7.5
10.0

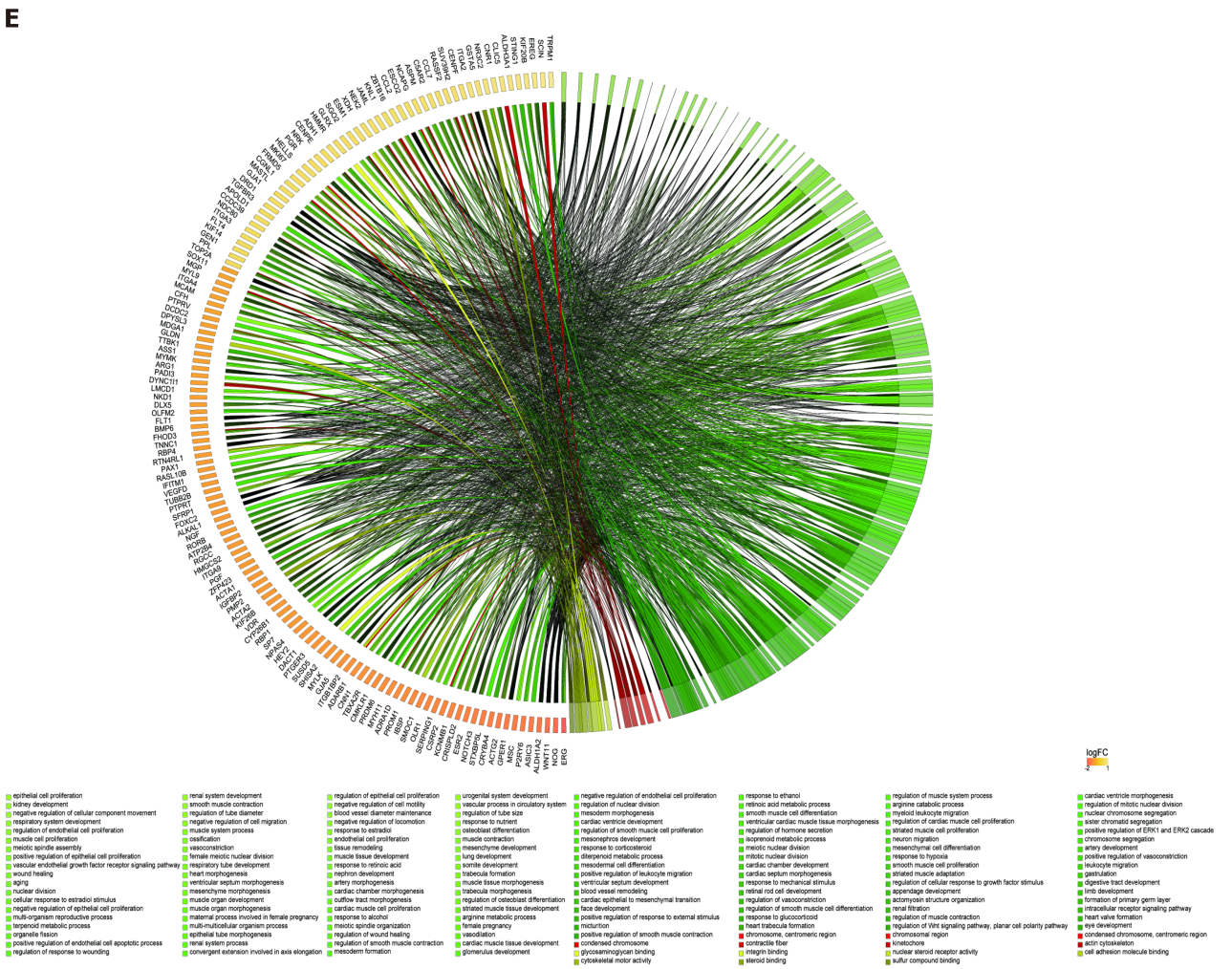

Figure 3 Gene Ontology and Kyoto Encyclopedia of Genes and Genomes enrichment analyses of DE messenger RNAs. A: Gene Ontology (GO) analysis of differentially expressed messenger RNAs (mRNAs). Bubble chart represents the significantly enriched pathways from the GO analysis. The color of dots in the bubble chart indicates the significance of the enriched category, and the size represents the scale of enriched genes in the terms; B: Kyoto Encyclopedia of Genes and Genomes (KEGG) analysis of differentially expressed mRNAs; C: Gene-concept network (cnetplot) of GO analysis; D: Gene-concept network (cnetplot)

of KEGG analysis; E: Chord diagram of GO; F: Waterfall plot of KEGG analysis. KECG: Kyoto Encyclopedia of Genes and Genomes.

fields were reported to regulate ECM structure[21] and synthesis[22]. On the other hand, the ECM was reported to participate in regeneration[23] and play an important role in stem cell fate[24]. The ECM may be involved in the regulation of cell fate by nsPEFs, which could be further investigated focusing on ECM-receptor interaction. KIF20B was reported to be involved in cell proliferation[25]. Scin belongs to the gelolysin protein superfamily, which is involved in the regulation of cytoskeleton and transport in cell vesicles. It has an important regulatory role in the release of intracellular calcium ions, behaving as a filamentous actin-severing and capping protein[26]. The actin filament network, which in turn leads to the release of secretory vesicles[27], plays an important role in actin-dependent membrane fusion [26]. Ereg belongs to the epidermal growth factor family and is separated from stem cells. It has been reported that Ereg can promote the migration and chemotactic ability of adipose stem cells through the MAPK signaling pathway[28]. Cenpf plays an important role in the microtubule network, which may be related to SNARE proteins which are involved in plasma membrane circulation[29]. These genes remain to be explored in nsPEFs-treated stem cells.

MiRNAs play an important biological function by regulating downstream gene translation. We found that nsPEFs had few effects on miRNAs, and the expression levels of novel.118 and novel.106 were significantly upregulated. GO/KEGG analyses of the target genes of miRNAs showed that nsPEFs may affect vesicle fusion to the plasma membrane, MAPK, *etc.* In addition, nsPEFs were reported to affect the MAPK signaling pathway by phosphorylation of p38, JNK, and ERK [30]. Bone regeneration can be regulated *via* the MAPK signaling pathway under specific hydrogel treatment[31]. High-voltage PEFs with short durations, can permeabilize cell membranes with a duration ranging from microseconds to nanoseconds[32]. nsPEFs can also regulate membrane pore formation and upregulate the release of exosomes[33], and vesicle fusion was related to exosome formation[34]. In addition, studies have shown that electroporation can increase the production of exosomes by increasing intracellular calcium ions[35]. Following nsPEFs treatment, exosome release from tumor cells was also significantly increased[33]. Exosomes, released from stem cells, could stimulate wound regeneration and bone regeneration[36,37]. Thus, nsPEFs may affect exosome formation through vesicle fusion to the plasma membrane in stem cells, which requires further investigation.

Based on the target genes of differentially expressed lncRNAs, the most significant MF involved tubulin binding after nsPEFs treatment and the most significant signaling pathways involved glycerophospholipid metabolism and mismatch repair. In addition, studies have shown that nsPEFs with certain parameters can be applied to regulate the level of cell differentiation[12], promote the release of the intracellular calcium pool[38], and trigger reversible perforation of the cell membrane[39]. A previous study showed that nsPEFs could affect chromosome structure by inducing extracellular release of chromosomal DNA in a calcium-dependent manner[40]. nsPEFs with high intensity (60 kV/cm) can induce damage to the cytoskeleton and nuclear membrane[41]. Chromosome structure is sensitive to physical stimulation. Extremely-low-frequency magnetic fields could stabilize active chromatin, partially depending upon chromatin status [42]. Chromosomes can be oriented, aligned, and translated by high-frequency electric fields, in a frequency-dependent manner[43]. Chromatin accessibility played an important role in gene expression and cell fate[44]. Chromatin undergoes a binary off/on switch during cell fate transitions[45]. Electric fields were reported to change cell fate partially through regulation of calcium and modulation of electrically charged cell-surface receptors in response to the electric field[46]. Thus, nsPEFs may affect the chromatin accessibility and fate of stem cells, which remains to be explored.

The calcium signaling pathway may play an important role in the process of reaction of MSCs to nsPEFs. A previous study showed that nsPEFs could induce calcium flux in osteoblasts[47]. In our study, DEGs and the target genes of lncRNAs and miRNAs were enriched in the calcium signaling pathway as shown by GO/KEGG analyses. Calcium release caused by nsPEFs may be due to nanopore formation in the endoplasmic reticulum[48]. Furthermore, nsPEFs may activate TMEM16F (or anoctamin 6), a protein functioning as a calcium-dependent scramblase, which contributes to the reaction of calcium release due to nsPEFs[49]. BAPTA-AM, a calcium chelator, could attenuate the upregulated phosphorylation level of JNK caused by nsPEFs[14]. Calcium may contribute to apoptosis in hair follicle stem cells through Piezo1[50]. Calcium uptake was reported to control mitochondrial calcium homeostasis and hematopoietic stem cell differentiation, two important determinants in stem cell fate[51]. Calcium-activated potassium channel activity can influence MSC differentiation through membrane potential and intracellular calcium oscillations[52]. Consequently, the calcium signaling pathway may play an important role in the effects caused by nsPEFs in stem cells.

CONCLUSION

There are few studies on the effect of nsPEFs on stem cells at the whole transcriptomic level. The effects of nsPEFs on stem cells were systematically studied, and 263 differentially expressed mRNAs, 2 differentially expressed miRNAs, and 65 differentially expressed lncRNAs were identified. It was shown that nsPEFs may affect stem cells *via* several signaling pathways and may involve vesicular transport, calcium ion transport, the cytoskeleton, and cell differentiation. Our study is the first to investigate the expression profile of the whole transcriptome in nsPEFs-treated stem cells. This study provides a certain basis for the application of nsPEFs in stem cell differentiation and tissue regeneration.

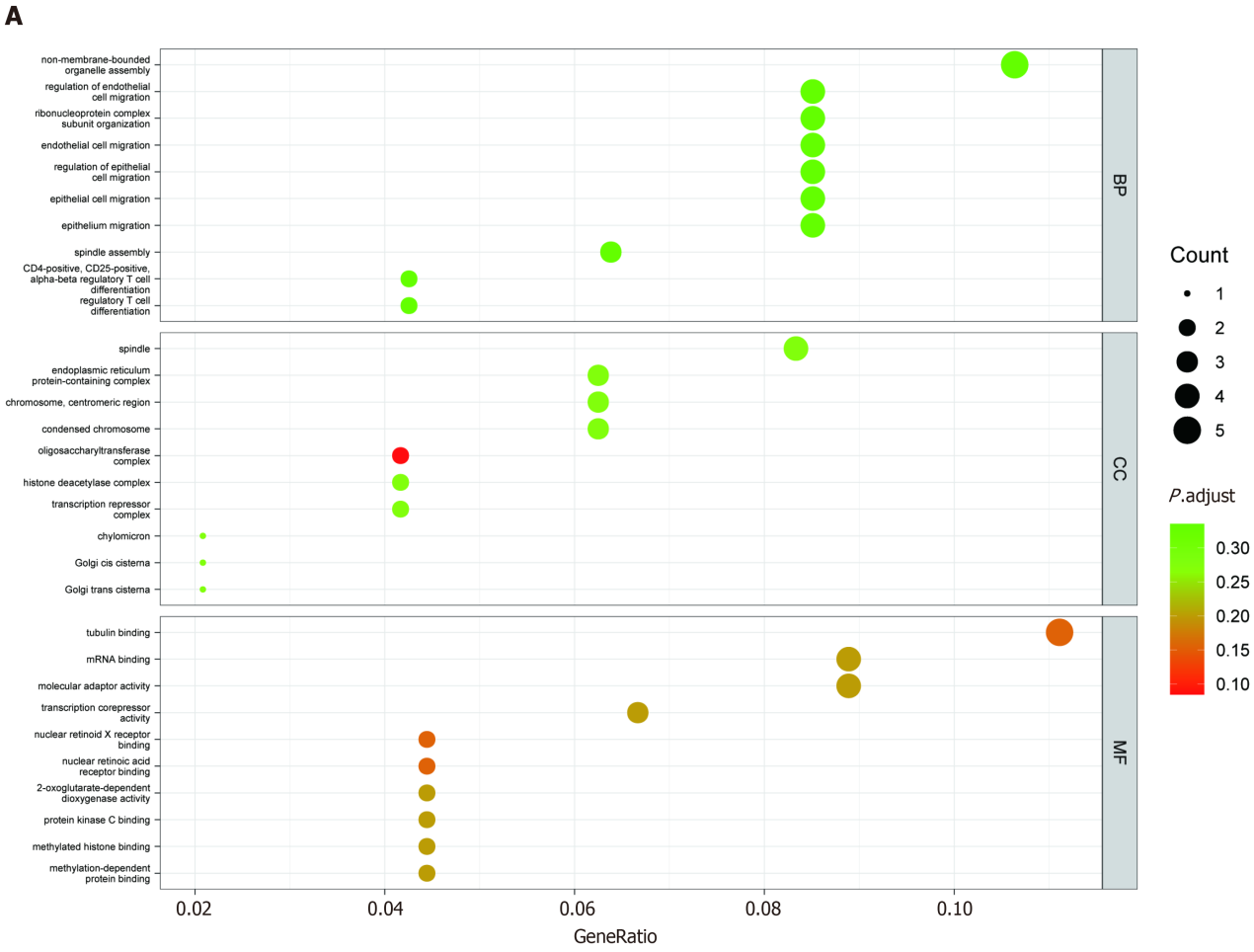
A
non-membrane-bounded organelle assembly
regulation of endothelial cell migration
ribonucleoprotein complex subunit organization
endothelial cell migration
regulation of epithelial cell migration
epithelial cell migration
epithelium migration
spindle assembly
CD4-positive, CD25-positive, alpha-beta regulatory T cell differentiation
regulatory T cell differentiation
BP
spindle
endoplasmic reticulum protein-containing complex
chromosome, centromeric region
condensed chromosome
oligosaccharyltransferase complex
histone deacetylase complex
transcription repressor complex
chylomicron
Golgi cis cisterna
Golgi trans cisterna
CC
tubulin binding
mRNA binding
molecular adaptor activity
transcription corepressor activity
nuclear retinoid X receptor binding
nuclear retinoic acid receptor binding
2-oxoglutarate-dependent dioxygenase activity
protein kinase C binding
methylated histone binding
methylation-dependent protein binding
MF
0.02
0.04
0.06
0.08
0.10
GeneRatio
Count
1
2
3
4
5
P.adjust
0.30
0.25
0.20
0.15
0.10

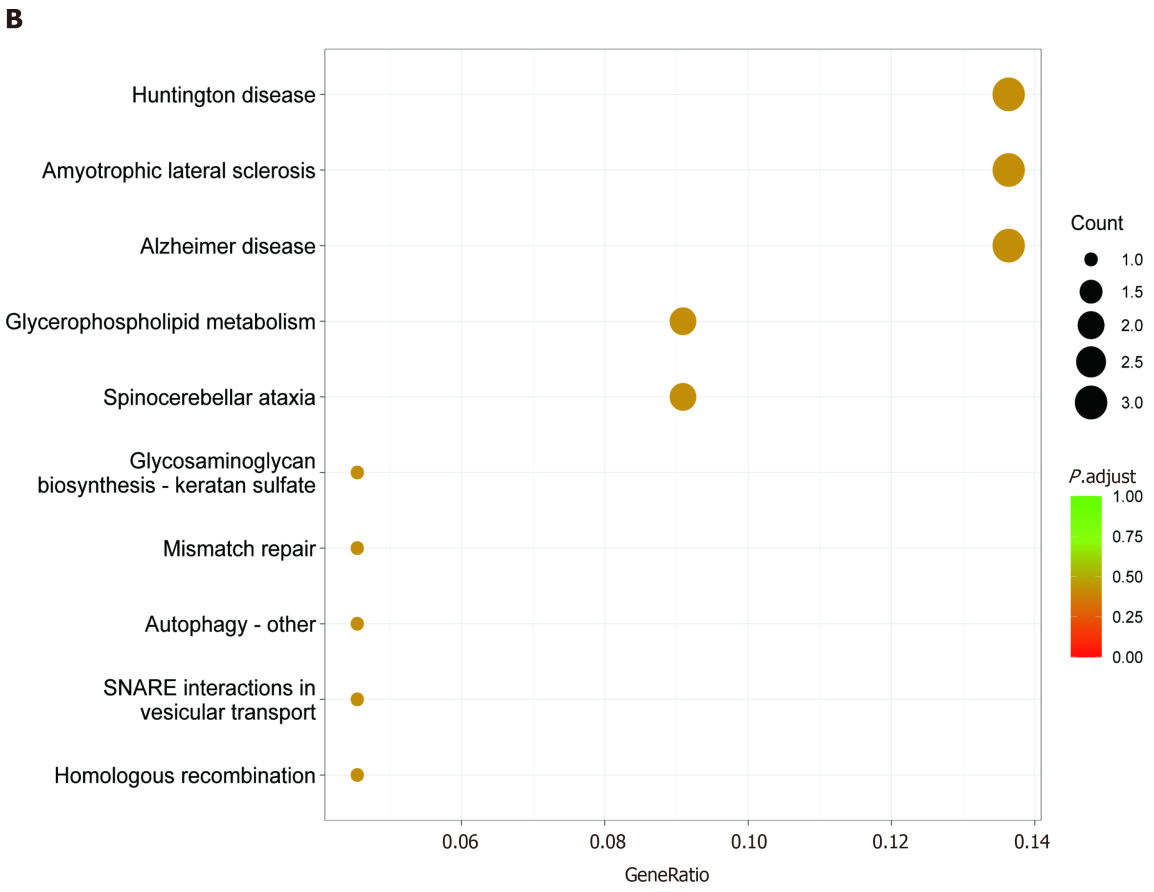
B
Huntington disease
Amyotrophic lateral sclerosis
Alzheimer disease
Glycerophospholipid metabolism
Spinocerebellar ataxia
Glycosaminoglycan biosynthesis - keratan sulfate
Mismatch repair
Autophagy - other
SNARE interactions in vesicular transport
Homologous recombination
0.06
0.08
0.10
0.12
0.14
GeneRatio
Count
1.0
1.5
2.0
2.5
3.0
P.adjust
1.00
0.75
0.50
0.25
0.00

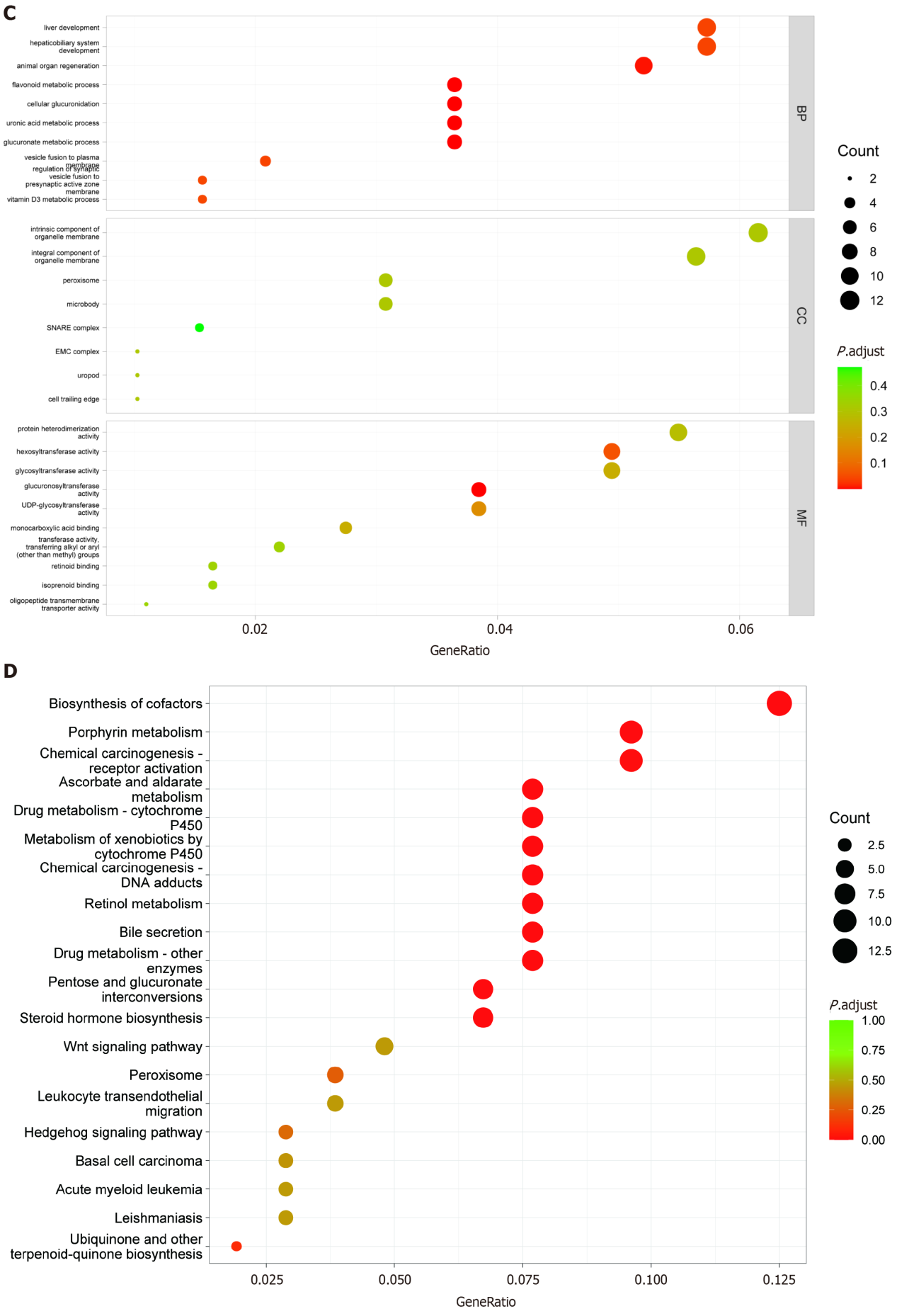

Figure 4 Gene Ontology and Kyoto Encyclopedia of Genes and Genomes enrichment analyses of target genes of differentially expressed

long noncoding RNAs and microRNAs. A: Gene Ontology (GO) analysis of target genes of differentially expressed long noncoding RNAs (lncRNAs); B: Kyoto Encyclopedia of Genes and Genomes (KEGG) analysis of target genes of differentially expressed lncRNAs; C: GO analysis of target genes of differentially expressed microRNAs (miRNAs); D: KEGG analysis of target genes of differentially expressed miRNAs.

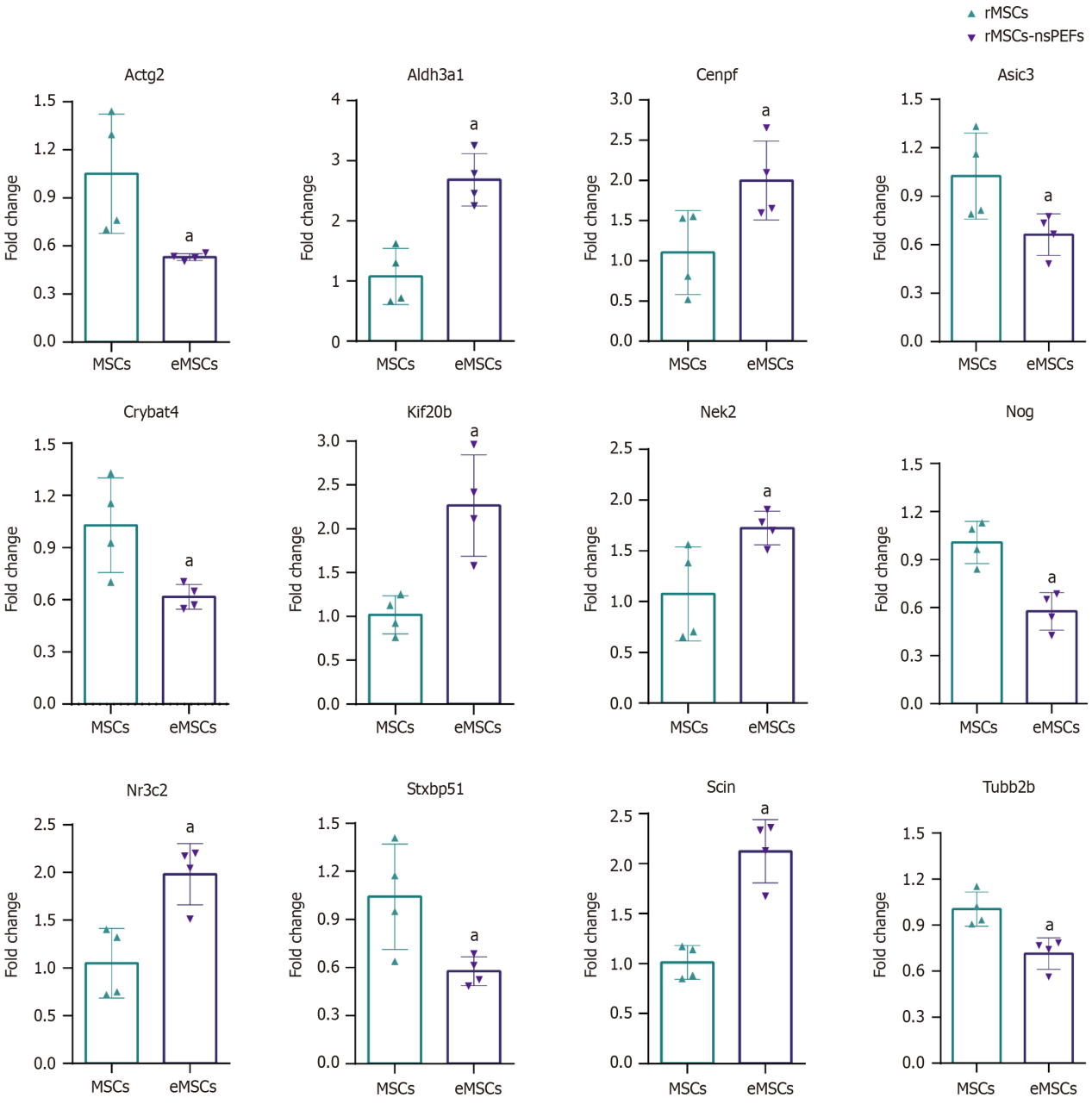

Figure 5 Gene expression validation by quantitative polymerase chain reaction. The error bars represent the standard deviations of measurements in three separate sample runs (n = 3). $^{a}P < 0.05$. rMSCs: Rat bone marrow mesenchymal stem cells; MSCs: Mesenchymal stem cells; eMSCs: Mesenchymal stem cells stimulated with nanosecond pulsed electric fields; nsPEFs: Nanosecond pulsed electric fields.

ARTICLE HIGHLIGHTS

Research background

Mesenchymal stem cells (MSCs) have been extensively applied in preclinical and clinical research in regenerative medicine. Their differentiation and function are modulated by various exogenous signals, which provide potential strategies for researchers to explore appropriate exogenous signals to regulate the functions and differentiation of stem cells. Nanosecond pulsed electric fields (nsPEFs) represent nanosecond-duration, high-strength electric fields to significantly influence cell phenotypes and regulate stem cell differentiation through multiple pathways. Thus, we used transcriptomics analysis to analyze messenger RNA (mRNA), long noncoding RNA (lncRNA), microRNA (miRNA), and circular RNA (circRNA) expression to identify changes in gene expression following treatment with nsPEFs.

Research motivation
The differentiation and function of MSCs are regulated by nsPEFs. However, the mechanism, especially changes in gene expression after nsPEFs treatment, remains unclear.

Research objectives
To reveal gene expression in MSCs pretreated with nsPEFs and explore the potential gene regulatory mechanism.

Research methods
We used whole transcriptome sequencing to investigate the effects of nsPEFs on MSC transcriptome. Five pulses of nsPEFs (100 ns at 10 kV/cm, 1 Hz) were applied to pretreat MSCs. Total RNA was isolated after pretreatment of MSCs; each transcript was normalized by fragments per kilobase per million. Fold change and difference significance were used to screen the differentially expressed genes (DEGs). Gene Ontology and Kyoto Encyclopedia of Genes and Genomes analyses were conducted to identify gene function, and the results were verified by quantitative polymerase chain reaction.

Research results
The top 20 differentially expressed lncRNAs and mRNAs were revealed. Two hundred and sixty-three DEGs were identified in the PRJNA931816 dataset, of which 92 were upregulated and 171 were significantly downregulated, respectively. DEGs were mainly enriched in epithelial cell proliferation, osteoblast differentiation, mesenchymal cell differentiation, nuclear division, and wound healing. As for cellular components, DEGs were mainly involved in condensed chromosome, chromosomal region, actin cytoskeleton, and the kinetochore. With regard to molecular functions, DEGs are mainly involved in glycosaminoglycan binding, integrin binding, nuclear steroid receptor activity, cytoskeletal motor activity, and steroid binding. Quantitative real-time polymerase chain reaction was used to verify the seven upregulated mRNAs, *Aldh3a1*, *Cenpf*, *Kif20b*, *Ereg*, *Nek2*, *Nr3c2*, and *Scin*, and six downregulated mRNAs, *Actg2*, *Asic3*, *Crybat4*, *Nog*, *Stxbp5 L*, and *Tubb2b*.

Research conclusions
Our systematic investigation of the wide-ranging transcriptional pattern modulated by nsPEFs revealed the differential expression of 263 mRNAs, 2 miRNAs, and 65 lncRNAs. We showed that nsPEFs may affect stem cells *via* several signaling pathways and involve vesicular transport, calcium ion transport, the cytoskeleton, and cell differentiation.

Research perspectives
This study is the first to investigate the expression profile of the whole transcriptome in nsPEFs-treated stem cells. The findings provide a certain basis for the application of nsPEFs in stem cell differentiation and tissue regeneration.

ACKNOWLEDGEMENTS

The authors are grateful to Peking University, Peking University People Hospital, and Peking University Shenzhen Hospital for providing the research instruments and workplace.

FOOTNOTES

Co-first authors: Jian-Jing Lin and Tong Ning.

Co-corresponding authors: Jian-Hao Lin and Xin-Tao Zhang.

Author contributions: Lin JJ, Ning T, and Jia SC designed the project, wrote the original draft, and edited the final version of the manuscript; Ning T and Li KJ analyzed the data; Jia SC drew the tables and figures; Huang YC, Liu Q, and Lin JH revised the manuscript; Lin JH and Zhang XT provided financial support and ensured the final manuscript, and they are the co-corresponding authors of this manuscript; Lin JJ and Ning T contributed equally to the work; and all authors have read and approved the final version of the manuscript.

Supported by the National Natural Science Foundation, China, No. 82272568, 81902247, and 32201013; Natural Science Foundation of Shandong Province, China, No. ZR2021QH275; Natural Science Foundation of Jinan City, China, No. 202225070; and Guangdong Basic and Applied Basic Research Foundation, China, No. 2022A1515220056.

Institutional animal care and use committee statement: This study was approved by the Ethics Committee of Peking University (No. COE-GeZ-7).

Conflict-of-interest statement: All the authors report no relevant conflicts of interest for this article.

Data sharing statement: The datasets supporting the conclusions of this article are available in the NCBI database, with unique accession code PRJNA931816. The hyperlink to dataset(s) is https://www.ncbi.nlm.nih.gov/bioproject/PRJNA931816/. All other data are

included in this article.

ARRIVE guidelines statement: The authors have read the ARRIVE guidelines, and the manuscript was prepared and revised according to the ARRIVE guidelines.

Country/Territory of origin: China

ORCID number: Jian-Jing Lin 0000-0002-1586-1415; Tong Ning 0000-0003-1664-4081; Shi-Cheng Jia 0009-0008-8489-0827; Ke-Jia Li 0000-0001-8711-1691; Yong-Can Huang 0000-0001-8548-8233; Qiang Liu 0000-0003-3029-2625; Jian-Hao Lin 0000-0003-1830-9244; Xin-Tao Zhang 0000-0001-9926-3756.

S-Editor: Wang JJ
L-Editor: Wang TQ
P-Editor: Zhao YQ

REFERENCES

1 **McKinney JM**, Pucha KA, Doan TN, Wang L, Weinstock LD, Tignor BT, Fowle KL, Levit RD, Wood LB, Willett NJ. Sodium alginate microencapsulation of human mesenchymal stromal cells modulates paracrine signaling response and enhances efficacy for treatment of established osteoarthritis. *Acta Biomater* 2022; **141**: 315-332 [PMID: 34979327 DOI: 10.1016/j.actbio.2021.12.034]
2 **Zhang J**, Zhang M, Lin R, Du Y, Wang L, Yao Q, Zannettino A, Zhang H. Chondrogenic preconditioning of mesenchymal stem/stromal cells within a magnetic scaffold for osteochondral repair. *Biofabrication* 2022; **14** [PMID: 35226893 DOI: 10.1088/1758-5090/ac5935]
3 **Choi DH**, Lee KE, Oh SY, Lee SM, Jo BS, Lee JY, Park JC, Park YJ, Park KD, Jo I, Park YS. Tonsil-derived mesenchymal stem cells incorporated in reactive oxygen species-releasing hydrogel promote bone formation by increasing the translocation of cell surface GRP78. *Biomaterials* 2021; **278**: 121156 [PMID: 34597900 DOI: 10.1016/j.biomaterials.2021.121156]
4 **Fan L**, Chen J, Tao Y, Heng BC, Yu J, Yang Z, Ge Z. Enhancement of the chondrogenic differentiation of mesenchymal stem cells and cartilage repair by ghrelin. *J Orthop Res* 2019; **37**: 1387-1397 [PMID: 30644571 DOI: 10.1002/jor.24224]
5 **Chen Y**, An X, Wang Z, Guan S, An H, Huang Q, Zhang H, Liang L, Huang B, Wang H, Lu M, Nie H, Wang J, Dai X, Lu X. Transcriptome and lipidome profile of human mesenchymal stem cells with reduced senescence and increased trilineage differentiation ability upon drug treatment. *Aging (Albany NY)* 2021; **13**: 9991-10014 [PMID: 33795523 DOI: 10.18632/aging.202759]
6 **Kusuyama J**, Bandow K, Shamoto M, Kakimoto K, Ohnishi T, Matsuguchi T. Low intensity pulsed ultrasound (LIPUS) influences the multilineage differentiation of mesenchymal stem and progenitor cell lines through ROCK-Cot/Tpl2-MEK-ERK signaling pathway. *J Biol Chem* 2014; **289**: 10330-10344 [PMID: 24550383 DOI: 10.1074/jbc.M113.546382]
7 **Hess R**, Jaeschke A, Neubert H, Hintze V, Moeller S, Schnabelrauch M, Wiesmann HP, Hart DA, Scharnweber D. Synergistic effect of defined artificial extracellular matrices and pulsed electric fields on osteogenic differentiation of human MSCs. *Biomaterials* 2012; **33**: 8975-8985 [PMID: 22995709 DOI: 10.1016/j.biomaterials.2012.08.056]
8 **Guo W**, Zhang X, Yu X, Wang S, Qiu J, Tang W, Li L, Liu H, Wang ZL. Self-Powered Electrical Stimulation for Enhancing Neural Differentiation of Mesenchymal Stem Cells on Graphene-Poly(3,4-ethylenedioxythiophene) Hybrid Microfibers. *ACS Nano* 2016; **10**: 5086-5095 [PMID: 27144593 DOI: 10.1021/acsnano.6b00200]
9 **Bicer M**, Sheard J, Iandolo D, Boateng SY, Cottrell GS, Widera D. Electrical Stimulation of Adipose-Derived Stem Cells in 3D Nanofibrillar Cellulose Increases Their Osteogenic Potential. *Biomolecules* 2020; **10** [PMID: 33353222 DOI: 10.3390/biom10121696]
10 **Yao C**, Hu X, Mi Y, Li C, Sun C. Window effect of pulsed electric field on biological cells. *IEEE Trans Dielectr Electr Insul* 2009; **16**: 1259-1266 [DOI: 10.1109/TDEI.2009.5293936]
11 **Ning T**, Zhang K, Heng BC, Ge Z. Diverse effects of pulsed electrical stimulation on cells - with a focus on chondrocytes and cartilage regeneration. *Eur Cell Mater* 2019; **38**: 79-93 [PMID: 31478555 DOI: 10.22203/eCM.v038a07]
12 **Li K**, Ning T, Wang H, Jiang Y, Zhang J, Ge Z. Nanosecond pulsed electric fields enhance mesenchymal stem cells differentiation *via* DNMT1-regulated OCT4/NANOG gene expression. *Stem Cell Res Ther* 2020; **11**: 308 [PMID: 32698858 DOI: 10.1186/s13287-020-01821-5]
13 **Li K**, Fan L, Lin J, Heng BC, Deng Z, Zheng Q, Zhang J, Jiang Y, Ge Z. Nanosecond pulsed electric fields prime mesenchymal stem cells to peptide ghrelin and enhance chondrogenesis and osteochondral defect repair in vivo. *Sci China Life Sci* 2022; **65**: 927-939 [PMID: 34586575 DOI: 10.1007/s11427-021-1983-y]
14 **Ning T**, Guo J, Zhang K, Li K, Zhang J, Yang Z, Ge Z. Nanosecond pulsed electric fields enhanced chondrogenic potential of mesenchymal stem cells *via* JNK/CREB-STAT3 signaling pathway. *Stem Cell Res Ther* 2019; **10**: 45 [PMID: 30678730 DOI: 10.1186/s13287-019-1133-0]
15 **Uusküla-Reimand L**, Wilson MD. Untangling the roles of TOP2A and TOP2B in transcription and cancer. *Sci Adv* 2022; **8**: eadd4920 [PMID: 36322662 DOI: 10.1126/sciadv.add4920]
16 **Heilig AK**, Nakamura R, Shimada A, Hashimoto Y, Nakamura Y, Wittbrodt J, Takeda H, Kawanishi T. Wnt11 acts on dermomyotome cells to guide epaxial myotome morphogenesis. *Elife* 2022; **11** [PMID: 35522214 DOI: 10.7554/eLife.71845]
17 **Kim JA**, Choi YA, Yun HS, Bae YC, Shin HI, Park EK. Extracellular calcium-binding peptide-modified ceramics stimulate regeneration of calvarial bone defects. *Tissue Eng Regen Med* 2016; **13**: 57-65 [PMID: 30603385 DOI: 10.1007/s13770-015-9066-x]
18 **Vadlamani RA**, Nie Y, Detwiler DA, Dhanabal A, Kraft AM, Kuang S, Gavin TP, Garner AL. Nanosecond pulsed electric field induced proliferation and differentiation of osteoblasts and myoblasts. *J R Soc Interface* 2019; **16**: 20190079 [PMID: 31213169 DOI:

10.1098/rsif.2019.0079]
19 **Kasprzycka W**, Trębińska-Stryjewska A, Lewandowski RB, Stępińska M, Osuchowska PN, Dobrzyńska M, Achour Y, Osuchowski ŁP, Starzyński J, Mierczyk Z, Trafny EA. Nanosecond Pulsed Electric Field Only Transiently Affects the Cellular and Molecular Processes of Leydig Cells. *Int J Mol Sci* 2021; **22** [PMID: 34681896 DOI: 10.3390/ijms222011236]
20 **Roth CC**, Glickman RD, Tolstykh GP, Estlack LE, Moen EK, Echchgadda I, Beier HT, Barnes RA Jr, Ibey BL. Evaluation of the Genetic Response of U937 and Jurkat Cells to 10-Nanosecond Electrical Pulses (nsEP). *PLoS One* 2016; **11**: e0154555 [PMID: 27135944 DOI: 10.1371/journal.pone.0154555]
21 **Nguyen HT**, Wei C, Chow JK, Nguy L, Nguyen HK, Schmidt CE. Electric field stimulation through a substrate influences Schwann cell and extracellular matrix structure. *J Neural Eng* 2013; **10**: 046011 [PMID: 23838058 DOI: 10.1088/1741-2560/10/4/046011]
22 **Aaron RK**, Ciombor DM, Simon BJ. Treatment of nonunions with electric and electromagnetic fields. *Clin Orthop Relat Res* 2004; 21-29 [PMID: 15021127 DOI: 10.1097/00003086-200402000-00005]
23 **Yang Y**, Lin H, Shen H, Wang B, Lei G, Tuan RS. Mesenchymal stem cell-derived extracellular matrix enhances chondrogenic phenotype of and cartilage formation by encapsulated chondrocytes in vitro and in vivo. *Acta Biomater* 2018; **69**: 71-82 [PMID: 29317369 DOI: 10.1016/j.actbio.2017.12.043]
24 **Chermnykh E**, Kalabusheva E, Vorotelyak E. Extracellular Matrix as a Regulator of Epidermal Stem Cell Fate. *Int J Mol Sci* 2018; **19** [PMID: 29584689 DOI: 10.3390/ijms19041003]
25 **Chen J**, Zhao CC, Chen FR, Feng GW, Luo F, Jiang T. KIF20B Promotes Cell Proliferation and May Be a Potential Therapeutic Target in Pancreatic Cancer. *J Oncol* 2021; **2021**: 5572402 [PMID: 34539784 DOI: 10.1155/2021/5572402]
26 **Wang X**, Shelton SD, Bordieanu B, Frank AR, Yi Y, Venigalla SSK, Gu Z, Lenser NP, Glogauer M, Chandel NS, Zhao H, Zhao Z, McFadden DG, Mishra P. Scinderin promotes fusion of electron transport chain dysfunctional muscle stem cells with myofibers. *Nat Aging* 2022; **2**: 155-169 [PMID: 35342888 DOI: 10.1038/s43587-021-00164-x]
27 **Chumnarnsilpa S**, Robinson RC, Grimes JM, Leyrat C. Calcium-controlled conformational choreography in the N-terminal half of adseverin. *Nat Commun* 2015; **6**: 8254 [PMID: 26365202 DOI: 10.1038/ncomms9254]
28 **Cao Y**, Wang L, Yang H, Lin X, Li G, Han N, Du J, Fan Z. Epiregulin promotes the migration and chemotaxis ability of adipose-derived mesenchymal stem cells *via* mitogen-activated protein kinase signaling pathways. *J Cell Biochem* 2018; **119**: 8450-8459 [PMID: 30011072 DOI: 10.1002/jcb.27069]
29 **Pooley RD**, Moynihan KL, Soukoulis V, Reddy S, Francis R, Lo C, Ma LJ, Bader DM. Murine CENPF interacts with syntaxin 4 in the regulation of vesicular transport. *J Cell Sci* 2008; **121**: 3413-3421 [PMID: 18827011 DOI: 10.1242/jcs.032847]
30 **Morotomi-Yano K**, Akiyama H, Yano K. Nanosecond pulsed electric fields activate MAPK pathways in human cells. *Arch Biochem Biophys* 2011; **515**: 99-106 [PMID: 21933660 DOI: 10.1016/j.abb.2011.09.002]
31 **Liu Y**, Zhang Y, Zheng Z, Zhong W, Wang H, Lin Z, Li L, Wu G. Incorporation of NGR1 promotes bone regeneration of injectable HA/nHAp hydrogels by anti-inflammation regulation *via* a MAPK/ERK signaling pathway. *Front Bioeng Biotechnol* 2022; **10**: 992961 [PMID: 36213055 DOI: 10.3389/fbioe.2022.992961]
32 **Safaei Z**, Thompson GL. Histone deacetylase 4 and 5 translocation elicited by microsecond pulsed electric field exposure is mediated by kinase activity. *Front Bioeng Biotechnol* 2022; **10**: 1047851 [PMID: 36466344 DOI: 10.3389/fbioe.2022.1047851]
33 **Qian J**, Chen T, Wu Q, Zhou L, Zhou W, Wu L, Wang S, Lu J, Wang W, Li D, Xie H, Su R, Guo D, Liu Z, He N, Yin S, Zheng S. Blocking exposed PD-L1 elicited by nanosecond pulsed electric field reverses dysfunction of CD8(+) T cells in liver cancer. *Cancer Lett* 2020; **495**: 1-11 [PMID: 32949680 DOI: 10.1016/j.canlet.2020.09.015]
34 **van Niel G**, D'Angelo G, Raposo G. Shedding light on the cell biology of extracellular vesicles. *Nat Rev Mol Cell Biol* 2018; **19**: 213-228 [PMID: 29339798 DOI: 10.1038/nrm.2017.125]
35 **Yang Z**, Shi J, Xie J, Wang Y, Sun J, Liu T, Zhao Y, Zhao X, Wang X, Ma Y, Malkoc V, Chiang C, Deng W, Chen Y, Fu Y, Kwak KJ, Fan Y, Kang C, Yin C, Rhee J, Bertani P, Otero J, Lu W, Yun K, Lee AS, Jiang W, Teng L, Kim BYS, Lee LJ. Large-scale generation of functional mRNA-encapsulating exosomes *via* cellular nanoporation. *Nat Biomed Eng* 2020; **4**: 69-83 [PMID: 31844155 DOI: 10.1038/s41551-019-0485-1]
36 **Zhang Y**, Shi L, Li X, Liu Y, Zhang G, Wang Y. Placental stem cells-derived exosomes stimulate cutaneous wound regeneration *via* engrailed-1 inhibition. *Front Bioeng Biotechnol* 2022; **10**: 1044773 [PMID: 36568306 DOI: 10.3389/fbioe.2022.1044773]
37 **Ma S**, Zhang Y, Li S, Li A, Li Y, Pei D. Engineering exosomes for bone defect repair. *Front Bioeng Biotechnol* 2022; **10**: 1091360 [PMID: 36568296 DOI: 10.3389/fbioe.2022.1091360]
38 **Mao Z**, Zhang Y, Lu N, Cheng S, Hong R, Liu QH. Carbon Nanotubes Enabling Highly Efficient Cell Apoptosis by Low-Intensity Nanosecond Electric Pulses *via* Perturbing Calcium Handling. *Small* 2020; **16**: e1904047 [PMID: 31799810 DOI: 10.1002/smll.201904047]
39 **Pakhomov AG**, Gianulis E, Vernier PT, Semenov I, Xiao S, Pakhomova ON. Multiple nanosecond electric pulses increase the number but not the size of long-lived nanopores in the cell membrane. *Biochim Biophys Acta* 2015; **1848**: 958-966 [PMID: 25585279 DOI: 10.1016/j.bbamem.2014.12.026]
40 **Koga T**, Morotomi-Yano K, Sakugawa T, Saitoh H, Yano KI. Nanosecond pulsed electric fields induce extracellular release of chromosomal DNA and histone citrullination in neutrophil-differentiated HL-60 cells. *Sci Rep* 2019; **9**: 8451 [PMID: 31186478 DOI: 10.1038/s41598-019-44817-9]
41 **Stacey M**, Fox P, Buescher S, Kolb J. Nanosecond pulsed electric field induced cytoskeleton, nuclear membrane and telomere damage adversely impact cell survival. *Bioelectrochemistry* 2011; **82**: 131-134 [PMID: 21719360 DOI: 10.1016/j.bioelechem.2011.06.002]
42 **Manser M**, Sater MR, Schmid CD, Noreen F, Murbach M, Kuster N, Schuermann D, Schär P. ELF-MF exposure affects the robustness of epigenetic programming during granulopoiesis. *Sci Rep* 2017; **7**: 43345 [PMID: 28266526 DOI: 10.1038/srep43345]
43 **Andrews MJ**, McClure JA. Effects of high frequency electric fields on mammalian chromosomes in vitro. *J Biol Phys* 1978; **6**: 69-86 [DOI: 10.1007/BF02311220]
44 **Klemm SL**, Shipony Z, Greenleaf WJ. Chromatin accessibility and the regulatory epigenome. *Nat Rev Genet* 2019; **20**: 207-220 [PMID: 30675018 DOI: 10.1038/s41576-018-0089-8]
45 **Li D**, Shu X, Zhu P, Pei D. Chromatin accessibility dynamics during cell fate reprogramming. *EMBO Rep* 2021; **22**: e51644 [PMID: 33480184 DOI: 10.15252/embr.202051644]
46 **Thrivikraman G**, Boda SK, Basu B. Unraveling the mechanistic effects of electric field stimulation towards directing stem cell fate and function: A tissue engineering perspective. *Biomaterials* 2018; **150**: 60-86 [PMID: 29032331 DOI: 10.1016/j.biomaterials.2017.10.003]
47 **Zhou P**, He F, Han Y, Liu B, Wei S. Nanosecond pulsed electric field induces calcium mobilization in osteoblasts. *Bioelectrochemistry* 2018;

124: 7-12 [PMID: 29990600 DOI: 10.1016/j.bioelechem.2018.06.009]

48 **Scarlett SS**, White JA, Blackmore PF, Schoenbach KH, Kolb JF. Regulation of intracellular calcium concentration by nanosecond pulsed electric fields. *Biochim Biophys Acta* 2009; **1788**: 1168-1175 [PMID: 19230822 DOI: 10.1016/j.bbamem.2009.02.006]

49 **Muratori C**, Pakhomov AG, Gianulis E, Meads J, Casciola M, Mollica PA, Pakhomova ON. Activation of the phospholipid scramblase TMEM16F by nanosecond pulsed electric fields (nsPEF) facilitates its diverse cytophysiological effects. *J Biol Chem* 2017; **292**: 19381-19391 [PMID: 28982976 DOI: 10.1074/jbc.M117.803049]

50 **Xie Y**, Chen D, Jiang K, Song L, Qian N, Du Y, Yang Y, Wang F, Chen T. Hair shaft miniaturization causes stem cell depletion through mechanosensory signals mediated by a Piezo1-calcium-TNF-α axis. *Cell Stem Cell* 2022; **29**: 70-85.e6 [PMID: 34624205 DOI: 10.1016/j.stem.2021.09.009]

51 **Bonora M**, Kahsay A, Pinton P. Mitochondrial calcium homeostasis in hematopoietic stem cell: Molecular regulation of quiescence, function, and differentiation. *Int Rev Cell Mol Biol* 2021; **362**: 111-140 [PMID: 34253293 DOI: 10.1016/bs.ircmb.2021.05.003]

52 **Pchelintseva E**, Djamgoz MBA. Mesenchymal stem cell differentiation: Control by calcium-activated potassium channels. *J Cell Physiol* 2018; **233**: 3755-3768 [PMID: 28776687 DOI: 10.1002/jcp.26120]

Published by **Baishideng Publishing Group Inc**
7041 Koll Center Parkway, Suite 160, Pleasanton, CA 94566, USA
Telephone: +1-925-3991568
E-mail: office@baishideng.com
Help Desk: https://www.f6publishing.com/helpdesk
https://www.wjgnet.com